The Dissertation Committee for Troy Powell Purvis Certifies that this is the approved version of the following dissertation:

Nanoparticle Formulations of Poorly Water Soluble Drugs and Their Action *In Vivo* and *In Vitro*

Committee:

Robert O. Williams III, Supervisor

James McGinity

Robert Talbert

Keith P. Johnston

Salomon Stavchansky

Nanoparticle Formulations of Poorly Water Soluble Drugs and Their Action *In Vivo* and *In Vitro*

by

Troy Powell Purvis, B.S.

Dissertation

Presented to the Faculty of the Graduate School of

The University of Texas at Austin

in Partial Fulfillment

of the Requirements

for the Degree of

Doctor of Philosophy

The University of Texas at Austin

December 2007

Dedication

To my role models and loving parents, Mr. O.J. "Jack" Purvis, Jr. and Mrs. Anita Purvis. To my friends, family members, teachers, and inspirational leaders who have supported me throughout my educational process, without whom none of this would be possible.

Acknowledgements

I acknowledge my God, who has lead me down the path which He has laid out for me, providing me with the intellect and capacity to complete my role in life - to better humankind through improvement in medicine and make life better for those who suffer. I would like to thank my graduate supervisor, Dr. Robert O. Williams, III for his intellect and guidance throughout my graduate education, seeing in me the potential to be a great pharmaceutical scientist. He has always been accessible as a mentor, and he has always been a caring and understanding professor. I would like to thank Dr. James McGinity for his practical knowledge of communication, as well as his unparalleled knowledge in the field of pharmaceutical science. His advice about public speaking - one of my greatest fears - has given me insight about the importance of a lot of confidence and little humor when presenting in front of an audience. I would like to thank Dr. Keith Johnston, who has aided me throughout this program with his knowledge of chemical engineering principles which have helped me to become a better scientist, and his meticulous deliberation, in all areas of research. I would like to thank Dr. Salomon Stavchansky, whose pharmacokinetic knowledge is superb, giving excellent lectures in both his undergraduate and graduate classes. Not only is he a great scientist and educator, he gives his truthful opinion about any question he is asked, backed by his own life experience. I would like to thank Dr. Robert Talbert for asking thought-provoking

questions, and challenging me to think about the answers to those questions. He is a great asset both to the University and to my committee.

I wish to thank all of the faculty members and staff of the College of Pharmacy. Dr. Robert Pearlman has been a great professor to work for as a teaching assistant, giving advice to his students as much as his teaching assistants. Dr. Jason McConville has brought invaluable experience in the areas of pharmacokinetics and animal care and treatment to the University, and he makes a great addition to the Pharmaceutics Division. The Departments of Chemical Engineering, Biomedical Engineering, and Aerospace Engineering have excellent faculty members who have helped with my research and education, especially, Dr. Keith Johnston, Dr. Krishnendu Roy, Dr. Noel Clemens, and Mr. Mirko Gamba. The faculty and staff at the University of Texas Health Science Center have brought their own clinical knowledge to my education. Dr. Jay I. Peters has given a plethora of ideas related to our research, given his knowledge of medicine and the human body. Dr. Nathan Wiederhold graciously allowed me to work with him in his lab, and continues to give advice on our collaborative publications. Dr. Jacqueline Coalson, with her knowledge of histology and tissue function, has contributed to my education in that area. Dr. Marilyn Pollack, Laura McNeish, Brooke Holt, Juan Segovia, and the staff in the histocompatibility lab have donated their time (and in some cases their blood) to helping with experiments there.

The staff at the University of Texas College of Pharmacy has been especially helpful during my doctorial pursuits. Ms. Mickie Sheppard has guided me through the admission process right through to the final dissertation, making certain that I had all of the paperwork and administrative requirements met. Ms. Yolanda Abasta-Ruiz has always been helpful in communication between faculty and students, as well as providing answers to administrative questions. The Systems Analysts have been willing and able to

help with technical issues that have arisen, from computer meltdowns to providing service for PowerPoint presentations. Ms. Joyce McClendon, Mr. David Fudell, Ms. Belinda Lehmkuhle, and Mr. Jay Hammon have been invaluable resources when it comes to technical problems I might have had.

I wish to thank the former and present graduate students with whom I have worked and collaborated. Specifically, I thank my fellow Pharmaceutics graduate students and graduates Mr. Dave Miller, Ms. Dorothea Sauer, Ms. Prapasri Sinswat, Dr. Kirk Overhoff, Dr. Jason Vaughn, Ms. Wei Yang, Mr. Justin Tolman, Ms. Caroline Bruce, Mr. Alan Watts, Mr. Shawn Kucera, Ms. Sandra Schilling, and Ms. Loni Coots (Ms. Coots, especially for her generosity). As well as Pharmaceutics students, Chemical Engineering students have been very helpful in assisting with my research, including Mrs. Michal Matteucci, Mr. Todd Crisp, Mr. Josh Engstrom, and Ms. Jasmine Tam. Without your friendship and support, this program would have been nearly impossible to complete.

Finally, I wish to thank my parents, Mr. and Mrs. O.J. "Jack", Jr. and Anita Purvis, as well as my sisters Shellie Purvis and Lena McWilliams and brother-in-law, Mason McWilliams for their moral support, unconditional love, and guiding examples. My friends here in Austin have also been an excellent support system, including Ms. Jerusha DeGroote, Ms. Autumn Wood, Ms. Amy Bonneau, and Ms. Sarah McGaffey, who have all lended me a hand when I needed it most.

Nanoparticle Formulations of Poorly Water Soluble Drugs and Their Action *In Vivo* and *In Vitro*

Publication No._____

Troy Powell Purvis, Ph.D.

The University of Texas at Austin, 2007

Supervisor: Robert O. Williams III

Poorly water soluble drugs have been manipulated to make them more soluble, increasing the bioavailability of these drugs. Several cryogenic processes allow for production of drug nanoparticles, without mechanical stress that could cause degradation. The Ultra Rapid Freezing (URF) process is a technique which improves water solubility of drugs by reducing primary drug particle size by producing amorphous solid dispersions. Heat conduction is improved, using a cryogenic material with a high thermal conductivity relative to the solution being frozen to maintain the surface temperature and heat transfer rate while the solution is being frozen. With URF technology, the freezing rate is fixed, which drives the particle formation and determines its characteristics.

Supersaturation of drug in aqueous solution can allow for better absorption of the drug via the oral and pulmonary routes. Drug formulations that supersaturate the dissolution media show the possibility for increased bioavailability from an amorphous drug form. If the concentration of drug in solution is significantly increased, higher

chemical potential will lead to an increase in flux across an exposed membrane, leading to higher blood levels for an amorphous drug, compared to an identical crystalline formulation. During oral delivery, supersaturated drug concentrations would also saturate PGP efflux sites in the gut lumen, increasing the drug's bioavailability. Saturated PGP sites show zero order efflux kinetics, so increasing the drug concentration in supersaturated biological fluid will increase serum drug levels. High supersaturation levels maintained for prolonged periods would have a beneficial effect on a drug's absolute bioavailability. Pulmonary administration offers therapeutic advantages over more invasive routes of administration. Limited amount of metabolizing enzymes like CYP 3A4 in lung tissue along with avoidance of first pass metabolism are advantages to pulmonary delivery.

The objective of the research presented in this dissertation is to show the versatility of nanoparticulate poorly water soluble drug formulations. Due to the reduced particle size and the URF manufacturing process, a wide range of applications can be used with these nanoparticles. Oral and pulmonary administration routes can be explored using nanoparticles, but *in vitro* cell culture testing can show clinical benefits from this type of processing technology.

Table of Contents

List of Tables

List of Figures

Chapter 1: Enhancing Therapeutic Outcomes of Immunosuppressant Drugs Using Novel Formulation Design

1.1 INTRODUCTION

Within the past few decades, the number of patients on the organ transplant waiting list has increased dramatically while the number of available organs has remained constant [3]. This shortage has led to a reduction in the acceptable criteria for organ transplants ("marginal" donor) and a higher risk for organ rejection. Coupled with the rise in incidence of autoimmune diseases, safer and more effective immunosuppressant medication is needed. Immunosuppressants are used to modulate and in some cases inhibit the cascade of reactions leading to an immune response. Classification of immunosuppressants is based on their mechanism of action, and each class has its own set of formulation challenges. Researchers have used several strategies to improve formulation design of these drugs to overcome some of these formulation challenges. Nanoparticle engineering (Nanocrystals®, solution based dispersion by supercritical fluids (SEDS), and emulsification techniques) is one example of formulation design that can overcome formulation challenges such as poor aqueous solubility. Choice of excipients (Gelucire 44/14 and Peceol) and different routes of administration of the drug can also improve bioavailability of immunosuppressants hindered by p-glycoprotein (PGP) efflux and cytochrome P450 (CYP 3A) metabolism. Changing the route of administration of these drugs can improve targeting and absorption of the drugs (e.g.

inhalation administration for lung transplantation), leading to improved therapeutic outcomes. Novel approaches to formulation design of immunosuppressant drugs have lead to enhanced therapeutic outcomes of these drugs for various disease states. While immunosuppressants are primarily used to treat solid organ (liver, kidney, heart, and lung) and tissue (bone marrow) transplant rejection, other disorders such as multiple sclerosis, psoriasis, ulcerative colitis, and asthma are all being aggressively treated with immunosuppressant drugs. Advanced design of drug delivery systems for delivering immunosuppressants shows promise in treating these disease states along with other autoimmune diseases. Immunosuppressant drugs are classified into one of four categories based on their mechanism of action in the body and the type of immunosuppressive effect that is observed *in vivo*. The categories of immunosuppressants are: glucocorticoids, immunophilin binders, cytostatics, and other immunosuppressant drugs (including monoclonal antibodies, interferons, and other proteins) [4]. For the purposes of this review, novel formulations of "small" molecule drugs, including glucocorticoids, immunophilin binders, and cytostatics, will be discussed.

Over a period of time, doses of the drug can be reduced in transplant patients as the chance of transplant rejection decreases, but most transplant patients must maintain administration of immunosuppressants for life. Therapeutic drug monitoring of blood drug concentrations typically accompanies long-term immunosuppressant therapy due to intrapatient variability of drug absorption. Normalizing the bioavailability of these medications and acquiring more stable blood levels has been the goal of formulation scientists. Frequently, patients are administered combinations of different types of

immunosuppressants in order to modulate all components of the immune response cascade.

Using novel drug delivery systems, immunosuppressant drugs can show increased efficacy *in vivo*. Various strategies have been used to develop drug delivery systems of immunosuppressants with enhanced therapeutic outcomes. Reducing primary particle size of the drug has shown increased absorption with various different types of immunosuppressants. Nanocrystal® wet-milling technology has shown promise in delivery of the poorly water soluble crystalline drugs [5], including immunosuppressants [6]. Various types of immunosuppressant-loaded microparticles and nanoparticles have been produced, showing promising therapeutic results *in vivo*. Solid lipid nanoparticles [7, 8], biodegradable encapsulating nanoparticles [1], and diffusion controlled release nanoparticles [9] have shown enhanced modes of delivery for various routes of administration. Overall, this review article summarizes advanced formulation designs of immunosuppressants resulting in enhanced therapeutic outcomes of these drugs with improved targeting and delivery.

1.2 GLUCOCORTICOIDS

The corticosteroids or glucocorticoids were the first type of drug found to have potent immunosuppressive effects [10] and current formulations containing glucocorticoids include those for pulmonary, oral, topical, and parenteral administration. These drugs include prednisone, prednisolone, hydrocortisone, betamethasone, budesonide, and other similar compounds. These drugs mimic cortisol, which is

produced by the adrenal glands, and they act to reduce the inflammatory response along with modulation of the immune response. Glucocorticoids were first used to treat acute transplant rejection and graft-vs-host disease in transplant patients, but now are frequently used in combination with other medications for transplant maintenance. Other indications for glucocorticoids include treatment of allergic reactions of varying types, and autoimmune disorders. The mechanism of action of the glucocorticoids is owed to their broad spectrum ability to suppress cell-mediated immunity [10]. These drugs inhibit the production of cytokines and the interleukins IL-1, IL-2, IL-3, IL-4, IL-5, IL-6, IL-8, and tumor necrosis factor gamma (TNF-γ) by inactivating the genes that code for them [11]. Reduction in the amount of free cytokines, specifically IL-2, reduces the rate of T-cell proliferation, leading to an overall reduction in the immune response. Humoral immunity results from the smaller amounts of IL-2 and IL-2 receptors expressed after glucocorticoid administration. Anti-inflammatory effects of glucocorticoids result from the synthesis and release of lipocortin-1 which binds to cell membranes and prevents phospholipase A2 from producing eicosanoids from arachadonic acid. Lipocortin-1 also acts to inhibit emigration, chemotaxis, and the release of immune system mediators from neutrophils, macrophages, and mast cells. Cyclooxygenases (COX-1 and COX-2) are also suppressed by glucocorticoids, adding to their anti-inflammatory action [11]. This broad spectrum of immunomodulatory activity has led to the use of glucocorticoids in treating a wide variety of chronic disorders including but not limited to asthma, rheumatoid and juvenile arthritis, lupus erythematosus, and inflammatory bowel disease (IBD). However, because of their broad immunomodulatory activity, glucocorticoids can

reduce the patient's ability to fight infection while inhibiting the reparative processes in the body. .

The physicochemical properties of the glucocorticoids have been studied extensively. In general, the glucocorticoid molecules contain a central steroidal backbone with differing functional groups which impart the anti-inflammatory action to the compound. The steroidal backbone includes three fused six-membered ring structures with a five-membered ring fused to it [12]. As a result, the glucocorticoids are generally lipophilic in nature with low aqueous solubility, and chemical alteration of these drugs can be performed to improve their solubility and potency. For example, prednisone is a derivative of the naturally occurring compound cortisone, having an extra degree of unsaturation in the steroidal structure. Despite the low aqueous solubility of these drugs in their native forms, steroids may be considered to have good intestinal absorption, having high apparent permeability (log P_{app}) values and showing good passive transport permeability. Formulation of steroids into salt forms generally increases their aqueous solubility and allows for increased bioavailability. Oral bioavailability of the glucocorticoids, however, can be negatively influenced by their interaction with p-glycoprotein (P-GP) and the cytochrome P450 3A4 isoenzymes (CYP 3A4) in the intestines [12]. The physicochemical properties of some drugs of interest have been summarized in Table 1.1. These physicochemical properties must be considered when devising novel drug delivery systems for these types of drugs.

1.2.1 Beclomethasone and Betamethasone

Beclomethasone and betamethasone are two very closely related glucocorticoid immunosuppressants with identical structures, except in betamethasone, the heteroatom substituent on the steroidal backbone is fluorine [13], while in beclomethasone, the heteroatom substituent is chlorine [14]. The chemical structures of beclomethasone and betamethasone dipropionate are depicted in Figure 1.1. Frequently, these two drugs are administered as salt forms (dipropionate, sodium phosphate) due to their low aqueous solubility in their native forms. Typically, betamethasone is administered parenterally, topically, or via the ophthalmic route, while beclomethasone is administered topically or inhaled.

Beclovent® Aerosol for Inhalation (Glaxo Smithkline, Research Triangle Park, NC) is a commercial formulation of beclomethasone dipropionate indicated for asthma and other pulmonary autoimmune conditions [15]. Beclomethasone dipropionate is sparingly water soluble and poorly mobilized from the injection site for subcutaneous or intramuscular administration, so pulmonary formulation of this drug is more efficacious than the parenteral formulation. This formulation is composed of microcrystalline beclomethasone dipropionate with oleic acid excipients added as a surfactant [15]. Beclovent® Aerosol is formulated in a pressurized metered dose inhaler (pMDI) device with chlorofluorocarbons (CFCs) such as trichloromonofluoromethane and dichlorodifluoromethane used as propellant agents. The propellants offer an additional advantage, forming a clathrate with beclomethasone dipropionate, trapping the drug molecule around a "cage" of propellant molecules through dispersion interactions. After

actuation of the pMDI, most of the drug is deposited in the mouth and throat areas, while only a fraction is deposited in the deep lung tissue. A considerable amount of the formulation is swallowed, indicating that the particle size of the drug after actuation is larger than the respirable fraction (3-5 μm) needed for lung deposition. Additionally, the Beclovent® Aerosol for Inhalation contains ozone-depleting chlorofluorocarbons which are being phased out of production [15].

Other pMDI formulations of beclomethasone have been reported which do not contain ozone-depleting chlorofluorocarbons. Rocca-Serra et al. have studied the efficacy and tolerability of beclomethasone pMDI formulations which contain hydrofluroalkane (HFA-134a) propellants as an alternative to CFCs [16]. These propellants do not show a propensity to form clathrates with the drug, but they do effectively propel the drug into the patients' respiratory system in the desired respirable fraction. This study involved monitoring asthmatic patients' in two treatment groups: one group using the commercial Beclojet® with CFC containing propellants and the other using the beclomethasone/HFA-containing propellant. The study did not involve a placebo group because of ethical concerns about harm to human asthmatic subjects not receiving treatment for their conditions. A double-blind study was designed with randomized groups receiving one of the two treatments over a 6 week study period. Blood cortisol concentrations, adverse events, and treatment efficacy were studied. Peak expiratory flow (PEF), the measure of breathing efficiency, was the main measure of efficacy of the formulations. PEF was measured both in the morning and in the evening following treatment with the two different beclomethasone pMDI's. In the protocol study group, the average starting baseline PEF for patients was measured at 392.6 L/min for the

HFA group and 407.3 L/min for the CFC group. Final PEF measurements showed 403.9 L/min in the HFA group and 414.7 L/min in the CFC group. The protocol study's baseline to final PEF ratios were similar, showing a ratio of 1.06 for the HFA group and 1.05 for the CFC group. The results of the study also showed that the particle sizes of aerosols produced by the HFA formulation were smaller than those produced by the CFC formulation, resulting in the need to half the dose when switching from the CFC to the HFA formulation. The present study demonstrated that beclomethasone HFA was not statistically inferior to the beclomethasone CFC formulation for adjusting morning PEF, evening PEF, or PEF variability. The study constituted 449 patients, with a total number of adverse events involving the respiratory system being 57 in the HFA group, compared with 35 in the CFC group, most of the adverse events being mild to moderate. The study concluded that non-extra fine beclomethasone HFA-134a formulation was equivalent to the CFC formulation used in the study with regard to clinical efficacy and tolerability in patients with mild to severe asthma [16].

Another study involving the use of HFA propellant over CFC propellant in pMDI formulations of beclomethasone was conducted, evaluating the quality of life of asthmatic patients using these treatments. Juniper et al. reported data using clinical indexes of patients switched from conventional beclomethasone treatment to approximately half the dose of extra fine beclomethasone aerosol [17]. This study involved human asthmatic volunteers with a total number of 152 male patients and 40 female patients. The formulation of the HFA-BDP pMDI was altered in one group to produce extra fine aerosols with an average particle size of 1.1 μm. The baseline (pre-treatment) quality of life scores were measured by a 7-point value score with instance of

severe asthma symptoms occurring (1 = severe asthma all the time to 7 = severe asthma none of the time). The average baseline score for male patients was 5.45, while the average baseline score for female patients was 5.36. Patients were randomized in a 3:1 HFA-BDP group (400-1600 μg/day), a 3:1 CFC-BDP group (400-1600 μg/day), and an HFA-BDP group with approximately half the dose of BDP administered (200-800 μg/day). The duration of the study was 12 months, and the mean change from baseline was analyzed. Results showed that the overall change in baseline quality of life was increased to about 0.18 with the HFA (200-800 μg/day) group at 2 months, while the CFC group (400-1600 μg/day) increased only 0.8 over the 2 month time period. At 4 months, the HFA group (200-800 μg/day) showed increased quality of life scores of about 2.4 and the CFC group (400-1600 μg/day) increased to 1.6, while at 8 months, the HFA group (200-800 μg/day) increased to 2.8, with the CFC group (400-1600 μg/day) decreasing to 0.7. At the final time point of 12 months, the HFA (200-800 μg/day) the scores had increased to 0.32 from baseline, while the HFA (400-1600 μg/day) remained constant at about 0.33. The study concluded that patients switched from CFC-BDP to approximately half the dose of HFA-BDP extra fine aerosol experienced significant improvement in asthma-specific quality of life. The reason for the discrepancy between quality of life and clinical outcomes was that HFA-BDP spray was deposited in more in the peripheral airways as well as alveolar sacs. Also, improvement in quality of life seen in the present study developed progressively over the 12 month time period, suggesting that improvement could be increased with even longer term use of HFA-BDP (200-800 μg/day). The difference in quality of life score was significant between the HFA-BDP group (200-800 μg/day) vs. the CFC (800-1600 μg/day) group by 0.24 standard

deviations. The study concludes that switching from CFC based BDP aerosols to extra fine aerosol mist with HFA-BDP (200-8000 μg/day) may experience clinically important improvements in quality of life. This study also confirmed from shorter studies that asthma control can be maintained with approximately half the dose of HFA-BDP vs. CFC based BDP treatment [17].

NanoSystems® particle size reduction technology has been used to produce drug formulations of immunosuppressants with improved physicochemical properties [18]. The Nanocrystal® process was initially developed by NanoSystems®, a division of Elan Pharmaceutical Company. This process involves the use of media milling technology to formulate poorly water soluble drugs into nanocrystalline particles which offer improved drug delivery [18]. In this process, large micron sized crystalline particles of poorly water soluble compounds are milled in aqueous solution containing water-soluble stabilizer solutions. This process produces physically stable dispersions consisting of nanometer sized drug crystals that do not spontaneously reaggregate due to the surface adsorption of stabilizing excipients. High energy wet milling of the crystals in the presence of the stabilizing excipients causes the drug crystals to fracture to nano-sized particles. Polymeric excipients then adsorb to the crystal surface of the particles, inhibiting aggregation and particle growth of the crystals and providing stable dispersions of the drug crystals. Following milling for 30-60 min, unimodal distribution profiles and mean particle diameters of <200nm have been reported. This type of processing is especially useful in formulating drugs that are poorly water soluble and do not dissolve readily in the stabilizer-containing aqueous media in which they are milled [18]. A schematic of the Nanocrystal® technology is shown in Figure 1.2 [18]. A comparison of

the size of beclomethasone dipropionate crystals both before and after Nanocrystal® processing is shown in Figure 1.3 [6].

The use of Nanocrystal® technology for enhancing delivery of beclomethasone dipropionate (BCD) is an example of novel formulation design of immunosuppressant drugs. An initial study involved the preparation of pulmonary BCD using polyvinyl alcohol (PVA) as a stabilizer. Unmilled BCD showed a mean particle size of 10.5 μm, and after Nanocrystal® processing of BCD in 2.5% PVA, the mean particle size was reduced to 267 ± 84 nm [19]. The particle size of the crystals remained constant throughout the study, and following 7 months of storage at room temperature, the mean size was found to increase only slightly to 282 ± 73 nm [19]. A second study was conducted, using BCD wet-milled with Tyloxapol 2% w/w solution in water [6]. Following production of the BCD aqueous dispersion, the formulation was nebulized using an Omron Micro-air® NEU-30 nebulizer. The droplet size of the nebulized dispersion was controlled within a range of 1-7 μm, and the nebulized dispersion was analyzed using Andersen cascade impaction [6]. When viewed as a percentage of emitted dose through the mouthpiece, the respirable fraction ranged from 56-72% for the nanocrystalline formulation versus 36% for the propellant system. In addition, the throat deposition was 9-10% of the emitted dose for the novel dispersion, as compared to 53% for the commercial product. Therefore, the novel dispersion technology provides greater deposition of drug to the conducting airways and deep lung tissue both in quantity and as a percent of emitted dose than the commercial BCD product, lowering the dose needed for therapy and decreasing potential side effects. Also, the use of nebulized aqueous

dispersions of nanocrystalline BCD represents an environmentally sound alternative to the use of chlorofluorocarbon based propellant formulations [6].

Dry powder pulmonary formulations of BCD within mucoadhesive microspheres were studied in order to increase the residence time in the lungs and decrease dosing frequency and overall dose[20]. The microspheres were spray-dried from either an aqueous suspension or ethanolic solution containing BCD and the mucoadhesive polymer hydroxypropyl cellulose (HPC). Formulations produced by aqueous suspension showed crystalline characteristics, while those produced from ethanolic solution showed amorphous character. Amorphous beclomethasone dipropionate and hydroxypropylcellulose (aBCD/HPC) microspheres showed rapid absorption of the drug. Crystalline beclomethasone dipropionate and hydroxypropylcellulose (cBDC/HPC) microspheres showed increased residence time, being retained in the lung longer (with 86% remaining after 180 minutes), and showed sustained drug release. Bulk crystalline BCD (cBCD) administered without formulation into HPC microspheres and aBCD/HPC showed less than 17% dose remaining and less than 5% dose remaining, respectively, after 180 minutes. The aBCD/HPC formulation, with a higher apparent solubility and dissolution rate, was able to be absorbed faster than the crystalline forms of the drug, despite being formulated with a mucoadhesive carrier. Both of the HPC microsphere formulations (cBCD/HPC and aBCD/HPC) showed better efficacy against eosinophil accumulation than did the bulk drug substance cBCD. Inhaled cBCD/HPC microspheres showed a 50-60% decrease in the accumulation of lung eosinophils at the 6 and 24 hour time points after dosing compared to the aerosolized bulk drug substance [20], even with overall dosing of the BCD reduced from 480 μg of the bulk BCD to 88 μg of the

cBCD/HPC formulation. It was shown that five times the dosing of BCD bulk was only effective from 1-6 hours compared to 24 hour efficacy with the cBCD/HPC formulations. Therefore, by controlling the release and retention of BCD in the airways, mucoadhesive BCD microspheres are able to prolong the pharmacokinetic/pharmacodynamic profiles of this drug without increasing drug dose, and, hence unwanted side-effects [20].

Betamethasone sodium phosphate (BSP) encapsulated into poly(lactic/glycolic acid) (PLGA) nanoparticles was evaluated for its effectiveness in the treatment of experimentally induced arthritis. Higaki et al. used the biodegradable nanoparticle/steroid formulation for adjuvant induced arthritis (AA) and antibody induced arthritis (AbIA) [1]. The PLGA/BSP nanoparticles were administered intravenous (IV), while the bulk BSP was administered subcutaneously at the site of induced arthritis. The inflammation rate in the test subject animals was evaluated against two control groups treated only with blank PLGA nanoparticles and saline. In the AA mice, at 1 day post treatment, the PLGA/BSP nanoparticles showed 64% inflammation rate, while the bulk BSP administered at 100 μg and 300 μg showed inflammation rates of 68% and 78%, respectively. All three treatment groups showed decreased inflammation rates compared with the control groups which still showed 100% inflammation. In the AA mice, at 7 days post treatment, the PLGA/BSP nanoparticles inflammation rate was 76% vs. 84% and 87% for the bulk BSP groups (100 μg and 300 μg dosing), while the control groups still had 100% inflammation rates. A 36-24% decrease in inflammation was obtained after 1 day and maintained for 1 week with a single injection of 100 μg of PLGA-nanosteroid. The PLGA-nanosteroid particles were also effective against AbIA in mice. The inflammation in the joints of mice induced with

AbIA was scored for inflammation on a scale of 0-5 (0=no inflammation; 5=maximum inflammation). Twelve days after treatment, the arthritis score for the vehicle alone (PLGA) was 3.9, while the arthritis score for the PLGA/BSP was 1.3 and the BSP 100 μg dose was 2.4. The authors state that the PLGA nanoparticles may protect BSP against conversion and degradation in circulation, preventing the rapid and extensive tissue distribution that occurs with free BSP. The results of this study indicate that a single IV dose of hydrophilic BSP encapsulated in PLGA nanoparticles can lead to rapid, complete, and durable resolution of arthritis inflammation, owing to the enhanced preferential localization of the BSP in the synovial tissue. The observed strong therapeutic benefit obtained with PLGA-nanosteroid is due to the sustained release of the BSP over the longer time period as compared to injection of the bulk BSP. Therefore, targeted drug delivery of BSP using a sustained release PLGA nanosteroid delivery system shows successful treatment against experimental arthritis.

1.2.2 Budesonide

Budesonide (BDS) is a structural analog of the naturally occurring mineralocorticoid, cortisone, produced by the adrenal glands. The chemical structure of budesonide is depicted in Figure 1.1. This drug was determined not to have the undesirable side effects of water retention, high blood pressure, and muscle weakness associated with other glucocorticoids like cortisone. Budesonide is most often given by oral, topical, and pulmonary administration.

Budesonide has been used to treat a number of autoimmune and autoinflammatory diseases, including those diseases which affect the digestive tract. Orally dosed budesonide has shown effectiveness against Crohn's disease, ulcerative colitis (UC), and IBD, all of which are believed to have an autoimmune component as part of their etiology [21]. Drug delivery systems containing budesonide have been used to effectively target the drug to the site of action, avoiding the side effects that could accompany systemic delivery of the drug. One study evaluated the colon specific delivery of budesonide in an enteric formulation [22]. This drug delivery system is a microparticulate formulation consisting of hydrophobic budesonide-containing cores of cellulose acetate butyrate (CAB) which are enterically coated with Eudragit® S. Scanning electron micrographs of this formulation are shown in Figure 1.4. Drug release profiles of the formulation showed no release of budesonide in the acid phase, with sustained release of the drug occurring after the buffer stage. Figure 1.5 shows the *in vitro* release profiles of the formulation. These formulations were then tested with rats *in vivo* to determine the degree of inflammation that the microparticulate budesonide formulation could inhibit. These experiments were designed to mimic the inflammation that occurs with ulcerative colitis using 2,4,6-trinitrobenzenesulfonic acid (TNBS) to induce inflammation. Histological evaluations of the intestinal tissue of rats showed substantially decreased inflammation, resulting in lower microscopic histological damage scores. Micrographs of rat intestinal mucosa showed much lower degrees of inflammation when the budesonide CAB microparticles were used (Figure 1.6). This colonic delivery system improved the efficacy, at the site of action, of budesonide in the healing of induced colitis in rats, demonstrating that the effects of budesonide were

generally improved compared to those obtained with budesonide enteric microparticles for upper intestinal drug release.

Based on previous research, development of the Entocort® EC capsule for delivery of budesonide to the site of action for Crohn's disease patients has been reported by AstraZeneca Pharmaceuticals [23]. Entocort® EC has a pH- and time-dependent release profile for budesonide, developed to optimize drug delivery to the ileum, the site of inflamed tissue in Crohn's patients. The dosage form is a capsule with beads consisting of a sugar core, coated first with a layer containing budesonide, ethylcellulose and surfactants, followed by an enteric polymer coating (Eudragit® L). This formulation design allows for both the pH- and time-dependent release of the drug. pH-dependent release of the drug was shown to be caused by the Eudragit-L® enteric coating, while time-release of the drug was caused by the ethylcellulose/surfactant coating layer. Since ethylcellulose is water-insoluble, the presence of the surfactantants in this layer allowed for partial dissolution and pore-formation in this coating allowing for the time-dependent release of the drug. Scintigraphic methods confirmed that the Entocort® formulation delays absorption and prolongs the rate of elimination, while maintaining complete absorption. This study evaluated the regional deposition and uptake of budesonide in the Entocort® capsules and the immediate release capsules [23]. Delivery of budesonide from Entocort® capsules was evaluated when the formulation was given both before and after a meal to determine absorption with varying intestinal transit times [24]. The time-to-peak (t_{max}) plasma concentration was significantly increased with controlled-release budesonide when compared to the immediate release formulation (before breakfast 4.5 hr. vs 1.8 hr; after breakfast 5.2 hr. vs. 2.9 hr.). When given after breakfast, the controlled

release formulation was associated with a mean residence time 1.6 hours longer than seen with the immediate release formulation [24]. The rate of absorption of budesonide from standard and controlled-release capsules taken before and after breakfast evaluated in this study. The proportions of the budesonide dose absorbed from immediate release and controlled-release capsules in the upper and lower gastrointestinal tract are shown to vary according to the dose delivery system. Controlled-release budesonide, therefore, effectively delivers most of the budesonide dose to the ileum and colon, the regions that are most often affected by IBD. In addition, the time of food intake had little effect on the site of absorption or the bioavailability of the controlled-release formulation [24].

Pulmonary formulations of budesonide have also been reported for use in other chronic inflammatory conditions such as asthma. Waldrep et al. reported inclusion of various types of immunosuppressants in liposomal formulations for aerosol delivery to the lungs [25, 26]. Liposomal formulations of cyclosporin, beclomethasone, and budesonide were prepared using different types of phospholipids with varying drug to phospholipid ratios. Aerosol particle size analysis demonstrated that the mass median aerodynamic diameter (MMAD) of aerosolized liposomal formulations of these drugs increased minimally with higher liposome concentrations, remaining in the desirable respirable fraction for pulmonary formulations (2-5 μm in diameter) [25]. Lobo et al. from Nektar Therapeutics has reported budesonide dry powder formulations for inhalation [27]. The powders were manufactured by dissolving the drug in acetone before processing via the Solution Enhanced Dispersion by Supercritical fluids (SEDS) technique [27]. These SEDS processed powders were characterized by their low density and a MMAD (2.4 μm average) within the respirable size range. The performance of the

budesonide powders were evaluated in a Turbospin® and Eclipse® dry powder inhaler (DPI) device. The capsules of the inhaler devices were filled with powder, and their emitted doses (ED), defined as the relative amount of powder loaded in the capsule that leaves the device, were studied. The SEDS processed powders dispersed well in the DPI devices, exhibiting high ED's (70-80%) and relatively low variability (RSD 8-13%). Regardless of the device, the SEDS processed powders outperformed both the micronized drug and the commercial powder while showing good batch-to-batch reproducibility (RSD <5%) [27]. Both of these formulation techniques offer more effective dosing options for the treatment of asthma. Clinical trials of these formulations are on-going, but preliminary results showed that SEDS powders formulated into DPI devices, using the Turbospin® and Eclipse® DPI's deposit drug in the deep lung, leading to enhanced treatment of asthmatic conditions.

1.2.3 Dexamethasone

Dexamethasone (DEX) is a synthetic adreno-corticosteroid with similar properties to the naturally occurring hydrocortisone and cortisol, being about 20-30 times more potent than hydrocortisone in its anti-inflammatory effect. This compound, however, has been chemically modified with a fluorine substituent on the steroid ring structure, allowing the drug to have reduced side-effects. The drug is a potent anti-inflammatory medication, lacking the unwanted effect of sodium retention by the body. The chemical structure of dexamethasone is depicted in Figure 1.1. Typically, dexamethasone is

administered orally or topically, but it can also show effectiveness when administered to the lungs of asthmatics, and is often used for IV treatment in patients.

Formulations of dexamethasone palmitate (DEXP) have been produced using liposomal formulations of the drug [28]. Liposomes were produced using DEXP, phosphatidylcholine, and cholesterol in proportions 4:3:0.3, and these formulations showed high drug loading (70%). These formulations were intratracheally administered to the rat model to determine the retention of the liposomes, their release profiles, and the resulting blood levels due to drug release. Lymphocyte and interferon production were shown to be comparable between liposomal and free DEXP, showing no loss of activity when the drug is formulated as a liposome. Liposomes of DEX in proportions of 9:1 DEX:PC were prepared, and pulmonary retention of these DEX in the liposomal formulations in rats was 50%, compared with 26% retention for free DEX after 1.5 hours [29]. Liposomal DEX was also shown to have a prolonged action on the proliferation of white blood cells after 72 hours, while free DEX showed no further anti-inflammatory effect after 24 hours. This study showed that pulmonary dexamethasone was significantly retained in the lungs of the rat model and that the anti-inflammatory action in the lung was prolonged using the liposomal formulations compared to the free DEX, and side effects of the liposomal DEX formulation were reduced. Blood levels of liposomal DEX were reported to be lower in the rat model after 24 hours (about 0.8 % recovery), compared with free DEX (about 0.3% recovery), however lung levels were much higher (10% recovery in the lungs vs. less than 1% in the lungs for free DEX), and remained high over a period of time. A lag time in lung to blood partitioning was noted in the liposomal DEX formulation over the free DEX, which is to be expected. In

another study, biomarkers of pulmonary inflammation were studied following prophylactic administration of the liposomal DEX formulations and free DEX [30]. Liposomal DEX provided more protection from inflammation than did free DEX, inhibiting the increase in inflammatory mediator activity. Liposomal DEX reduced myleoperoxidase activity by 15%, elastase activity by 68%, and chloramine activity by 50% compared to free DEX. Of the pro-inflammatory mediators studied, liposomal DEX inhibited phospholipase A2 (62% vs. free DEX 45%), leukotriene B4 (76% vs. free DEX 64%), and thromboxane B2 (76% vs. free DEX 64%) [30]. Overall, liposomal treatment with DEX showed sustained release of the drug, when administered via the intratracheal route, with lower total dosage needed and a lower side effect profile, with increased prophylaxis against inflammation.

Incorporation of immunosuppressant drugs into the structure of implantable devices has been investigated due to the biofouling and rejection of these devices by the body due to the body's immune response. Dexamethasone has been encapsulated into PLGA microspheres to determine the feasibility of this drug to inhibit inflammation around implantable devices [31]. In this study, PLGA microspheres loaded with DEX were prepared with an O/W emulsion technique using polyethylene glycol (PEG) or PVA as aqueous stabilizers. Solvent evaporation and lyophilization yielded microspheres, which were sized with an average diameter of 11±1 μm. These microspheres did not show sufficient initial drug release, so microspheres were also pre-degraded to show the effect of weakening the PLGA, and hence fast initial drug release. These microspheres were shown to have a mean diameter of 12±2 μm. *In vitro* studies evaluated the DEX release from the microspheres. The non-degraded and pre-degraded microspheres were

mixed to allow for optimum release of drug, and release kinetics of pre-degraded microspheres showed an initial burst release followed by approximately zero order release rate for 1 month [31]. Delivery of dexamethasone at the site of the implant has been shown to reduce the inflammatory response and reduce the formation of pericardial adhesions of implants [32]. Chorny et al. examined efficacy of DEX loaded polylactide-polyethylene glycol (PLA-PEG) films implanted for inhibition of the formation of pericardial lesions in rabbits. *In vitro* results showed biphasic drug release rates in serum, with 69% drug released in 72 hours. The implants produced sustained drug release at the implantation site after that with low distribution in peripheral tissues. Tendency and density of scarring was evaluated 21 days post-op, and rabbits treated with blank implants were compared to DEX loaded implants. Epicardial adhesions' formation was reduced and the anatomy was preserved in treated animals. It is concluded that local delivery of DEX from biodegradable implants provides a new approach to prevention of scarring, notably pericardial adhesions, while minimizing drug distribution in surrounding tissues and systemic delivery [32].

1.3 IMMUNOPHILIN BINDING COMPOUNDS

The immunophilin binding compounds are a class of immunosuppressant drugs consisting of different medications from a broad range of natural and synthetic sources. These drugs include: cyclosporin, tacrolimus, sirolimus, everolimus, and other similar macrolide lactone molecules. Although differences in the individual drugs' mechanisms of action are observed, each of these drugs binds with cytosolic immunophilin proteins to

produce complexes which exert their immunosuppressive effects. In the case of cyclosporin and tacrolimus, the first phase of T-lymphocyte activation is halted. Because the immunophilin/drug complex inhibits the production of calcineurin, the dephosphorylation of key transcription factors for the production of interleukins is reduced [33]. Phosphorylated factors cannot cross the nuclear membrane, and the production of key factors for lymphocyte activation and proliferation is halted. In this way, cyclosporin and tacrolimus prevent lymphocytes from entering the G0 to G1 cell growth phases. Along with reducing interleukin release, the immunophilin/drug complex reduces the function of effector T-cells by reducing lymphokine production [33]. Cyclosporin (Sandimmune® [34], Neoral®) has been used to treat acute graft rejection in liver, kidney, and bone marrow transplant patients. Neoral® (cyclosporin microemulsion preconcentrate) [35] has also been used to treat severe psoriasis, rheumatoid arthritis, multiple sclerosis, and myesthenia gravis. Tacrolimus (Prograf® capsules, oral liquid [36]) has shown effectiveness against host-vs-graft disease in kidney and liver transplant patients, and the topical formulation of the drug (Protopic® ointment [37]) is used to treat psoriasis.

In the case of sirolimus and everolimus, the second phase of T-lymphocyte activation is halted by reducing signal transduction and clonal proliferation. Sirolimus and everolimus bind to immunophilin, but the drug/immunophilin complex does not inhibit calcineurin, instead inhibiting another related protein (mammalian target of rapamycin, m-TOR) [38]. Sirolimus and everolimus inhibit the binding of m-TOR to interleukin growth factors necessary for the production of kinases and phosphatases in the T-lymphocytes [39]. mRNA for key proteins required for the G1 cycle are blocked, and

progress of T-lymphocytes from the G1 to S phase in the cell cycle is inhibited. Sirolimus and everolimus act synergistically with the calcineurin inhibitors (cyclosporin and tacrolimus), and can be administered as combination therapies without increasing side effects. For example, sirolimus (Rapamune® tablets, oral liquid) and everolimus have been used in combination with cyclosporin and glucocorticoids in the treatment for long term transplant maintenance. Sirolimus is also effective against psoriasis.

The immunophilin binding compounds vary widely in their molecular structure, but they share common physicochemical properties, and they undergo similar metabolism in the body. Since all of the immunophilin binding compounds have high lipophilic character, shown by their high logP values, they are all substrates for the P-GP efflux pump [40]. This class of immunosuppressants has a common characteristic of being P-GP substrates inherent in their hydrophobic nature, containing positively or neutrally charged domains with a large planar molecular structure. Since these compounds are removed from the systemic circulation by P-GP and other multi-drug resistance (MDR) systems, the immunophilin binding compounds show erratic and extremely variable bioavailability [40]. Additionally, the immunophilin binding compounds are metabolized by the CYP 3A4 family of isoenzymes. The main function of these enzymes is to convert non-polar foreign chemicals into more polar (and therefore more excretable) substances. Oral bioavailability of these drugs is adversely affected by the intestinal and first-pass metabolic effects of these enzymes. The P-GP efflux mechanism coupled with the intestinal metabolic activity of CYP 3A4 work synergistically, contributing to the low oral bioavailability of these drugs [40].

1.3.1 Cyclosporin A

Cyclosporin A (CSA) is a peptide made up of 11 amino acids, derived from the *Trichoderma polysporum* fungus, and having highly lipophilic character and low aqueous solubility [41]. The chemical structure of CSA is depicted in Figure 1.1. As discussed previously, this compound is a calcineurin inhibitor type immunosuppressant. Selected physicochemical properties of this drug are shown in Table 1.1.

The commercial formulations of CSA, including Sandimmune® and Neoral® (Novartis, East Hanover, NJ), have found widespread therapeutic applications for a variety of immunosuppressive indications. Sandimmune® and Neoral® are approved for treatment of kidney, liver, and heart transplant patients as well as patients with rheumatoid arthritis and psoriasis. These formulations are available as oral liquids and liquid-containing capsules, and they allow for increased bioavailability of this poorly water soluble drug. Dressman et al. have determined that oral absorption of poorly water soluble and highly permeable drugs is limited by their dissolution rate [42], so formulation of CSA into a more soluble form allows for increased absorption of the drug. Neoral® and Sandimmune® are oral formulations where the drug is essentially presolubilized in the formulations. The Sandimmune® formulation contains CSA dissolved in corn oil and polyoxyethylated glycolyzed glycerides [34] and will not be discussed in depth. However, the Neoral® formulations are produced using advanced formulation design. Neoral® contains dehydrated alcohol, corn oil mono and di-glycerides, and polyoxyl 40 hydrogenated castor oil [35] formulated as a fine emulsion system. Neoral® has shown increased bioavailability over Sandimmune® because

Neoral® contains increased amounts of solubilizers, allowing better absorption than the Sandimmune®. For this reason, the two medications cannot easily be substituted for one another without therapeutic drug monitoring. The absolute bioavailability of cyclosporin administered as Sandimmune® is population dependent, estimated to be less than 10% in liver transplant patients and as great as 89% in some renal transplant patients. The absolute bioavailability of cyclosporin administered as Neoral® has not been determined in adults. In studies of renal transplant, rheumatoid arthritis and psoriasis patients, the mean CSA AUC was approximately 20% to 50% greater and the peak blood CSA concentration (C_{max}) was approximately 40% to 106% greater following administration of Neoral® compared to following administration of Sandimmune®. The dose normalized AUC in *de novo* liver transplant patients administered Neoral® 28 days after transplantation was 50% greater and C_{max} was 90% greater than in those patients administered Sandimmune®. AUC and C_{max} are also increased (Neoral® relative to Sandimmune®) in heart transplant patients, but data are very limited. Although the AUC and C_{max} values are higher on Neoral® relative to Sandimmune®, the pre-dose trough concentrations are similar for the two formulations. Cyclosporin in the Neoral® formulation shows high volume of distribution (3-5 L/kg in liver transplant patients), with excretion of the drug occurring mainly from the biliary route [35].

The main challenges with administration of the commercial CSA formulations are absorption variability and nephrotoxicity. While Neoral® is considered to be a substantial improvement over Sandimmune®, the emulsion formulation still suffers from considerable absorption variability and nephrotoxicity [35]. The commercial formulations exhibit high inter- and intra-patient absorption variability due to various

factors. In addition, high oral doses of CSA needed for relief of dermal psoriasis symptoms can lead to nephrotoxicity. Other formulation techniques have been developed to attempt to deal with these problems. The effects of adding micellar solubilizing agents, like the bile acid tauroursodeoxycholate (TUDC), to the oral formulations was investigated for improving oral dosage of CSA [43]. Oral doses of cyclosporin in the TUDC-monoolein micellar formula and co-administration of Sandimmune® with TUDC was studied in comparison with standard Sandimmune® administration for promoting and regulating CSA bioavailability in the rat. Pharmacokinetic parameters were determined in the fasted state with either an IV injection of CSA 5 mg/kg or a single oral dose of CSA with and without TUDC 10 mg/kg. Compared to Sandimmune®, the micellar solution of cyclosporin improved the drug's bioavailability by 160% and decreased interindividual variability expressed as a percent of variation from 32% to 15%. The plasma drug concentration vs time curves are shown in Figure 1.7. Bioavailability of the drug slightly improved in rats receiving Sandimmune® plus co-administered TUDC, though not significantly. Data indicate that the carriers used in delivery systems for cyclosporin greatly affect drug bioavailability, and that aqueous micellar vehicles provide for high cyclosporin absorption with low variability [43].

Parenteral delivery of CSA has been studied using microparticulate and nanoparticulate formulations of the drug. Sanchez et al. produced CSA loaded polyester nanoparticles for IV administration and studied the immunosuppressive and nephrotoxic properties of these formulations [44]. Compared with the commercial Sandimmune® injectable product, the microparticulate system investigated in the study offered extended release of CSA over the study time period. The study evaluated the *in vivo* release of

CSA from these particles in mice, showing differences in release dependant on the size of the particles - from 0.2 μm to 1 μm to 30 μm in size. These particles showed increased drug AUC compared to the commercial product. Among the formulations investigated, the 30 μm microspheres provided constant levels of CSA to be released over the 3 week test period. Figure 1.8 shows the blood-concentration vs. time curve for the microparticulate formulations, showing the differences between the formulations particle sizes. The Sandimmune formulation shows rapid increase in blood levels following administration, followed by rapid blood concentration decline, undetectable after 4 days. The nanosphere and microsphere formulations increased blood CSA concentrations to a t_{max} of 0.5 days, followed by a slow decline in drug concentration, depending on the size of the particle. Particles of sized 0.2-1 μm follow the same trend, having t_{max} values of 0.5 days and extending the CSA release from up to 21 days. Particles sized 30 μm show slower drug release, with a t_{max} of 7 days, constantly releasing drug for over 21 days. Further investigations showed CSA preferentially accumulates in the liver, kidney, spleen, and adipose tissues, with lower levels detected in the blood. These data show that CSA therapy by this route can decrease the likelihood of rejection on liver and kidney transplants. Figure 1.9 shows the length of time immunosuppression can be extended with the microparticulate formulations. Incorporation of CSA into these sustained-release formulations could offer better therapeutic outcomes by reducing the peak drug concentrations and reducing the likelihood of nephrotoxic events associated with high drug concentrations. The authors conclude that release of CSA from microparticles is dependent on the size of the microparticle and its catastrophic degradation rate. A single subcutaneous dose of encapsulated CSA can maintain long-term levels of the drug in

tissues which are most frequently transplanted, indicating the modulating ability of the immunosuppression therapy. Also, the sustained-release nature of these formulations can reduce the frequency of IV dosing and improve patient compliance.

In order to improve delivery of CSA to the site of action in lung transplant and asthma patients, pulmonary delivery of the drug has been explored. Mitruka et al. have experimented with pulmonary delivery of CSA using aerosolized solutions of the drug in ethanol, delivered to rats [45, 46]. Aerosol delivery of CSA resulted in higher and more rapid peak drug levels in lung tissue than did systemic delivery. CSA AUC was three times higher in lung tissue with aerosol delivery than with intramuscular delivery (477,965 ng hr/g and 157,706 ng hr/g, respectively). The lung tissue to blood ratio was higher in the aerosol groups (27.3:1 and 17.4:1) when compared with the intramuscular groups (8.1:1 and 9.4:1). CSA concentrations in blood as a function of time following the first 24 hours of drug administration are shown in Figure 1.10, and CSA concentrations in lung tissue as a function of time is shown in Figure 1.11. Area under the concentration vs. time curve (AUC)/dose of CSA (mg/kg) for each of the 4 study groups is shown in Figure 1.12. Therefore, local aerosol inhalation delivery of CSA provided a regional advantage over systemic intramuscular administration by providing higher peak drug concentrations and lung tissue exposure [46]. Additionally, local delivery of CSA by aerosol inhalation dose-dependently prevented acute pulmonary allograft rejection. Effective graft levels and low systemic drug delivery required significantly lower doses than systemic therapy alone [45]. Also, expression of inflammatory cytokines involved with graft rejection was suppressed by CSA therapy [45]. These data indicate that

pulmonary delivery of CSA can be effective at lower systemic levels, reducing the possibility for nephrotoxic side effects seen with high dose immunosuppressant therapy.

1.3.2 Tacrolimus

Tacrolimus (TAC) or FK506 is a macrolide lactone derived from the bacteria *Streptomyces tsukubaensis*, extracted as one of three tautomeric forms of the molecule from bacterial fermentation. The chemical structure of TAC is depicted in Fig. 1. As discussed previously, TAC is a calcineurin inhibitor similar in its effects to cyclosporin. It exhibits higher potency than cyclosporin, but it is similarly lipophilic and poorly water soluble [47]. Selected physicochemical properties of this drug are shown in Table 1.1.

The commercial formulations of TAC include the Prograf® capsules for oral administration [36] and the Protopic® ointment for dermal application [37]. Protopic® ointment is a simple mixture of tacrolimus in a base of white petrolatum, mineral oil, paraffin, propylene carbonate, and white wax, and since the design of this formulation is not novel, it will not be discussed. Prograf® capsules, however, are produced using a novel solid dispersion processing technique. The production of this solid dispersion formulation (SDF) is described by Yamashita et al. [1]. TAC is dissolved in ethanol and a stabilizing hydrophilic polymer is then added. After complete dissolution or swelling of the polymer, the ethanol is removed under reduced pressure and increased heat leading to formation of the SDF. Studies show that the SDF produced using this process contains tacrolimus in an amorphous state, which exhibits higher apparent solubility in dissolution

media than does the corresponding crystalline form [1]. The resulting SDF yields high supersaturation drug concentrations *in vitro* that are maintained for an extended period of time. The ability of these formulations to supersaturate the dissolution media highlights the possibility for increased bioavailability from an amorphous drug form. The meta-stable solubility of amorphous drug form may be as high as 100-times greater than its crystalline form [48]. If the concentration of drug in solution is significantly increased, the higher chemical potential will lead to an increase in flux across an exposed membrane. This would lead to much higher blood levels for an amorphous drug form, compared to an identical crystalline formulation [49]. The blood concentration of tacrolimus after oral administration of the SDF with hydroxypropyl methylcellulose (HPMC) to beagle dogs was measured against oral administration of the crystalline TAC powder (Figure 1.13). The pharmacokinetic parameters derived from the analysis of blood concentration vs. time curves are shown in Table 1.2. The AUC (0 to 8 hrs) of the SDF composition is almost 10-times higher than that of crystalline TAC, and the C_{max} of the SDF composition shows similar 10-fold increases in magnitude compared to the crystalline form [1]. Honbo et al. compared tacrolimus SDF's with oily ethanol formulations (OEF) of TAC for efficacy against allograft rejection [50]. A rat skin allograft transplantation study was conducted to determine the length of time the graft could remain viable when administered doses of oral TAC of 0, 1, 3.2, 10, and 32 mg/kg/day. At 1 and 3.2 mg/kg/day TAC, the animals in both OEF and SDF groups survived for over 30 days. The mean survival time was 14.4 days in the SDF-treated group and 11.2 days in the OEF treated group [50]. Survival graphs are shown in Figure 1.14.

For oral absorption, the major site of absorption for TAC was identified to be the upper small intestine [36]. Following administration, TAC has a high volume of distribution and binds extensively into red blood cells and blood proteins. Clearance occurs mainly through the biliary route. Prograf® is rapidly absorbed in some patients, with t_{max} occurring within 0.5-3 hours, while in other patients, a relatively flat absorption profile was observed, indicating continuous and prolonged absorption. The poor dissolution of TAC in gastric fluids, its low aqueous solubility, and variable gastric motility is thought to be responsible for this observation. For kidney transplant patients, single oral doses of 0.1, 0.15, and 0.2 mg/kg resulted in C_{max} of 19.2, 24.2, and 47.9 ng/mL, respectively. The t_{max} for these measurements varied from 0.7-6 hours. The mean bioavailability of Prograf® capsules was 21.8% for liver transplant patients, 20.1% for kidney transplant patients, and 14.4-17.4% for healthy subjects. Oral bioavailability was reduced when co-administered with a fatty meal. Decreases in AUC (-35% in whole blood) and C_{max} (-57% in whole blood) and increases in t_{max} (173% in whole blood) were observed, showing that both rate and extent of absorption is affected by food [36]. Oral absorption of TAC in Prograf®, therefore, is incomplete and highly variable, indicating problems with the commercial dosage form.

In addition to its primary use in inhibiting organ transplant rejection, TAC has been used for treatment in a variety of other disorders where reduction of an inflammatory/immune response is critical. Targeted delivery of TAC to the large intestine was investigated by Lamprecht et al. with sustained local release of TAC for treatment of ulcerative colitis [51-53]. Microspheres, manufactured using Eudragit P-4135F, show pH-dependent release in the colon using an emulsification/solvent extraction

method. In vitro release studies showed the TAC microspheres limited drug release at pH 6.8 and below (less than 10% release over 6 hours) and rapid release (100% within 30 min) at pH ≥ 7.4 [51]. Myeloperoxidase activity in the rat animal model was used to indicate the severity of colitis, with decreasing activity showing less colonic inflammation. TAC microspheres were shown to be as effective in mitigation of colitis induced inflammation when administered subcutaneously, and they are more effective than when administered orally as a solution. The TAC subcutaneous group, however, showed increased levels of adverse effects, including kidney impairment indicated by lower creatinine clearance, than the tacrolimus microsphere formulation. This was mainly due to the higher bioavailability of the TAC, due to the avoidance of the PGP efflux and CYP 3A4 effects seen with the oral administration of TAC [53]

1.3.3 Sirolimus and Everolimus

Sirolimus (SRL) or rapamycin is a macrolide lactone derived from the bacteria *Streptomyces hygroscopicus*, found in the soil on the south Pacific island of Rapa Nui [54]. As discussed previously, SRL has a mechanism of action different from that of cyclosporin and tacrolimus type calcineurin inhibitors. The chemical structure of SRL is depicted in Figure 1.1. Everolimus (EVR) is structurally very similar to SRL, with a 2-hydroxyethyl substitution at position 40 [55], and it can be produced by semisynthesis of SRL [56]. SRL, along with EVR, is structurally much different than tacrolimus, but it shares common pharmacophores with tacrolimus and other macrolides [57]. SRL and

EVR are similarly poorly water soluble and highly lipophilic [58]. Selected physicochemical properties of sirolimus are shown in Table 1.1.

The commercial formulations of SRL include the Rapamune® tablets for oral administration and Rapamune® oral solution [59]. There is currently no approved commercial formulation for EVR, but this drug shows promise with its immunosuppressive effects. Rapamune® is currently approved for prophylaxis of rejection for kidney allograft patients. The oral solution contains SRL dissolved in ethanol with solubilizers (Phosal® PG and polysorbate 80) present to allow for the drug to remain in solution following exposure to aqueous media and oral administration. Rapamune® oral liquid requires refrigeration and must be mixed with water or juice prior to administration, so an alternative tablet form of the drug was developed [59]. The SRL drug substance for the Rapamune® tablet formulation is manufactured according to the Nanosystems® wet-milling process described previously [5, 18]. For Rapamune® tablets, crystalline sirolimus is wet-milled with polymeric stabilizers (polyethylene glycol 8000, povidone, poloxamer 188, and polyethylene glycol 20,000) to decrease the primary particle size of the crystals to below 400 nm. The Nanosystems® process stabilizes the surface of the nanosized SRL crystals using these excipients to prevent aggregation of the particles, allowing for increased dissolution rates afforded by the smaller particle size. The resulting aqueous dispersion of SRL behaves like a solution, which is then processed into the finished tablet dosage form. In the case of Rapamune® tablets, the drug dispersion is then applied onto placebo tablet cores using spray-drying, followed by an overcoat of pharmaceutical glaze.

Following administration of Rapamune® Oral Solution, SRL is rapidly absorbed, with a mean t_{max} of approximately 1 hour after a single dose in healthy subjects and approximately 2 hours after multiple oral doses in renal transplant recipients [59]. The systemic availability of SRL was estimated to be approximately 14% after the administration of Rapamune® Oral Solution. The mean bioavailability of SRL after administration of the tablet is about 27% higher relative to the oral solution. Rapamune® oral tablets show improved bioavailability relative to the oral solution, and, therefore, are not bioequivalent to the oral solution [59].

Inclusion of immunosuppressant drugs within the exterior coating of implant devices has also been investigated to improve drug efficacy (drug delivery vehicle) and biocompatibility of the device (prevention of an immune response). Biosensors International developed an implantable stent covered by a resorbable "composite" coating containing a model immunosuppressive drug (the SRL-analog EVR and TAC) within a poly-hydroxyacid biodegradable polymer matrix for the local inhibition of in-stent restenosis [55]. Preclinical and clinical trials of the stents were conducted in coronary patients, and safety and efficacy of the new stent design was evaluated against the traditional bare metal S-stent. Stents were implanted into coronary arteries, and patients were monitored for various conditions related to stent implantation. Following preclinical examinations, both biocompatibility and efficacy of the EVR-eluting stents compared to the bare metal stent at 30 days. Clinical evaluation of the stents showed that no major adverse cardiac events or stent thromboses occurred within either group. The everolimus stent group showed an 87% reduction in neointimal volume. The binary restenosis rate at follow-up and 3 months was 0% for the everolimus-eluting stent and

9.1% for the bare metal stent. Release of drug from the stent, therefore, disrupts the restenosis cascade, while allowing sufficient neointimal growth to promote healing and avoid late stent thromboses. Future studies and post-operative follow-up will allow for determination of long-term stent biocompatibility [55].

1.4 CYTOSTATICS

Cytostatic compounds are most often used in chemotherapy against carcinoma, but smaller doses can be used as immunosuppressant agents. These drugs inhibit cell division, reducing the proliferation of T- and B-lymphocytes. Antimetabolite drugs are the most common cytostatic compounds used for immunosuppression. These are typically analogs of naturally occurring compounds, like nucleic acid bases, which interfere with DNA and RNA synthesis. Azathioprine and 6-mercaptopurine are analogs of purine, while methotrexate is an analog of folic acid. Alkylating agents such as nitrosoureas, platinum compounds, and cyclophosphamides are cytostatic drugs which work differently from the antimetabolite analog compounds, but also function as immunosuppressant cytostatics. Certain antibiotics are cytostatic and cytotoxic agents which have been used for immunosuppression. These include the antibiotics dactinomycin, mitomycin C, mitramycin, and bleomycin.

1.4.1 Methotrexate

In normal metabolism, folic acid is converted to dihydrofolate, followed by its conversion to tetrahydrofolate, a substance essential for the *de novo* synthesis of nucleic acids. Methotrexate (MTX), as stated previously, is an analog of folic acid, inhibits the enzyme responsible for folic acid conversion (dihydrofolic acid reductase) by competitively binding to the enzyme with a higher affinity than folic acid, thereby inactivating the enzyme. Therefore, MTX interferes with DNA and RNA synthesis, cell repair, and cellular replication. Active proliferation of cells, like those in the immune system, is subsequently halted, and immunosuppression results. MTX has been shown to be effective against transplant rejection as well as other autoimmune conditions such as rheumatoid arthritis and psoriasis [60]. MTX free acid shows some aqueous solubility, but the drug is most commonly formulated as the sodium salt. Unlike other drugs mentioned in this review, MTX oral absorption is actually enhanced by drug transporters in the gastrointestinal tract. Since it is chemically similar to folic acid, the folic acid transporter is utilized to increase MTX bioavailability [40]. Trexall® is the trade name for commercially available tablets and injectable formulations of MTX [61]. The chemical structure for MTX is shown in Figure 1.1, and relevant physicochemical properties of the drug are shown in Table 1.1.

Microspheres of MTX were developed for intra-articular delivery of drug to the synovial fluid for treatment of rheumatoid arthritis. Biodegradable poly-lactic acid (PLLA) microspheres were produced with entrapped MTX which were then injected into the joint cavity of animals with induced arthritis [62]. The purpose of this study was to minimize the systemic bioavailability of the drug to reduce toxic side-effects, while maximizing the immunosuppressive properties of the drug to alleviate symptoms of

rheumatoid arthritis. MTX plasma concentrations were analyzed and tolerability of the microspheres as well as their degradation and drug release rates were evaluated *in vivo*. Biocompatibility was evaluated by observing the swelling of the joints of the rabbits, and histological analysis was performed following the injection of the microspheres. Encapsulation efficiency (EE) of the microspheres increased with increasing molecular weight (MW) of PLLA used. Encapsulation efficiencies of 63.6% to 68% were achieved with 2,000 MW PLLA, while a PLLA polymer MW of 50,000 showed an EE of 89.2%. The mean particle diameter of microspheres increased from 79.5 μm with 2,000 MW polymer to 187.6 μm for 100,000 MW polymer. Degradation of the microspheres occurred fastest with the 2,000 MW polymer and slowed as polymer molecular weight increased. Microspheres loaded with MTX and 2000 MW PLLA showed a rapid burst phase followed by a slow release rate *in vitro*. *In vivo* results showed sustained release of MTX into the systemic circulation in the microsphere formulation, compared to high plasma MTX levels followed by decreasing MTX upon elimination. The t_{max} values of both the microsphere MTX and free MTX showed similar results with a time of 0.5 hours. The C_{max} values, however varied significantly, with free MTX reaching a peak plasma concentration of about 0.6 μg/mL at the t_{max}, while the microsphere MTX formulation only achieved a C_{max} of about 0.05 μg/mL. The free MTX showed an exponential decline in plasma concentration following administration, while the microspherical MTX showed nearly constant release over the 8 hour time period. Both formulations showed plasma levels of 0.04 μg/mL at the end of the study time period of 8 hours. This shows that nearly zero-order release of MTX is observed using the microsphere formulation. Other *in vivo* results showed that, after sacrificing the rabbits,

no MTX was detected in knee joints of animals dosed with free MTX, while approximately 0.6 μg MTX was detected in knee joints of rabbits treated with MTX microspheres. The MTX concentrations in plasma vs. time were plotted to evaluate the systemic bioavailability of free MTX and MTX microspheres. The plasma concentration vs. time curve is shown in Figure 1.15. Although the MTX microspheres showed lower systemic bioavailability, histological scoring showed decreased inflammation and joint swelling due to rheumatoid arthritis in animals treated with MTX microspheres over free MTX. Increasing attention is being paid to development of polymeric microspheres for delivery of drugs locally to the joints for sustained drug release. Following intra-articular injection, these microspheres demonstrated good biocompatibility and decreased the clearance rate of MTX from the joint cavity, providing for decreased inflammation in rheumatoid arthritis [62].

Other studies have been conducted to improve delivery of methotrexate to the joints of rheumatoid arthritis patients. Wunder et al. have used albumin-based formulation design for the delivery of MTX [63]. They state the main features of appropriate drug carriers are high accumulation in target tissues, low uptake rates by normal tissue, low toxicity, and biochemical potential to be linked to drugs. This research group has found that albumin acts as a good carrier for MTX because it satisfies all of these characteristics when considering tumor tissue as the target. They stated that albumin might also be a suitable drug carrier for drug targeting to inflamed joints of patients with rheumatoid arthritis. Using albumin labeled with aminofluorescein, the study showed that albumin did, indeed, preferentially accumulate in inflamed joints with rheumatoid arthritis. This observation was confirmed using radiolabeled human serum

albumin (HSA), which showed significant accumulation in joints of collagen-induced arthritis (CIA) rats. This study evaluated the uptake kinetics of radiolabeled HSA and radiolabeled MTX in the paws of mice both with and without CIA. Significant albumin amounts accumulated in arthritic hind paws, exceeding the uptake in non-inflamed hind paws by 6- to 7-fold. In contrast, uptake of radiolabeled MTX in arthritic hind paws was found to be significantly less, decreasing rapidly over time [63]. Different dosages of MTX and MTX-HSA were then administered to rats that had been given CIA, and the incidence of arthritis in these animals was observed. Treatment was started two weeks before onset of disease, and the animals were treated for 4 weeks and received two injections weekly. MTX-HSA was significantly more effective in the suppression of the onset of arthritis than were comparable doses of MTX. At least a 5-fold higher dose of MTX was required to achieve the levels of arthritis suppression seen with MTX-HSA. The effect of different doses of MTX and MTX-HSA on the development of CIA in mice is evaluated in this study. These results indicate that MTX, in contrast with albumin, is rapidly removed from blood circulation and does not accumulate in inflamed paws. When complexed together, however, MTX and HSA target inflammation in CIA mice, allowing for delivery of the drug to the site of action.

Methotrexate formulations for the treatment of psoriasis were developed using solid lipid nanoparticles (SLN) loaded with the drug [2]. Topical application of methotrexate was developed to minimize the systemic bioavailability of MTX, while using the immunosuppressive properties of the drug to treat psoriasis. MTX-SLNs were prepared by melting the lipid components and adding the drug to the lipid phase (containing Tween® 80), preparing an aqueous phase using a co-surfactant, followed by

emulsification of the two phases with heating and mechanical stirring to form an O/W emulsion. SLNs were then formed by cooling the emulsion and dispersing it in a mixture of cold water and propylene glycol. They were further purified using dialysis to remove any unentrapped drug. Particle size distribution and other *in vitro* tests were performed to characterize the SLNs. The SLNs were then incorporated into a carbopol gel for application to psoriatic lesions. Deposition of the drug was evaluated on cadaver skin. The tolerability of the formulations, as well as their ability to heal psoriatic lesions was evaluated in psoriasis patients. Average amount of MTX deposited on the skin increased from 36.4% for free MTX to 39.1% for the lipid/MTX physical mixture to 74.5% for the MTX-SLN formulation. In human subjects afflicted with psoriasis, the average percent improvement in lesion healing was evaluated, and consistently, the MTX-SLN formulation showed much improved healing over the plain MTX and MTX/lipid physical mixture. Table 1.3 shows the gel formulations evaluated in this study, with plain MTX, MTX/lipid physical mixtures, and MTX-SLN's detailed. Table 1.4 shows the average percent improvement in healing of psoriatic lesions using the different MTX formulations. *In vivo* skin deposition of the free MTX and the physical mixture of MTX/lipids on the skin than the SLN formulation, but upon washing of the applied areas, >99% of the MTX was removed from the skin. The SLN formulations, however, showed higher drug retention on the skin surface. Patient scoring was conducted after treatment with MTX, MTX/lipid mixture, and MTX SLN formulations, from 0-4 (0 = no degree of erythema and scaling, and 4 = severe erythema and scaling). Baseline scoring showed high degrees of psoriatic symptoms (ranging from 3.8-4). Treatment was administered using the three formulations for 6 weeks, and scoring for the psoriatic symptoms

decreased in all treatment groups. Most notably, however, the MTX SLN group showed the fastest recovery time from psoriatic symptoms, showing a score of 0 at the 3 week time period. The free MTX showed a score of 1.9, while the physical mixture showed a scoring of 2.2. The trend continued through the end of the study, (6 weeks), when the final scoring for the MTX was 0.4, the scoring for the MTX/lipid mixture was 0.5, and the scoring for the MTX SLN continued to show 0. While plain MTX is shown to be effective against psoriasis, the physicochemical properties of the drug hinder the drug's ability to penetrate the epidermis. The SLN formulations appear to allow for penetration of the drug deeper into the skin surface, and, therefore lend themselves to more effective treatment against topical skin maladies such as psoriasis. The findings of this investigation, therefore, demonstrate the promising role of MTX SLN in treatment of psoriasis [2].

1.4.2 Azathioprine

Azathioprine (AZA) is a cytostatic drug, which, as stated previously, is a prodrug analog of the purine molecule, a component of nucleic acids. Until the discovery of cyclosporin in 1978, the combination of azathioprine and corticosteroid medications was the standard for treatment of transplant rejection. In the body, the AZA molecule is cleaved and converted to 6-mercaptopurine, the active form of the drug. This metabolite then goes on to antagonize purine synthesis which halts the synthesis of DNA, RNA, and some proteins [64]. This drug therefore inhibits mitosis and cell metabolism, reducing the proliferation of lymphocytes, leukocytes, and mast cells, and subsequently reducing

the body's immune response. AZA has also been shown to reduce the amount of free antibodies in circulation, stemming from the reduced number of immune-related cells [65]. As a result of its mechanism of action, this drug has been shown to be toxic in large amounts and over long therapeutic dosing schedules. For this reason, therapeutic drug monitoring should accompany the administration of azathioprine. AZA free acid is poorly soluble in water, and it shows varying solubility with pH. The sodium salt of azathioprine is typically used in formulating dosage forms because it shows increased aqueous solubility compared to the free acid [65]. AZA, with the commercial trade name Imuran®, is traditionally administered orally as a 50 mg AZA tablet or parenterally as a reconstituted aqueous solution of the drug produced from its lyophilized sodium salt [64]. The chemical structure of AZA is depicted in Figure 1.1, and relevant physicochemical properties are shown in Table 1.1.

AZA has been studied for its immunosuppressive effect on a number of autoimmune conditions, including Crohn's disease. However, use of this drug has been limited by concerns over its systemic toxicity [65]. Because systemic delivery of immunosuppressants can cause opportunistic infection or other harmful side-effects, in many instances, these drugs are desired to be delivered locally, with limited systemic absorption. Colonic delivery has been evaluated as a strategy limit the systemic delivery of AZA thereby reducing much if its toxicity. Zins et al. have developed a delayed-release oral formulation of AZA which shows lower systemic bioavailability than standard AZA tablets, retaining the effectiveness against autoimmune intestinal disorders while decreasing toxicity [66]. This study aimed to determine the bioavailability and pharmacokinetic parameters of delayed-release oral AZA capsules at doses of 200, 400,

and 600 mg while comparing them to the 100 mg standard capsule. The relative bioavailabilities after ileocolonic administration via delayed-release capsules were 15%, 15%, and 12% for the 200, 400, and 600 mg capsules, compared to 100% for the standard 100 mg dose. Ileocolonic delivery of AZA by this formulation, therefore, reduced the systemic bioavailability, while alleviating the symptoms of Crohn's disease. The therapeutic potential of this ileocolonic delivery formulation, which can limit toxicity by local delivery of AZA, should be investigated in patients with refractory IBD [66].

In addition, AZA was formulated into either a hydrophilic or hydrophobic foam for rectal administration for the treatment of IBD [67]. The foams were evaluated for their pharmacokinetic parameters and compared to the delayed-release and standard capsule formulations mentioned above. The bioavailabilities of the drug after colonic AZA administration via an oral delayed release form, a hydrophobic rectal foam, and a hydrophilic rectal foam (7%, 5%, and 1%, respectively) were significantly lower than the bioavailability of AZA after oral administration with the immediate release capsule. The study concluded that AZA delivered directly to the colon by either delayed release oral or rectal foam formulations considerably reduced the systemic AZA bioavailability. The therapeutic potential of these colonic delivery methods, which can potentially limit toxicity by local delivery of high doses of AZA could be beneficial in treatment of IBD [67].

1.5 CONCLUSION

Immunosuppressant drugs have been used to treat a wide variety of autoimmune conditions and have shown promise in suppressing the immune response for prevention of organ rejection post-transplantation. Overcoming the drug's physicochemical properties of low water solubility, PGP or CYP 3A4 interaction, or cellular toxicity are needed to produce safe and effective drug products. Some drugs, however, benefit from lower systemic bioavailability and higher drug concentration at the site of action. As shown herein, advanced formulation design has allowed for more efficient delivery of these drugs to their site of action, leading to higher efficacy, reduced toxicity, and lower dosing required to reach a therapeutic response. Alternative routes of administration, such as pulmonary, topical, and oral enteric routes have all shown significant improvement in alleviation of various disease states over conventional treatments. Several currently marketed commercial products utilize novel formulation design in delivery of immunosuppressant drugs, but more research is needed to develop new drug products with yet more enhanced therapeutic outcomes. Future studies of these drugs on solid organ transplants can improve the survival of these transplants, allowing patients to live more normal lives. Improved formulation design could allow for less frequent dosing of these medications to transplant patients, while lessening the occurrence of opportunistic infections which could occur in patients on immunosuppressant therapy. Continuing research in the area of delivery of immunosuppressants is required so that improved transplantation techniques can improve long-term patient survival. Along with transplant patients, other patients having autoimmune disorders can benefit from immunosuppressant therapy, and these areas must be studied to improve quality of life and alleviate symptoms of these types of immune disorders.

1.6 REFERENCES

1. M. M. Chakinala, M. H. Kollef, and E. P. Trulock, Critical Care Aspects in Lung Transplant Patients, J Intens Care Med. 17 (2002) 8-33.

2. Wilson, Shannon, Shields, and Stang, *Drug Guide*. 2003, Upper Saddle River, NJ: Prentice Hall Health.

3. G. G. Liversidge and P. Conzentino, Drug Particle Size Reduction for Decreasing Gastric Irritancy and Enhancing Absorption of Naproxen in Rats, Int J Pharm. 125 (1995) 309-315.

4. K. D. Ostrander, H. W. Bosch, and D. M. Bondanza, An In-Vitro Assessment of a Nanocrystal Beclomethasone Dipropionate Colloidal Dispersion via Ultrasonic Nebulization, Eur J Pharm Biopharm. 48 (1999) 207-215.

5. C. S. Maia, W. Mehnert, and M. Schafer-Korting, Solid Lipid Nanoparticles as Drug Carriers for Topical Glucocorticoids, Int J Pharm. 196 (2000) 165-167.

6. C. S. Maia, A. Gysler, W. Mehnert, R. H. Muller, and M. Schafer-Korting, Local Tolerability of Solid Lipid Nanoparticles for Dermal Use, Proceedings of the International Symposium of Controlled Release of Bioactive Materials. 26 (1999) 399-400.

7. M. Higaki, T. Ishihara, N. Izumo, M. Takatsu, and Y. Mizushima, Treatment of Experimental Arthritis with Poly (D,L Lactic/Glycolic) Acid Nanoparticles Encapsulating Betamethasone Sodium Phosphate, Ann Rheum Dis. 64 (2005) 1132-1136.

8. M. Guzman, J. Molpeceres, F. Garcia, M. R. Aberturas, and M. Rodriguez, Formation and Characterization of Cyclosporin Loaded Nanoparticles, J Pharm Sci. 82 (1993) 498-502.

9. E. F. Morand, Corticosteroids in the Treatment of Rheumatologic Diseases, Current Opin Rheumatol. 12 (2000) 171-177.

10. V. H. J. Van Der Velden, Glucocorticoids: Mechanism of Action and Anti-Inflammatory Potential in Asthma, Mediators Inflamm. 7 (1998) 229-237.

11. F. Faassen, J. Kelder, J. Lenders, R. Onderwater, and H. Vromans, Physicochemical Properties and Transport of Steroids Across CACO-2 Cells, Pharm Res. 20 (2003) 177-186.

12. S. Wang, Y. Zheng, and W. Zhang, Betamethasone dipropionate, Acta Crystallographica, Section E: Structure Reports. E60 (2004) O1063-O1064.

13. W. L. Duax, V. Cody, and P. D. Strong, Structure of the asthma drug beclomethasone dipropionate, Acta Crystallograph B: Struct Crystallog Cryst Chem. B37 (1981) 383-387.

14. Beclovent Aerosol for Inhalation: professional literature. 1998, Glaxo Smithkline Pharmaceuticals: Research Triangle Park, NC.

15. J. P. Rocca-Serra, E. Vicaut, G. Lefrancois, and A. Umile, Efficacy and Tolerability of a New Non-Extrafine Formulation of Beclomethasone HFA-134a in Patients with Asthma, Clin Drug Invest. 22 (2002) 653-665.

16. E. Juniper, D. B. Price, P. Stampone, J. Creemers, S. Mol, and P. Fireman, Clinically Important Improvements in Asthma-Specific Quality of Life, but No Difference in Conventional Clinical Indexes in Patients Changed from Conventional Beclomethasone to Approximately Half the Dose of Extrafine Beclomethasone Dipropionate, Chest. 121 (2002) 1824-1832.

17. E. Merisko-Liversidge, G. G. Liversidge, and E. Cooper, Nanosizing: A Formulation Approach for Poorly Water Soluble Compounds, Eur J Pharm Sci. 18 (2003) 113-120.

18. T. S. Wiedmann, L. DeCastro, and R. W. Wood, Nebulization of Nanocrystals: Production of Respirable Solid-in-Liquid-in-Air Colloidal Dispersion, Pharm Res. 14 (1997) 112-116.

19. M. Sakagami, W. Kinoshita, Y. Makino, and T. Fujii, Mucoadhesive BDP Microspheres for Powder Inhalation - Their Unique Pharmacokinetic/Pharmacodynamic Properties, Respir Drug Del. 4 (1998) 193-199.

20. S. Edsbacker, P. Wollmer, A. Nilsson, and M. Nilsson, Pharmacokinetics and gastrointestinal transit of budesonide controlled ileal release (CIR) capsules, Gastroenter. 104 (1993) A695.

21. M. Rodriguez, J. Antunez, C. Taboada, B. Seijo, and D. Torres, Colon specific delivery of budesonide from Microencapsulated cellulosic cores: Evaluation of the efficacy against colonic inflammation in rats, J Pharm Pharmacol. 53 (2001) 1207-1215.

22. S. Edsbacker and T. Andersson, Pharmacokinetics of Budesonide (Entocort EC) Capsules for Crohn's Disease, Clin Pharmaco. 43 (2004) 803-821.

23. S. Edsbacker, P. Larsson, and P. Wollmer, Gut Delivery of Budesonide, a Locally Active Corticosteroid from Plain and Controlled-Release Capsules, Eur J Gastroenterol Hepatol. 14 (2002) 1357-1362.

24. J. C. Waldrep, J. Arppe, K. A. Jansa, and V. Knight, High Dose Cyclosporin A and Budesonide Liposome Aerosols, Int J Pharm. 152 (1997) 27-36.

25. J. C. Waldrep, B. E. Gilbert, C. M. Knight, M. B. Black, and P. W. Sherer, Pulmonary Delivery of Beclomethasone Aerosol in Volunteers, Chest. 11 (1996) 316-323.

26. J. M. Lobo, H. Schiavone, S. Palakodaty, P. York, A. Clark, and S. Tzannis, SCF-Engineered Powders for Delivery of Budesonide from Passive DPI Devices, J Pharm Sci. 94 (2005) 2276-2288.

27. H. Benameur, N. Latour, L. Schandene, J. P. Van Vooren, B. Flamion, and F. Legros, Liposome-incorporated dexamethasone palmitate inhibits in-vitro lymphocyte response to a mitogen, J Pharm Pharmacol. 47 (1995) 812-817.

28. Z. Suntres and P. Shek, Liposomes promote pulmonary glucocorticoid delivery, J Drug Targ. 6 (1998) 175-182.

29. Z. Suntres and P. Shek, Prophylaxis against lipopolysaccharide-induced lung injuries by liposome-entrapped dexamethasone in rats, Biochem Pharmacol. 59 (2000) 1155-1161.

30. T. Hickey, D. Kreutzer, D. J. Burgess, and F. Moussy, Dexamethasone/PLGA Microspheres for Continuous Delivery of an Anti-Inflammatory Drug for Implantable Medical Devices, Biomat. 23 (2002) 1649-1656.

31. M. Chorny, D. Mishaly, A. Leibowitz, A. Domb, and G. Golomb, Site-specific Delivery of Dexamethasone from Biodegradable Implants Reduces Formation of Pericardial Adhesions in Rabbits, J Biomed Materials Res A. 78A (2006) 276-282.

32. S. Ho, N. Clipstone, L. Timmerman, J. Northrop, I. Graef, D. Fiorentino, J. Nourse, and G. Crabtree, Mechanism of Action of Cyclosporin A and FK506, Clin Immunol Immunop. 80 (1996) S40-S45.

33. Sandimmune Capsules and Oral Liquid: professional literature. 1999, Novartis Pharmaceuticals: East Hanover, NJ.

34. Neoral Soft Gelatin Capsules and Oral Liquid: professional literature. 1998, Novartis Pharmaceuticals: East Hanover, NJ.

35. Prograf Capsules: professional literature. 2004, Fujisawa Pharmaceuticals: Osaka, Japan.

36. Protopic ointment: professional literature. 2002, Fujisawa Pharmaceuticals: Osaka, Japan.

37. R. E. Morris, Prevention and Treatment of Allograft Rejection in vivo by Rapamycin: Molecular and Cellular Mechanisms of Action, Annals of the New York Academy of Sciences. 1 (1992) 68-72.

38. K. L. Molnar-Kimber, Mechanism of action of rapamycin (Sirolimus, Rapamune), Transplant Proc 28 (1996) 964-969.

39. C. Kruijtzer, J. Beijnnen, and J. Schellens, Improvement of Oral Drug Treatment by Temporary Inhibition of Drug Transporters or CYP 450 in the Gastrointestinal Tract and Liver: an Overview, Oncologist. 7 (2002) 516-530.

40. Y. Ran, L. Zhao, Q. Xu, and S. Yalkowsky, Solubilization of Cyclosporin A, AAPS Pharm Sci Tech. 2 (2001.

41. J. B. Dressman, Reppas, C., In vitro-in vivo correlations for lipophilic, poorly water soluble drugs, Eur J Pharm Sci. 11 (2000) S73-S80.

42. N. Balandrand-Pieri, P. Queneau, F. Caroli-Bosc, P. Bertault-Peres, A. Montet, A. Durand, and J. Montet, Effects of Tauroursodeoxycholate Solutions on Cyclosporin A Bioavailability in Rats, Drug Metabol Distrib. 25 (1997) 912-916.

43. A. Sanchez, R. Seoane, O. Quireza, and M. J. Alonso, In Vivo Study of the Tissue Distribution and Immunosuppressive Response of Cyclosporin A-Loaded Polyester Micro and Nanospheres, Drug Deliv. 2 (1995) 21-28.

44. S. N. Mitruka, S. M. Pham, A. Zeevi, S. Li, J. Cai, G. J. Burckart, S. A. Yousem, R. J. Keenan, and B. P. Griffith, Aerosol Cyclosporin Prevents Acute Allograft Rejection in Experimental Lung Transplantation, J Thoracic Cardiovasc Surg. 115 (1997) 28-37.

45. S. N. Mitruka, A. Won, K. R. McCurry, A. Zeevi, T. McKaveney, R. Venkataramanan, A. Iacono, B. P. Griffith, and G. J. Burckart, In the Lung Aerosol Cyclosporine Provides a Regional Concentration Advantage over Intramuscular Cyclosporine, Clin Lung Heart/Lung Transplant. 19 (2000) 969-975.

46. S. Soeda, T. Akashi, K. Maeda, and T. Kawagita, Studies on the Development of Tacrolimus Production, Seibutsu Kogaku Kaishi. 76 (1998) 389-397.

47. K. Yamashita, T. Nakate, K. Okimoto, A. Ohike, Y. Tokunaga, R. Ibuki, K. Higaki, and T. Kimura, Establishment of New Preparation Method for Solid Dispersion Formulation of Tacrolimus, Int J Pharm. 267 (2003) 79-91.

48. B. C. Hancock and G. Zograffi, Characteristics and significance of the amorphous state in pharmaceutical systems, J Pharm Sci. 86 (1997) 1-12.

49. S. L. Raghavan, Effect of cellulose polymers on supersaturation and in vitro membrane transport of hydrocortisone acetate, Int J Pharm. 193 (2000) 231-237.

50. T. Honbo, M. Kobayahi, K. Hane, T. Hata, and Y. Ueda, The Oral Dosage form of FK-506, Transplant Proc. 19 (1987) 17-22.

51. A. Lamprecht, H. Yamamoto, H. Takeuchi, and Y. Kawashima, Design of pH-Sensitive Microspheres for the Colonic Delivery of Immunosuppressive Drug Tacrolimus, Eur J Pharm Biopharm. 58 (2004) 37-43.

52. Y. Meissner, Y. Pellequer, and A. Lamprecht, Nanoparticles in Inflammatory Bowel Disease: Particle Targeting vs. pH Sensitive Delivery, Int J Pharm. 316 (2006) 138-143.

53. A. Lamprecht, H. Yamamoto, N. Ubrich, H. Takeuchi, P. Maincent, and Y. Kawashima, FK-506 Microparticles Mitigate Experimental Colitis with Minor Renal Calcineurin Suppression, Pharm Res. 22 (2005) 193-199.

54. S. N. Sehgal, J. S. Camardo, J. A. Scarola, and B. T. Maida, Rapamycin (Sirolimus, Rapamune), Dialys Transplant. (1995) 482-487.

55. E. Grube and L. Buellesfeld, Rapamycin Analogs for Stent Based Local Drug Delivery, Herz. 29 (2004) 162-166.

56. L. A. Sorbera, P. A. Leeson, and J. Castaner, SDZ-RAD, Drugs Fut. 24 (1999) 22.

57. P. Simamora, J. M. Alvarez, and S. H. Yalkowsky, Solubilization of Rapamycin, Int J Pharm. 213 (2001) 25-29.

58. S. N. Sehgal, K. Molnar-Kimber, T. D. Ocain, and B. M. Weichman, Rapamycin: A Novel Immunosuppressive Macrolide, Medicinal Res Review. 14 (1994) 1-22.

59. Rapamune Tablets and Oral Liquid: professional literature. 2004, Wyeth Pharmaceuticals: Philadelphia, PA.

60. D. S. Wishart, Drug Bank: A Comprehensive Resource for In Silico Drug Discovery and Exploration, *Nucleic Acids Res*. 2006.

61. Trexall Tablets: professional literature. 2005, Duramed Pharmaceuticals: Pomona, NY.

62. L. Liang, J. Jackson, W. Min, V. Risovic, K. Wasan, and H. Burt, Methotrexate Loaded Poly (L-Lactic) Acid Microspheres for Intra-Articular Delivery of Methotrexate to the Joint, J Pharm Sci. 93 (2004) 943-955.

63. A. Wunder, U. Muller-Ladner, E. Stelzer, J. Funk, E. Neumann, G. Stehle, T. Pap, H. Sinn, S. Gay, and C. Fiehn, Albumin-Based Drug Delivery as Novel Therapeutic Approach for Rheumatoid Arthritis, J Immunol. 170 (2003) 4793-4801.

64. M. Kalariya, B. Padhi, M. Chougule, and A. Misra, Methotrexate Loaded Solid Lipid Nanoparticles for Topical Treatment of Psoriasis: Formulation and Clinical Implications, Drug Del Tech. 4 (2004) 65-71.

65. Imuran Tablets: professional literature. 2005, Glaxo-Smithkline Pharmaceuticals: Mississagua, Ontario.

66. Report on Carcinogens, 11th Edition, U.D.o.H.a.H. Services, Editor. 2004, Public Health Service, National Toxicology Program.

67. B. J. Zins, W. J. Sandborn, J. A. McKinney, D. C. Mays, E. C. Van Os, W. J. Tremaine, D. W. Mahoney, A. R. Zinsmeister, and J. J. Lipsky, A Dose Ranging Study of Azathioprine Pharmacokinetics After Single-Dose Administration of a Delayed-Release Oral Formulation, J Clin Pharmacol. 37 (1997) 38-46.

68. E. C. Van Os, B. J. Zins, W. J. Sandborn, D. C. Mays, W. J. Tremaine, D. W. Mahoney, A. R. Zinsmeister, and J. J. Lipsky, Azathioprine Pharmacokinetics After Intravenous, Oral, Delayed Release Oral, and Rectal Foam Administration, Gut. 39 (1996) 63-68.

Chapter 2: Rapidly Dissolving Repaglinide Powders Produced by the Ultra-Rapid Freezing Process

2.1 ABSTRACT

The objective of the study was to produce rapidly-dissolving formulations of the poorly water soluble drug, repaglinide, using an innovative new technology, Ultra-Rapid Freezing (URF), and to investigate the influence of excipient type on repaglinide stability. Repaglinide (REP) compositions containing different types and levels of excipients and different drug potencies (50 to 86%) were produced by the URF technology. Repaglinide/excipient solutions were frozen on a cryogenic substrate, collected, and lyophilized to form a dry powder. Surfactants, including sodium dodecyl sulfate (SDS), and alkalizing agents such as diethanolamine (DEA) and tromethamine (TRIS) were incorporated into the compositions. Forced degradation of repaglinide was conducted under stressed conditions (e.g. elevated temperature, exposure to peroxide) to determine stability of the drug in such environments. The solubility of repaglinide increased as a function of increasing pH, therefore incorporation of an alkalizing agent into the URF formulations increased the drug's solubility. Instability of the drug resulted when the drug was exposed to pH values above 9.0. URF formulations containing alkalizing agents showed no degradation or spontaneous recrystallization in the formulation, indicating increased stability afforded by processing. URF processing created nanostructured drug/excipient particles with high dissolution rates as compared to unprocessed drug.

Alkalizing agents such as TRIS and DEA, present at levels of 25-33% w/w in the formulations did not cause degradation of the drug when processed using URF. URF processing, therefore, yielded fast-dissolving formulations that were physically and chemically stable, resistant to alkali degradation or spontaneous recrystallization in the formulation.

2.2 INTRODUCTION

The biopharmaceutical classification system (BCS) is used to group pharmaceutical actives depending upon the solubility and lipophilicity (permeability) characteristics of the drug. BCS Class II compounds are poorly soluble but highly permeable, and they exhibit bioavailability that is limited by dissolution rate[1]. The dissolution rate of BCS Class II drug substances may be accelerated by improvement of the wetting characteristics of the bulk powder[2]. Reduction of primary particle size is also critical for increasing the dissolution rate of poorly water soluble drugs.

Cryogenic processing techniques have been developed to enhance the dissolution rate by creating nanostructured amorphous particles with high degrees of porosity [3-9]. Cryogenic processes allow for reduction of primary particle size of drug particles without the intense frictional or mechanical forces involved in ball-milling or other processes relying on frictional comminution or trituration with a mortar and pestle, which can cause degradation of the drug through thermal stress [10]. Previous studies have shown that the cryogenic spray-freezing into liquid (SFL) process produces amorphous solid solutions of drug and excipients [3]. The formation of metastable amorphous solid solutions yields

higher energy states for the drug, and thus a greater thermodynamic driving force for dissolution.

Vaughn et al. and Hu et al. have studied the cryogenic SFL technique extensively [3, 8]. Based on these studies, SFL particles have been shown to have a large specific surface area, producing powders with rapid dissolution. Additionally, the SFL process produces powders consistent with a solid solution [8]. SFL powders were formulated with small amounts of surfactant to achieve high drug loadings (50-86% drug/total solids) while maintaining high dissolution rates. SFL powders require smaller amounts of surfactant to achieve high dissolution rates [3]. These high drug loaded SFL powders contain amorphous nanostructured aggregates with high surface area and excellent wettability.

Another cryogenic process, the spray freeze drying (SFD) method, typically involves the atomization of a drug containing solution in the gaseous nitrogen above a pool of liquid nitrogen. The fine droplets of drug/solvent are frozen, then lyophilized to remove the solvent. Rapid freezing rates in the cryogenic liquid substrate do not allow for molecular arrangement into crystalline domains, so SFD processing produces amorphous drug nanoparticle aggregates with improved dissolution rates [11]. The scalability of this type of technology, however, has limited its widespread industrial use [12].

The URF technology involves the use of a solid cryogenic substrate with a thermal conductivity between 10-20 W/m degrees K. A solution of the drug is applied to the solid surface of the substrate, where instantaneous freezing takes place. Brownian motion of the particles in solution is slowed significantly, so reactive species have little

time to react before being frozen into the solid state. Removal of the frozen particles and lyophilization of the solvent produces stable amorphous drug particles. The URF technology has been shown to produce uniform, amorphous, drug particle/excipient aggregates [13]. Additionally, the process is continuous, allowing for improved scale up applications. A reservoir of boiling cryogenic liquid is not required, allowing for lower operating costs and more convenient operation.

Numerous citations report solvent/drug/excipient compositions being frozen in liquid or gaseous nitrogen or other cryogenic fluids. All of these approaches face the same challenge in transferring the heat necessary to cool and freeze the solution forming the drug particle domains. The heat transfer is forced to pass through a gas film at the surface of the particle. This imparts a rate limiting step in the heat transfer and will define the maximum freeze rate[14].

The URF technology overcomes the limitation of transferring heat through a gas film by eliminating the gas interface element and utilizing direct contact with the cryogenic substrate. Drug solutions that come into direct contact with a boiling liquid cryogenic substrate transfer heat through a gas bubble film until the temperature of the particle comes into thermal equilibrium with the liquid at its boiling point [15]. Note that conduction is improved by using a cryogenic material with a high thermal conductivity, density, and mass relative to the solution being frozen so as to maintain the surface temperature and heat transfer rate while the solution is being frozen. With the URF technology, the thickness of the freezing solution may be controlled to fix its minimum freezing rate since the freezing rate drives the particle formation and determines its characteristics.

Repaglinide, a BCS Class II compound for treatment of Type II diabetes [16-18], was chosen as a model drug to study dissolution enhancement of drug formulations formed using the novel URF technology. Preformulation studies indicate that a pH-dependent dissolution profile for repaglinide exists, the drug having a greater aqueous solubility at higher pH. Since this drug is needed to regulate post-prandial glucose levels, the drug should ideally dissolve rapidly in the stomach (where the pH of the contents can be low). Additionally, the drug undergoes hydrolysis at high pH, owing to the drug's instability in basic solutions. URF technology has the ability to produce stable amorphous drug formulations with high dissolution rates, so repaglinide would be good candidate for the application of URF. The objective of this study is, using URF processing, to prepare repaglinide as a stable formulation with stable amorphous character. Additionally, the incorporation of alkalizing agents as well as non-polymeric surfactants will allow for the production of a rapidly dissolving, yet chemically stable repaglinide powder formulation.

2.3 MATERIALS AND METHODS

2.3.1 Materials

Micronized repaglinide was purchased from Kingchem (Lot # 040701; Allendale, NJ, USA). Repaglinide USP reference standard (Rockville, MD, USA), 200 mg, (Lot # FOB265, Cat # 1600813) was gifted from the Dow Chemical Company. Sodium dodecyl sulfate (SDS) was supplied by Pierce Chemicals (Rockford, IL, USA). Tromethamine

buffer (TRIS), t-butanol, sodium phosphate monobasic, potassium phosphate dibasic, citric acid monohydrate, and diethanolamine (DEA) were purchased from Spectrum Chemicals (Gardena, CA, USA). Hypromellose (Methocel E5, HPMC) was purchased from The Dow Chemical Company (Midland, MI, USA). High performance liquid chromatography (HPLC) grade acetonitrile and methanol were obtained from EM Science (Gibbstown, NJ, USA). 1,3 dioxolane was supplied by Acros Organics (Geel, Belgium).

2.3.1.1 Preformulation Studies: pH-Solubility Study

The solubility of repaglinide in various buffered media at various time points and 37^{o}C was investigated in this study, based on methods described elsewhere by Higuchi and Connors [19]. Buffer species were prepared, ranging in pH values from 1 to 9. For acidic media, 0.1N HCl (pH 1.1) was used, as well as 0.1M sodium phosphate (pH 3), and the USP dissolution medium containing citric acid and sodium phosphate (pH 4.5). For neutral pH values, a 0.1M sodium phosphate buffer (pH 7) was used, while for basic conditions, a 0.1M Tris buffer was used (pH 9). In addition to the 5 types of buffer solutions prepared above, solutions of each buffer containing 0.1% and 0.2% SDS were prepared. The procedure for determining the pH-solubility of the repaglinide was as follows: 10 mg of repaglinide was weighed into each of 36 vials. A 10 mL aliquot of each type of buffer (containing 0%, 0.1%, or 0.2% SDS) was added to each of the drug-containing vials and allowed to equilibrate at 37^{o}C with shaking (Environ Orbital Shaker, Lab-Line Instruments, Melrose Park, IL, USA) for 12, 24, and 48 hours. A 1 mL aliquot was taken from each sample and filtered through a 0.2 μm Whatman PTFE syringe filter

(Florham Park, NJ, USA) at 12, 24, and 48 hours. Each sample was analyzed using HPLC for the repaglinide concentration using the method as reported by Gandhimathi and Reddy [20]. Equilibrium solubility of repaglinide was determined in each type of buffer.

2.3.1.2 Repaglinide Degradation Study

The accelerated degradation of repaglinide was studied upon exposure to a series of harsh environments. Samples of bulk repaglinide were subjected to acidic, basic, thermal, and oxidative stress conditions, as recommended by the International Conference on Harmonisation (ICH) [21]. Acid degradation was accomplished by weighing out about 1 mg on a microbalance scale to the 1/1000 mg (Mettler Toledo M3/36, Hightstown, NJ, USA, calibrated by Aldingen Company, validated through 9/2007) repaglinide into a 100 mL volumetric flask, dissolving it in 5 mL methanol, then exposing it to 10 mL of 1N HCl for 1 hour at 25^{o}C. The reaction was then quenched with 10 mL of 1N NaOH and diluted to volume with water. Base degradation involved weighing out about 1 mg repaglinide, on the same microbalance mentioned above, into a 100 mL volumetric flask, dissolving it in 5 mL methanol, then exposing the drug solution to 10 mL 1N NaOH for 15 minutes at 25^{o}C. The reaction was quenched with 10 mL of 1N HCl then diluted to volume with water. Additionally, forced base degradation was carried out using 0.1M TRIS base, similar to the NaOH degradation above. About 1 mg of repaglinide, weighed on the same microbalance mentioned above, was added to a 100 mL volumetric flask and dissolved in 5 mL methanol. The drug solution was exposed to 10 mL of the basic 0.1M TRIS (pH 9.0) solution for 1 hour at 25^{o}C. The reaction was

quenched with 0.1N HCl after completion of the reaction. Oxidative degradation occurred by weighing out 1 mg of repaglinide, on the same microbalance mentioned above, dissolving it in 5 mL methanol, then adding 1 mL 30% hydrogen peroxide (H_2O_2) to the solution (total hydrogen peroxide concentration prior to dilution was 5% peroxide), allowing it to be exposed for 1 hour at 25^{o}C. Finally this solution was diluted to 100 mL volume with water (to a final H_2O_2 of 0.3% H_2O_2). Thermal degradation was completed with repaglinide in methanolic solution (1 mg % w/v) at 60^{o}C for 6 hours. A 1 mL aliquot was taken from each sample and filtered through a 0.2 μm Whatman PTFE syringe filter (Florham Park, NJ, USA) and injected into the chromatograph. Chromatographic purity of the resulting stressed solutions was analyzed by HPLC (chromatographic procedure detailed below in "Dissolution Performed Under Sink Conditions" section) to determine the extent of degradation and to identify primary degradation products or impurities left over after drug synthesis [20]. The results of the forced REP degradation study are shown in Table 2.1Table 2.2, with the standard REP USP Standard chromatographic purity results given for comparison.

2.3.2 Preparation of URF Formulations

Repaglinide formulations were processed using the novel URF technology. Repaglinide, which is poorly water soluble, was dissolved in 1,3 dioxolane (12.5% w/v), an organic solvent which is water-miscible. Water soluble excipients in the formulations (SLS, TRIS) were dissolved in either water or a water/t-butanol (30:70 v/w) cosolvent system to produce a 0.01-0.02% w/v solids loading in the aqueous phase. T-butanol, with

a melting point of 24-27°C, was employed to raise the freezing point of the final drug solution. The 1,3 dioxolane and water/*t*-butanol solutions were mixed to produce a final solids content of about 1% w/v, and the resulting organic/aqueous co-solvent system was frozen on the cryogenic substrate maintained at -45°C. The frozen droplets were then removed from the substrate and lyophilized using a Virtis Advantage Tray Lyophilizer (Virtis Company, Gardiner, NY), removing all of the frozen solvent to produce a powder. The formulations were packaged in hermetically sealed glass containers under dry nitrogen. Table 2.1 shows the compositions investigated in this study including the drug-to-excipient ratios.

2.3.3 Preparation of Co-Ground Physical Mixtures

Co-ground physical mixtures containing repaglinide (control) with varying proportions of excipients, corresponding to the two of the URF compositions listed in Table 2.1, were mixed by geometric dilution in a mortar and pestle.

2.3.4 X-ray Powder Diffraction

A Philips 1710 X-ray diffractometer with a copper target and nickel filter (Philips Electronic Inst.; Mahwah, NJ) was used to obtain XRD results for the samples. Powders were mounted on aluminum stages with glass bottoms and smoothed to a level surface. The XRD pattern of each sample was measured from 10 to 50 degrees 2θ using a step increment of 0.1 2-theta degrees and a dwell time of 1 sec at each step.

2.3.5 Conventional Differential Scanning Calorimetry (DSC)

Samples weighing 8 to 15 mg were added to an aluminum pan which was then crimped and sealed, and these samples were evaluated on a TA Instruments model 2820 DSC (New Castle, DE). Samples were heated at a rate of 10^{o}C/min from 25^{o}C to 250^{o}C using a conventional DSC ramping method. Samples were purged with nitrogen gas at 150 mL/min. Melting points and phase transitions were measured at the peak minimum of each DSC thermogram. The DSC was calibrated with an indium standard. DSC was used to determine the melting point and purity of REP bulk and standards (data not shown).

2.3.6 Scanning Electron Microscopy (SEM)

A Hitachi S-4500 field emission scanning electron microscope (Hitachi, Ltd., Tarrytown, NY) was used to obtain SEM micrographs of the powder samples. Samples were gold-palladium sputter coated for 30 seconds prior to viewing under an acceleration voltage of 5kV.

2.3.7 Dissolution Performed Under Sink Conditions

Dissolution testing of the samples was performed according to the USP 27 Apparatus II (Vankel Model VK6010 Dissolution Tester with a Vanderkamp Model VK650A heater/circulator, Varian, Inc. Palo Alto, CA). Dissolution parameters were set up according to the United States Pharmacopoeia (USP) monograph for repaglinide tablets, using 50 mM citric acid/ 100mM sodium phosphate dibasic buffer with a pH of 4.5. Powder samples corresponding to a repaglinide content of 2-5 mg were introduced into 900 mL of dissolution medium. A sample volume of 5 mL was collected at 3, 7, 11, 15, 20, 25, and 30 minutes (n=6) using a VK8000 autosampler (Varian, Inc. Cary, NC). There was no medium replacement. Paddle speed and bath temperature were maintained at 50 rpm and 37^{o}C, respectively. The collected aliquots were filtered then analyzed using HPLC at a wavelength of 240 nm using a Shimadzu LC-10 liquid chromatograph (Shimadzu Corp., Columbia, MD) equipped with a Waters Symmetry C18 5µm 4.6 x 150mm reverse-phase column (Waters Corp., Milford, MA). The 10mM phosphate mobile phase buffer consisted of 10 mM potassium phosphate monobasic dissolved in deionized water with the pH adjusted to 3.5 with o-phosphoric acid. The mobile phase was composed of the 10mM phosphate buffer and acetonitrile in a 50/50 proportion. The repaglinide peak eluted with an average retention time of 6 minutes at a flow rate of 1 mL/min [22]. Sink conditions were maintained throughout the dissolution studies at <10% of solubility as determined in the pH-solubility study.

2.3.8 Dissolution Performed Under Supersaturation Conditions

Supersaturated dissolution was performed, using a small volume dissolution apparatus equipped with a paddle stirring mechanism (Vankel VK6010 Dissolution Tester, Varian Inc., Palo Alto, CA) [23]. Amounts of drug compositions were weighed out corresponding to about 25-times the aqueous solubility of repaglinide (about 53 mg repaglinide in each sample). The dissolution media was the same as described above (e.g. 50 mM citric acid/100 mM sodium phosphate dibasic pH 4.5), using 100 mL of medium for this procedure. Paddle speed and bath temperature were maintained at 50 RPM and 37^{o}C respectively. A 1 mL aliquot of sample was taken manually at 2, 5, 10, 20, 30, 60, 120, and 1440 minutes, with no medium replacement. This aliquot was filtered through a 0.2 μm Whatman nylon filter (Florham Park, NJ), and a 0.5 mL aliquot of this solution was immediately diluted in 1 mL of acetonitrile and analyzed for repaglinide concentration using the HPLC procedure described above.

2.4 RESULTS AND DISCUSSION

2.4.1 pH-Solubility Study

Figure 2.1 shows the chemical structure of repaglinide along with some possible hydrolysis products predicted by Reddy et al [20]. Figure 2.2 shows the results of the pH solubility study in terms of solubility versus pH in the presence of SDS. Results from the pH solubility study showed much higher solubility of the drug at pH values greater than 7. Repaglinide exhibits two pKa values of 4.19 and 5.78 [24], and being a weakly acidic compound, the drug is ionized at higher pH values, owing to its higher aqueous solubility

at higher pH values. During the pH solubility study, it was observed that an insoluble mass was formed in the vials containing 0.1N HCl and 0.1M sodium phosphate pH 3 with 0.1% and 0.2% SDS. This instability resulted from the SDS hydrolyzing to lauryl alcohol and sodium bisulfite in the acidic solution [25]. The unionized repaglinide could bind to or dissolve into the oily and immiscible phase that was present in the acidic aqueous solutions (lauryl alcohol), causing the formation of the water insoluble mass in the vial. This phenomenon was only observed in the acidic solutions containing SDS and repaglinide. This insoluble mass was isolated and dissolved in HPLC mobile phase and analyzed using the HPLC method described above for repaglinide and impurity content, and these results are presented in Table 2.2.

All of the samples from the pH solubility study were analyzed by HPLC. Repaglinide was observed to be relatively stable under acidic conditions (1N HCl, 37^{o}C, 1 hour). Samples exposed to higher pH (0.1M TRIS buffer, pH 9), impurity peaks were observed after 1 hour. Table 2.3 shows degradation of repaglinide in TRIS buffer after 1 hour. From this data, it can be concluded that repaglinide, although more soluble at a higher pH, is also more unstable at higher pH values.

2.4.2 Forced Degradation Study

Results of the forced degradation study showed chemical instability under all stressed conditions, most notably under the base degradation condition (pH 12, 1N NaOH). Alkaline instability was expected due to the degradation of the drug that was observed in the pH solubility study. After 15 minutes of reaction time in 1N NaOH,

repaglinide degraded more than 13%. It is hypothesized that some of the degradation observed in basic conditions results from the base catalyzed hydrolysis of the amide bond in the drug molecule [20]. Oxidative conditions created by adding hydrogen peroxide to the drug solution, and thermal stresses caused by heating the solution also yielded degradation peaks in the chromatograms. Repaglinide appears to be most resistant to degradation when exposed to acidic conditions. Few degradation peaks were observed in the HPLC chromatograms, using 1N HCl at 25^{o}C for 1 hour. Table 2.2 shows the results of the forced degradation study, including amount of REP remaining after forced degradation and retention times for degradants/impurities observed under accelerated conditions.

2.4.3 Solid State Characterization of Bulk Drug Substance

The melting point of repaglinide was 129.97^{o}C, as measured by DSC (data not shown), was similar to the reported melting point of 130-131^{o}C [24]. HPLC analysis of the bulk drug substance confirmed the potency at >99%, with few degradation peaks seen in the chromatograms (Table 2.3), when compared to the USP repaglinide reference standard. Degradation peaks accounted for less than 0.1% of the total repaglinide peak area individually and less than 0.5% of the total repaglinide peak area in total, conforming to USP specifications. Scanning electron micrographs (SEM's) showed that repaglinide existed in long needle-shaped crystal habit, with a wide particle size distribution, the average particle size being 20-23 μm in size (Figure 2.3). X-ray

diffraction of the bulk powder yielded characteristic crystalline peaks at 12.5, 15, 25.25, 27.85, and 35.85 2-theta.

2.4.4 Results of Dissolution Under Sink Conditions

Dissolution rates of URF formulations, bulk drug substance, and Prandin tablets were evaluated at sink conditions according to the USP monograph for repaglinide tablets. SEM's of URF formulations revealed a porous network of nanostructured aggregates with significantly reduced particle sizes over the bulk drug (Figure 2.3). The physical particle morphology, therefore, is responsible for the increased dissolution rate of the URF powders over the bulk REP drug substance. Results of the sink dissolution testing are shown in Figure 2.4. Upon addition of bulk repaglinide to the dissolution media, the powder did not wet, but remained floating at the air-liquid interface. Incorporation of a wetting agent, SDS [26-28] into the URF formulation (URF-A) resulted in rapid wetting of the powder upon addition to the dissolution media, with the formulation rapidly sinking into the media and wetting upon initiation of the dissolution test. The level of SDS studied during dissolution was about 2.5 mg SDS in 900 mL of dissolution medium, which is below the critical micelle concentration of SDS. Based on results from the solubility study, a higher pH media would result in a greater driving force for dissolution due to an increase in the equilibrium solubility. In the case of pH 9, for example, the solubility would be increased by a factor of about 25-times the equilibrium solubility at pH 4.5. DEA and TRIS were employed as alkalizing agents in formulations URF-B and URF-E, respectively. By adding these alkalizing agents to the URF

formulations, the dissolving drug particles should experience an increase in the surrounding microenvironmental pH, allowing for faster dissolution to occur. Results shown in Figure 2.4 confirm a significant increase in dissolution rate compared to URF-A with SDS alone (no alkalizing agent).

Within the first 5 minutes, 90% and 88% of the repaglinide in URF-B and URF-E, respectively, was dissolved in the dissolution media, compared with about 60% and 55% for URF-A and Prandin tablets, respectively, further indicating the advantage of an increase in local environmental pH. The bulk drug showed only about 30% drug release after 5 minutes, due to the poor wettability of the powder. Complete (100%) dissolution of URF-B and URF-E was observed in 30 minutes, while Prandin tablets and URF-A showed only 90% and 85% release after 30 minutes, respectively. All formulations tested, including Prandin® tablets, showed an increase in dissolution over bulk repaglinide, which showed only about 63% release after 30 minutes.

2.4.5 Results of Dissolution Under Supersaturated Conditions

The goal of the dissolution study at supersaturated conditions was to determine the meta-stable solubility of amorphous URF repaglinide in 4.5 dissolution buffer, and how long repaglinide remained at supersaturated concentration before recrystallization of the drug occurred [29].

Figure 2.5 shows the results of the dissolution conducted under supersaturated conditions of formulation URF-E, containing the alkalizing agent, TRIS. URF formulations showed increased solubility of the amorphous drug in the dissolution

medium followed by slow reprecipitation over 24 hours. Equilibrium solubility of crystalline repaglinide in the dissolution medium (accounting for 0.01% SDS added to the medium from the formulation itself) was determined to be 150 μg/mL. URF-E quickly produced a supersaturated solution, achieving a maximum concentration of approximately 2.5-times the equilibrium solubility. Dissolution media remained supersaturated over a 24 hour period where the concentration fell only to approximately 1.5-times equilibrium solubility. Since supersaturation is the main driving force for nucleation and growth, the elevated concentration produced during the first 60 minutes of dissolution lead to reprecipitation of particles from solution. From these results, the amorphous form of repaglinide with an alkalizing agent and SDS as a surfactant present in the formulation was important in achieving and maintaining supersaturated levels of repaglinide in the dissolution media.

Figure 2.6 shows the results of the supersaturated dissolution study of formulation URF-A, containing drug and surfactant (Rep:SDS, 1:1 ratio). Compared to the similar physical mixture, URF-A exhibited a much faster dissolution rate. Crystalline drug in the physical mixture approached the measured equilibrium solubility of the drug in dissolution medium (accounting for 0.03% SDS added to the medium from the formulation itself). The amorphous URF-A formulation, however, reached a maximum concentration of approximately 600 μg/mL within 20 minutes, corresponding to a supersaturation level of 2.4-times equilibrium solubility. Upon reaching the maximum supersaturation, the drug quickly reprecipitated out of solution which reduced the supersaturation to approximately 1.5-times equilibrium solubility in less than 2 hours. Similar to formulation URF-E, the SDS present in the drug powder was able to reduce the

interfacial tension between the dissolution media and the drug formulation which allowed the amorphous drug to dissolve quickly and the solution to remain supersaturated 1.4-times the equilibrium solubility even after 24 hours.

The ability of these formulations to supersaturate the dissolution media highlights the possibility for increased bioavailability from an amorphous drug form. The meta-stable solubility of an amorphous drug form may be as high as 100-times greater than its crystalline form [30]. If the concentration of drug in solution is significantly increased, the higher chemical potential will lead to increased flux across an exposed membrane [31], leading to blood levels much higher for an amorphous drug form, compared to an identical crystalline formulation. URF formulations presented in this work were highly amorphous and supersaturated buffered media up to 24 hours, showing physicochemical stability. These properties should lead to high concentration levels during gastrointestinal tract transit and thus significant improvement in bioavailability.

2.4.6 X-ray Diffraction

URF formulations were evaluated for their physicochemical stability. Samples of each formulation were tested after preparation, using X-ray diffraction (Figure 2.7). Formation of an amorphous solid solution has inherent instability when using certain wetting agents to enhance dissolution. Use of poloxamer polymers for their wetting ability has produced formulations with fast dissolution rates [32], however these formulations have a tendency to spontaneously recrystallize in the presence of humidity. Formulations presented in this study do not contain polymers, but do show amorphous

character. XRD patterns of URF formulations show no characteristic crystallinity peaks observed in the bulk drug substance. The amorphous character of the dispersed repaglinide in the formulations is retained and spontaneous recrystallization of the drug in the solid state is inhibited by using the URF process.

2.4.7 Chromatographic Purity and Potency

URF formulations were also evaluated for chromatographic purity. Repaglinide shows instability at pH values greater than 9, therefore base-catalyzed degradation was evaluated after URF formulations were produced. Impurities in each formulation were calculated by comparing the peak areas of each impurity peak against the peak area of the repaglinide peak in the HPLC chromatograms. Results from chromatographic purity tests for selected formulations are shown in Table 2.3. Comparing the impurities in each formulation with the repaglinide standard showed comparable percent impurities, probably residuals from drug synthesis. Therefore, further degradation of the repaglinide was not observed in the URF formulations, even though they contained an alkalizing agent. Rapid freezing rates allowed for the formation of solid solutions of the drug, reducing Brownian motion of the drug/excipient particles, making the formulations resistant to degradation experienced by the drug in liquid solutions [6].

2.5 CONCLUSIONS

Preformulation results showed instability of repaglinide to alkali conditions, but URF formulations containing alkalizing agents, however, showed no increased amounts of degradation products. Additionally, these formulations show a faster rate of dissolution and higher supersaturated dissolution concentration than does the equivalent physical mixture, due to their amorphous character indicated by XRD results. The rapid freezing of the drug/co-solvent mixture produces a stable formulation, in addition to being a scalable and continuous process. Based on the results, repaglinide has been processed using the URF technology into stable formulations with high dissolution rates that should show greater bioavailability than the crystalline bulk drug.

2.6 ACKNOWLEDGMENTS

The authors wish to gratefully acknowledge The Dow Chemical Company for its financial support (grant number UTA04-076).

2.7 REFERENCES

1. G. L. Amidon, A theoretical basis for a biopharmaceutic drug classification: the correlation of in vitro drug product dissolution and in vivo bioavailability, Pharm Res. 13 (1995) 413-420.

2. J. B. Dressman and C. Reppas, In vitro-in vivo correlations for lipophilic, poorly water soluble drugs, Eur J Pharm Sci. 11 (2000) S73-S80.

3. J. H. Hu, K. P. Johnston, and R. O. Williams III, Spray-freezing into liquid (SFL) particle engineering technology to enhance dissolution of poorly water soluble drugs: organic solvent versus organic/aqueous co-solvent systems, Eur J Pharm Sci. 20 (2003) 295-303.

4. J. H. Hu, K. P. Johnston, and R. O. Williams III, Rapid dissolving high potency danazol powders produced by spray freezing into liquid process, Int J Pharm. 271 (2004) 145-154.

5. Z. S. Yu, T. L. Rogers, J. H. Hu, K. P. Johnston, and R. O. Williams III, Preparation and characterization of microparticles containing peptide produced by a novel process: spray-freezing into liquid, Eur J Pharm Biopharm. 54 (2002) 221-228.

6. T. L. Rogers, A. C. Nelson, J. H. Hu, J. N. Brown, M. Sakari, T. J. Young, K. P. Johnston, and R. O. Williams III, A novel particle engineering technology to enhance dissolution of poorly water soluble drugs: spray-freezing into liquid, Eur J Pharm Biopharm. 54 (2002) 271-280.

7. T. L. Rogers, K. P. Johnston, and R. O. Williams III, Solution Based Particle Formation of Pharmaceutical Powders by Supercritical or Compressed Fluid Carbon Dioxide and Cryogenic Spray-Freezing Technologies, Drug Dev Ind Pharm. 27 (2001) 1003-1015.

8. J. M. Vaughn, X. Gao, J. M. Yacaman, K. P. Johnston, and R. O. Williams III, Comparison of powder produced by evaporative precipitation into aqueous solution (EPAS) and spray freezing into liquid (SFL) technologies using Z-contrast STEM and complimentary techniques, Eur J Pharm Biopharm. 60 (2005) 81-89.

9. F. M. Etzler and M. S. Sanderson, Particle Size Analysis: A Comparative Study of Various Methods, Part Part Syst Charact. 12 (1995) 217-224.

10. J. O. Waltersson and P. Lundgren, The effect of mechanical comminution on drug stability, Acta Pharm Suec. 22 (1985) 291-300.

11. H. Leuenberger, Spray Freeze Drying: The process of choice for low water soluble drugs?, J Nanoparticle Res. 4 (2002) 111-119.

12. H. R. Costantino, L. Firouzabadian, and K. Hogeland, Protein spray freeze drying. Effect of atomization conditions on particle size and stability, Pharm Res. 17 (2000) 1374-1383.

13. J. C. Evans, B. D. Scherzer, C. D. Tocco, G. B. Kupperblatt, J. N. Becker, D. L. Wilson, S. A. Saghir, and E. J. Elder, *Preparation of nanostructured particles of poorly water soluble drugs via a novel ultra-rapid freezing technology*, in *Polymeric Drug Delivery - Polymeric Matrices and Drug Particle Engineering*, S. Svenson, Editor. 2006, American Chemical Society: Washington, DC. p. 320-328.

14. R. S. Hall, S. J. Board, A. J. Clare, R. B. Duffey, T. S. Playle, and D. H. Poole, Inverse Leidenfrost Phenomenon, Nature. 224 (1969) 266-267.

15. B. S. Gottfried, C. J. Lee, and K. J. Bell, The Leidenfrost Phenomenon: Film Boiling of Liquid Droplets, Int J Heat and Mass Transfer. 9 (1966) 1167-1187.

16. W. Malaisse, Repaglinide, a new oral antidiabetic agent: a review of recent preclinical studies, Eur J Clin Invest. 29 (1999) 21-29.

17. R. Landgraf, M. Frank, C. Bauer, and M. Dieken, Prandial glucose regulation with repaglinide: its clinical and lifestyle impact in a large cohort of patients with Type II diabetes, Int J Obesity. 24 (2000) S38-S44.

18. F. Wang, Focus on repaglinide: an oral hypoglycemic agent with a more rapid onset and shorter duration of action than the sulfonylureas, Formulary. 33 (1998) 1028-1081.

19. T. Higuchi and K. Connors, Phase solubility diagram, Adv Anal Chem Instru. 4 (1965) 117-122.

20. K. Reddy, J. Babu, and V. Mathad, Impurity profile study of repaglinide, J Pharm Biomed Anal. 32 (2003) 461-467.

21. *International Conference on Harmonization of Technical Requirements for Registration of Pharmaceuticals for Human Use*. Stability Testing: Drug substance stress testing. 2003, Rockville, MD: US Food and Drug Administration

22. M. Gandhimathi, T. Ravi, and S. Renu, Determination of repaglinide in pharmaceutical formulations by HPLC and UV detection, Anal Sci. 19 (2003) 1675-1677.

23. K. Yamashita, T. Nakate, K. Okimoto, A. Ohike, Y. Tokunaga, R. Ibuki, K. Higaki, and T. Kimura, Establishment of New Preparation Method for Solid Dispersion Formulation of Tacrolimus, Int J Pharm. 267 (2003) 79-91.

24. W. Grell, R. Hurnaus, and G. Griss, Repaglinide and related hypoglycemic benzoic acid derivatives, J Med Chem. 41 (1998) 5219-5246.

25. M. Nakagaki and S. Yokoyama, Acid catalyzed hydrolysis of sodium dodecyl sulfate, J Pharm Sci. 74 (1985) 1047-1052.

26. K. C. Patel, G. S. Banker, and H. G. DeKay, Anionic and cationic wetting agents in a hydrophilic ointment-base. I. Choice of wetting agents, J Pharm Sci. 50 (1961) 294-300.

27. J. M. Newton, G. Rowley, and J. F. V. Tornblom, Effect of additives on the release of drug from hard gelatin capsules, J Pharm Pharmacol. 23 (1971) 452-453.

28. J. M. Newton and F. N. Razzo, Interaction of formulation factors and dissolution fluid and the in vitro release of drug from hard gelatin capsules, J Pharm Pharmacol. 27 (1975) 78P.

29. G. Valsami, A. Dokoumetzidis, and P. Macheras, Modeling of supersaturated dissolution data, Int J Pharm. 181 (1999) 153-157.

30. B. C. Hancock and M. Parks, What is the True Solubility Advantage for Amorphous Pharmaceuticals?, Pharm Res. 17 (2000) 397-404.

31. S. L. Raghavan, Effect of cellulose polymers on supersaturation and in vitro membrane transport of hydrocortisone acetate, Int J Pharm. 193 (2000) 231-237.

32. G. Couarraze, B. Leclerc, G. Conrath, F. Falson-Rieg, and F. Puisieux, Diffusion of a dispersed solute in a polymeric matrix, Int J Pharm. 56 (1989) 197-206.

Chapter 3: Sirolimus Rapidly Dissolving Powders Prepared by the Ultra-Rapid Freezing Process

3.1 ABSTRACT

Stable wettable particles containing the poorly water soluble drug, sirolimus (SRL), produced by the Ultra-Rapid Freezing (URF) process, dissolved rapidly to produce highly supersaturated solutions. Additionally, International Committee of Harmonization (ICH) guidelines were followed to determine the stability of the drug against degradation by acid, base, peroxide, and heat. The by-products of degradation of SRL were determined by HPLC to observe if interference in the retention times of the SRL isomers would occur due to the degradation products of the drug.

The particles were formed by the ultra rapid freezing (URF) process for various levels of SRL and types of stabilizers including poloxamer 407 (P407), hydroxypropylmethylcellulose E5 (HPMC), and sodium lauryl sulfate (SDS). SRL/stabilizer solution was applied to a rotating drum filled with a cryogenic liquid, instantly frozen, collected, and lyophilized to form a dry powder. Powders were characterized by x-ray diffraction (XRD), scanning electron microscopy (SEM), and dissolution testing (USP Apparatus II, paddle method, 3mg SRL (15% solubility, 900mL of 0.1% SDS/water, 50 RPM, 37^{o}C). Dissolution testing was also performed at supersaturated conditions, by loading SRL at 12.5X the aqueous equilibrium solubility of 2.6 μg/mL. Here6.5 mg SRL was added to 100mL in a small volume paddle dissolution

apparatus, with 0.1% SDS/water, 50 RPM, and 37^{o}C. The results were compared to those for the commercially available Rapamune® at the same 12.5X drug loading.

SEM revealed a highly porous network composed of nanometer-sized primary drug/excipient particles aggregated into micron size aggregates. Drug release of SRL from the compositions prepared by URF was faster at sink conditions compared to that of Rapamune® tablets. The amorphous nature, determined by XRD, of the SRL formulations allowed for supersaturation of the dissolution media. Rapamune®, containing crystalline SRL, however, relies on high surfactant/solubilizer content (1mg SRL in 350mg tablet) to achieve supersaturated conditions. Although Rapamune® shows high, sustained supersaturation, the potency of the tablets is low.. The dissolution of SRL in Rapamune® tablets was due to micellar solubilization, solubilization by surfactants [1]. High potency URF SRL formulations (50-65% w/w SRL) show high initial supersaturation, whereas the 65% SRL formulations showed a lower initial, but more prolonged supersaturation. Formulations of 50% SRL potency with URF-SRL Formulation 3 showed the highest supersaturation (8.8 x Ceq) at 24 hours, URF-SRL Formulation 2 showed (7.6 x Ceq) at 24 hours, and URF-SRL Formulation 1 showed supersaturation of (3.5 x Ceq) at 24 hours. Formulations of 65% SRL potency (URF-SRL 4) showed prolonged supersaturation of 5.1 x C/Ceq, while URF-SRL 5 showed prolonged supersaturation of 2.8 x C/Ceq, and formulation URF-SRL 6 showed prolonged supersaturation of 2.6 x C/Ceq.

The URF process created amorphous nanostructured aggregates of SRL/excipient with high dissolution rates. Dissolution under supersaturated conditions showed that drug supersaturation is dependent on excipient type and level in the formulation. The

stable high potency compositions (50-65% w/w SRL), produce supersaturation, indicating the high apparent solubility of the amorphous SRL. The high supersaturation may be expected to increase the flux across biological membranes, and to saturate PGP efflux and CYP 3A4 metabolism. Therefore, the oral bioavailability from these compositions may be expected to be enhanced. The cryogenic process (URF) is favorable for producing minimal drug degradation, and preserving the potency of SRL in the formulation.

3.2 INTRODUCTION

Sirolimus (SRL), or rapamycin, is a potent macrolide antibiotic isolated from the bacterium *Streptomyces hygoscopicus,* a soil microbe found on the South Pacific island of Rapa Nui [2, 3]. In addition to its antibiotic characteristics, sirolimus has also been found to have potent immunosuppressive and antifungal capabilities along with anti-cancer properties. Currently, sirolimus is approved for immunosuppression in kidney transplant recipients, both alone and in combination with other immunosuppressants. The drug has shown efficacy in the treatment of allograft rejection, both prophylactically and during acute rejection [2]. Graft and patient survival were studied for up to 12 months following kidney transplantation to determine the effectiveness of the sirolimus formulations in preventing organ rejection. Kidney graft survival was 92% and 88.7% for the oral solution and tablet treatment groups, respectively, while patient survival rates were 95.8% and 96.2% with the commercially available SRL oral solution and SRL tablets,

respectively [4]. Sirolimus, therefore, shows efficacy when treating transplant patients over a long period of time. The drug also shows promise in the treatment of autoimmune diseases such as lupus, Type-1 diabetes, and rheumatoid arthritis. Scientists are also working to develop sirolimus-eluting stents which are resistant to scar tissue build-up and biofouling [5]. Sirolimus, therefore, has the potential to treat a variety of indications, both autoimmune and infectious diseases.

The major hurdle to its widespread therapeutic use for these indications is the commercial product's low bioavailability and erratic and incomplete oral absorption [6, 7]. This is due to the low aqueous solubility of the drug is 2.6 μg/mL [8]. The commercial sirolimus product, Rapamune®, shows efficacy against tissue and organ rejection following kidney and liver transplantation [4]. Along with liver and kidney allografts, heart and lung transplantation surgery remains an important treatment for organ failure, and treatment opportunities exist for maintenance and survival of these transplants. If sirolimus is formulated for better absorption and higher bioavailability, orally dosed sirolimus may hold the possibility for improved treatment for the different indications for which it is effective.

Although sirolimus exhibits a wide range of therapeutic properties, its unique mechanism of action among the immunosuppressants allows for the potential to augment current immunosuppressant treatments and to reduce the potential nephrotoxicity of immunosuppressing drugs. Instead of binding directly to calcineurin like other immunosuppressants (cyclosporin A and tacrolimus), sirolimus binds with a receptor in the lymphocyte, the mitochondrial target of rapamycin (m-TOR) receptor [2]. Sirolimus blocks lymphocyte proliferation without inhibiting calcineurin phosphatase, and, it

interferes with post-receptor interleukin (IL-2) signaling, resulting in the arrest of cell maturation at the G1 to S phase transition, thereby inhibiting T-cell proliferation. Sirolimus, therefore, can be used alone or in combination with these other immunophilin binding-type immunosuppressants to alleviate the symptoms of host vs. graft disease or allograft rejection that is observed in transplant recipients [3].

The low and erratic bioavailability of sirolimus has limited its use in oral administration due to its poor water solubility and the fact that it is a substrate for the P-glycoprotein (PGP) efflux pump and CYP 3A4 isoenzyme. The compound is distributed widely in tissues due to its highly lipophilic nature (calculated log P = 3.58) , but it shows wide intra-subject and inter-subject variability as far as absorption and clearance are concerned [9]. The main fraction of the administered SRL dose is sequestered in red blood cells (94.5%), while a small amount of the dose partitions into lymphocytes (1.1%), granulocytes (1%), and blood serum (3.1%) [10]. SRL is metabolized by several different pathways. SRL undergoes counter-transport from enterocytes of the small intestine into the gut lumen, pumping available drug from systemic circulation into the waste excreted by the large intestine [6]. Pharmacokinetic studies have shown that the drug is eliminated mainly from the feces (98%) [9], confirming the observations that the drug is a substrate for the PGP efflux pump. First-pass metabolism of the drug occurs following oral administration, with CYP 3A4 isoenzymes in the liver converting the drug to the inactive O-demethylated metabolite [11]. Also, the CYP 3A4 isoenzymes in the intestinal wall have contributed to lower oral bioavailability of the drug. Mixed function oxidase enzymes in the body fluids also convert SRL into different metabolites [12]. Seven major metabolites, including the hydroxy, demethyl, and hydroxydemethyl forms,

have been identified in whole blood, indicating that sirolimus is a substrate for more cytochromes than CYP 3A4 alone [7]. Inducers of CYP 3A4 and PGP have been shown to decrease circulating sirolimus concentrations [4]. Additionally, sirolimus is also very highly bound (92%) to cytosolic binding proteins like serum albumin and α-1 glycoprotein, making the compound less available systemically [6].

Cryogenic processes are used to increase the aqueous solubility of poorly water soluble drugs, and formulations of these poorly water soluble drugs have been used for oral and pulmonary administration [13-19]. In addition, these processes have been shown to produce stable amorphous nanoparticles of drug formulations, and these formulations show increased ability to supersaturate dissolution media [20]. Supersaturation of the drug in solution will cause increased drug flux across biological membranes, allowing the drug to saturate PGP efflux sites and increasing its oral bioavailability *in vivo* [21, 22]. The Ultra Rapid Freezing (URF) process is a cryogenic technique which improves water solubility of drugs by reducing primary drug particle size and producing amorphous solid dispersions [20, 23-25]. URF produces very similar particle morphologies as a related process spray-freezing into liquid (SFL) [19, 26, 27], consistent with the similar heat transfer rates. In URF, the solution is contacted directly with a cryogenic substrate [20, 24, 25]. Direct contact with a boiling liquid cryogenic substrate transfers heat through a gas bubble film until the temperature of the particle comes in thermal equilibrium with the liquid at its boiling point [28]. Heat conduction is enhanced by using a cryogenic material with a high thermal conductivity, density, and mass relative to the solution being frozen so as to maintain low surface temperatures and high heat transfer rates while the solution is being frozen. With the URF technology, the thickness of the freezing solution

may be controlled to fix its minimum freezing rate since the freezing rate drives the particle formation and determines its characteristics [23, 25]. The result of the URF process is a porous amorphous aggregated system of nanosized primary particles with enhanced dissolution rates, as observed previously for particles produce by SFL.

The objective of the study was to produce stable, highly wettable, rapidly dissolving compositions with high drug loading, containing the poorly water soluble drug, sirolimus (SRL). Also, SRL was observed under ICH forced degradation criteria to determine the degradation products of the drug under acid, base, peroxide, and heated conditions. It is critical to determine whether degradation products are formed drug processing and whether these degradation products interfere with analysis of SRL isomers. The dissolution behavior to produce highly supersaturated solutions was investigated for a variety of formulations of SRL made by URF.

3.3 MATERIALS AND METHODS

3.3.1 Materials

Sirolimus (Lot # B-0510554) was provided by The Dow Chemical Company. Rapamune® tablets (Lot # B00468) and Rapamune Oral Solution (Lot # A90732) were purchased. Sodium dodecyl sulfate (SDS), (Pierce Chemicals, Rockford, IL), Poloxamer 407 (P407) (Spectrum Chemical Company, Gardena, CA) and Hydroxypropylmethylcellulose E5 (Methocel E5) (The Dow Chemical Company, Midland, MI) were used as received. 1,3 dioxolane (Acros Organics, Geel, Belgium) and

T-butanol (Fisher Scientific, Fair Lawn, NJ) were used as received. High performance liquid chromatography (HPLC) grade acetonitrile and methanol (EM Industries, Inc., Gibbstown, NJ). Sodium hydroxide pellets (Sigma-Aldrich Inc., St. Louis, MO), as well as hydrochloric acid, (12.1N), trifluoroacetic acid, and acetic acid (HPLC grade) (Fisher Scientific, Fair Lawn, NJ) were used as received. Liquid nitrogen was obtained from BOC gases (Murray Hill, NJ). Deionized water was prepared by a Milli-Q purification system from Millipore (Molsheim, France).

3.3.2 Preparation of SRL Samples by URF

The preparation of SRL samples was accomplished using the URF process [20, 25]. Sirolimus was dissolved in 1,3 dioxolane (12.5% w/v), while the water soluble excipients in the formulations (sodium dodecyl sulfate (SDS), poloxamer 407, hydroxypropylmethylcellulose (HPMC E5) were dissolved in either water or a water/t-butanol (30:70 ratio) cosolvent system. The 1,3 dioxolane and water/*t*-butanol solutions were mixed, and the resulting organic/aqueous co-solvent system was frozen on the cryogenic substrate maintained at -85^{o}C. The frozen droplets were then removed from the substrate and lyophilized, using a Virtis Advantage Tray Lyophilizer (Virtis Company, Gardiner, NY), to produce a powder.

3.3.3 Dissolution Testing at Sink and Supersaturated Conditions

Dissolution of URF-SRL formulations at sink conditions was conducted according to the United States Pharmacopoeia (USP) guidelines for immediate release dosage forms, using 0.1% w/v SDS in deionized water as the dissolution medium. Powder samples corresponding to a sirolimus content of 3-5 mg were introduced into 900 mL of dissolution medium. A sample volume of 5 mL is collected at 15, 30, 60, 90, and 120 minutes (n=3) using a VK8000 autosampler (Varian, Inc.; Cary, NC). There was no medium replacement. Paddle speed and bath temperature are maintained at 50 rpm and 37^{o}C, respectively. The 400µL aliquots were collected, and the filtered samples were then diluted with 600µL 50/50 v/v acetonitrile/methanol. Sink conditions were maintained throughout the dissolution. The equilibrium solubility of SRL in the dissolution media at 37^{o}C was determined to be 5.1 µg/mL during preformulation.

Dissolution at supersaturated conditions was performed, using a small volume dissolution apparatus (100 mL vessel) equipped with a paddle stirring mechanism (Vankel VK6010 Dissolution Tester, Varian Inc., Palo Alto, CA). Drug compositions to 50-times the aqueous equilibrium solubility of SRL (about 6.5-7 mg SRL in each sample in 100 mL of dissolution media) were weighed out. For comparison with the commercial Rapamune® product, 6 Rapamune® (Wyeth Pharmaceuticals, Lot # B00468) tablets were used in the same manner for conducting dissolution testing at supersaturated conditions. The dissolution media was 0.1% SDS in water, using 100 mL volume of medium for this procedure. Paddle speed and bath temperature were maintained at 50 RPM and 37^{o}C, respectively. A 1 mL aliquot of sample was taken manually at 2, 5, 10, 20, 30, 60, 120, and 1440 minutes, with no medium replacement. Aliquots was filtered through a 0.2 µm Whatman nylon filters (Florham Park, NJ), and a 0.5 mL aliquot of this

filtered solution was diluted in 1 mL of acetonitrile/methanol 50/50 v/v and analyzed for sirolimus concentration using the HPLC procedure.

3.3.4 Determination of SRL by HPLC

The HPLC method for measuring SRL in the samples was as follows: potency, chromatographic purity, and dissolution samples were analyzed at 278 nm using a Waters 515 liquid chromatograph with a Waters 996 Photo Diode Array (Waters Corp., Milford, MA) equipped with a Waters Symmetry C8 3.5µm 4.6 x 75mm reverse-phase column and Waters Symmetry C18 5µm guard column (Waters Corp., Milford, MA). The column temperature is maintained at 35^{o}C. The mobile phase consisted of 1360 mL deionized water, 1200 mL methanol, and 1440 mL acetonitrile. Sirolimus exists in two isomeric forms in solution: a lactone form and a lactam form, with both isomers showing equivalent therapeutic activity [29]. The major isomer sirolimus (lactone) peak elutes with an average retention time of 21 minutes while the minor isomer sirolimus (lactam) peak elutes with an average retention time of 27 minutes at a flow rate of 1 mL/min [30]. The summation of the minor isomer peak area and the major isomer peak area was used to quantify the sirolimus present in the samples. Additionally, the SRL isomers were fractionated using a Shimadzu FRC 10-A fractionator to collect the eluent that eluted from the column from 19.5 to 22 minutes (for the major isomer) and the eluent that eluted from the column from 26 to 28 minutes (for the minor isomer). These fractions were analyzed by mass spectrometry to confirm the identity of these compounds (they were found to have the same m/z number, indicating they are isomers). This HPLC method is

linear and reproducible over a range of concentrations 100-0.1 μg/mL (r^2=0.9999) sirolimus. The LOQ was 0.1 μg/mL, and LOD was 0.02 μg/mL.

3.3.5 Mass Spectrometry (LC-MS)

High-performance LC-MS was performed on samples using a Finnigan-MAT LCQ (ThermoFisher, San Jose, CA) electrospray ion-trap mass spectrometer coupled with a MAGIC 2002™ microbore HPLC (Michrom BioResources, Auburn, CA). Twenty microliters of sample was injected through the injector port, passed through a small molecular desalt trap, and eluted with 50% mobile phase A (acetonitrile:water:acetic acid:trifluoroacetic acid, 2:98:0.1:0.02) and 50% B (acetonitrile: water:acetic acid:trifluoroacetic acid, 90:10:0.09:0.02) at 20μl/min. The eluent was analyzed by LCQ using Finnigan Excalibur™ software (ThermoFisher) manual control to obtain full scan and MSMS scan spectra. The settings for the ESI were as follows: spray voltage, 3.5kV; sheath gas and auxiliary gas flow rates, 60 and 5 (arbitrary number), respectively; capillary temperature, 200ºC; capillary voltage, 22 V; tube lens offset, 40V. The electron multiplier was set at –860V; the scan time settings were performed with 3 microscans and 50 msec of max injection time for full scan, and with 3 microscans and 200 msec of max injection time for MSMS scan. The target number of ions for MS was $1X10^8$ and for MSMS was $2X10^7$. MSMS scan was performed with an isolation width of 2 amu, and a normalized collision energy level at 35%.

3.3.6 Scanning Electron Microscopy (SEM)

The powder samples were sputter coated using a model K575 sputter coater (Emitech Products, Inc., Houston, TX) with gold-palladium for 30 sec and viewed using a Hitachi S-4500 field emission scanning electron microscope (Hitachi High-Technologies Corp. Tokyo, Japan). An acceleration voltage of 5-15kV was used to view the images.

3.3.7 Polar Surface Area (PSA) Determination

The polar surface area of the isomers was calculated using ChemDraw® program to derive the simplified molecular input line entry system (SMILES) string for the two isomers and the Advanced Chemistry Development (ACD/Labs) Software V8.14 for Solaris (© 1994-2007 ACD/Labs) program was used to calculate their polar surface areas.

3.3.8 X-Ray Powder Diffraction

The X-ray diffraction patterns of all powder samples were analyzed using a Philips 1710 X-ray diffractometer with a copper target and nickel filter (Philips Electronic Instruments, Inc. Mahwah, NJ). The leveled powder sample was measured from 5-45 2θ degrees using a step time of 0.05 2θ degrees and a dwell time of 1 sec.

3.3.9 Stability Studies of Sirolimus

SRL was evaluated for its stability and degradation under a variety of accelerated conditions, according to the International Committee of Harmonization (ICH) guidelines [31]. The stability of SRL was determined following exposure to acid, base, hydrogen peroxide, and heat. Specifically, a stock solution of SRL was prepared containing 1 mg/mL of the drug in acetonitrile, and this stock was diluted to 100 μg/mL SRL after dilution with the appropriate forced degradative reagent. In the acidic condition (SRL-acid solution), 1 mL of 1N HCl was added to a 10 mL volumetric flask, and 3 mL of water was added to it. One milliliter of the diluted SRL solution was added to the flask, and the flask was diluted to volume with water. The SRL solution was incubated for 1 hour at 25^{o}C. In the basic condition (SRL-base solution), 1 mL of 1N NaOH was added to a 10 mL volumetric flask, and 3 mL of water was added to it. One milliliter of the SRL solution was added to the flask and diluted to volume with water. The SRL solution was incubated for 30 min at 25^{o}C. In the oxidative condition (SRL-peroxide solution), 1 mL of 3% hydrogen peroxide (H_2O_2) was added to a 10 mL volumetric flask, followed by 3 mL of water. One milliliter of the diluted SRL solution was added to the flask and diluted to volume with water. The reactants were allowed to react for 1 hour at 25^{o}C. The acidic condition solution was quenched with 0.1N NaOH, while the basic condition solution was quenched with 0.1N HCl. For the thermal degradation study (SRL-heat solution), 1 mL of the sirolimus stock solution (1 mg/mL in acetonitrile) was diluted with water in a 10 mL volumetric flask to volume with diluent. The flask was maintained at 40^{o}C for 6 hours to observe thermal degradation of the drug.

3.4 RESULTS

Sirolimus was exposed to acid, base, peroxide, and elevated temperature in solution, and the objective was to determine the amount and rate of degradation of sirolimus that each accelerated condition caused. It was also of concern to observe whether or not the possible metabolites or degradation products of sirolimus would interfere with the analysis of the SRL isomers themselves using HPLC.

Sirolimus undergoes isomerization in aqueous solution, shown in Figure 3.1 [2]. The results show two distinct peaks present in HPLC/UV chromatograms, the lactone form (major isomer), which elutes at about 16 minutes and the lactam form (minor isomer), which elutes at about 21 minutes. In aqueous solution, SRL exists primarily as an intramolecular hemiketal, forming a six-membered ring (major isomer), while the minor isomer also exists as an intramolecular hemiketal, but with a neighboring keto group, forming a seven membered ring (oxepane) [32]. Depending on the concentration of water in the co-solvent system in which sirolimus is dissolved, there are differing proportions of major to minor isomerization that can occur. Typically with the mobile phase that is used for HPLC analysis of SRL, the major isomer accounts for 85.7%-87.5% of the SRL peak area, while the minor isomer accounts for 12.5-14.3% of the SRL peak area, depending on the amount of water in the mobile phase, diluent, and other components of the solution. The order of elution of the major and minor isomers has to do with the polar surface area of the isomers. Since the major isomer has a higher polar

surface area (195Å^2) than does the minor isomer (192 Å^2), the compounds will elute in the same order each time.

The column and guard column used in the HPLC method also play a part in separation of the SRL isomers. The C8 guard column coupled with the C18 analytical column allowed for further resolution of the isomers, due to the polarity differences in the columns themselves. The peak areas of the two isomeric forms were summed, and reported to be the total SRL. Separation of the two isomeric forms was not entirely possible, as the isomers interconvert faster than can be injected into an HPLC [33]. However, the two isomers show the same UV spectrum [12], and are considered to have the same therapeutic activity, since they interconvert so rapidly (within 1 minute) in aqueous solution. Using mass spectrometry, the isomers were confirmed to be the same, having the same m/z values of 936, which is consistent with the literature [33]. There are also two transient open ring tautomeric forms of SRL that interconvert instantaneously to either the major or minor isomer, and they are detectible by HPLC/UV at retention times 11.4 and 12.6 min, respectively [34]. Other literature values have shown different ratios of the SRL major to minor isomer in different solvents. In organic solvents, for example, a 4:1 major to minor isomer ratio was shown [2]. Since the work that is presented here is all in organic/aqueous solution during analysis, the above ratios for the SRL major to minor peak areas are more relevant than the 4:1 ratios reported previously [2]. The typical chromatogram of SRL in the diluent that was used in this study (40/30/30 v/v/v water/acetonitrile/methanol) with the above described HPLC conditions is shown in Figure 3.2.

Sirolimus is extensively metabolized through the CYP 3A4 isoenzymes and mixed function oxidases in the intestinal tract and liver. In addition, DSRL is a PGP efflux pump substrate which further reduces the drug's bioavailability [10]. The main metabolites of SRL identified in human, pig, and rat tissue include: 39-O-demethylated rapamycin [34], 28-O-acetyl rapamycin [33], 16-hydroxylated rapamycin [33], and 40-O-(2-hydroxyethyl)-rapamycin [33]. All of the metabolite compounds, except 39-O-demethylated rapamycin, are less polar than the SRL isomeric forms, so they elute from the column before the SRL isomers. The 39-O-demethylated rapamycin metabolite, being less polar in nature than sirolimus, elutes later than the both SRL isomer peaks. In this study, there are no pure reference standard metabolites available, but references to studies on sirolimus metabolites have been cited [33, 34], and these compounds can be identified in the appropriate HPLC chromatograms. Given the higher polarity and higher polar surface area of most of the metabolites, they should elute before the SRL isomers, while not interfering with the analysis of SRL. Conversely, lower polarity and lower polar surface area metabolites (39-O-demethylated rapamycin) elute after the both SRL isomer peaks [34].

Forced degradation of SRL in basic solution showed the highest degree of SRL degradation. Even after only 30 min of reaction time, all of the SRL isomers had been degraded, and none was detected in the HPLC chromatograms. The HPLC chromatogram of the forced degradation of SRL with base is shown in Figure 3.3, along with the corresponding UV spectrum of the sample. In the UV spectrum as well as the HPLC chromatogram itself, however, it is noticed that a small amount of the transient tautomeric forms of SRL are still present, even after all of the detectable SRL has been

degraded. Since the current study was conducted under organic/aqueous (0.1N NaOH aqueous, with no methanol present) conditions and quenched following the reaction time, a ring closing reaction occurs [35]. Therefore, after a short reaction time in aqueous solution with low amounts of sodium hydroxide, a small amount of the transient intermediates were left in solution, when the degradation was quenched with acid, even though the SRL isomeric compounds are not detected. In the chromatograms, most of the degradant products are small and very highly polar molecules [35], which elute very early in the analysis, and only one identifiable degradant (16-hydroxylated sirolimus) was detected (Table 3.1).

Acid degradation of SRL was also observed during the preformulation studies. The acid degradation of SRL showed greater degradation of the SRL isomers than did the oxidative degradation, but less than that of the base degradation study. More of the SRL tautomers I and II were detected, as well as more of the 16-hydroxylated SRL degradant, as well as two unidentified degradants (Table 3.1). No literature references were found to show previous work done with acid degradation of the SRL isomers, but the presence of acid (0.1N hydrochloric acid) was observed to increase the amount of transient SRL tautomers I and II, indicating that the acidic conditions stabilize these transient compounds, preventing them from reverting back into their SRL isomers. Example chromatograms are shown in Figure 3.4.

Oxidative degradation of SRL was also observed during preformulation in this study. The present forced degradation study was conducted under mild aqueous conditions with 3% aqueous hydrogen peroxide. Although there were some identifiable degradation products produced by the forced oxidation (16-hydroxylated SRL and 40-O-

(2-hydroxyethyl) SRL, the SRL isomers were still present and in tact for the most part (Table 3.1). Also, the SRL tautomers I and II were present at higher levels in the oxidative conditions than in the working standards used to compare the chromatograms. The oxidative conditions seem to stabilize the tautomers and reduce the chance of them reverting back to their original SRL isomeric forms [36]. Overall, mild oxidative conditions have an effect on SRL isomers, producing known metabolic byproducts, but 54% of the SRL remained unreacted. This is in contrast to the catastrophic degradation of the SRL shown in the base degradation of SRL, which showed no SRL present after the reaction time. Example chromatograms are shown in Figure 3.5.

Thermal degradation of SRL was also observed during the preformulation study. The conditions of 40^{o}C for 6 hours was chosen because these conditions are similar to those described by ICH (40^{o}C and 75% relative humidity), and because this temperature/humidity condition is thought to show 10% degradation of the SRL compound. In this study, low levels of SRL degradation were observed (94.1% SRL remaining), even though SRL was exposed to heat in an aqueous/organic diluent solution. Accelerated thermal conditions showed small amounts of the SRL degradant 16-hydroxylated SRL, but no other degradation products of the SRL isomers were detected (Table 3.1). Therefore, SRL appears to be stable under mild thermal conditions, such as those to which normal pharmaceutical products are exposed (37^{o}C and 40^{o}C). Example chromatograms are shown in Figure 3.6.

X-ray diffraction (XRD) analysis of the powder formulations show the drug is present in an amorphous state, with no characteristic SRL XRD peaks noted in any of the samples (Figure 1). Figure 3.7 shows the XRD of the bulk sirolimus material, and URF-

SRL formulations 1, 3, and 4, respectively. XRD patterns of the sirolimus raw material show the characteristic diffraction peaks at 13, 15, 18, 21, 25, 27, 28, and 30 2-θ, as did the URF-SRL only processed by URF. XRD patterns of URF samples 1, 3, 4, 11, 12, and 13 do not exhibit the characteristic SRL XRD patterns, indicating amorphous formulations were produced by URF.

Scanning Electron Micrographs (SEM's) show the bulk SRL and the URF-SRL formulations' morphology (Figures 3.8-3.11). Bulk sirolimus is shown to have an irregular crystal habit, with large crystals of 100-200 μm in diameter, mixed with smaller crystals, exhibiting large degrees of polydispersity (Figure 3.8). Sirolimus URF formulations 1, 3 and 4 showed porous nanoparticle aggregates (Figures 3.9-3.11).

These porous, amorphous, nanostructured aggregates of sirolimus and excipients are intended for oral administration. The URF formulations of SRL show enhanced dissolution rates when compared to the commercial product (Figure 3.12, 3.13), despite the higher potency of the SRL formulations. SRL formulations produced using URF exhibit lower apparent supersaturated dissolution (Figure 3.14, 3.15) does the commercial product whose apparent dissolution is dependent upon high levels of solubilizers.

Addition of a good wetting agent, such as SDS or poloxamer 407, to the formulation allows for much improved wetting of sirolimus, and the enhanced wetting of the sirolimus formulations causes increased dissolution rates at sink conditions for the formulation. Addition of a cellulosic polymer, such as HPMC E5, allow for the formulation to supersaturate dissolution media for longer periods of time. The porous nature of the particles allows for aqueous media to interpenetrate the particles, while the amorphous character of the particles allows the drug to exhibit a higher apparent

solubility. URF formulations 1, 2, and 3 have 50% drug loading, while URF formulations 4, 5, and 6 have 65% drug loading. Figure 3.12 shows the dissolution profile of SRL formulations 1, 2, and 3, along with the Rapamune tablet dissolution, while Figure 3.13 shows the dissolution profiles of formulations 4-6. All of the higher drug loaded formulations show higher drug dissolution rates than the Rapamune® tablet. Formulations containing wetting agents showed improved dissolution *in vitro*. The high potency URF formulations of SRL, therefore, show higher dissolution rates than does the commercial product, due to the solid solutions produced in the URF processing.

Dissolution under supersaturated conditions of the SRL formulations, incorporating excipients, occurred and was maintained at above the equilibrium solubility of SRL alone [37]. URF formulation 1 showed some high initial supersaturation (9.8X at 2 minutes), due to the amorphous character of the solid solution particles, but crystallization was observed after only 120 minutes, and it showed the least amount of extended supersaturation. URF SRL only showed no supersaturation, because it was crystalline in structure, having no stabilizers to make it amorphous, and, as a result, this formulation did not supersaturate, but it stayed at the equilibrium solubility (Figure 3.13). In the current study, URF Formulation 3 showed high initial supersaturation (10.6X at 2 minutes), and prolonged supersaturation. URF formulation 2, using 1:1 TAC:HPMC E5 showed the best initial supersaturation profile (11.7X at 2 minutes). These high potency formulations showed initially high supersaturation, but recrystallization of the drug occurred, though there is still a high apparent SRL solubility. URF SRL-3 formulation showed 8.8X supersaturation over the 24 hour time period, while URF SRL-2 formulation showed 7.6X supersaturation over the 24 hour time period, and URF SRL-1

formulation showed 3.5X supersaturation over the 24 hour time period, showing that theses formulations can supersaturate dissolution media for long periods of time, even though they have high drug potency (50% SRL). Increasing the potency of the drug (to 65% SRL) in the formulations, as expected, showed lower supersaturation, due to the reduced amounts of excipients in the formulations, however, supersaturation was maintained for longer periods of time due to the presence of HPMC, which stabilizes the particle size growth. URF SRL-4 formulation showed 5.1X supersaturation after 400 minutes, followed by URF SRL-5 formulation, which showed 2.8X supersaturation, and URF SRL-6 formulation which showed 2.6X supersaturation.

It is critical that the processing of sirolimus produces porous amorphous particles with high surface area in order for the higher dissolution rates to be achieved. Other drug processing techniques can be used to produce the formulation with similar excipients, provided amorphous aggregates of microparticles are produced, and the particle size and morphology may be controlled by the type and level of stabilizers (Figures 3.9 and 3.10). In addition, supersaturation of the drug can be optimized by choice and level of the excipients used in the formulations.

3.5 DISCUSSION

As compared to this study, previous studies have been conducted on the degradation of SRL. These previous studies, however, did not follow ICH guidelines in regard to acid, base, oxidative, and thermal conditions specified by these guidelines. In a previous base degradation study of SRL, Steffan et al. have shown degradation of SRL in

extremely basic conditions for long periods of reflux, using 1N methanolic sodium hydroxide [35]. The authors then went on to elucidate the mechanism by which the SRL is degraded, and they isolated the byproducts of the reaction mechanism [35]. In the present study, the concentration of hydroxide was much lower (0.1N sodium hydroxide in aqueous solution, with no methanol present), yet the degradation of the SRL was complete within 30 min. Steffan et al. have shown that the SRL ring opening is due to retroaldol cleavage of the drug in methanolic solution, due to C-28 being epimerized instantaneously. Steffan et al. used a variety of strongly to mildly basic compounds to degrade SRL, and found that less nucleophilic bases such as diethylamine and 4-N,N-dimethylaminopyridine had the same ring opening effect, resulting in α,β-unsaturated ketones of the carboxylic acid salt of SRL [35], leading ultimately to the complete SRL isomers' degradation.

In a previous oxidative degradation study of SRL harsh conditions of oxidation were conducted in organic solution. Goulet et al. used oxidative conditions, but their experiments used ozonolysis in dichloromethane and methanol [36]. They used organic solvents to preserve the single SRL isomer, rather than using aqueous/organic solutions which show two isomers of SRL in solution. Goulet showed complete ring opening of the SRL isomers, and further degradation into smaller, more polar compounds [36]. No SRL isomers remained after the reaction mechanism performed by Goulet et al.

Under acidic conditions, Zhou et al. showed that ionic hydrogen bonds (as in acid conditions) stabilize the cis-amide rotamer of a ring-opened SRL tautomer, so this could explain why the SRL tautomers were more stable in acidic solution [38]. This stabilization effect, however, is small and short-lived. The chromatograms of the acidic

degradation of SRL isomers (Figure 3.10) show that it this is a possible mechanism for the presence of increased amount of SRL tautomers in acidic solution.

Thermal degradation experiments on SRL have shown stability of the compound in whole blood at various temperature conditions (4^oC to 37^oC), but not at the ICH recommended 40^oC in HPLC mobile phase diluent. Salm et al. have studied the stability of SRL in whole blood under similar temperature conditions and found very little degradation of SRL at body temperature (37^oC), even when compared to whole blood stored at 4^oC [39]. Even though whole blood has enzymatic entities (CYP 3A4, mixed function oxidases, etc.) that can degrade the SRL, no significant degradation of SRL was detected in the whole blood samples. They found that the degradation of the compound at elevated temperatures (37^oC) was clinically insignificant compared to the samples stored at 4^oC [39]. The Salm et al. study was conducted over 8 days, but they found that this data also compares to the Yatscoff et al. study, which was conducted over 30 days [40].

As with other URF processed drugs, XRD and SEM analysis showed porous, amorphous nanosized drug particles, forming into micron sized aggregates. Cryogenic processes allow for reduction of primary particle size of drug particles without the intense frictional or mechanical forces involved in ball-milling or other processes relying on frictional comminution or trituration with a mortar and pestle, which can cause degradation of the drug through thermal stress [41]. URF technology involves the use of a rotating drum with a thermal conductivity between 10-20 W/m degree Kelvin filled with a cryogenic liquid. When the drug/excipient solution is applied to the drum, the droplets freeze instantaneously. Instantaneous freezing does not allow the drug to

organize itself into crystals, and the result is amorphous drug aggregates. Because of the small amount of solids present in the drug containing solution (0.75% w/v), most of the solvent is driven off during the lyophilization process, leaving nanosized primary particles aggregated into micron sized particles. With the SRL formulations, t-butanol, with a melting point of 24-27°C, was employed to raise the freezing point of the final drug solution, causing more rapid freezing, and allowing for the amorphous character of the formulations. The reduction in primary particle size, as well as its amorphous character allows for the supersaturation of SRL in dissolution media. Experiments have produced rapidly dissolving, high potency (50-65% potency) URF formulations of the drug (Table 3.3).

Commercial formulations involve incorporation of sirolimus into a solid dosage form (Rapamune® tablets, Wyeth). This composition has a high levels of excipients (including solubilizing agents like PEG's 8000 and 20,000, Poloxamer 188, glyceryl monooleate, and povidone), and therefore have low drug loading (1 mg sirolimus in a 350 mg tablet, or 1:350 w/w) [4]. Although the SRL in the commercial tablet is crystalline in nature, it relies on increased levels of surfactant and solubilizer content in order to produce sufficient supersaturated dissolution rates [1]. URF formulations rely on high apparent solubility of the drug in its amorphous form along with solubilization to produce high supersaturated dissolution rates. URF formulations also wet readily in dissolution media and dissolve faster at sink conditions than does the Rapamune® tablet. High energy wet milling of the crystals in the presence of the stabilizing excipients causes the drug crystals to fracture to nano-sized particles 100-300 nm in size [42]. Polymeric

excipients then adsorb to the crystal surface of the particles, inhibiting aggregation and particle growth of the crystals and providing stable dispersions of the drug crystals [43]. This process is time consuming compared to URF, requiring the drug to be processed and milled with surfactant for extended periods [43], allowing for the potential of drug degradation. URF formulations provide for short processing times of about 15 minutes for a lab scale batch [25].

Other studies [20, 44] have shown that HPMC acts to inhibit recrystallization of drug particles by forming a structure around the growing drug crystal and stabilizing it to a sub-micron size [45]. Dissolution of high potency (up to 94%) amorphous itraconazole particles yielded high plateau levels in supersaturation up to 90-times the equilibrium solubility [46]. High surface areas led to more rapid and higher levels of supersaturation than for traditional low surface area solid dispersions which crystallized during slow dissolution. Sinswat et al. have shown that various excipients included in the formulations at different levels accounts for the higher apparent solubility of the formulations, compared to the equilibrium solubility of the drug [44]. Other excipients investigated showed high apparent supersaturation, but crystals of the drug precipitated out of solution faster than the HPMC formulations. For example, Yamashita et al. showed that TAC:PVP, initially produced about 25X apparent solubility, but after 24 hours, the solubility was only about 10X apparent solubility, while PEG 6000 showed 25X apparent solubility, but quickly dropped to about 3X apparent solubility [47]. Yamashita et al have shown that solid dispersion formulations of tacrolimus (TAC) in HPMC have high apparent supersaturation values (25X equilibrium solubility), maintained for up to 24 hours, only reducing to 20X equilibrium solubility [47]. The

formulations reported by both Sinswat et al. and Yamashita et al. were high potency formulations [44, 47]. The Nanosystems® process in the commercial Rapamune® uses excipients to stabilize particle size of the drug particles [43]. Rapamune®, with the high amount of surfactantants/solubilizers in the tablet (1:350 w/w drug/excipient ratio), shows an "apparent" supersaturation, but this is not a true supersaturation, but merely the solubility of the drug in micellar form and very small particle size stabilization in the presence of surfactants, which might have gone through the filter. Higher potency formulations showed supersaturation, but not the extended supersaturation observed with Rapamune tablets, due to the lower amounts of excipients.

URF-SRL Formulations 1, 2, and 3 showed very high initial supersaturation, but this effect was prolonged only in URF SRL-2 and URF-SRL 3, due to the increase in surfactants and possible mixed micelle formation (adding 6.5 mg SRL and 6.5 mg surfactant - SDS or P407 or both) in the 0.1% dissolution medium. Increasing potency of the SRL to 65% (URF Formulations 4, 5, and 6) show extended supersaturation due to the HPMC effect discussed earlier. The URF-4 formulation showed the highest degree of supersaturation among these 65% SRL potency formulations. This could be due to increased solubilizer/surfactant content in the formulations, along with the higher amount of HPMC E5 present in the formulation.

3.6 CONCLUSIONS

The preformulation studies of SRL using ICH guidelines indicated a relatively stable drug upon exposure to peroxide and temperatures of 40^{o}C. During processing,

alkaline excipients should be avoided. The use of peroxides to accelerate oxidation produced moderate degradation of the SRL isomers, but not to the extent of the acidic and basic conditions. The study also showed that, though we are using cryogenic techniques to process the SRL, relatively high temperatures (40^{o}C for 6 hours) does not seem to affect the degradation of the drug on the time scale that the drug can be processed using URF.

The optimum formulation studied was URF-SRL Formulation 3. Despite the high potency (50%)and unusually low amounts of solubilizers, high levels of supersaturation were observed over long periods of time (8.8 x Ceq) up to 24 hours. Other formulations (URF-SRL Formulation 2 and URF-SRL Formulation 1) with smaller amounts of wetting agents produced lower supersaturation values, (7.6 x C/Ceq, and 3.5 x C/Ceq) and slower dissolution rates. Higher potency formulations of SRL (65%), showed enhanced dissolution rates, but the supersaturation levels of these formulations was not as high as the 50% SRL formulations (with the exception of URF-SRL Formulation 2). They did, however, supersaturate for longer periods of time, due to the presence of HPMC, which stabilizes recrystallizing drug particles and prevent particle growth.

3.7 ACKNOWLEDGEMENTS

The authors of this paper wish to gratefully thank The Dow Chemical Company for their partial financial support of the research contained therein. The authors would also like to thank Dr. Herng-Hsiang Lo in the CRED Analytical Instrumentation Facility Core supported by NIEHS center grant ES07784 for his help with the mass spectrometry

(LC-MS) analysis and interpretation.

3.8 REFERENCES

1. S. H. Yalkowsky, *Solubility and solubilization in aqueous media*. American Chemical Society. Vol. 1. 1999, New York: Oxford University Press

2. S. N. Sehgal, K. Molnar-Kimber, T. D. Ocain, and B. M. Weichman, Rapamycin: A Novel Immunosuppressive Macrolide, Medicinal Res Review. 14 (1994) 1-22.

3. S. N. Sehgal, J. S. Camardo, J. A. Scarola, and B. T. Maida, Rapamycin (Sirolimus, Rapamune), Dialys Transplant. (1995) 482-487.

4. W. Laboratories, Rapamune (sirolimus) Oral Solution and Tablets, *US Package Insert*. 2000, Wyeth Laboratories.

5. S. Windecker, A. Remondino, F. R. Eberli, P. Jüni, L. Räber, P. Wenaweser, M. Togni, M. Billinger, D. Tüller, C. Seiler, and B. Meier, Sirolimus-Eluting and Paclitaxel-Eluting Stents for Coronary Revascularization, New England Journal of Medicine. 353 (2005) 653-662.

6. D. L. Davis, J. N. Murthy, H. Gallant-Haidner, R. W. Yatscoff, and S. Soldin, Minor Immunophilin Binding of Tacrolimus and Sirolimus Metabolites, Clin Biochem. 33 (2000) 1-6.

7. H. L. Gallant-Haidner, D. J. Trepanier, D. G. Freitag, and R. W. Yatscoff, Pharmacokinetics and Metabolism of Sirolimus, Therapeutic Drug Monitoring. 22 (2000) 31-35.

8. P. Simamora, J. M. Alvarez, and S. H. Yalkowsky, Solubilization of rapamycin, Int. J. Pharm. 213 (2001) 25-29.

9. D. T. Trepanier, H. Gallant, D. F. Legatt, and R. W. Yatscoff, Rapamycin: Distribution, Pharmacokinetics, and Therapeutic Range Investigations: An Update, Clin Biochem. 31 (1998) 345-351.

10. K. Mahalati and B. D. Kahan, Clinical Pharmacokinetics of Sirolimus, Clin Pharmaco. 40 (2001) 573-585.

11. S. Zhang and M. E. Morris, *Efflux Transporters in Drug Excretion*. Drug Delivery Principles and Applications, ed. B. Wang, T. Siahaan, and R. Soltero. 2005, Hoboken, NJ: Wiley and Sons.

12. C. Vezina, A. Kudelski, and S. N. Sehgal, Rapamycin, A New Antifungal Antibiotic I. Taxonomy of the Producing Streptomycete and Isolation of the Active Principle, J Antibiot. (1975) 721-731.

13. J. H. Hu., Johnston, K.P., Williams, R.O., Rapid dissolving high potency danazol powders produced by spray freezing into liquid process, Int. J. Pharm. 271 (2004) 145-154.

14. J. T. McConville, K. A. Overhoff, P. Sinswat, J. M. Vaughn, B. L. Frei, D. S. Burgess, R. L. Talbert, J. I. Peters, K. P. Johnston, and R. O. Williams, Targeted High Lung Concentrations of Itraconazole Using Nebulized Dispersions in a Murine Model, Pharm. Res. 23 (2006) 901-911.

15. B. J. Hoeben, D. S. Burgess, J. T. McConville, L. K. Najvar, R. L. Talbert, J. I. Peters, N. P. Wiederhold, B. L. Frei, J. R. Graybill, R. Bocanegra, K. A. Overhoff, P. Sinswat, K. P. Johnston, and R. O. Williams, In vivo efficacy of aerosolized nanostructured itraconazole formulations for prevention of invasive pulmonary aspergillosis, Antimicrob. Agents and Chemotherapy. 50 (2006) 1552-1554.

16. J. H. Hu., Johnston, K.P., Williams, R.O., Spray-freezing into liquid (SFL) particle engineering technology to enhance dissolution of poorly water soluble drugs: organic solvent versus organic/aqueous co-solvent systems, Eur. J. Pharm. Sci. 20 (2003) 295-303.

17. J. H. Hu., Johnston, K.P., Williams, R.O., Stable amorphous danazol nanostructured powders with rapid dissolution rates produced by spray freezing into liquid, Drug Dev. Ind. Pharm. 30 (2004) 695-704.

18. J. H. Hu., Johnston, K.P., Williams, R.O., Nanoparticle Engineering Processes for Enhancing the Dissolution Rates of Poorly Water Soluble Drugs, Drug Dev. Ind. Pharm. 30 (2004) 233-245.

19. J. Hu, T. L. Rogers, J. Brown, T. Young, K. P. Johnston, and R. O. Williams III, Improvement of Dissolution Rates of Poorly Water Soluble APIs Using Novel Spray Freezing into Liquid Technology, Pharm Res. 19 (2002) 1278-1284.

20. T. Purvis, M. E. Matteucci, M. T. Crisp, K. P. Johnston, and R. O. Williams III, Rapidly Dissolving Repaglinide Powders Produced by the Ultra-Rapid Freezing Process, AAPS Pharm Sci Tech. in press (2007.

21. S. Jang, M. Weintjes, and J. Au, Kinetics of P-glycoprotein Mediated Efflux of Paclitaxel, J Pharmacol Exp Therap. 298 (2001) 1236-1242.

22. C. Kruijtzer, J. Beijen, and J. Schellens, Improvement of Oral Drug Treatment by Temporary Inhibition of Drug Transporters CYP 450 in the GI Tract and Liver: An Overview, Oncologist. 7 (2002) 516-530.

23. J. C. Evans, B. D. Scherzer, C. D. Tocco, G. B. Kupperblatt, J. N. Becker, D. L. Wilson, S. A. Saghir, and E. J. Elder, *Preparation of nanostructured particles of poorly water soluble drugs via a novel ultra-rapid freezing technology*, in

Polymeric Drug Delivery - Polymeric Matrices and Drug Particle Engineering, S. Svenson, Editor. 2006, American Chemical Society: Washington, DC. p. 320-328.

24. P. Sinswat, K. A. Overhoff, J. T. McConville, K. P. Johnston, and R. O. Williams III, Nebulization of Nanoparticulate Amorphous or Crystalline Tacrolimus - Single Dose Pharmacokinetics Study in Mice, Eur J Pharm Biopharm. in press (2007.

25. K. A. Overhoff, J. D. Engstrom, B. Chen, B. D. Scherzer, T. E. Milner, K. P. Johnston, and R. O. Williams III, Novel Ultra-Rapid Freezing Particle Engineering Process for Enhancement of Dissolution Rates of Poorly Water Soluble Drugs, Eur J Pharm Biopharm. 65 (2007) 57-67.

26. T. L. Rogers, K. P. Johnston, and R. O. Williams III, Solution-based particle formation of pharmaceutical powders by supercritical or compressed fluid CO2 and cryogenic spray-freezing technologies, Drug Development and Industrial Pharmacy. 27 (2001) 1003-1015.

27. T. L. Rogers, A. C. Nelsen, M. Sarkari, T. J. Young, K. P. Johnston, and R. O. Williams III, Enhanced Aqueous Dissolution of a Poorly Water Soluble Drug by Novel Particle Engineering Technology: Spray-Freezing into Liquid with Atmospheric Freeze-Drying, Pharm Res. 20 (2003) 485-493.

28. B. S. Gottfried, C. J. Lee, and K. J. Bell, The Leidenfrost Phenomenon: Film Boiling of Liquid Droplets, International Journal of Heat and Mass Transfer. 9 (1966) 1167-1187.

29. M. Ricciutelli, P. Di Martino, L. Barboni, and S. Martelli, Evaluation of rapamycin chemical stability in volatile-organic solvents by HPLC, J Pharm Biomed Anal. 41 (2006) 1070-1074.

30. D. Cattaneo, N. Perico, and F. Gaspari, Assessment of Sirolimus Concentrations in Whole Blood by High-Performance Liquid Chromatography with UV Detection, J Chromatogr B. 774 (2002) 187-194.

31. FDA. *Stability Testing: Drug substance stress testing*. in *International Conference on Harmonization of Technical Requirements for Registration of Pharmaceuticals for Human Use.* 2003. Rockville, MD, USA.

32. S. Edsbacker, P. Wollmer, A. Nilsson, and M. Nilsson, Pharmacokinetics and gastrointestinal transit of budesonide controlled ileal release (CIR) capsules, Gastroenter. 104 (1993) A695.

33. F. Streit, U. Christians, H. Schiebel, K. Napoli, L. Ernst, A. Linck, B. Kahan, and K. Sewing, Sensitive and specific quantification of sirolimus (rapamycin) and its

metabolites in blood of kidney graft recipients by HPLC/electrospraymass spectrometry, Clin. Chem. 42 (1996) 1417-1425.

34. M. Nickmilder, D. Latinne, J. De Houx, R. Verbeeck, and G. Lhoest, Isolation and identification of a C39 demethylated metabolite of rapamycin from pig liver microsomes and evaluation of its immunosuppressive activity, Clin. Chem. 44 (1998) 532-538.

35. R. J. Steffan, R. M. Kearney, D. C. Hu, A. A. Failli, J. S. Skotnicki, R. A. Schiksnis, J. F. Mattes, K. W. Chan, and C. E. Caufield, Base Catalyzed Degradation of Rapamycin, Tetrahedron Letters. 34 (1993) 3699-3702.

36. M. T. Goulet and J. Boger, Degradative Studies on the Tricarbonyl Containing Macrolide Rapamycin, Tetra Let. 31 (1990) 4845-4848.

37. G. Valsami, A. Dokoumetzidis, and P. Macheras, Modeling of Supersaturated Dissolution Data, Int J Pharm. 181 (1999) 153-157.

38. C. C. Zhou, K. D. Stewart, and M. K. Dhaon, An Intramolecular Ionic Hydrogen Bond Stabilizes a cis amide rotamer of a ring-opened Rapamycin Degradation Product, Magn. Res. Chem. 43 (2005) 41-46.

39. P. Salm, M. J. Tresillian, P. J. Taylor, and P. I. Pillians, Stability of Sirolimus (Rapamycin) in Whole Blood, Therapeutic Drug Monitoring. 22 (2000) 423-426.

40. R. W. Yatscoff, R. Boeckx, and D. W. Holt, Concensus Guidelines for Therapeutic Drug Monitoring of Rapamycin: Report of the Consensus Panel, Ther Drug Monit. 17 (1995) 676-680.

41. J. O. Waltersson, Lundgren, P., The effect of mechanical comminution on drug stability, Acta Pharm. Suec. 22 (1985) 291-300.

42. T. S. Wiedmann, L. DeCastro, and R. W. Wood, Nebulization of Nanocrystals: Production of Respirable Solid-in-Liquid-in-Air Colloidal Dispersion, Pharm Res. 14 (1997) 112-116.

43. E. Merisko-Liversidge, G. G. Liversidge, and E. Cooper, Nanosizing: A Formulation Approach for Poorly Water Soluble Compounds, Eur J Pharm Sci. 18 (2003) 113-120.

44. P. Sinswat, M. E. Matteucci, K. P. Johnston, and R. O. Williams, Dissolution rates and supersaturation behavior of amorphous repaglinide particles produced by controlled precipitation, J Biomed Nanotech. 3 (2007) 18-27.

45. Y. Yokoi, E. Yonemochi, and K. Terada, Effects of sugar ester and hydroxypropyl methylcellulose on the physicochemical stability of amorphous cefditoren pivoxil in aqueous suspension, Int J Pharm. 290 (2005) 91-99.

46. M. E. Matteucci, B. K. Brettmann, T. L. Rogers, E. J. Elder, R. O. Williams III, and K. P. Johnston, Design of Potent Amorphous Drug Nanoparticles for Rapid Generation of Highly Supersaturated Media, Molecular Pharmaceutics. in press (2007.

47. K. Yamashita, T. Nakate, K. Okimoto, A. Ohike, Y. Tokunaga, R. Ibuki, K. Higaki, and T. Kimura, Establishment of New Preparation Method for Solid Dispersion Formulation of Tacrolimus, Int J Pharm. 267 (2003) 79-91.

Chapter 4: Multiple Dose Pharmacokinetics of Pulmonary-Dosed Nebulized Amorphous Tacrolimus Nanoparticles in Mice

4.1 ABSTRACT

The objective of this study was to determine steady state trough levels and investigate the effect of chronic exposure of tacrolimus/lactose (TAC:LAC in a 1:1 ratio) produced by the Ultra-Rapid Freezing (URF) process and administered as a colloidal dispersion by nebulization to mice. Drug distribution in multiple organs and lung histology after chronic exposure was confirmed, and theoretical modeling techniques for estimating dissolution of drug *in vivo* are proposed.

Colloidal dispersions of TAC:LAC were administered by nebulization for 7 and 14 days to mice using a nose only dosing apparatus. URF processed TAC:LAC powders were redispersed (3 mL of water; 10 mg/mL TAC) to make the colloidal dispersions for nebulization using an ultrasonic nebulizer (Aeroneb® Pro) for a 10 minute dosing period. Immediately following dosing at days 7 and 14, the lungs, blood, heart, liver, kidneys, and spleen were removed and analyzed for TAC concentration by HPLC (lung TAC levels) and ELISA (blood and other organs). Lung histology of the mice in the experimental group versus control group (administered placebo), was studied using the Cimolai scoring. Computational methods were used to model dissolution of TAC nanoparticles *in vivo*.

Steady state trough levels of TAC showed high lung (6.97 μg/g wet lung weight) and blood levels (2.5 ng/mL). TAC partitioned from lungs into blood and organs (kidney

= 2.52 ng/g weight; liver = 1.86 ng/g weight; heart = 0.5 ng/g weight; and spleen = 1.3 ng/g weight). Histology analysis indicated no tissue damage following chronic lung exposure for 14 days using Cimolai scoring (0 - no inflammation). Computational modeling indicated fast dissolution of TAC:LAC nanoparticles *in vivo* after pulmonary administration primarily due to TAC nanoparticle characteristics (particle size, partitioning into various organs, degree and extent of supersaturation, and clogP values). URF compositions of TAC:LAC are dispersible and readily delivered by nebulization to mice. Drug distribution was observed in the mouse's organs, and chronic exposure to lung tissue caused no damage. Computational methods predicted rapid dissolution of TAC nanoparticles in the lungs.

4.2 INTRODUCTION

Tacrolimus (TAC) is a potent immunosuppressant drug derived from the soil bacterium *Streptomyces tsukubaensis* [1]. The main challenge with the drug is the low and erratic oral bioavailability that is exhibited by TAC formulations [2]. TAC is a calcineurin inhibitor having a similar mechanism of action to Cyclosporin A (CSA), but its immunosuppressive activity is 10-100 times greater than CSA [3, 4]. Orally dosed TAC, despite having high potency, exhibits low and erratic bioavailability due to first pass metabolism, extensive cytochrome P-450 (CYP 3A4) metabolism in the intestines, and high affinity for the p-glycoprotein (PGP) efflux pump [5-8]. The bioavailability of the drug can vary between 4% to 93%, showing extensive variability both inter- and intra-patient [9, 10].

The commercial formulations of TAC are Prograf® Oral Solution and Prograf® tablets, intended for oral administration. The challenges of oral inter- and intrapatient bioavailability exists when delivering this drug, due mainly to transporter activity and metabolic inactivation. The Prograf® tablet delivery system is a solid dispersion of TAC in a hydrophilic polymer matrix of hydroxypropylmethylcellulose (HPMC). The manufacture of this solid dispersion has been described by Yamashita et al. [11]. Briefly, the TAC is dissolved in ethanol, while the HPMC is swelled in the ethanol, but not dissolved. The resulting dispersion is homogenized and vacuum dried at 40^{o}C. The pulverized material is then incorporated with diluents into the tablet form for oral administration.

Other routes of administration of TAC have been evaluated for their effect, specifically improving bioavailability and inter- and intrapatient variability [12-14]. TAC was delivered by nebulization to the lungs to avoid the unfavorable side-effects of transporter activity and metabolic inactivation commonly associated with oral delivery [15]. Sinswat et al. evaluated the efficacy of dosing of TAC to the lungs of healthy mice [16]. The main mechanism of absorption of drugs from the pulmonary route is diffusion [17]. Lung tissue is highly vascularized, so sink conditions are often maintained [18]. Maintaining sink conditions in the lungs promotes diffusion of drugs into the blood from the lung tissue [17]. Solid drugs dissolve in the bronchial fluid and solubilized drug molecules, administered by the pulmonary route, diffuse across the alveolar monolayer into systemic circulation or act topically to exert their effect [19-21]. Gaseous drugs like nitrous oxide rely on the differences in partial pressures between the lung gases and dissolved gas in the blood in order to diffuse into the body [18]. Additionally, Vaughn et

al.[22] and Makino et al.[23] have shown uptake of nanoparticles by alveolar macrophages. This is also a mechanism by which drug particles can be delivered to the lungs and transported to the lymphatic system for systemic delivery [24]. Vaughn et al. showed uptake of itraconazole nanoparticles by the alveolar macrophages [22], using qualitative methods, while Makino et al. showed uptake of polystyrene microparticles in the size range of 2-5 μm by alveolar macrophages [23]. The mechanisms of supersaturated diffusion [25, 26] and macrophage uptake work concurrently to produce higher bioavailability in pulmonary formulations versus formulations delivered by the oral route. Pulmonary delivery of TAC allows for no intestinal metabolism by CYP 3A4 in the intestines, avoidance of first pass metabolism, and no PGP efflux into the large intestinal lumen.

Tacrolimus/lactose (TAC:LAC 1:1) nanoparticles were produced using the ultra-rapid freezing (URF) technology, which has been studied extensively [16, 27-29]. Micron-sized nano-structured aggregates of the TAC/LAC nanoparticles manufactured by URF have an amorphous morphology and, thus, have the ability to supersaturate dissolution media, which greatly enhances dissolution of poorly water soluble drugs in aqueous media. Previous studies by [16] have shown that nebulization of this TAC formulation can improve bioavailability and absorption, resulting in high lung and blood levels of the drug following lung to blood partitioning as described by Patton et al. [30]. A single- dose pharmacokinetic study confirmed that the maximum drug concentration (C_{max}) and area under the curve concentration vs. time curve (AUC's) for inhaled nebulized TAC:LAC formulations achieve very high lung concentration. This is important for patients receiving lung transplants and for preventing chronic graft

rejection post-transplant [16]. The physicochemical properties of the TAC:LAC formulation used in this study have been reported previously (i.e. surface area, dissolution properties, amorphous morphology, particle size) [16]. Although these studies showed promise for acute dosing of TAC:LAC via nebulized colloidal dispersion, it is important to study the effects of chronic dosing TAC:LAC to the lungs. The current research focuses on determining the long-term effects of multiple dosing of TAC:LAC to the lungs.

Additionally, a more thorough understanding of dissolution and absorption of nanodispersions in the lung tissue was sought. Thus, estimates of TAC:LAC dissolution and permeation times in the alveoli were used to determine if absorption times were sufficient to minimize macrophage uptake. Tam et al. have studied the *in vivo* effects of cyclosporin A dosed to the lungs of mice, and reported high lung blood levels with in a single-dose pharmacokinetic study [31]. This research also utilized computer-assisted computation to estimate the dissolution of nanoparticles and their partitioning into the lung epithelium [32]. Tam et al., however, used antisolvent precipitation for the production of the stabilized nanoparticles. Behavior of TAC:LAC nanoparticles in the lungs was studied using the model reported by Tam et al. [31]. Patton et al. have performed similar studies using *in vivo* modeling to predict particle dissolution [30].

The objective of this study was to determine the lung and blood trough levels of TAC after once a day dosing for 7 and 14 days, and to observe the potential long term effects of TAC:LAC dosing on lung tissue. The goal was to use non-polymeric, non-toxic generally regarded as safe (GRAS) excipients to deliver the TAC. Lactose, being a GRAS material should not cause irritation in lung tissue when a formulation containing

this excipient is delivered pulmonarily. Additionally, a second animal study, using rats was performed at a lower dosing level to compare results with Ide et al. [33]. This research confirmed dosing of TAC:LAC nanoparticles at a lower dose in rats to confirm the pharmacokinetic parameters. An *in silico* model of the dissolution of TAC:LAC nanoparticles in the lung surfactant fluid and subsequent diffusion into blood was also proposed, and showed agreement with the results *in vivo*.

4.3 MATERIALS AND METHODS

4.3.1 Materials

TAC was provided by The Dow Chemical Company (Midland, MI). Lactose monohydrate was USP grade, while, magnesium chloride hexahydrate, sodium chloride, potassium chloride, sodium phosphate dibasic, sodium sulfate, calcium chloride dihydrate, sodium acetate trihydrate, sodium bicarbonate, and sodium citrate dihydrate were analytical grade and purchased from Spectrum Chemicals (Gardena, CA). High performance liquid chromatography (HPLC) grade acetonitrile (ACN) and methanol (MeOH) were purchased from EM Industries, Inc. (Gibbstown, NJ). Liquid nitrogen was obtained from BOC Gases Company (Murray Hill, NJ). Deionized water was prepared by a Milli-Q purification system from Millipore Corporation (Molsheim, France). PRO-Trac® II Tacrolimus (FK-506) Enzyme-Linked Immunosorbant Assay (ELISA) assay kits were purchased from Diasorin Inc. (Stillwater, MN).

4.3.2 Preparation of Formulations by the URF Process

TAC:LAC formulations prepared by the URF process have been described previously [16]. Briefly, the compositions were prepared by dissolving TAC in ACN (60%), and lactose in water (40%), to make a drug/excipient ratio of 1:1 by weight. The two solvent preparations were mixed, creating a cosolvent system with a solids content of 0.75%. The cosolvent solution of drug/excipient was applied to the surface of a solid substrate, which was cooled using liquid nitrogen maintained at -80^{o}C, as described previously [28]. The frozen compositions were then collected and the solvents were removed using a Virtis Advantage Tray Lyophilizer (Virtis Company, Inc. Gardenier, NY), following the lyophilization protocol previously described [16]. The dry powders were packaged under dry nitrogen and stored at room temperature.

4.3.3 *In Vivo* Mouse Studies: Pulmonary Administration of URF Formulations

Pulmonary dosing of URF TAC:LAC the formulation was performed on healthy male ICR mice (Harlan Sprague Dawley, Inc. Indianapolis, IN). The study protocol was approved by the Institutional Animal Care and Use Committee (IACUC) at the University of Texas at Austin. All animals were maintained in accordance with the American Association for Accreditation of Laboratory Animal Care. A pulmonary dosing apparatus for the mice was used, which conveniently dosed up to four mice simultaneously, exposing only the nose of the animal to the drug-containing aerosol droplets [16]. The

nose-only dosing apparatus consists of a cylindrical tube of about 0.22 L volume into which the drug dispersion is nebulized, creating a cloud of drug-containing aerosol droplets measuring about 3 microns in diameter. Connected to the dosing cylindrical tube are up to four mouse restraint tubes (Battelle Toxicology, Inc., Columbus, OH). A small fan located behind the nebulizer insures that a constant cloud of drug is produced in the tube and circulated through the apparatus. This nose-only dosing apparatus is a closed system and has shown reproducible dosing results using nebulization [16]. Animals are acclimated for 15 minutes per day for 2 days prior to dosing, and their breathing and respiration rates are comparable to animals that are not confined.

The URF processed TAC:LAC powders were redispersed in 3 mL of water (10 mg/mL TAC) to make the colloidal dispersion using probe sonication in an ice bath for 1 minute and bath sonication at room temperature for 2 minutes prior to nebulization. Nebulization of the colloidal dispersion was conducted using an Aeroneb Pro® ultrasonic nebulizer (Aerogen, Ltd., Galway, Ireland) for a 10 minute dosing period. Animals were dosed once a day at every half-life (half life of TAC in lungs is approximately 20-22 hours) of the drug in the lungs, as determined previously by the single-dose pharmacokinetic study [16]. Mice were sacrificed at 24 hours after the last dosing period. A total of eight mice were used in the experimental group (dosed using TAC:LAC), and a total of four mice were used in the control group (dosed using nebulized lactose as a 10 mg/mL solution), as shown in Figure 4.1. On days 7 and 14, four mice were sacrificed from the experimental group, and two mice were sacrificed from the control group. Prior to euthanasia, the animals were examined for signs of unkempt grooming, loss of body hair, loss of weight, and uncontrolled diarrhea which might indicate toxicity of the

TAC:LAC formulation. Euthanasia was performed using gaseous isoflurane. Bronchio-alveolar lavage (BAL) with phosphate buffered saline was performed at the days 7 and 14 on two mice from the experimental group and one mouse from the control group, as described previously [22]. Lungs were removed from the remaining mice of the experimental group and the control group, inflated and treated using formalin (10% formaldehyde solution. Whole blood (1 mL aliquot) was obtained by cardiac puncture, and organs (lungs, heart, kidneys, liver, and spleen) were extracted from each mouse. The organs were visually inspected for scarring, irritation, tumor growth, hematoma, or other abnormalities [34]. Whole blood aliquots were mixed with heparinized saline (20 μL of 200 IU sodium heparin/mL) to prevent clotting. All organ weights were measured before TAC analysis was begun. Samples were stored at -20^{o}C until assayed for TAC concentration. TAC concentration in lung tissue was evaluated by HPLC assay, while TAC concentration in whole blood and other organs was evaluated using ELISA. Histological evaluation of the lung tissue was performed using matched lung tissue samples from experimental (TAC:LAC) and control mice (LAC only) embedded in paraffin wax. The stained lung sections from both the experimental and control groups were viewed by light microscopy and evaluated for tissue histology using the Cimolai scoring system.

An additional single dose study was performed in four rats dosed at 3.2 mg TAC to determine the 1 hour TAC blood and lung levels. Validation of TAC efficacy has been confirmed at lower lung levels (270.4 ng/g lung weight) by Ide et al. in a previous study [33]. Dosing was performed as described above; however, URF processed TAC:LAC powders containing 3.2mg TAC were redispersed in 3 mL of water for lower dosing of

the rats relative to the mouse study. All four rats were euthanized by CO_2 inhalation 1 hour after dosing. Whole blood (3 mL aliquot) was obtained by cardiac puncture immediately after sacrifice. Lungs were excised and stored at -20°C until homogenization and assay using ELISA.

4.3.4 ELISA for Analysis of TAC in Blood and Organs

The determination of TAC in whole blood and organs (kidney, spleen, heart, liver in higher dosed mice; lungs in lower dosed rats) was performed using the PRO-Trac® II FK 506 ELISA assay kit (Diasorin Inc., Stillwater, MN), in accordance with the manufacturer's instructions. Specifically, 50 µL of whole blood or tissue homogenate, along with standards included with the kit, were placed in conical 1.5 mL polypropylene tubes. Digestion reagent was freshly reconstituted, and 300 µL was added to all samples. The tubes were vortexed for 30 sec and incubated at room temperature for 15 min. The samples were then placed in a water bath maintained at 75^{o}C for 15 min to stop proteolysis. After vortexing for 1 min, the tubes were centrifuged at room temperature and 1800 X g for 10 min. The supernatant (100 µL) was transferred to the microtiter plate wells in duplicate from each of the centrifuged samples. Capture monoclonal anti-FK 506 antibody (50 µL) was added to each well, and the plate was shaken at room temperature and 700 RPM for 30 min. TAC horseradish peroxidase conjugate (50 µL) was then added to each well, and the plate was shaken at room temperature and 700 RPM for an additional 60 min. The plate was washed in triplicate with 300 µL of washing solution, before the addition of 200 µL chromogen. The plate was shaken again at 700

RPM for another 15 min at room temperature. The subsequent reaction was stopped by the addition of 100 μL of stop solution. The absorbance in each well was read using the microtiter plate reader (μQuant Microtiter Plate Reader, Biotek Instruments, Inc., Winooski, VT) at dual wavelengths of 450 and 630 nm. Data was plotted according to a four-parameter logistic (4PL) curve-fitting program.

4.3.5 Solid Phase Extraction of Lung Tissue

Lungs which were previously washed using the BAL procedure were analyzed using solid phase extraction followed by reverse phase HPLC. The total wet lung weight was recorded individually from each mouse dosed at 10 mg/mL. Lung tissue was homogenized using a Polytron rotor-stator homogenizer (VWR Scientific, West Chester, PA) for 45 sec in 1 mL of normal saline. The lung homogenate was then mixed with 0.5 mL of 0.4N zinc sulfate heptahydrate solution, and then a 1 mL aliquot of a mixture of methanol/water (70:30) was added to the homogenate. Acetonitrile (1 mL) was added to the homogenized samples before further vortexing for 1.5 minutes, followed by centrifugation at 3000 RPM for 15 min to obtain a clear supernatant. Next, the supernatant was collected into a clean vial containing 1 mL of purified water. Meanwhile, C18 cartridges for solid phase extraction (Supelco Inc., Bellfonte, PA) were preconditioned. The columns were pretreated with 2 mL ACN, followed by 1 mL MeOH, then washed with 1 mL of water before loading them with the supernatant. The sample was transferred and drawn through the column with slight vacuum pressure. The column was washed with 1.5 mL of methanol/water (70/30) solution, followed by 0.5 mL of n-

hexane and allowed to dry under vacuum. The sample was eluted with 2 mL of ACN (4 X 0.5 mL aliquots). The eluted material was evaporated to dryness with a nitrogen stream, and then reconstituted with 250 µL of mobile phase using the HPLC method for TAC analysis. The data is expressed as µg TAC/gram wet lung weight tissue.

4.3.6 HPLC Assay for Analyzing TAC

The HPLC method for analyzing TAC in mouse tissue samples (dosed at 10mg/mL) was adapted from Akashi et al [35]. The samples were analyzed with an HPLC at a wavelength of 215 nm using a Waters 515 liquid chromatograph with a Waters 996 Photo Diode Array (Waters Corp., Milford, MA) equipped with a Lichosphere RP C18 column 4 mm X 250 mm, 5 µm, part number CP28827 (Varian Corp. Lake Forest, CA). The column temperature is maintained at 50^{o}C. The mobile phase consists of 600 mL acetonitrile, 400 mL water, and 1 mL phosphoric acid. Tacrolimus exists in three tautomeric forms in solution, with all tautomers showing equivalent therapeutic activity [36]. The three tautomers elute at 6.6, 10.5, and 13.5 minutes, respectively, at a flow rate of 2 mL/min, and an injection volume of 20 µL was used. The summation of the tautomer peak areas is used to quantify the tacrolimus present in the samples. This HPLC method is linear and reproducible over a range of concentrations 100-1 µg/mL (r^2=0.9999) sirolimus with an limit of quantitation (LOQ) of 5 µg/mL and limit of detection (LOD) of 1 µg/mL TAC [35].

4.3.7 Particle Size Analysis

Atmospheric dynamic light scattering (DLS) measurements of the dispersed URF TAC:LAC (1:1) formulation in water were conducted using a BI-ZetaPlus from Brookhaven Instruments Corporation. The dispersion was sonicated for 15 minutes prior to measurement. Data analysis was conducted using a digital autocorrelator (Brookhaven Instruments Corporation, model BI-9000AT) with 522 real time channels and the NNLS program. The detection angle was 90°.

4.3.8 Statistical Analysis

Where applicable, data are given as mean with standard deviations. In vivo weights were analyzed by the one-way subjects ANOVA comparing experimentally dosed animals with control animals. Statistical significance was set at $p < 0.05$.

4.4 RESULTS AND DISCUSSION

4.4.1 Whole Blood and Organ TAC Concentrations at Steady State Trough Levels

The animals were dosed at every half-life for over 4-5 half lives (for the lung pharmacokinetic analysis), so the theoretical steady state of TAC *in vivo* was achieved. The half life of the TAC in the lungs was determined previously to be 20.75 hours [16]. Dosing of the drug at every half-life for 4-5 half lives has been shown to produce steady

state trough levels of drug, and mice were dosed for 7 and 14 days for this multi-dose study [32-34]. There were no adverse events or deaths of the mice in either the group receiving the TAC:LAC composition or the control group receiving LAC only, indicating that the treatment was well tolerated [37]. Both treatment groups exhibited normal behavior, grooming habits, and fecal excretion [34]. Weights of the animals in both groups were taken before sacrificing them, and the weights are shown in Table 4.1. Ide et al. previously reported that weight loss, diarrhea, and unkempt grooming accompanied pulmonary dosing of TAC [33], but none of these were observed in this multi-dose study.

In the experimental groups, TAC concentration in whole blood and organs was determined at steady state trough levels following 7 and 14 days of pulmonary dosing (whole blood, lungs, kidneys, spleen, heart, and liver). The results of the 7 and 14 day TAC analysis are shown in Table 4.2. The average lung level of TAC was 6.97 μg TAC/g wet lung weight over the study period, and the average blood TAC level was 2.5 ng TAC/mL over the study period. TAC was also found to have partitioned from the blood and distributed to the kidneys, spleen, heart, and liver. Of these organs, the kidneys showed the highest TAC concentration, indicating that the drug accumulates in the kidneys. This is significant because nephrotoxicity is associated with high level dosing of TAC [2, 9]. The kidneys showed an average of 2.52 ng TAC/g wet organ weight over the study period. It has been reported that kidney toxicity in rats begins at 10 mg/kg/day for subcutaneous TAC at Day 14 in a multi-dose study [38]. In the present study, the maximum dosing of mice was 0.55 mg TAC/day (3 mg/mL nebulized dispersion TAC/day, with a respirable fraction of 74%, in 4 animals). The kidneys of the experimental group were visually similar to those of control animals, with no hematoma

or kidney scarring observed, therefore, nephrotoxicity was not indicated in the 7 and 14 day multi-dose study. The TAC level in the kidneys was comparable to that of the blood, and since the kidneys are highly vascularized and blood is continuously filtered through this organ, a similar level of TAC was expected in this organ. The liver TAC concentration was lower than that measured in the blood and kidney (average 1.86 ng TAC/g liver weight). This is possibly due to the metabolism of the drug which occurs in the liver tissue. Since TAC is a known CYP 3A4 substrate [1, 8], the lower liver TAC concentrations were possibly due to the inactivation and metabolism of the drug in this organ. Lower levels of TAC were measured in the heart and spleen, specifically 0.5 ng TAC/g wet heart weight and 1.3 ng TAC/g wet spleen weight, respectively. Blood was collected by cardiac puncture, and there was no blood left in the heart prior to TAC tissue analysis, therefore partitioning of drug into these tissues was not as pronounced as in other tissues, probably due to protein binding of the drug in whole blood [1].

Transporters which can assist in pulmonary drug delivery have been found in lung tissue. Some of these transporters that have been discussed previously [7, 39, 40] in relation to oral drug delivery, also have application in pulmonary delivery. Efflux transporters, such as PGP, have been detected in normal and pathological lung tissue, though at a significantly lower amount than in the gastrointestinal tract [41]. PGP is expressed on the apical side of the ciliated epithelial cells in the connecting ducts of the lung, while smaller airways and alveoli contain little to none of the PGP transporters. Additionally, PGP is present in the lateral membranes of respiratory nasal mucosa. Expression of PGP in the lungs leads to the efflux of hydrophobic drugs from systemic circulation out of the lungs [42]. Drugs particles are incorporated into mucous in the

upper airways and ciliated cells move the particles up the mucociliary escalator, ultimately to the digestive tract. Drug particles can also be phagocytized by alveolar macrophages in the lower airways and moved to the lymphatic system [23]. Although present in lower amounts than in the intestine, multi-drug resistant protein 1A (MDR1A) has been detected in normal lung tissue (2% of the normal gastrointestinal tract concentration). Overexpression of the multi-drug resistant proteins 1, 3, and 8 (MDR1), (MDR3), and (MDR8) has been observed in non-small cell lung cancer cells, complicating the administration of chemotherapy for this disease [42]. Other adenosine triphosphate (ATP)-binding cassette (ABC) proteins like breast cancer resistant protein (BCRP) have also been detected in certain diseased lung tissue, and these transporters should be considered when formulating drugs for pulmonary delivery.

Other transporter proteins are located exclusively in the lung. Cystic fibrosis transmembrane conductance regulator (CFTR) is the most studied of the lung protein transporters. These proteins are highly expressed on the luminal side of serous cells and the apical side of the lung epithelium. They function as a chloride efflux pump in normal lung tissue, regulating the ionic balance between Na^+ and Cl^- that is essential for proper lung function. Mutations in the expression of this protein lead to cystic fibrosis (CF) and excess lung fluid build-up. Animal studies have shown that mice with the CFTR gene knocked out develop CF symptoms and frequently die of complications [42]. The therapeutic effect of drugs affecting the balance of chloride and sodium ions in the lung will be altered by the CFTR protein transporter. ATP-binding cassette A1 (ABCA1) is a protein transporter which controls the transport of cholesterols and phospholipids onto the surface of the lung alveoli [42]. These substances are critical in the formation of lung

surfactant fluid which lubricates the lung tissue during respiration. Bioavailability of sterol drugs deposited in the lungs could be affected by this protein transport system, reducing a drug's systemic concentration [42]. Although the lungs contain fewer transport mechanisms than the gastrointestinal tract [41], some protein transporters in the lungs can have an effect on pulmonary drug delivery. Scientists must understand these mechanisms when formulating drugs for pulmonary delivery since these transports can have an effect on a drug's bioavailability (either lowering the bioavailability or enhancing bioavailability, depending on the transporter/drug interaction) when delivering drugs to the lungs.

In comparison to the results reported by Ide et al. involving delivery of TAC to the lungs, the colloidal dispersion of TAC:LAC showed higher drug trough levels in the lung and blood than did the pMDI formulation at its C_{max} [33]. A TAC concentration of 0.1% in the pMDI was administered to rats. Similar total doses were administered in both the Ide et al. study and the Sinswat et al. study.(e.g. 1800 μg TAC/day; Ide et al. study and 1900 μg TAC/day; Sinswat et al. study [16]). The total lung levels of TAC at 1 hour for the Ide et al. study was 270 ng TAC/g wet lung weight, compared to the Sinswat et al. study which reported 6.5 μg TAC/g wet lung weight. The total blood concentration of TAC at 1 hour for the Ide et al. study was 4.9 ng TAC/mL whole blood, compared to the Sinswat et al. study which reported 268 ng TAC/mL whole blood. Even with the lower TAC levels, however, the Ide et al. study showed a significantly lower rejection rate than observed in the control group (no immunosuppressive treatment) when the TAC was administered to rats that had undergone unilateral left lung transplantation. These results were similar to the intramuscular injection of TAC at 1 mg/kg/day. Therefore, the

TAC:LAC nanoparticulate formulation dosed by nebulization should demonstrate efficacy against lung allograft rejection based on these reported lung and blood levels of the drug.

4.4.2 Lung Tissue Histology

Lung tissue histology was evaluated in both the experimental and control groups used in the TAC multi-dose study. After inflating of the lungs with formalin solution post-mortem, and matching similar sections of lungs which were stained and embedded in paraffin wax, a histological evaluation was performed on the lung tissue. Evidence of bronchiolar ulceration and tissue repair was also assessed. It is important to evaluate histological differences in lungs of the experimental versus lungs of the control group in order to observe if TAC caused damage to the lung tissue following chronic administration to the mice. The TAC:LAC formulations do not contain excipients that are known to damage the lung tissue [43]. Lactose in the nebulized control formulation did not elicit immune response or cause toxicity at the levels which were dosed. The images from microscopic evaluation are shown in Figure 4.2-4.5.

The images show that the alveoli are intact and do not display damage. Inflammation of the airways and cellular migration into the airways was not observed and the airways appeared clear. The airways show a distinct single cell layer consistent with alveolar physiology. There was no evidence of bronchiolar, peribronchiolar, or perivascular infiltrates in any of these groups [44]. Mice were euthanized with isoflurane which does not cause vascular congestion or edema associated with CO_2 narcosis. Additionally, no epithelial ulceration or evidence of cell repair was noted in either the

experimental or control groups. Common signs of lung tissue damage include peribronchial infiltrates, luminal discharge, and parenchymal pneumonia, along with infiltration of lung tissue by immune cells [45]. Additionally, perivascular edema was not observed, as expected, since the animals were euthanized using isoflurane gas. The only observations that were found in lung histology were a.) alveolar spaces, b.) capillaries, c.) lymph tissue, and d.) arterioles with red blood cells present. The lungs appeared to be normal, when compared to lungs that had not been dosed with any medication or lactose control. Based on the histology results, the TAC:LAC nebulized colloidal dispersion administered to the mice did not elicit an immune response or cause histology changes over the study period. Therefore, tacrolimus dosed to the lungs was demonstrated to be well tolerated in mice.

4.4.3 Modeling of TAC Nanoparticle Dissolution *In Vivo*

In order to better understand the role of dissolution and permeation of poorly water soluble drugs in the lungs, a model reported by Tam et al.[31] was used to predict absorption half lives of TAC in the lungs. Furthermore, the model was used to shed insight as to why the lung levels were significantly higher than in the blood and other organs. Briefly, the Noyes-Whitney equation was used to describe the dissolution rate of TAC spherical nanoparticles,

$$\frac{\partial M}{\partial t} = -\frac{D}{2r} 4\pi r^2 (C_{sat} - C) \qquad (1)$$

where the boundary layer thickness was approximated by the particle diameter, M is the mass of undissolved drug, r is the particle radius, C_{sat} is the drug equilibrium solubility, and C is the dissolved drug concentration in lung fluid. To account for a changing radius with time, the relationship $M = (4/3)\pi r^3 \rho$ was used to give the following equation.

$$\frac{\partial r}{\partial t} = -\frac{D}{2r\rho}(C_{sat} - C) \qquad (2)$$

The dissolved drug concentration over time was comprised of a generation term from particle dissolution and a depletion term from drug permeation

$$\frac{\partial C}{\partial t} = N_p D \frac{2\pi r}{V}(C_{sat} - C) - \frac{AP}{V} C \qquad (3)$$

where N_p is the number of drug particles deposited in an alveolus, and V and A are the volume of lung fluid and surface area for a single alveolus, respectively. It was assumed that the absorption of drug from each alveolus into the lung tissue was independent of absorption from other alveoli.

A solver program was used to simultaneously solve equations (2) and (3) (Matlab ode15s solver (Natick, MA)) with the initial conditions of t=0, $r=r_0$ and C=0. The Wilke-Chang equation was used to estimate a diffusion coefficient of $4.02*10^{-6}$ cm^2/s [46] based upon physical properties of TAC. A permeability value of 1.0×10^{-5} cm/s was chosen to model TAC lung permeability since common permeabilities of poorly water soluble drugs in lung cell cultures range between 10^{-6}-10^{-4} cm/s[47]. The number of drug particles deposited in the lungs was calculated from an estimated total mass of deposited drug and the average particle volume. The average TAC particle diameter was 468 nm, as measured by dynamic light scattering (Figure 4.6). The lung tissue C_{max} (14.1 μg/g) and

the corresponding blood concentration (402 ng/mL) from the single-dose pharmacokinetic study conducted by Sinswat et al.[16] were used to approximate the maximum mass of drug deposited in the lung at a given time. This value was chosen instead of the 7 day trough levels because it is believed to be a more accurate representation of the maximum deposited drug dose available for dissolution. The number of alveoli in a mouse was estimated to be ~2.25 x10^7, calculated using an alveolar surface area of 680 cm^2 [48] and alveolus diameter of 31 μm [49]. Total alveolar fluid volume was estimated to be 8.3 μL, based on a human alveolar surface fluid volume of 15 mL [30, 50] and the ratio of human lung to mouse lung weight. A value of 74.8 μg/mL was chosen for C_{sat} based on supersaturation dissolution results reported by Sinswat et al., which showed that the amorphous TAC:LAC (1:1) formulation was able to achieve dissolved concentrations 11 times the crystalline, bulk equilibrium solubility (6.8 μg/mL) in simulated lung fluid [16]. The mass of permeated drug, $M_{permeated}$, was determined from the mass of deposited drug $M_{o,}$ and the masses of undissolved and dissolved drug via the material balance

$$M_0 = N_p \frac{4}{3}\pi r^3 \rho + CV + M_{permeated} \qquad (4)$$

Figure 4.7 shows that the predicted absorption half-life for amorphous TAC:LAC nanoparticles is less than 10 seconds, indicating that the dissolution and permeation of the nanoparticles is extremely rapid. The absorption half-life is still predicted to be just over one minute even for a lower permeability of 10^{-6} cm/s, which is the lower limit of typical lung permeabilities for poorly water soluble drugs. However, crystalline, 3 μm TAC particles were not expected to dissolve and permeate quickly according to the model,

yielding absorption half-lives between 1-10 hours depending on the assigned permeability value. Thus, the formation of smaller particles with enhanced dissolution properties, as compared to traditionally aerosolized crystalline microparticles, have the potential to significantly decrease absorption half-lives of poorly water soluble drugs, in some cases by as much as two orders of magnitude. Rapid absorption of many drugs, including TAC, by the lung tissues is important to avoid uptake by macrophages, the primary clearance mechanism in the alveoli, as macrophage uptake of 1 μm particles has been observed as early as 15 minutes after particle deposition [51]. Even though phagocytosis is most prevalent for particles with diameters of approximately 1 μm and is less common for smaller particles [52-54], rapid particle dissolution is desired to further minimize macrophage clearance.

It is interesting to note that the model predicts that drug deposited on the alveoli should rapidly permeate to blood, yet lung levels are at least three orders of magnitude larger than the blood and organ levels 20 hours after dosing. A possible reason for this inconsistency is that TAC has been reported to have a high affinity for proteins found in lung tissue, such as serum albumin, membrane bound glycoproteins, and membrane bound protein receptors. (>98% protein bound) [2]. Consequently, drug absorption from the lung tissue into the blood compartment could be significantly retarded. Additionally, based upon dissolution results for the TAC:LAC formulation [16] and results from the model, particle dissolution should be rapid and is not expected to be the limiting factor in drug absorption. Thus, it is probable that the TAC:LAC nanoparticles dissolve rapidly upon deposition in the lung and permeate into the lung tissue. However, protein binding of TAC in the tissues is responsible for the low drug levels in the blood and the other

organs, and not insufficient drug dissolution. This result is desirable in the case of TAC, as it is an immunosuppressant often used by lung transplant recipients, where therapeutic levels in the lung tissue have not been easily achieved by non-pulmonary routes of delivery.

4.5 CONCLUSIONS

Pulmonary dosing of colloidal dispersions containing tacrolimus in the TAC:LAC formulation maintains high lung levels for chronic dosing for up to 14 days. Inflammation and irritation of the lung tissue were not observed histologically, and the formulation was well tolerated in the healthy mouse model. Computational methods predicted high theoretical dissolution rates *in vivo* upon deposition in the lung tissue, and partitioning of the drug is shown to occur from the lung tissue to the blood, and subsequent distribution of tacrolimus throughout the organs of the mouse show high levels of tacrolimus in the blood and organs of the mouse. Overall, the pulmonary route of administration for tacrolimus offers the advantages of higher bioavailability at the site of action, decreased drug metabolism, and systemic absorption of the drug, allowing for immunosuppressant activity throughout the body, compared to the conventional oral administration of TAC.

4.6 REFERENCES

1. M. A. Hooks, Tacrolimus - A New Immunosuppresant - Review of the Literature, Ann. Pharmacother. 28 (1994) 501-511.

2. R. Venkataramanan, A. Swaminathan, T. Prasad, A. Jain, S. Zuckerman, V. Warty, J. McMichael, J. Lever, G. Burckart, and T. Starzl, Clinical Pharmacokinetics of Tacrolimus, Clin. Pharmacokin. 29 (1995) 404-430.

3. M. D. Tacca, Prospects for Personalized Immunosuppression: Pharmacologic Tools - A Review, Transplant Proc. 36 (2004) 687-689.

4. A. B. Jain and J. J. Fung, Cyclosporin and Tacrolimus in Clinical Transplantation - A Comparative Review, Clin. Immunotherapeutics. 5 (1996) 351-373.

5. K. S. Pang, Modeling of Intestinal Drug Absorption: Roles of Transporters and Metabolic Enzymes, Drug Metabolism and Disposition. 31 (2003) 1507-1519.

6. A. M. Calcagno and T. J. Siahaan, *Physiological, Biochemical, and Chemical Barriers to Oral Drug Delivery*. Drug Delivery Principles and Applications, ed. B. Wang, T. Siahaan, and R. Soltero. 2005, Hoboken, NJ: Wiley and Sons.

7. S. Jang, M. Weintjes, and J. Au, Kinetics of P-glycoprotein Mediated Efflux of Paclitaxel, J Pharmacol Exp Therap. 298 (2001) 1236-1242.

8. W. G. Humphreys, *Presystemic and First-Pass Metabolism*. Drug Delivery Principles and Applications, ed. B. Wang, T. Siahaan, and R. Soltero. 2005, Hoboken, NJ: Wiley and Sons.

9. R. Venkataramanan, L. M. Shaw, L. Sarkozi, R. Mullins, J. Pirsch, G. MacFarlane, D. Scheller, D. Ersfeld, M. Frick, W. E. Fitzsimmons, M. Virji, A. Jain, K. L. Brayman, and A. Shaked, Clinical Utility of Monitoring Tacrolimus Blood Concentrations in Liver Transplant Patients, J. Clin. Pharmacol. 41 (2001) 542-551.

10. S. Zhang and M. E. Morris, *Efflux Transporters in Drug Excretion*. Drug Delivery Principles and Applications, ed. B. Wang, T. Siahaan, and R. Soltero. 2005, Hoboken, NJ: Wiley and Sons.

11. K. Yamashita, T. Nakate, K. Okimoto, A. Ohike, Y. Tokunaga, R. Ibuki, K. Higaki, and T. Kimura, Establishment of New Preparation Method for Solid Dispersion Formulation of Tacrolimus, Int J Pharm. 267 (2003) 79-91.

12. B. B. Ceyhan, M. Sungur, C. A. Celikel, and T. Celikel, Effect of Inhaled Cyclosporin on th Rat Airway: Histologic and Brochioalveolar Lavage Assessment, Respiration. 65 (1998) 71-78.

13. P. J. Atkins, N. P. Barker, and D. Mathisen, *The Design and Development of Inhalation Drug Delivery Systems*. Pharmaceutical Inhalation Aerosol Technology, ed. A.J. Hickey. Vol. 54. 1992, New York: Marcel Dekker.

14. J. C. Waldrep, New Aerosol Drug Delivery Systems for the Treatment of Immune-Mediated Pulmonary Diseases, Drugs of Today. 34 (1998) 549-561.

15. S. Tamura, Y. Tokunaga, R. Ibuki, G. L. Amidon, H. Sezai, and S. Yamashita, The Site-Specific Transport and Metabolism of Tacrolimus in Rat Small Intestine, J. Pharmacol. Exp. Therap. 306 (2003) 310-316.

16. P. Sinswat, K. A. Overhoff, J. T. McConville, K. P. Johnston, and R. O. Williams III, Nebulization of Nanoparticulate Amorphous or Crystalline Tacrolimus - Single Dose Pharmacokinetics Study in Mice, Eur J Pharm Biopharm. in press (2007.

17. M. G. Levitsky, *Pulmonary Physiology*. Vol. 1. 1982, New York: McGraw Hill.

18. J. H. Fleish, *Physiology and Pharmacology of the Airways*. Lung Biology in Health and Disease, ed. J.A. Nadel. Vol. 15. 1980, New York: Marcel Dekker.

19. I. Gonda, *Targeting by Deposition*. Pharmaceutical Inhalation Aerosol Technology, ed. A.J. Hickey. Vol. 54. 1992, New York: Marcel Dekker.

20. D. C. Thompson, *Pharmacology of Therapeutic Aerosols*. Pharmaceutical Inhalation Aerosol Technology, ed. A.J. Hickey. Vol. 54. 1992, New York: Marcel Dekker.

21. A. J. Hickey, *Pulmonary Drug Delivery: Pharmaceutical Chemistry and Aerosol Technology*. Drug Delivery Principles and Applications, ed. B. Wang, T. Siahaan, and R. Soltero. 2005, Hoboken, NJ: Wiley and Sons.

22. J. M. Vaughn, N. P. Wiederhold, J. T. McConville, J. J. Coalson, R. L. Talbert, D. S. Burgess, K. P. Johnston, R. O. Williams III, and J. I. Peters, Murine airway histology and intracellular uptake of inhaled amorphous itraconazole, Int. J. Pharmaceutics. in press (2007.

23. K. Makino, N. Yamamoto, K. Higuchi, N. Harada, H. Ohshima, and H. Terada, Phagocytic Uptake of Polystyrene Microspheres by Alveolar Macrophages: Effects of the size and surface properties of the microspheres, Colloids and Surfaces B: Biointerfaces. 27 (2003) 33-39.

24. M. Geiser, Morphological aspects of particle uptake by lung phagocytes, Micros. Res. Tech. 57 (2002) 512-522.

25. P. Sinswat, M. E. Matteucci, K. P. Johnston, and R. O. Williams III, Dissolution Rates and Supersaturation Behavior of Amorphous Repaglinide Particles Produced by Controlled Precipitation, J. Biomed. Nanotechnol. 3 (2007) 18-27.

26. J. M. Vaughn, J. T. McConville, M. T. Crisp, K. P. Johnston, and R. O. Williams III, Supersaturation produces high bioavailability of amorphous danazol particles formed by evaporative precipitation into aqueous solution and spray freezing into liquid technologies, Drug Development and Industrial Pharmacy. 32 (2006) 559-567.

27. J. C. Evans, B. D. Scherzer, C. D. Tocco, G. B. Kupperblatt, J. N. Becker, D. L. Wilson, S. A. Saghir, and E. J. Elder, *Preparation of nanostructured particles of poorly water soluble drugs via a novel ultra-rapid freezing technology*, in *Polymeric Drug Delivery - Polymeric Matrices and Drug Particle Engineering*, S. Svenson, Editor. 2006, American Chemical Society: Washington, DC. p. 320-328.

28. K. A. Overhoff, J. D. Engstrom, B. Chen, B. D. Scherzer, T. E. Milner, K. P. Johnston, and R. O. Williams III, Novel Ultra-Rapid Freezing Particle Engineering Process for Enhancement of Dissolution Rates of Poorly Water Soluble Drugs, Eur J Pharm Biopharm. 65 (2007) 57-67.

29. T. Purvis, M. E. Matteucci, M. T. Crisp, K. P. Johnston, and R. O. Williams III, Rapidly Dissolving Repaglinide Powders Produced by the Ultra-Rapid Freezing Process, AAPS Pharm Sci Tech. in press (2007.

30. J. S. Patton, C. S. Fishburn, and J. G. Weers, The Lungs as Portal Entry for Systemic Drug Delivery, Proc Am Thorac Soc. 1 (2004) 338-344.

31. J. Tam, J. T. McConville, R. O. Williams III, and K. P. Johnston, Antisolvent Precipitation of Cyclosporin A Nanoparticles for Enhanced Pulmonary Delivery, in review. (2007.

32. E. E. Schneeberger, *Structural Basis of Pulmonary Endothelial Permeability*. Lung Biology in Health and Disease, ed. U.S. Ryan. Vol. 32. 1987, New York: Marcel Dekker.

33. N. Ide, T. Nagayasu, K. Matsumoto, T. Tagawa, K. Tanaka, T. Taguchi, Y. Sumida, and M. Nakashima, Efficacy and Safety of Inhaled Tacrolimus in Rat Lung Transplantation, J. Thorac. Cardiovasc. Surg. 133 (2007) 548-553.

34. H. Hendrich, *The Laboratory Mouse*. 2 ed. Handbook of Experimental Animals, ed. H. Hendrich. Vol. 3. 2004, New York: Academic Press. 656.

35. T. Akashi, T. Nefuji, M. Yoshida, and J. Hosoda, Quantitative Determination of Tautomeric FK 506 by Reversed Phase Liquid Chromatography, J. Pharm. Biomed. Analy. 14 (1996) 339-346.

36. M. Ricciutelli, P. Di Martino, L. Barboni, and S. Martelli, Evaluation of rapamycin chemical stability in volatile-organic solvents by HPLC, J Pharm Biomed Anal. 41 (2006) 1070-1074.

37. K. Loser, S. Balkow, T. Higuchi, J. Apelt, A. Kuhn, T. A. Luger, and S. Beissert, FK-506 Controls CD40L-Induced Systemic Autoimmunity in Mice, J. Invest. Dermatol. 126 (2006) 1307-1315.

38. K. W. Mollison, T. Fey, R. A. Krause, J. M. Andrews, P. T. Bretheim, P. K. Cusick, G. C. Hsieh, and J. R. Luly, Nephrotoxicity studies of the immunosuppressants tacrolimus (FK506) and ascomycin in rat models, Toxicology. 125 (1998) 169-181.

39. C. Kruijtzer, J. Beijen, and J. Schellens, Improvement of Oral Drug Treatment by Temporary Inhibition of Drug Transporters CYP 450 in the GI Tract and Liver: An Overview, Oncologist. 7 (2002) 516-530.

40. C. P. Leamon and P. S. Low, *Receptor-Mediated Drug Delivery*. Drug Delivery Principles and Applications, ed. B. Wang, T. Siahaan, and R. Soltero. 2005, Hoboken, NJ: Wiley and Sons.

41. D. A. Groneberg, A. Fischer, K. Chung, and H. Daniel, Molecular Mechanisms of Pulmonary Peptidomimetic Drug and Peptide Transport, Am J Resp Cell Mol Biol. 30 (2004) 251-260.

42. M. V. D. Deen, E. D. Vries, W. Timens, R. Scheper, and D. S. Postma, ATP binding cassette (ABC) transporters in normal and pathological lung, Respiratory Research. 6 (2005) 1-16.

43. P. Baldrick and D. G. Bamford, A toxicological review of lactose to support clinical administration by inhalation Food Chem Toxicol. 35 (1997) 719-733.

44. N. Cimolai, G. P. Taylor, D. Mah, and B. J. Morrison, Definition and Application of a Histopathological Scoring Scheme for an Animal Model of Acute Mycoplasma-Pneumoniae Pulmonary Infection, Microb. Immunol. 36 (1992) 465-478.

45. T. Whelan and M. Hertz, Allograft Rejection After Lung Transplantation, Clinics in Chest Medicine. 26 (2005) 599-612.

46. W. L. McCabe, J. C. Smith, and P. Harriott, *Unit Operations of Chemical Engineering*. 6th ed. 2001, Boston, MA: McGraw Hill Inc.

47. B. Forbes and C. Ehrhardt, Human respiratory epithelial cell culture for drug delivery applications, European Journal of Pharmaceutics and Biopharmaceutics. 60 (2005) 193-205.

48. A. Geelhaar and E. R. Weibel, Morphometric estimation of pulmonary diffusion capacity. 3. The effect of increased oxygen consumption in Japanese Waltzing mice, Respiration Physiology. 11 (1971) 354-66.

49. H. Lum and W. Mitzner, A species comparison of alveolar size and surface forces, Journal of applied physiology 62 (1987) 1865-71.

50. R. W. Niven, *Pharmaceutical Inhalation Aerosol Technology*. Drugs and the Pharmaceutical Sciences, ed. A.J. Hickey. Vol. 54. 1992, New York, New York: Marcel Dekker, Inc. 340.

51. P. Forsgren, J. Modig, B. Gerdin, B. Axelsson, and M. Dahlback, Intrapulmonary deposition of aerosolized Evans blue dye and liposomes in an experimental porcine model of early ARDS, Upsala Journal of Medical Sciences. 95 (1990) 117-36.

52. W. G. Kreyling and G. Scheuch, *Clearance of Particles Deposited in the Lungs* Lung Biology in Health and Disease, ed. P. Gehr and J. Heyder. Vol. 143. 2000, New York: New York Marcel Dekker Inc.

53. H. M. Courrier, N. Butz, and T. F. Vandamme, Pulmonary Drug Delivery Systems: Recent Developments and Prospects, Critical Reviews in Therapeutic Drug Carrier Systems. 19 (2002) 425-498.

54. G. Oberdoerster, Effects and fate of inhaled ultrafine particles, ACS Symposium Series. 890 (2005) 37-59.

Chapter 5: Efficacy of Tacrolimus Nanoparticles Using *In Vitro* Cellular Assays for Immune Function

5.1 ABSTRACT

Tacrolimus (TAC) has been shown to be an effective treatment for a variety of autoimmune conditions, specifically host/graft disease and allograft transplant maintenance in transplant patients. However, the current TAC commercial products, the Prograf capsule and the Prograf oral solution show low and often variable serum levels, partially related to first pass metabolism and cytochrome P450 isoenzymes (CYP 3A4) within the gastrointestinal tract. Other routes of administration have been explored to improve the bioavailability of this drug and reduce the dose, so as to overcome the nephrotoxicity associated with high doses often required with this drug. A novel ultra-rapid freezing technology (URF) has been developed which allows for the drug to be reduced to a 200-800 nm amorphous particles, which produces a fine drug dispersion in saline. The purpose of this study was to evaluate the efficacy of these particles using the mixed leukocyte culture (MLC) assay to assess the inhibition of lymphocytes by commercial tacrolimus and nanoparticles of tacrolimus.

MLC assays have previously been used to determine matched host/donor compatibility in transplant patients. Phytohemagglutinin (PHA) assays have also been used to determine the proliferative capability of lymphocytes. Using PHA, abnormal lymphocyte proliferation occurs in subjects with aplastic lymphoma and other hematological disorders. In previous studies, investigators have used the MLC assay and

PHA assay to assess the ability of drugs to suppress lymphocyte function. In one study, Wright et al. [1] tested the efficacy of several immunosuppressive compounds, including cyclosporine and tacrolimus, by assessing the degree of lymphocyte proliferation utilizing MLC and PHA assays.

In the present study, we utilized a similar model to compare commercial tacrolimus to two formulations of nanoparticles of tacrolimus created in our lab.. The three formulations tested in this study were: commercial tacrolimus (TAC) prepared by dissolving Prograf® capsules as described by Wright [1], and two nanoparticulate TAC formulations produced by ultra rapid freezing: URF-TAC (a crystalline nanoparticle of pure tacrolimus) and TAC:LAC (an amorphous nanoparticle of tacrolimus stabilized by lactose). Both nanoparticle preparations, TAC:LAC and TAC:URF, showed greater suppression of lymphocytes proliferation than commercial tacrolimus (TAC) on a milligram to milligram basis. This finding was true for both the MLC and PHA assays.

5.2 INTRODUCTION

Tacrolimus (TAC) is an immunosuppressant drug derived from *Streptomyces tsukubaensis*, classified as a macrolide lactone that inhibits calceneurin within lymphocytes [2]. The drug is primarily used in solid organ transplants to prevent rejection of the allograft . Mechanistically, it binds to an immunophilin, followed by the binding of the TAC-immunophilin complex to calceneurin and the inhibition of the phosphatase activity. In this way, it prevents the passage of lymphocytes from G0 to the G1 phase of growth [2]. TAC has been shown to be more potent than cyclosporin, with an improved

side effect profile [3]. Despite its widespread use, the current forulation has several linitations including its low water solubility, variability in its bioavailability [4], and its metabolic transformation by cytochrome enzymes in both the gastrointestinal tract and the liver [4, 5].

TAC has been processed into a more water-dispersible formulation, by our group, using a cryogenic process called Ultra-Rapid Freezing (URF) and utilizing lactose (LAC) as an excipient [6]. Using this process, the drug/excipient solution is dissolved in a co-solvent system and rapidly frozen. Lyophilization of the solvent produces amorphous nanoparticle aggregates of the drug/excipient in solid solution (URF-TAC:LAC, 1:1). Pure tacrolimus has also been processed using URF (URF-TAC), showing crystalline structure due to the absence of stabilizers to keep it in an amorphous form. *In vitro* characterization of formulations produced by these processes confirmed that individual primary nanoparticles are produced in size ranging from 200-800 nm in size, aggregated into larger secondary particles which can be deaggregated with probe sonication [6]. These particles have the potential to enhance oral administration as well as being delivered to the lung by means of nebulization [7, 8].

Previous studies have used MLC and PHA to determine the effectiveness of immunosuppressive drugs on lymphocytes. Wright et al have used human and pig lymphocytes to evaluate various immunosuppressants on lymphocyte proliferation [1]. This study evaluated many different kinds of immunosuppressants such as cyclosporin A, azathioprine, sirolimus, tacrolimus, and mycophenolate mofetil using these techniques. In these studies, Wright et al used the various immunosuppressants at various concentrations, in solution, to derive the results for pig and human immunosuppression [1].

In the present study, the method outlined by Wright was used, and a dose was chosen of commercial tacrolimus that should suppress lymphocyte function by 40-50%. Additionally, we used the same concentration of tacrolimus nanoparticles (TAC:LAC and URF-TAC) dispersed in suspension, to determine the efficacy of these formulations on suppression of human lymphocytes *in vitro*. The objective of this study, therefore, was to establish the stability of TAC nanoparticles in cell growth medium, and to evaluate the *in vitro* efficacy of the three formulations.

5.3 MATERIALS AND METHODS

5.3.1 Materials

For testing of TAC (both URF-TAC and TAC:LAC) nanoparticles in the growth medium, the materials that were used were RPMI 1640 tissue culture medium (Fisher Scientific Product #MT15040CN, Fair Lawn, NJ) (mixed with 1M Hepes buffer (Fisher Scientific Product #MT250CI, Fair Lawn, NJ), L-glutamine (100X) (Fisher Scientific Product #ICN1680149, Fair Lawn, NJ), MEM vitamins (Fisher Scientific Product #BW13114E, Fair Lawn, NJ), and an antibiotic/antimycotic solution containing penicillin (10,000 u/mL, streptomycin (10,000 u/mL), and amphotericin B (25 µg/mL) (Fisher Scientific Product #SV3007901, Fair Lawn, NJ)). This is a growth medium, provided by the histocompatibility laboratory at the University of Texas Health Science Center, San Antonio, TX, which has been shown to stimulate proliferation of lymphocytes, when a

specific mitogen is added, and inhibiting growth of undesirable microorganisms (bacteria and fungi). This growth medium will be referred to as RPMI 1640, throughout this manuscript because it is the medium used in all tests performed. 96-well plates (BD Falcon, Franklin Lakes, NJ) were purchased and used to observe stability of the nanoparticles over a 5 day incubation period at 37^{o}C. Tacrolimus (99%+ purity) was purchased from Haorui Pharma-Chem, Inc (Edison, NJ), and lactose monohydrate, USP was purchased from Spectrum Chemicals (Gardena, CA). Prograf® capsules 5mg were purchased from University Hospital Pharmacy, San Antonio, TX. Absolute ethanol, USP was purchased from Aaper Alcohols (Lot # 06H30GA, Shelbyville, KY). Saline solution was purchased from Sigma, Inc. (St. Louis, MO).

For the MLC/PHA tests, the following items were provided by the University of Texas Health Science Center Histocompatibility Lab, San Antonio, TX: RPMI 1640 (with added ingredients listed above), heat inactivated pooled human serum (Atlanta Biologics, Atlanta, GA; Product # 5401101), sterile plastic tissue culture tubes (15 mL, conical) (Medsupply Partners, San Antonio, TX), sterile serologic pipettes (BD Falcon, Franklin Lakes, NJ), sterile 96-well round bottom tissue culture plates with lids (BD Falcon, Franklin Lakes, NJ), tritiated thymidine (specific activity 6.7 Ci/mM) (Perkin Elmer, Waltham, MA), Microscint® scintillation cocktail (Perkin Elmer, Boston, MA), phytohemagglutinin (Sigma Company, Lot # L8754), trypticase soy broth (Fisher Scientific Product #EB21715, Fair Lawn, NJ), pooled panel lymphocytes collectively representing all DR and DQ types (prepared at UTHSCSA), tabletop centrifuge (Eppendorf Micro Centrifuge, Product #5415C, Westbury, NY), Eppendorf pipettes (Westbury, NY), Coulter counter (Perkin Elmer TopCount NXT, Boston, MA), 5% CO_2

incubator (Queue Systems, Product # 2200, North Branch, NJ), and cell sample harvester (Filtermate Harvester Unifilter, Perkin Elmer, Boston, MA)..

5.3.2 Methods

5.3.2.1 *MLC and PHA Assays*

The MLC assay and PHA assay were conducted at the histocompatibility lab at the University of Texas Health Science Center in San Antonio. During these tests, TAC (from 5mg Prograf® capsules) was dissolved in absolute ethanol to 1mg/mL, similar to Wright et al [1]. The Wright et al. paper notes that the small amount of ethanol used to dissolve the TAC should have no effect on the proliferation rate of the lymphocytes in culture [1]. Briefly, the URF-TAC and TAC:LAC were dispersed in normal saline at a concentration of 1mg/mL for 2 minutes with a probe sonication in an ice bath, followed by 5 minutes of standing, and another 1 minute of sonication at room temperature. A uniform dispersion of both formulations was obtained. Two dilutions of all three formulations were made, then a third dilution was made from the second stock solution, because different concentrations of TAC are needed for the MLC and PHA assays. For the MLC assay, the IC_{50} was calculated to be 0.4-0.5 ng/mL [16, 17], while the PHA IC_{50} was calculated to be 0.23 ng/mL [17]. Dilutions of each of the three formulations were made accordingly. The MLC and PHA assays were then carried out per the protocol set up in the histocompatibility lab, and described by Segall et al [18] and others [1, 19]. In a 96-well plate, for the MLC assay, 100 µL of lymphocytes ($5x10^5$ cells/mL) from one donor and

100 μL of lymphocytes ($5x10^5$ cells/mL) from another donor, in RPMI 1640 growth medium with added serum was pipetted in triplicate. A 50 μL aliquot of each of the three TAC formulations was then added to the cell cultures. In another 96-well plate, for the PHA assay, 200 μL of lymphocytes ($5x10^5$ cells/mL) from the same donor, in RPMI 1640 growth medium with added serum was pipetted in triplicate. A 50 μL aliquot of each of the three TAC formulations was the added to the cell cultures. A control group (Panel X) was also used to compare the proliferation of lymphocytes in the experimental groups containing the three TAC formulations. Incubation of the cells at 37^oC, 5%CO_2 was then performed for 3 days. The trays were then labeled with 1 μCi of tritiated thymidine on day 5. Eighteen hours after labeling the trays, the cells were harvested, and the scintillation counter was used to determine the counts per minute (CPM) of radiation from the triplicate set of each sample. The percent relative response (%RR) was then calculated for each triplicate set of samples, and the results were reported as percent inhibition [18].

5.3.2.2 Statistical Analysis

Statistical analysis was performed with analysis of variance (ANOVA), using Excel. The Tukey's post-hoc analysis was then performed with Minitab Release 14. For the purposes of the statistical analysis, p-values < 0.05 were considered significant. The statistical significance of the inhibition ability of TAC:LAC, URF-TAC, and TAC in both experiments (with MLC data and PHA data) was analyzed and reported.

5.4 RESULTS AND DISCUSSION

For oral administration, the reduced particle size, along with the amorphous nature of the particles, allows for more rapid dissolution as well as supersaturation dissolution, with apparent solubility above the equilibrium solubility of the drug. Increased supersaturation can allow for increased drug flux across biological membranes, and, thus, increased drug bioavailability [9, 10]. For pulmonary administration, when nebulized in aqueous dispersion, these particles fit into aerosol droplets in the respirable size range of 3-5 μm [6]. The advantage of pulmonary administration in lung transplant patients is that the drug is localized to the site of action and acts at therapeutically relevant levels systemically.

The mechanism of action of TAC is important in understanding the methods of *in vitro* testing used in this study. TAC, like cyclosporin A (CSA), is a calcineurin phosphatase inhibitor [11]. They both have the end result of halting the cascade of reactions that allow for the maturation of lymphocyte cells into the specialized B- and T-lymphocytes needed in the immunosuppressive action of the immune system. CSA, however, binds to CyP-18, whereas TAC binds with FKBP-12. Both of these binding mechanisms result in the same suppression of calcineurin phosphatase, an enzyme involved in the activation of the transcription factor NF-AT, required for the expression of interleukin-12 (IL-12), interferon-gamma (INF-γ), and tumor necrosis factor alpha (TNF-α) genes. These genes in turn inhibit the immunophilin that begins the maturation cascade for lymphocytes. Since the binding of CSA to CyP-18 is 50-100 times less potent in the inhibition of calcineurin phosphatases than the TAC/FKBP-12, TAC is dosed at a lower level, and shows less nephrotoxic side effects than does CSA [12].

In vitro lymphocyte assays have been used to determine the compatibility of hosts with potential donors in transplant operations. Mixed lymphocyte culture (MLC) is an assay which uses lymphocytes from the host and the donors [13]. When these lymphocytes are mixed and incubated in growth medium, they will proliferate, as in response to one another, like a foreign antigen. A high rate of lymphocyte proliferation indicates poor host/donor compatibility, while a low rate of lymphocyte proliferation indicates good host/donor compatibility. These assays are routinely used in histocompatibility and immunogenics laboratories to determine potential transplant matches. Briefly, the host lymphocytes are added to the potential donor lymphocytes in triplicate into a 96 well plate containing Roswell Park Memorial Institute (RPMI) growth medium. Incubation of the cells at 37^{o}C and 5% CO_2 for 5 days produces the antigenic response. After the 5 days (120 hours) of incubation, 1μCi of tritiated thymidine (^{3}H-Thy) is added to the cells in order to radiolabel new cell proliferation. Eighteen hours after labeling the cells with ^{3}H-Thy, the cells are removed from incubation, rinsed from the growth medium and ^{3}H-Thy, and harvested. The new proliferated cells that have grown (and hence taken up the ^{3}H-Thy) in the 18 hours since the radiolabeled thymidine was added are then used to determine the counts per minute (CPM) of radiation that is released from the cells. High amounts of radiation indicate high levels of proliferation, and poor host/donor compatibility. Low amounts of radiation indicate low levels of proliferation, and good host/donor compatibility. Data analysis determines the CPM for each of the samples, and relative response (%RR) values are determined using the mean CPM of the controls, autologous cells, and test samples [13].

Another *in vitro* test for lymphocyte proliferation involves exposing the lymphocytes to an agent which is known to cause proliferation. These agents are called mitogens, and there are several available, including: phytohemagglutinin (PHA), concanavilin A (ConA), concavolin (CON) and pokeweed extract mitogen (PWM) [14]. These are non-specific mitogens which cause variable proliferation rates of lymphocytes, so test controls must be used when running a PHA assay. These tests evaluate the viability and ability of the lymphocytes to proliferate properly under a controlled set of conditions. These tests can determine several disease states such as lymphoma, autoimmune diseases involving lymphocytes, or other such autoimmune deficiencies.

5.4.1 MLC Assay

The MLC assays were performed twice, with 4 different donors' lymphocytes, to ensure that the results were consistent. In the first experiment, all three formulations of TAC inhibited the proliferative responses of pooled allogenic cells, with URF-TAC having the greatest inhibitory effect (65% inhibition), followed by TAC:LAC (55% inhibition), and the least effect was observed with Prograf® TAC (39% inhibition). These results are shown in Table 5.1. In the second experiment, different donors were used, and inhibition of lymphocyte proliferation was observed in each TAC formulation. The second experiment, however, showed TAC:LAC (86% inhibition) having a greater inhibitory effect than did the URF-TAC (66% inhibition), with Prograf® TAC (45% inhibition) showing the least inhibition. Effects were similar with two different cell sources used as responders. Triplicates of the samples were reasonably close in both the

first and second experiments. The results are shown in Table 5.1. Also, in the second experiment, it is interesting to note that the MLC assay with no drug added showed a much higher proliferation, shown in CPM, indicating that the second host/donor pair was much less compatible than the first. The human leukocyte antigen response for the DP and DQ antigens may have been more active in proliferating and reproducing lymphocytes [20]. In all cases, proliferation of cells without drug present was evident by the high CPM rate, indicating that the cells reproduced rapidly and absorbed the ^{3}H-Thy at a high amount. For the MLC experiment, ANOVA showed the p-value = 0.002, therefore these results are statistically significant. The variance between TAC:LAC, URF-TAC, and TAC dissolved in ethanol were 0.02, 0.01, and 0.01, respectively, showing reasonable variability between experiments. Tukey's post-hoc analysis of the MLC samples demonstrated that the TAC:LAC and URF-TAC groups provided statistically significant increases in inhibition over TAC dissolved in ethanol. Furthermore, TAC:LAC and URF-TAC did not show significant improvement in inhibition when compared to each other.

A possible reason for differences in results between the first and second experiment deals with the calcineurin and immunophilin binding of TAC between responders in the two different tests [21]. The same responders were not used in both tests, allowing for possible differences in TAC binding to lymphocytes. Previous studies have shown that calcineurin is expressed at different levels in different individuals [22, 23], and since binding to calcineurin is the first step in the cascade mechanism of immunophilin binding in the TAC immunosuppressive response, different levels of calcineurin could play a role in the proliferation of lymphocytes [24, 25]. The Human Leukocyte Antigen

(HLA) response system is a major factor for determining host/donor compatibility during allograft transplantation [26]. Three major classes of HLA have been reported, while minor Class II proteins are encoded on these genes. The major classes of HLA are: HLA-A, HLA-B, and HLA-C [27]. The minor classes of proteins encoded on these genes are DP, DQ, and DR [27]. Depending on the HLA serotyping of the responders used in these tests, high or low proliferation of lymphocytes could result in the MLC study. This could introduce variability in the study, and that is why triplicate readings are necessary for the MLC assay. In our studies, the triplicate values for inhibition were very similar, and results with the 3 TAC formulations were similar in the first and second tests. Therefore, URF processing of TAC, whether the formulation was crystalline (URF-TAC) or amorphous (TAC:LAC), showed significant improvement in inhibition of proliferation of cell cultures than TAC dissolved in ethanol.

5.4.2 PHA Assay

The PHA assays were performed twice, with 2 different donors' lymphocytes, to ensure that the results were consistent. The results of test one and test two are shown in Table 5.2. Since PHA is a non-specific mitogen with different affinities for different responders [28], there is an inherent slight difference between proliferation of lymphocytes when performing this test. Mitogens such as PHA are chemicals, usually proteins that encourage a cell to commence cell division, triggering the proliferation of these cells [29]. Mitogens trigger signal transduction pathways in which mitogen-activated protein kinase is involved, leading to mitosis. Depending on the genes present in the responder's cells,

these mitogens can elicit a large proliferative response, or a small proliferative response. Controls groups (Panel X) are used to normalize the results of the PHA test.

The first run of the PHA test corroborated the results shown in the MLC study. The mean results showing URF-TAC having the greatest inhibition (75% inhibition), followed by TAC:LAC (65% inhibition) and Prograf® (43.% inhibition). The second run had mean values of TAC:LAC (70% inhibition), URF-TAC (65% inhibition), and Prograf® (52% inhibition). In all cases, however, proliferation of cells without drug present was evident by the consistent CPM rate, indicating that the cells reproduced rapidly and absorbed the ^{3}H-Thy. In analyzing the ANOVA statistics, the p-value of the group was not < 0.05 (p-value=0.04), therefore the results are not significantly different between groups. The ANOVA variance between TAC:LAC, URF-TAC, and TAC dissolved in ethanol were 0.01, 0.02, and 0.03, respectively. In the Tukey's post-hoc test, TAC:LAC was shown to statistically improve inhibition over TAC dissolved in ethanol, however, the improvement of URF-TAC compared to TAC dissolved in ethanol was not statistically significant. Additionally, the improvement of inhibition of TAC:LAC over URF-TAC was not statistically significant. The data in the PHA tests are variable, but this is not unexpected due to the biological nature of the work being done, and using PHA, which has affinity for some cells more than others. However, the mean values for inhibition indicated a trend that showed a significant improvement in URF processed TAC, whether crystalline (URF-TAC) or amorphous (TAC:LAC), in the inhibition of lymphocyte proliferation than does TAC dissolved in ethanol.

5.5 CONCLUSIONS

The results of the MLC test clearly demonstrate that the nanoparticles of TAC (e.g. TAC:LAC and URF:TAC) show greater inhibition of proliferation than solubilized TAC. A similar trend is observed with the PHA test. These results may have important clinical applications and indicate that the form of TAC that is being administered influences the degree of immunosuppression.

5.6 ACKNOWLEDGEMENTS

The authors of this manuscript wish to thank the Histocompatibility lab at the University of Texas Health Science Center, San Antonio, TX for their support, specifically Brooke Holt, Laura McNeish, and Juan Segovia for donation of their blood and their help with the MLC and PHA assays.

5.7 REFERENCES

1. Wright DC, Deol HS, Tuch BE. A comparison of the sensitivity of pig and human peripheral blood mononuclear cells to the antiproliferative effects of traditional and newer immunosuppressive agents. Transplant Immunology 1999; 7:141-147.

2. Hooks MA. Tacrolimus - A New Immunosuppresant - Review of the Literature. Ann. Pharmacother. 1994; 28:501-511.

3. Jain AB, Fung JJ. Cyclosporin and Tacrolimus in Clinical Transplantation - A Comparative Review. Clin. Immunotherapeutics 1996; 5:351-373.

4. Venkataramanan R, Swaminathan A, Prasad T, et al. Clinical Pharmacokinetics of Tacrolimus. Clin. Pharmacokin. 1995; 29:404-430.

5. Humphreys WG. Presystemic and First-Pass Metabolism. In: Wang B, Siahaan T, Soltero R, eds. Drug Delivery Principles and Applications. Hoboken, NJ: Wiley and Sons, 2005.

6. Sinswat P, Overhoff KA, McConville JT, Johnston KP, Williams III RO. Nebulization of Nanoparticulate Amorphous or Crystalline Tacrolimus - Single Dose Pharmacokinetics Study in Mice. Eur J Pharm Biopharm 2007; in press.

7. Vaughn JM, McConville JT, Burgess D, et al. Single dose and multiple dose studies of itraconazole nanoparticles. European Journal of Pharmaceutics and Biopharmaceutics 2006; 62:95-102.

8. Vaughn JM, Wiederhold NP, McConville JT, et al. Murine airway histology and intracellular uptake of inhaled amorphous itraconazole. Int. J. Pharmaceutics 2007; in press.

9. Vaughn JM, McConville JT, Crisp MT, Johnston KP, Williams RO. Supersaturation produces high bioavailability of amorphous danazol particles formed by evaporative precipitation into aqueous solution and spray freezing into liquid technologies. Drug Development and Industrial Pharmacy 2006; 32:559-567.

10. Sinswat P, Matteucci ME, Johnston KP, Williams RO. Dissolution rates and supersaturation behavior of amorphous repaglinide particles produced by controlled precipitation. J Biomed Nanotech 2007; 3:18-27.

11. Loser K, Balkow S, Higuchi T, et al. FK-506 Controls CD40L-Induced Systemic Autoimmunity in Mice. J. Invest. Dermatol. 2006; 126:1307-1315.

12. Hutchinson IV, W BA, P BA, B PA, P GA, A BI. Differences in the Mode of Action of Cyclosporine and FK 506. Transplant Proc. 1998; 30:959-960.

13. Dubey DP, Yunis I, Yunis EJ. Cellular Typing: Mixed Lymphocyte Response and Cell-Mediated Lympholysis. In: Rose NR, Friedman H, Fahey JL, eds. Manual of Clinical Laboratory Immunology. Washington, DC: American Society for Microbiology, 1986:847-858.

14. Maluish AE, Strong DM. Lymphocyte Proliferation. In: Rose NR, Friedman H, Fahey JL, eds. Manual of Clinical Laboratory Immunology. Washington, DC: American Society of Microbiology, 1986:274-281.

15. Smith G, Ryoo W, Johnston KP. Electrostatically Stabilized Metal Oxide Particle Dispersions in Carbon Dioxide. J. Phys. Chem. B 2005; 109:20155-20165.

16. Miyaji S, Nishiyama T, Takada O, Hayahshi R, Suzuki S, Amemiya H. Comparative Study of Immunosuppressants Effects of Various

Immunosuppressants on Response of Canine Mixed Lymphocyte Culture. Iryo 1993; 47:200-204.

17. Ma A, Qi S, Xu D, Zhang X, Daloze P, Chen H. Baohuoside-1, a Novel Immunosuppressive Molecule, Inhibits Lymphocyte Activation In Vitro and In Vivo. Transplantation 2004; 78:831-838.

18. Segall M, Bach F. Pooled Stimulating Cells as a "Standard Stimulator" in Mixed Lymphocyte Culture. Transplantation 1976; 22:79-85.

19. Lauricella AM, Garbossa G, Nesse A. Dissimilar behavior of lymph cells in response to the action of aluminum. In vitro and in vivo studies International Immunopharmacology 2001; 1:1725-1732.

20. Parham P, Ohta T. Population Biology of Antigen Presentation by MHC Class I Molecules. Science 1996; 272:67-74.

21. Yardin C, Terro F, Lesort M, Esclaire F, Hugon J. FK506 antagonizes apoptosis and c-jun protein expression in neuronal cultures. NeuroReport 1998; 9:2077-2080.

22. Scammell JG, Denny WB, Valentine DL, Smith DF. Overexpression of the FK506-Binding Immunophilin FKBP51 Is the Common Cause of Glucocorticoid Resistance in Three New World Primates. Gen Compar Endocrin 2001; 124:152-165.

23. Mancinelli LM, Frassetto L, Floren LC, et al. The pharmacokinetics and metabolic disposition of tacrolimus: A comparison across ethnic groups. Clin. Pharmacol. Therapeut. 2001; 69.

24. Marsh SG, Albert ED, Bodmer WF, et al. Nomenclature for Factors of the HLA System. Tissue Antigens 2005; 65:301-369.

25. Fruman DA, Wood MA, Gjertson CK, Katz HR, Burakoff SJ, Bierer BE. FK506 binding protein 12 mediates sensitivity to both FK506 and rapamycin in murine mast cells. European Journal of Immunology 2005; 25:563-571.

26. Apanius V, Penn D, Slev PR, Ruff LR, Potts WK. The nature of selection on the major histocompatibility complex. Critical Reviews in Immunology 1997; 17:179-224.

27. Guo Z, Gatterman MS, Hood L, Hansen JA, Petersdorf EW. Oligonucleotide Arrays for High-Throughput SNPs Detection in the MHC Class I Genes: HLA-B as a Model System. Genome Res 2002; 12:447-457.

28. Hamelryck T, Dao-Thi M, Poortmans F, Chrispeels M, Wyns L, Lorris R. The crystallographic structure of phytohemmaglutinin-L. J Biolog Chem 1996; 271:20479-85.

29. Lang JM, Oberling F, Mendel C, Grenier JF, Mayer S, Waitz R. Hydrostatics and lymphocyte reactivity to phytohemagglutinin. Report of the Society of the Science of Biology and Its Affiliates 1974; 168:112-11.

Table 1.1: Selected immunosuppressant drugs' physicochemical properties. BCS Classification is based on aqueous solubility. PGP interaction and CYP 3A4 interaction is qualitative. LogP values are calculated. * Solubility is given as the value in water at 25°C.

Drug	BCS Classification	Aqueous Solubility *	log P app	PGP Interaction	CYP 3A4 Interaction
Prednisolone	1 (for salt form)	481.1 mg/L [9]	1.4 [9]	PGP Substrate [9]	CYP3A4 Substrate [9]
Hydrocortisone	1 (for salt form)	896.6 mg/L [9]	1.7 [9]	PGP Substrate [9]	CYP3A4 Substrate [9]
Dexamethasone	1 (for salt form)	254.8 mg/L [9]	1.8 [9]	PGP Substrate [9]	CYP3A4 Substrate [9]
Cyclosporin	2	0.028 mg/mL [36]	3.0 [36]	PGP Substrate [35]	CYP3A4 Substrate [35]
Tacrolimus	2	0.012 mg/mL [42]	4.6 [42]	PGP Substrate [35]	CYP3A4 Substrate [35]
Sirolimus	2	0.026 mg/mL [53]	3.6 [53]	PGP Substrate [35]	CYP3A4 Substrate [35]
Azithioprine	1 (for sodium salt)	272 mg/L [56]	0.1 [56]	none known	none known
Methotrexate	1 (for sodium salt)	2600 mg/L [56]	-1.08 [56]	none known	none known

Table 1.2: Pharmacokinetic parameters of tacrolimus after its oral administration to dogs as crystalline powders or SDF of tacrolimus with HPMC. (Reprinted with permission from Yamashita et al. IJP 267 (2003) 79-91).

Sample	$AUC_{0\text{-}8h}$ (ng h/mL)	C_{max} (ng/mL)	T_{max} (h)	MRT (h)
Crystalline Powder	1.1 ± 1.4	0.4 ± 0.3	3.1 ± 3.0	3.3 ± 0.9
SDF with HPMC	10.9 ± 6.1 *	4.0 ± 1.2 *	0.6 ± 0.2	2.7 ± 0.1

Table 1.3: Code of different MTX gels evaluated in the study. (Reprinted with permission from Kalariya et al. Drug Dev Tech. 4 (2004) 65-71. [2])

Gel Code	Content *
MTxG1	Plain MTx (marketed)
MTxG2	MTx and Lipid Physical Mixture
MTxG3	MTx-SLN

Table 1.4: Average percent improvement of healing of psoriasis lesions. (Reprinted with permission from Kalariya et al. Drug Dev Tech. 4 (2004) 65-71. [2]).

Time (weeks)	Mean % (± SEM) for Formulations Tested *		
	MTxG1	MTxG2	MTxG3
1	14.1 (0.14)	14.3 (0.26)	33.7 (0.46)
2	29.8 (0.29)	31.1 (0.73)	66.5 (0.38)
3	50.7 (0.95)	52.7 (0.49)	89.1 (0.78)
4	67.6 (1.13)	69.3 (1.09)	99.4 (0.93)
5	79.4 (0.89)	80.4 (0.99)	99.8 (0.24)
6	86.1 (1.16)	86.9 (1.21)	99.8 (0.35)

Table 2.1: Summary of URF Formulations Evaluated in This Study

Formulation Acronym	Components	Ratio
URF-A	Rep:SDS	1:1
URF-B	Rep:SDS:DEA	1:0.5:0.5
URF-C	Rep:SDS:DEA	1:0.17:0.17
URF-D	Rep:SDS:Tris	1:0.5:0.5
URF-E	Rep:SDS:Tris	1:0.17:0.17
Co-ground Physical Mixture A	Rep:SDS	1:1
Co-ground Physical Mixture D	Rep:SDS:Tris	1:0.5:0.5

Table 2.2: Results of the Repaglinide Forced Degradation Study (N/D = not detected, RRT = relative retention time)

Forced Degradation Condition	Reaction Time (hr)	Total % REP Recovered	% Peak 1 Area (RRT = 0.27)	% Peak 2 Area (RRT = 0.42)	% Peak 3 Area (RRT = 0.69)	% Peak 4 Area (RRT = 0.78)	% Peak 5 Area (RRT = 1.24)	Total % Peak Area Impurity
Acid (1N HCl, 25 degrees C)	1	92.1	5.1	1.1	N/D	N/D	N/D	6.2
Base (1N NaOH, 25 degrees C)	0.25	86.3	3.5	8.2	1.7	N/D	N/D	13.4
Base (0.1M TRIS, 25 degrees C)	1	88.7	1.4	5.6	2.8	1.2	N/D	11.0
Oxidation (6% hydrogen peroxide)	1	91.9	N/D	4	4.7	0.8	2.1	11.6
Thermal (1 mg% in methanol, 60 degrees C)	6	81.1	6.7	5.2	2.9	3.1	0.7	18.6
HCl/SDS Insoluble Mass	-	89.3	2.7	3.3	1.4	N/D	N/D	7.4
USP REP reference standard	-	99.82	N/D	N/D	0.07	0.04	N/D	0.11

Table 2.3: Potency and Impurity Analysis of Repaglinide and REP URF Formulations
(N/D = not detected, RRT = relative retention time)

Sample	Total REP Recovered (%)	% Peak Area 1 (RRT = 0.58)	% Peak Area 2 (RRT = 0.71)	% Peak Area 3 (RRT = 0.78)	% Peak Area 4 (RRT = 1.29)	% Peak Area 5 (RRT = 2.32)	% Peak Area 6 (RRT = 3.45)	Total % Peak Area Impurity
URF-B	99.65	0.07	0.07	0.05	0.05	0.05	0.06	0.35
URF-C	99.62	0.05	0.06	0.08	0.07	0.06	0.06	0.38
URF-D	99.69	0.05	0.06	0.04	N/D	0.05	0.04	0.24
URF-E	99.72	0.05	0.06	0.05	0.04	0.05	0.06	0.31
Bulk Repaglinide	99.54	0.09	0.07	0.07	0.07	0.08	0.08	0.46
USP REP reference standard	99.82	N/D	0.07	0.04	N/D	N/D	0.05	0.16

Table 3.1: Degradation results from acid, base, oxidation, and thermal degradation of SRL. The table shows the amount of SRL recovered in each sample and the total number of each degradant or observed, not each individual degradant specified by name.

Working Standard SRL 100µg/mL	Peak Area	% Peak Area
Sirolimus Major Isomer	8917485	89.96
Sirolimus Minor Isomer	768436	7.75
SRL Tautomer I	152689	1.54
SRL Tautomer II	53874	0.54
Degradants (summed)	20595	0.21

SRL Potency (including tautomers)	99.8%
SRL Potency (excluding tautomers)	97.7%
Total Degradation Products	0.2%

SRL-Acid Solution (100 µg/mL TAC initially)	Peak Area	% Peak Area
Sirolimus Major Isomer	6108358	68.5
Sirolimus Minor Isomer	517847	5.22
SRL Tautomer I	130776	1.31
SRL Tautomer II	107501	1.08
Degradants (summed)	143255	2.05

SRL Potency (including tautomers)	76.1%
SRL Potency (excluding tautomers)	73.7%
Total Degradation Products	2.1%

SRL-Base Solution (100 µg/mL TAC initially)	Peak Area	% Peak Area
Sirolimus Major Isomer	0	0
Sirolimus Minor Isomer	0	0
SRL Tautomer I	39659	0.43
SRL Tautomer II	18405	0.21
Degradants (summed)	56728	0.64

SRL Potency (including tautomers)	0.6%
SRL Potency (excluding tautomers)	0.0%
Total Degradation Products	0.6%

Table 3.2: Degradation results from acid, base, oxidation, and thermal degradation of SRL. The table shows the amount of SRL recovered in each sample and the total number of each degradant or observed, not each individual degradant specified by name. (continued)

SRL-Peroxide Solution(100µg/mLTAC initially)	Peak Area	% Peak Area
Sirolimus Major Isomer	2599642	29.20%
Sirolimus Minor Isomer	110922	14.40%
SRL Tautomer I	98571	6.46%
SRL Tautomer II	22816	4.23%
Degradants (summed)	27803	0.97

SRL Potency (including tautomers)	54.3%
SRL Potency (excluding tautomers)	43.6%
Total Degradation Products	1.0%

SRL-Heated Solution(100 µg/mL TAC initially)	Peak Area	% Peak Area
Sirolimus Major Isomer	8423235	84.2
Sirolimus Minor Isomer	687524	8.0
SRL Tautomer I	146426	0.95
SRL Tautomer II	52481	0.97
Degradants (summed)	17512	0.19

SRL Potency (including tautomers)	94.1%
SRL Potency (excluding tautomers)	92.2%
Total Degradation Products	0.2%

*- Note: Some degradation products are not retained by the column, so they do not give peak area response in chromatograms

Table 3.3: SRL Formulations tested for this study.

Formulation Name	Composition	Ratio	SRL Potency
URF-SRL Form 1	SRL:P407	50:50	98.20%
URF-SRL Form 2	SRL:HPMC E5	50:50	99.14%
URF-SRL Form 3	SRL:SDS:P407	50:25:25	98.37%
URF-SRL Form 4	SRL:SDS:HPMC E5	65:17.5:17.5	99.17%
URF-SRL Form 5	SRL:SDS:HPMC E5	65:25:10	97.90%
URF-SRL Form 6	SRL:SDS:HPMC E5:P407	65:11.6:11.6:11.6	98.32%

SRL: sirolimus
SDS: sodium dodecyl sulfate
HPMC E5 hydroxypropylmethylcellulose E5
P407: poloxamer 407

Table 4.1: Weights of mice taken just before euthanasia. Approximate weight of mice before the study was initiated was 20 grams. No significant differences in weights were observed between the control and experimental groups (p-value < 0.05 for day 7, and p-value < 0.05 for day 14), and no trending of weights were observed in either group.

Weights of Mice at Day 7 and 14, Prior to Euthanasia (grams)					
Day 7 Mice					
Experimental Mouse 1	22.0		Control Mouse 1	24.1	
Experimental Mouse 2	26.1		Control Mouse 2	23.5	
Experimental Mouse 3*	20.9				
Experimental Mouse 4	24.5				
Day 14 Mice					
Experimental Mouse 1	30.4		Control Mouse 1	31.5	
Experimental Mouse 2	27.5		Control Mouse 2	32.5	
Experimental Mouse 3	27.0				
Experimental Mouse 4	28.1				
* - Note: This mouse got his face stuck in the restraint tube, and suffered eye trauma. This did not affect the outcome of the TAC multi-dose test.					

Table 4.2: Organ and blood distribution of pulmonary dosed TAC in mice dosed for 7 and 14 days (n = 8 mice; 4 mice for day 7 and 4 mice for day 14).

Tissue	Avg Tissue wt.(g) or vol.(mL)	Avg TAC Conc. in Tissue	Std Deviation	Amount of TAC in tissue (µg)
			Over 7 & 14 Days	
	(mL)	(ng/mL)		
Blood 7 Days	2.4	2.39	0.183	
Blood 14 Days	2.4	2.649		0.0057
				0.0064
	(g)	(µg/g)		
Lung 7 Days	0.2205	7.19	0.322	1.5850
Lung 14 Days	0.2193	6.735		1.4770
	(g)	(ng/g)		
Liver 7 Days	1.3512	1.76	0.134	0.0024
Liver 14 Days	1.4569	1.95		0.0028
Kidney 7 Days	0.3748	2.51	0.014	0.0009
Kidney 14 Days	0.4001	2.53		0.0010
Spleen (7 and 14 days pooled)	0.0987	1.3	-	0.0001
Heart (7 and 14 days pooled)	0.1213	0.45	-	0.0001
			Total TAC remaining after 7 days (µg)	1.5943
			Total TAC remaining after 14 days (µg)	1.4874

Table 5.1: MLC results for histocompatibility, using the 3 formulations of TAC plus the control (first run and second runs); p=0.002.

Run 1

	Experiment 1A		Experiment 1B		
Cells-MLC	Net CPM*	Inhibition	Net CPM*	Inhibition	**Average Inhibition**
TAC:LAC	21,677	53%	10,795	56%	55%
URF-TAC	16,782	63%	8196	67%	65%
TAC	25,402	44%	16,474	39%	42%
No Drug	45,647		24,721		

Run 2

	Experiment 2A		Experiment 2B		Experiment 3A		Experiment 3B		
Cells-MLC	Net CPM*	Inhibition	Net CPM*	Inhibition	Net CPM*	Inhibition	Net CPM*	Inhibition	**Average Inhibition**
TAC:LAC	14,942	83%	20,300	82%	5,807	93%	16,623	85%	86%
URF-TAC	42,250	51%	42,760	63%	14,069	83%	37,747	66%	66%
TAC	54,035	37%	74,247	35%	30,852	64%	61,364	44%	45%
No Drug	85,932		114,254		84,680		109,686		

Table 5.2: PHA results for histocompatibility, using the 3 formulations of TAC plus the control (first run and second runs); p=0.04.

Run 1

	Experiment 1A		Experiment 1B		Experiment 2A		Experiment 2B		
Cells+PHA	Net CPM*	Inhibition	Net CPM*	Inhibition	Net CPM*	Inhibition	Net CPM*	Inhibition	**Average Inhibition**
TAC:LAC	27,000	53%	17,716	60%	19,156	62%	13,272	56%	57%
URF-TAC	18,404	68%	11826	73%	16195	68%	10036	67%	71%
TAC	41,105	29%	23,668	46%	31,204	37%	20,264	39%	38%
No Drug	57,825		44,233		49,881		38154		

Run 2

	Experiment 3A		Experiment 3B		Experiment 4A		Experiment 4B		
Cells+PHA	Net CPM*	Inhibition	Net CPM*	Inhibition	Net CPM*	Inhibition	Net CPM*	Inhibition	**Average Inhibition**
TAC:LAC	1,639	82%	1,158	83%	1,161	76%	1,518	75%	79%
URF-TAC	2,712	69%	2,842	59%	3,325	32%	1,676	72%	58%
TAC	2,396	73%	1,923	72%	2,474	50%	2,485	59%	63%
No Drug	8,889		6,988		4,900		6,009		

Table 5.3: ANOVA statistical analysis for MLC runs 1 and 2 (top), and Tukey's Post-Hoc Analysis (bottom).

Anova: Single Factor - MLC Experiments 1,2, and 3

SUMMARY

Groups	*Count*	*Sum*	*Average*	*Variance*
TAC LAC	6	4.5183	0.75305	0.02762
TAC URF	6	3.9238	0.65397	0.01104
TAC	6	2.5676	0.42793	0.01246

ANOVA

Source of Variation	*SS*	*df*	*MS*	*F*	*P-value*	*F crit*
Between Groups	0.3332	2	0.16662	9.778360	0.00191	3.682
Within Groups	0.2556	15	0.01704			
Total	0.5888	17				

Tukey's Post-Hoc Analysis of MLC samples comparing TAC to TAC:LAC and URF-TAC

Tukey 95% Simultaneous Confidence Intervals
All Pairwise Comparisons among Levels of Group
Individual confidence level = 97.97%

Group = TAC subtracted from:

Group	Lower	Center	Upper
TAC:LAC	12.94	32.5	56.06
URF-TAC	3.11	22.67	42.22

Group = TAC:LAC subtracted from:

Group	Lower	Center	Upper
URF-TAC	-29.39	-9.83	9.72

Table 5.4: ANOVA statistical analysis for PHA runs 1 and 2(top), and Tukey's Post-Hoc Analysis (bottom).

Anova: Single Factor for Experiments 1,2,3, and 4

SUMMARY

Groups	*Count*	*Sum*	*Average*	*Variance*
TAC LAC	8	5.560342	0.695043	0.012174966
TAC URF	8	5.160720	0.645090	0.019192904
TAC	8	4.126823	0.515853	0.024662541

ANOVA

Source of Variation	*SS*	*df*	*MS*	*F*	*P-value*	*F crit*
Between Groups	0.13682	2	0.068409	3.662763947	0.043195	3.46679
Within Groups	0.39221	21	0.018677			
Total	0.52903	23				

Tukey's Post-Hoc Analysis of PHA samples comparing TAC to TAC:LAC and URF-TAC

Tukey 95% Simultaneous Confidence Intervals
All Pairwise Comparisons among Levels of Group
Individual confidence level = 98.00%

Group = TAC subtracted from:

Group	Lower	Center	Upper
TAC:LAC	0.71	17.88	35.04
URF-TAC	-4.42	12.75	29.92

Group = TAC:LAC subtracted from:

Group	Lower	Center	Upper
URF-TAC	-22.29	-5.13	12.04

Table B.1 Tabulation of solubility of REP (ug/mL) in different buffers with different % SDS present in the media.

Solubility of REP in Various Buffers 0% SDS	
Buffer (Type/pH)	Solubility (µg/mL)
pH 1 0.1N HCl	130.3
pH 3 NaPO4	150
pH 4.5 citrate/sodium phosphate	21
pH 7 NaPO4	53
pH 9 0.1M Tris	541

Solubility of REP in Various Buffers 0.1% SDS

Buffer (Type/pH)	Solubility (µg/mL)
pH 1 0.1N HCl	231
pH 3 NaPO4	199
pH 4.5 citrate/sodium phosphate	282
pH 7 NaPO4	217
pH 9 0.1M Tris	1144

Solubility of REP in Various Buffers 0.2% SDS

Buffer (Type/pH)	Solubility (µg/mL)
pH 1 0.1N HCl	549
pH 3 NaPO4	911
pH 4.5 citrate/sodium phosphate	597
pH 7 NaPO4	455
pH 9 0.1M Tris	1597

Note: Graph of pH vs. Solubility is the 48 hour solubility; n=3

Table C.1 Tabulation of results for REP formulations dissolution under sink conditions.

URF-A (REP:SDS 1:1) n=3

Time (min)	% Drug Released	%RSD
0	0.00	0.00
3	55.18	3.54
7	68.91	4.51
11	73.80	2.37
15	78.69	3.10
20	79.70	2.95
23	82.34	1.85
30	84.39	1.10
60	100.08	0.91

Prandin Tablets (5 mg) n=3

Time (min)	% Drug Released	%RSD
0	0.0	0
3	54.1	3.54
7	65.9	4.12
11	75.6	2.39
15	82.8	2.54
20	87.6	1.97
23	90.3	1.02
30	93.4	0.09
60	100.05	0.13

URF-B (REP:SDS:DEA, 1:0.75:0.25) n=3

Time (min)	% Drug Released	%RSD
0	0.00	0.00
3	84.85	4.01
7	93.88	3.96
11	92.83	3.74
15	93.27	2.00
20	94.10	1.74
25	93.19	1.30
60	100.10	0.82

Bulk Repaglinide n=3

Time (min)	% Drug Released	%RSD
0	0.0	0
3	13.1	6.21
5	31.7	7.89
10	47.2	5.41
20	60.5	4.32
30	64.3	2.13
60	99.8	0.92

URF-D (REP:SDS:TRIS, 1:0.5:0.5) n=3

Time (min)	% Drug Released	%RSD
0	0.00	0.00
3	88.32	2.35
7	93.02	3.78
11	94.73	1.25
15	95.45	1.14
20	95.04	0.96
25	96.75	0.88
30	100.62	0.74
60	100.02	0.38

Table C.2: Tabulation of SRL Formulations Dissolution Under Sink Conditions

URF-2 (SRL:HPMC E5, 1:1) n=3

Time (min)	% Drug Released	%RSD
0	0.00	0.00
15	73.01	2.10
30	92.44	1.38
60	96.99	0.92
90	98.74	0.54
120	100.00	0.39

URF-3 (SRL:P407:SDS, 1:0.5:0.5) n=3

Time (min)	% Drug Released	%RSD
0	0.00	0.00
15	96.77	1.32
30	99.04	0.93
60	99.70	0.82
90	99.93	0.41
120	100.00	0.11

URF-4 (SRL:SDS:HPMC E5) (65:17.5:17.5) n=3

Time (min)	% Drug Released	%RSD
0	0.00	0.00
15	86.93	2.36
30	86.98	2.44
60	88.21	1.23
90	91.82	1.84
120	100.00	0.71

URF-6 (SRL:SDS:HPMC E5:P407) (65:11.6:11.6:11.6) n=3

Time (min)	% Drug Released	%RSD
0	0.00	0.00
15	94.60	2.31
30	92.62	4.25
60	97.95	1.11
90	99.91	1.96
120	100.00	0.27

Rapamune® (2-1 mg tablets) Dissolution n=3

Time (min)	% Drug Released	%RSD
0	0.00	0.00
15	60.29	3.65
30	79.30	4.41
60	94.33	2.19
90	98.76	1.78
120	96.59	1.90

Table D.1: Tabulation of REP formulations Dissolution under supersaturated conditions

Supersaturated Dissolution of REP URF-A (REP:SDS, 1:1)

Time (min)	Conc. (µg/mL)
0	0
2	216.1
5	365.1
10	490.7
20	604.8
30	397.4
60	404.1
120	382.5
1440	344.7

Supersaturated Dissolution Physical Mixture (REP:SDS, 1:1)

Time (min)	Conc. (µg/mL)
0	0
2	37.8
5	47.7
10	56.5
20	72.9
30	89.3
60	107.6
225	146.7
1440	213.1

Solubility of REP in SDS 0.03% = 256 µg/mL

Supersaturated Dissolution of REP URF-E (REP:SDS:TRIS, 1:0.17:0.17)

Time (min)	Conc. (µg/mL)
0	0
2	216.1
5	365.1
10	490.7
20	604.8
30	397.4
60	404.1
120	382.5
1440	344.7

Solubility of REP in SDS 0.01% = 152 µg/mL

Table D.2: Tabulation of REP formulations Dissolution under supersaturated conditions

Supersaturated Dissolution of SRL Formulation 1 (SRL:P407, 1:1)

Time (min)	Conc. (µg/mL)
0	0
2	10.2
5	9.8
15	8.4
30	7.8
60	6.3
120	4.2
1200	3.8

Supersaturated Dissolution of SRL Formulation 2 (SRL:HPMC E5, 1:1)

Time (min)	Conc. (µg/mL)
0	0
2	11.9
5	8.9
15	9.5
30	6.2
60	7.2
120	8.4
1200	7.9

Supersaturated Dissolution of SRL Formulation 3 (SRL:SDS:P407, 1:0.5:0.5)

Time (min)	Conc. (µg/mL)
0	0
2	11.6
5	10.9
15	10.3
30	8.4
60	8.4
120	9.1
1200	9.1

Solubility of SRL in 0.1% SDS = 5.1 µg/mL

Supersaturated Dissolution of Rapamune (6 tablets)

Time (min)	Conc. (µg/mL)
0	0
2	11.6
5	9.9
15	10.2
30	9.4
60	11.4
120	11.6
1200	11

Supersaturated Dissolution SRL Form 4 (65/17.5/17.5 SRL/SDS/HPMC)

Time (min)	Conc. (µg/mL)
0	0
2	4.4
5	7.5
15	4.7
30	6
60	5.4
270	5.9
1020	6.2

Supersaturated Dissolution SRL Form 5 (65/25/10 SRL/SDS/HPMC E5)

Time (min)	Conc. (µg/mL)
0	0
2	8.9
5	9.9
15	11.2
30	8.5
60	7.4
270	4
1020	7

Supersaturated Dissolution SRL Form 6 (65/12/12/12 SRL/SDS/HPMC/P407)

Time (min)	Conc. (µg/mL)
0	0
2	9.1
5	10.9
15	12.7
30	13.3
60	12.6
270	13.7
1020	19.7

Table E.1: Tabulation of Results from IL-12p70 Mouse ELISA

Test 1	Test 2	Test 3	Test 4	Test 5	Average	St. Dev.	
52	56	54	54	58	54.8	2.3	**Positive Control**
15	19	18	14	20	17.2	2.6	**Negative Control**
12	9	16	11	9	11.4	2.9	**Exp Group 1 BAL - Day 7**
11	10	13	12	14	12	1.6	**Exp Group 2 BAL - Day 7**
16	11	9	10	11	11.4	2.7	**Exp Group BAL - Day 14**
13	12	15	11	12	12.6	1.5	**Control Group 1 - Day 7**
14	17	9	12	10	12.4	3.2	**Control Group 2 - Day 14**

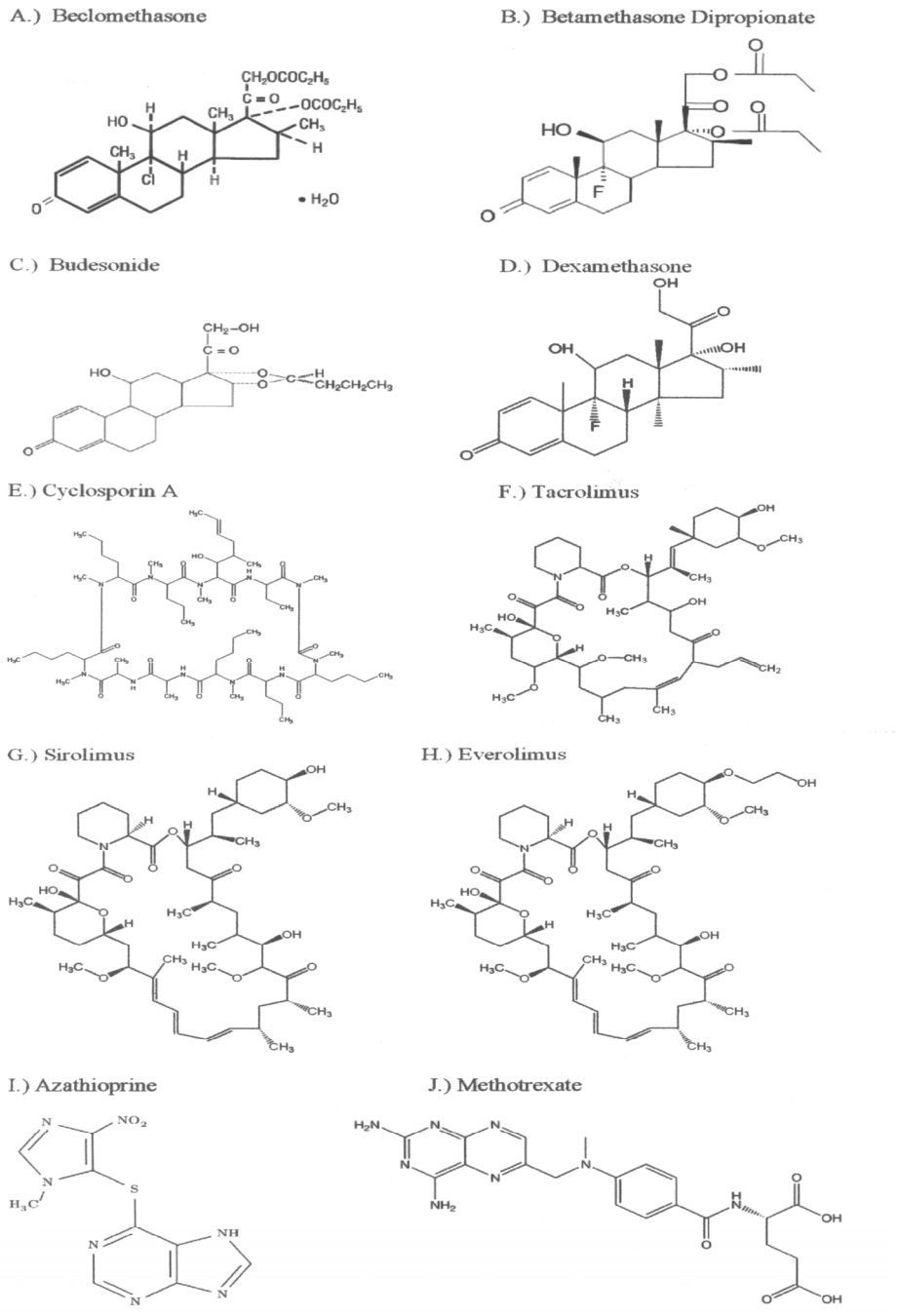

Figure 1.1: The chemical structures of immunosuppressant drugs detailed in this article. A.) Beclomethasone, B.) Betamethasone Dipropionate, C.) Budesonide, D.) Dexamethasone, E.) Cyclosporin A, F.) Tacrolimus, G.) Sirolimus, H.) Azathioprine, I.) Methotrexate.

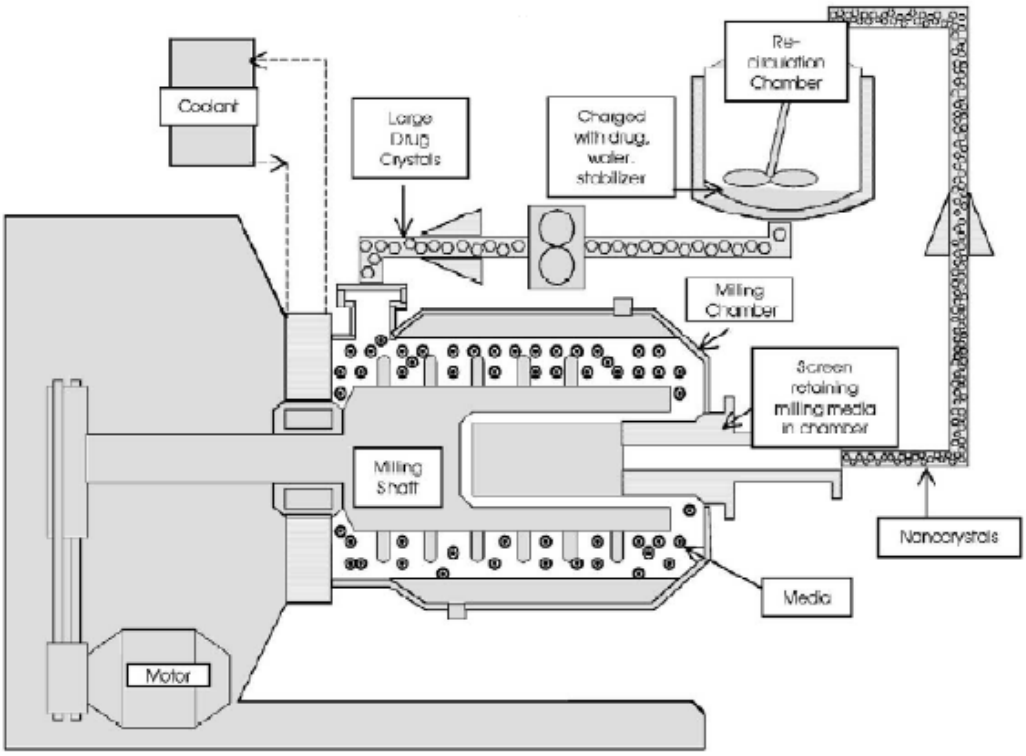

Figure 1.2: The media milling process is shown in a schematic representation. The milling chamber charged with polymeric media is the active component of the mill. The mill can be operated in a batch or recirculation mode. A crude slurry consisting of drug, water, and stabilizer is fed into the milling chamber and processed into a nanocrystal dispersion. The typical residence time required to generate a nanometer-sized dispersion with a mean diameter of <200 nm is 30-60 min. (Reprinted with permission from Merisko-Liversidge et al. Eur. J. Pharm Sci 18 (2003) 113-120.)

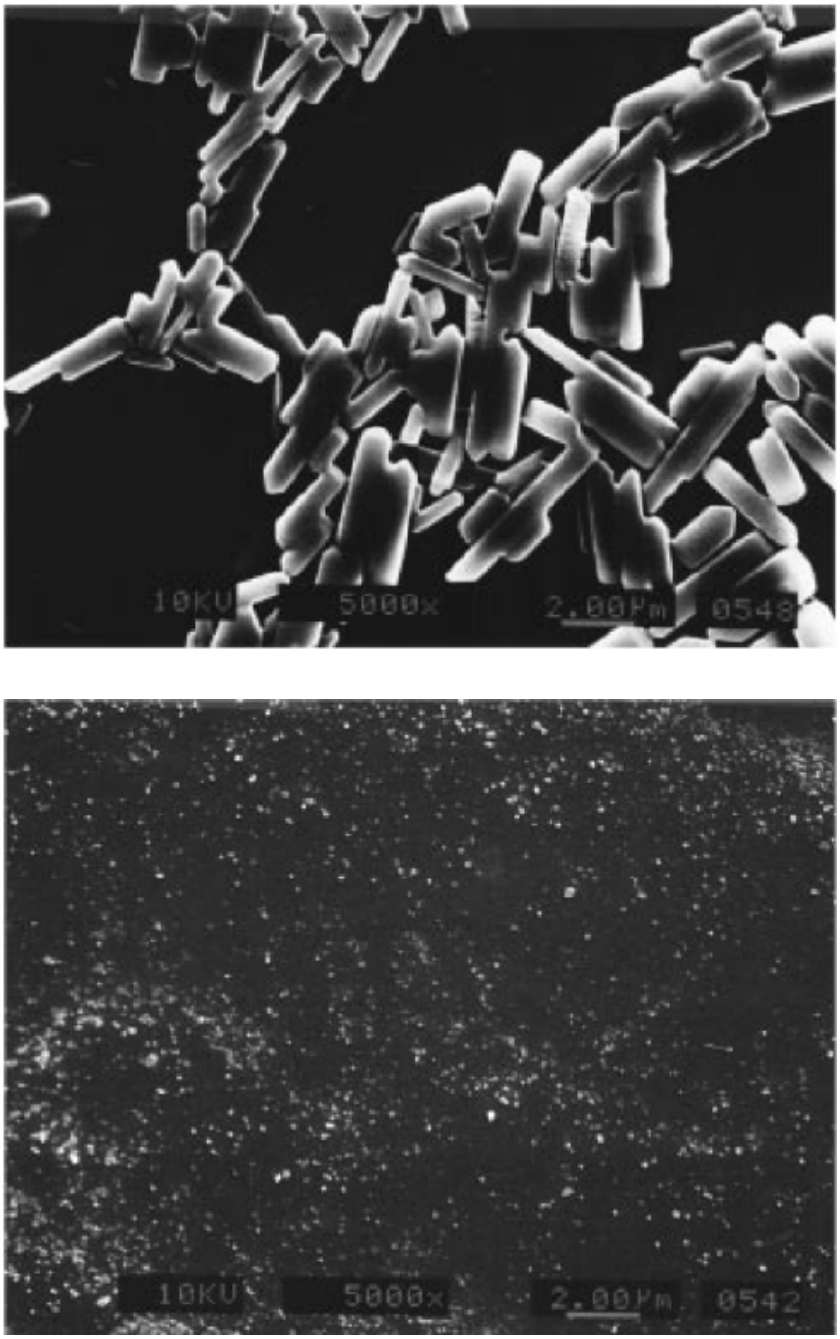

Figure 1.3: SEM of (A) micronized bulk beclomethasone dipropionate; and (B) beclomethasone dipropionate media milled using the Nanosystems® process. (Reprinted with permission from Ostrander et al. Eur. J. Pharm. Biopharm. 48 (1999) 207-215.)

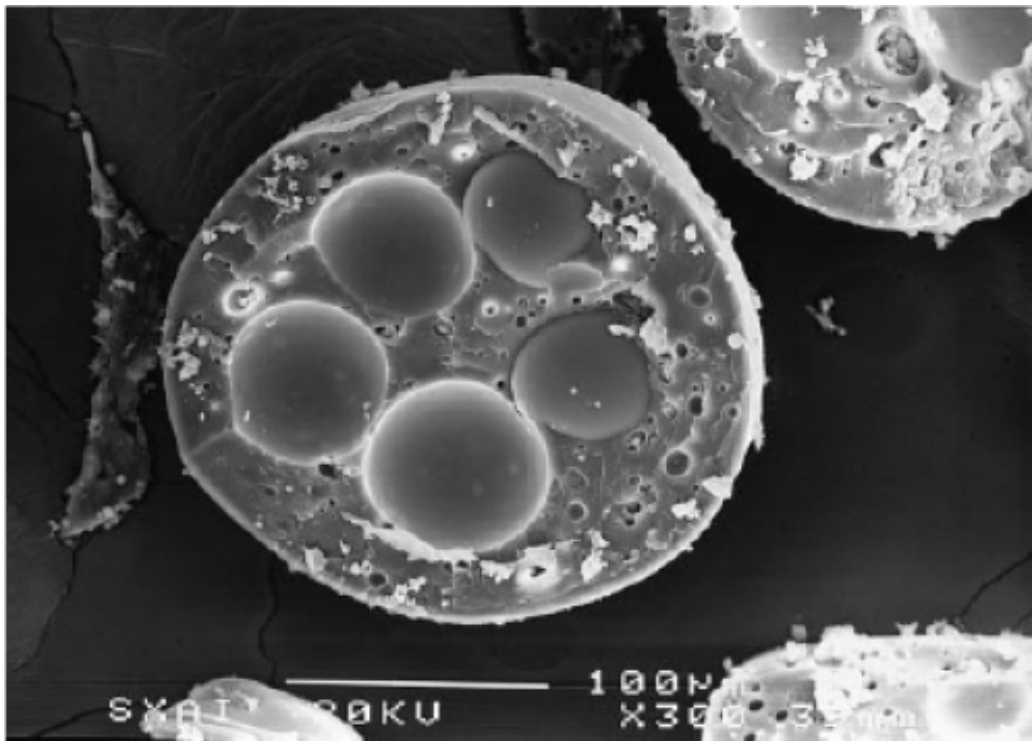

Figure 1.4: Scanning electron micrograph of a cross section of Eudragit S microparticles containing budesonide-loaded cellulose acetate butyrate cores. (Reprinted with permission from Rodriguez et al. J. Pharm. Pharmacol. 2001 53 1207-1215.)

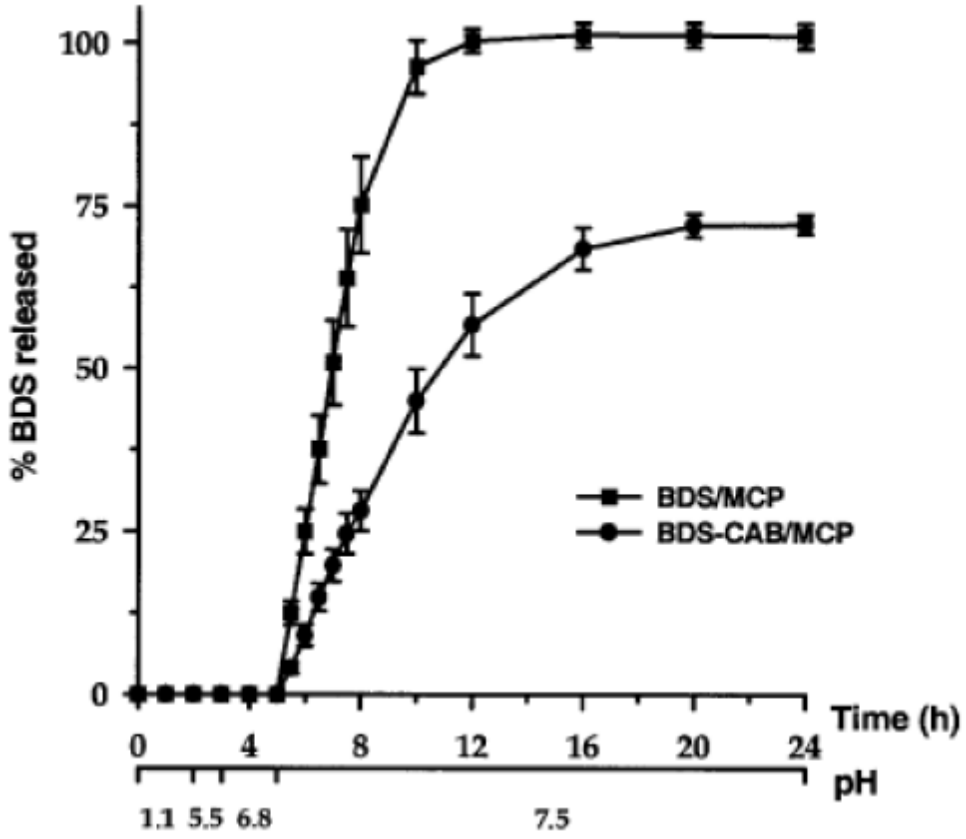

Figure 1.5: *In vitro* release profiles obtained from Eudragit S microparticles containing budesonide (BDS) directly encapsulated (BDS/MCP) or included in CAB cores (BDS-CAB/MCP). Data re mean ± standard deviation n=4. Reprinted with permission from Rodriguez et al. J. Pharm. Pharmacol. 53 2001 1207-1215)

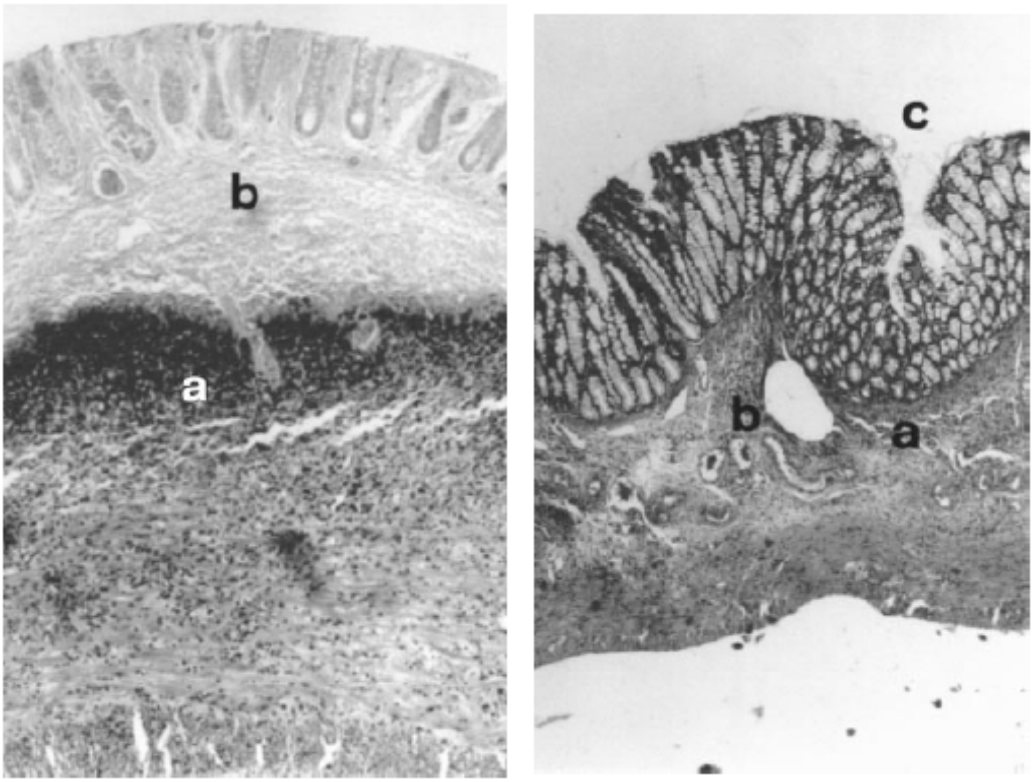

Figure 1.6: Optical micrographs of the colon of (Left) a TNBS-treated rat after oral administration of blank microparticles, showing mucosa with severe inflammatory infiltrate (a) extensive areas of necrosis (b). This colon was given a damage score of 6; and (Right) optical micrograph of colon of a TNBS-treated rat after oral administration of Eudragit S microparticles containing budesonide loaded CAB cores, showing mucosa with mild inflammatory infiltrate (a), vascular congestion (b), and well-conserved mucosa (c). This colon was given a tissue damage score of 2. (Reprinted with permission from Rodriguez et al. J Pharm Pharmacol. 53 2001 1207-1215.).

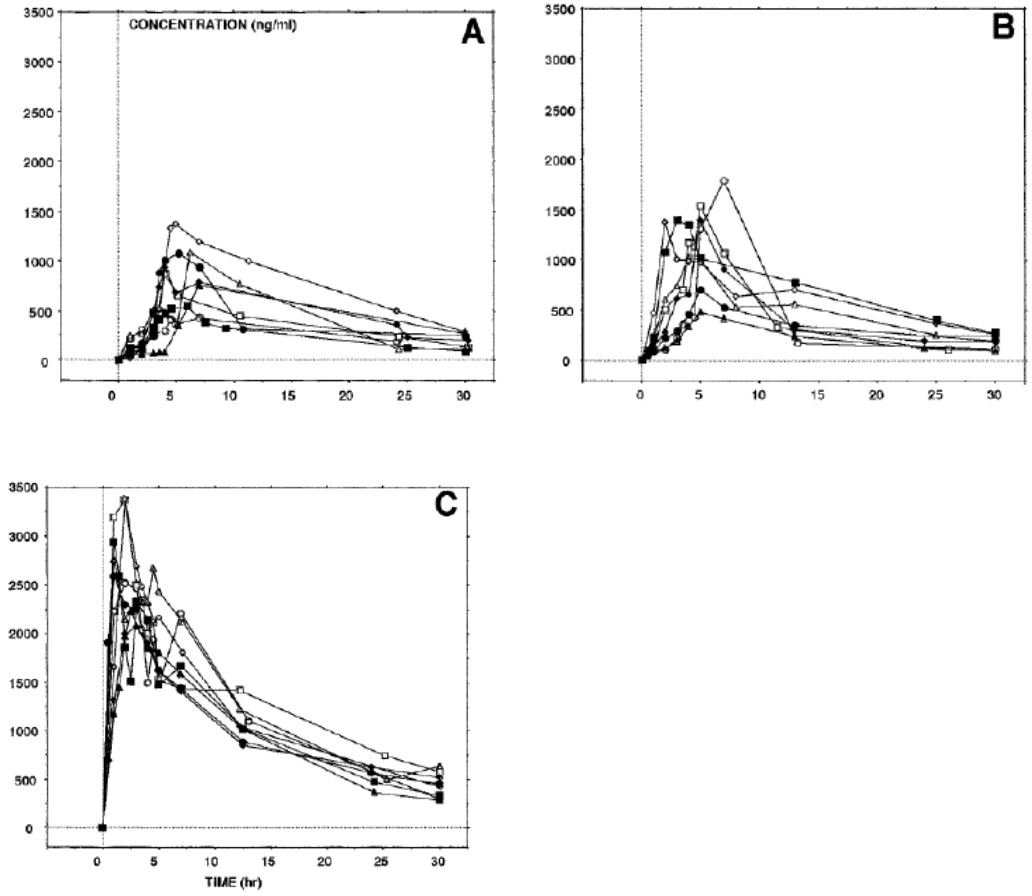

Figure 1.7: Individual cyclosporin concentrations vs. time after single oral administration of 10 mg/kg in rats. (Top Left) Group II: Sandimmune oral oily formulation. (Top Right) Group III: Oral coadministration of Sandimmune + TUDC. (Bottom Left) Group IV: TUDC-monoolein-cyclosporin micellar solution. (Reprinted with permission from Balandrand-Pieri et al. Drug Metabolism and Disposition 25 (8) 1997).

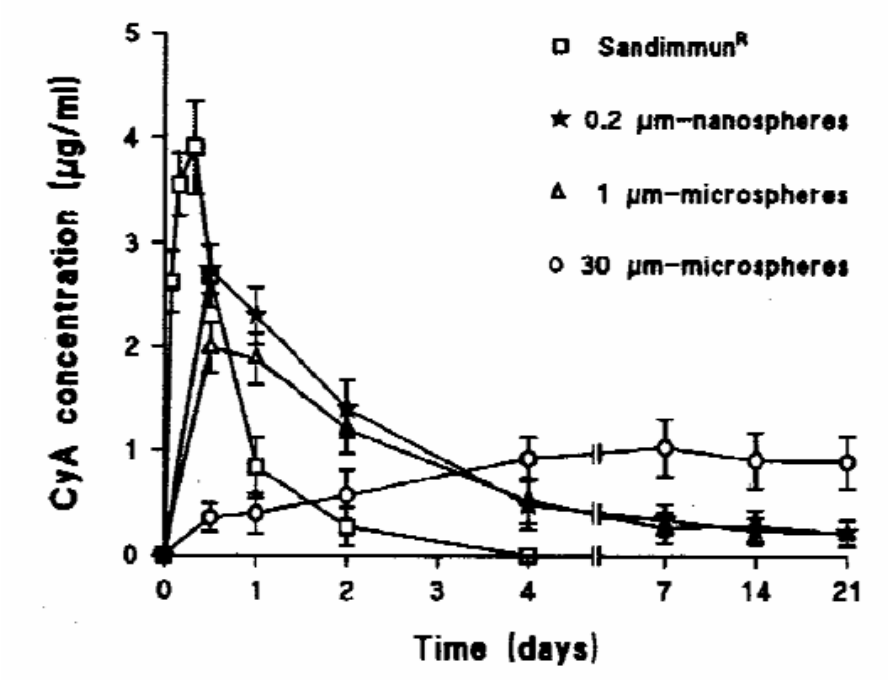

Figure 1.8: Blood-concentration vs time profiles observed after a single subcutaneous injection of free (Sandimmune) or microencapsulated cyclosporin. Each point represents the average ± SD of 4 determinations. (Reprinted with permission from Sanchez et al. Drug Delivery 2 1995 21-28).

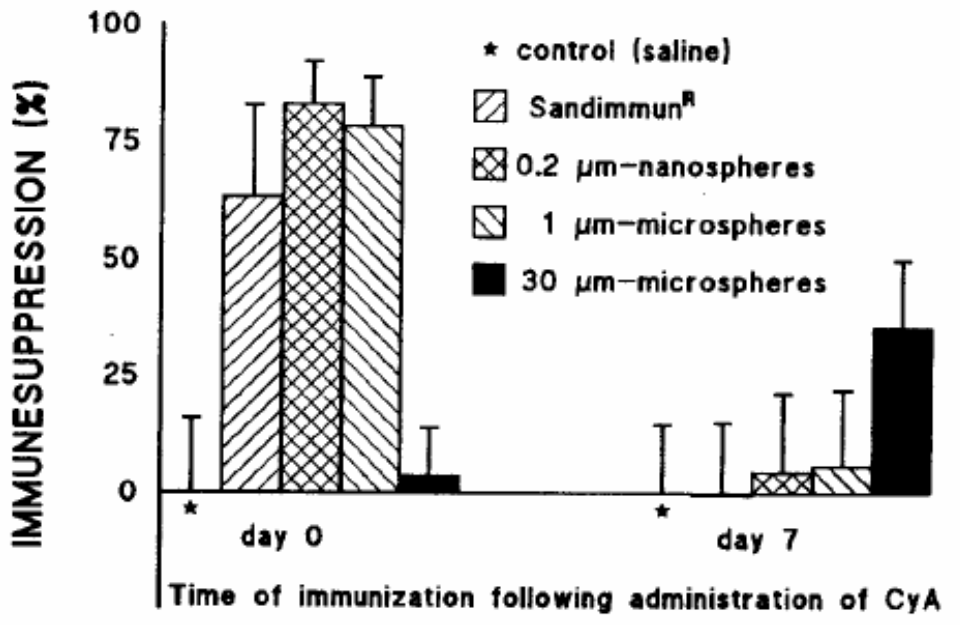

Figure 1. 9: Immunosuppressive effect corresponding to Day 0 and Day 7 postintraperitoneal injection into mice of a single dose (70mg/kg) of free cyclosporin (Sandimmune®) and microencapsulated cyclosporin. Each value represents the average ± SD of four determinations. The mean number of direct PFC per spleen of control animals was taken as 100% of immune response (0% immunosuppression). (Reprinted with permission from Sanchez et al. Drug Delivery 2 1995 21-28).

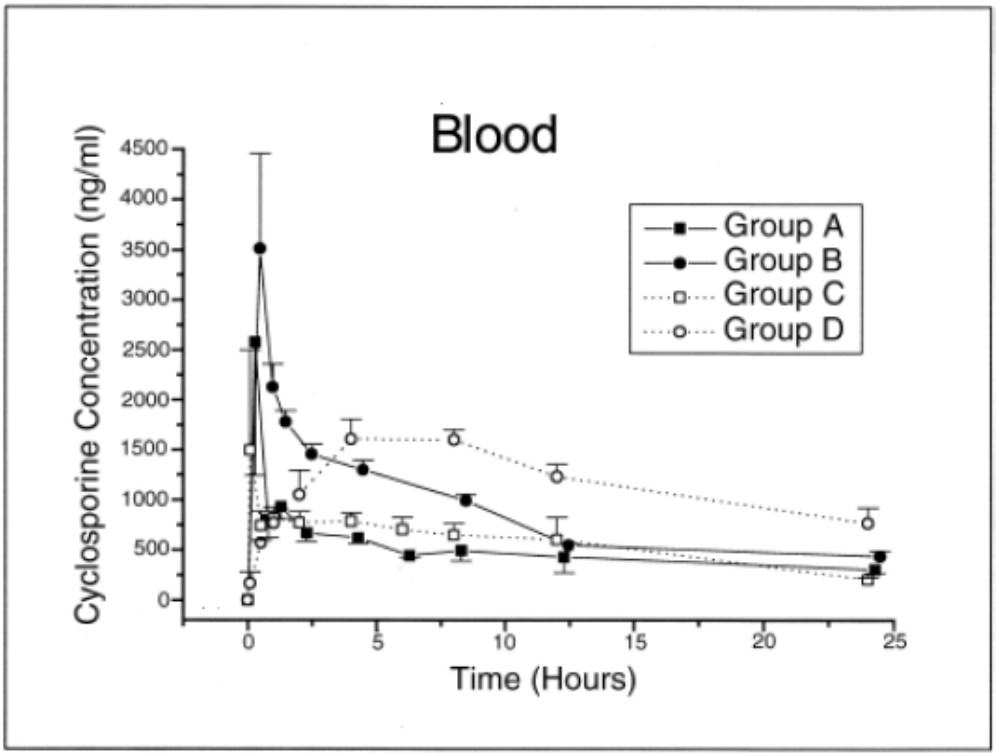

Figure 1.10: Cyclosporin concentrations in blood as a function of time following the first 24 hours after administration of the drug. Group A, aerosol cyclosporin 3mg/kg; Group B, aerosol cyclosporin 5mg/kg; Group C, intramuscular cyclosporin 5mg/kg; Group D, intramuscular cyclosporin 15mg/kg. (Reprinted with permission from Mitruka et al. J. Heart Lung Trans. 19 (10) 2000, 969-975).

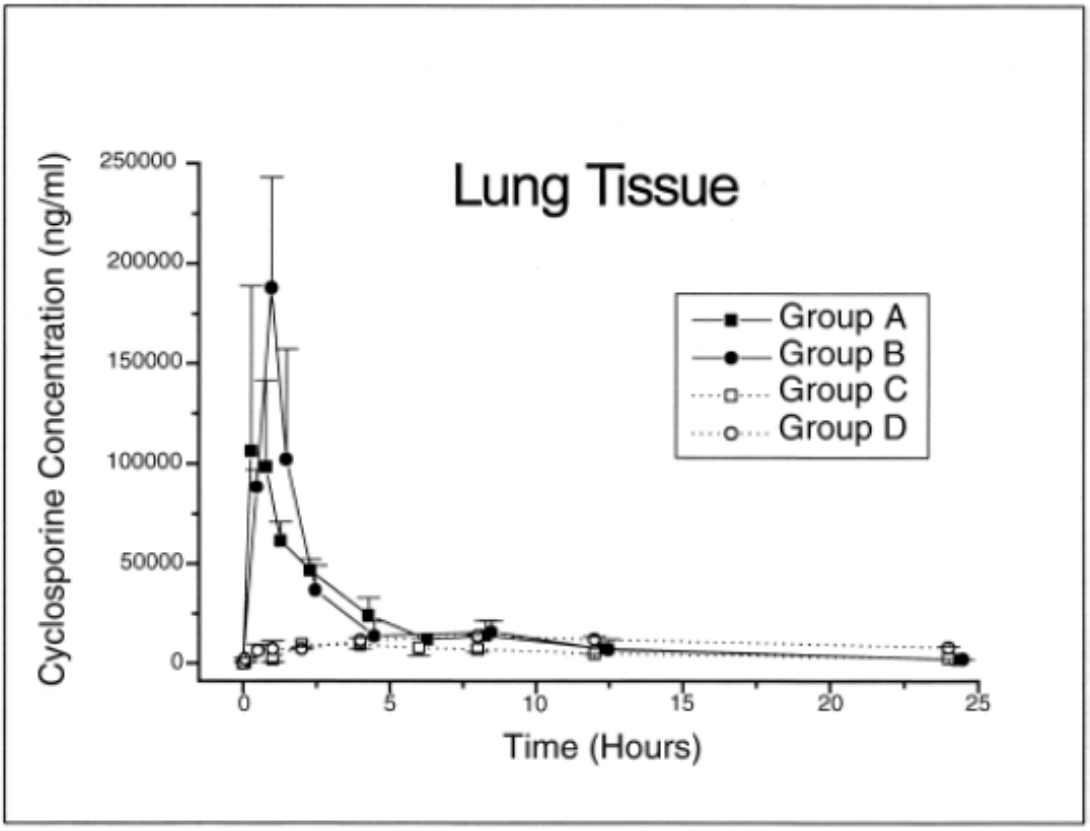

Figure 1.11 Cyclosporin concentrations in lung tissue with respect to time following the first 24 hours after administration of drug. Group A, aerosol cyclosporin 3mg/kg; Group B, aerosol cyclosporin 5mg/kg; Group C, intramuscular cyclosporin 5mg/kg; Group D, intramuscular cyclosporin 15mg/kg. (Reprinted with permission from Mitruka et al. J. Heart Lung Trans. 19 (10) 2000, 969-975)

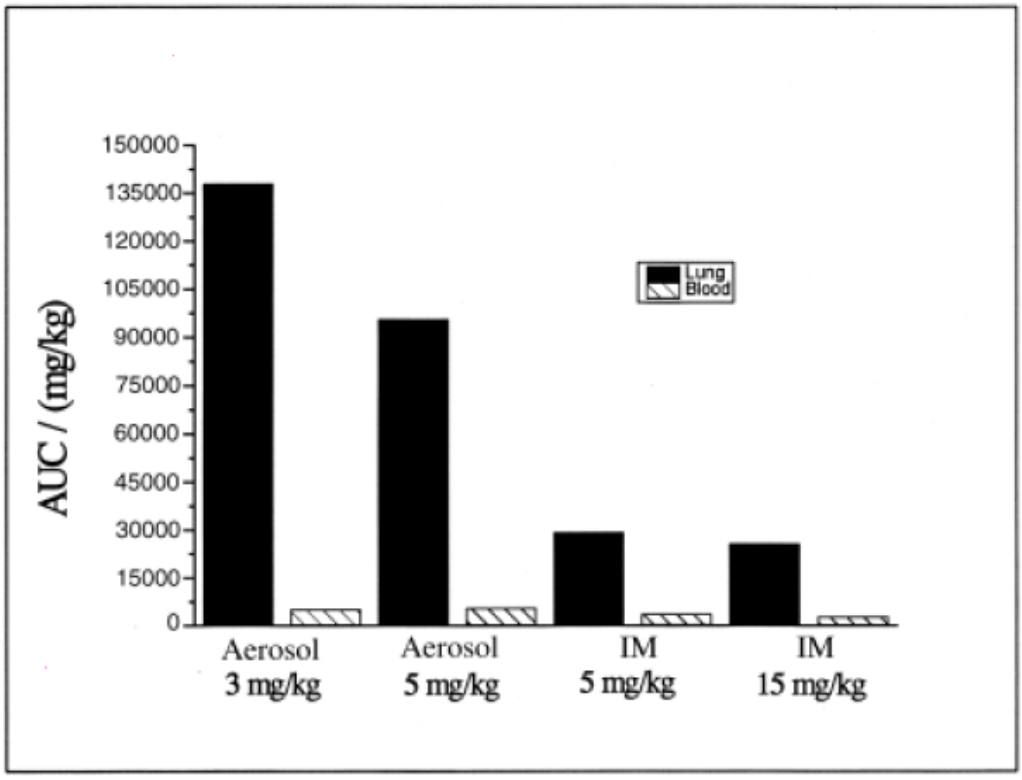

Figure 1.12: Area under the concentration vs. time curve (AUC)/dose of cyclosporin (mg/kg) for each of the 4 study groups. IM, intramuscular (Reprinted with permission from Mitruka et al. J. Heart Lung Trans. 19 (10) 2000, 969-975).

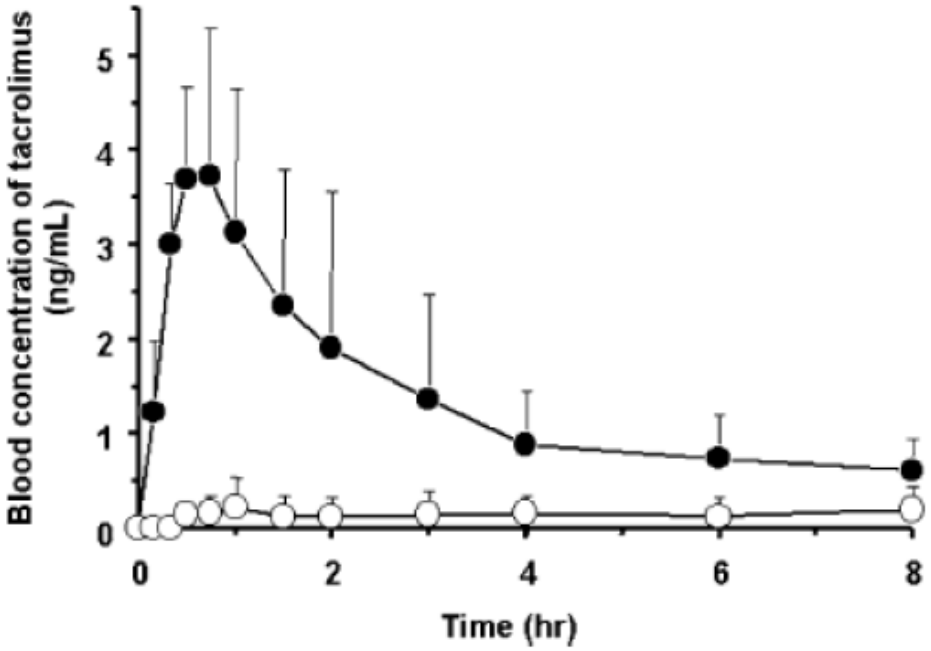

Figure 1.13 Blood concentration of tacrolimus after oral administration of SDF with HPMC to beagle dogs. (○) tacrolimus crystalline powders; (●) SDF of tacrolimus with HPMC. Values are expressed as the mean with a vertical bar showing SE of six animals. Each dosage form was administered at the dose of 1 mg tacrolimus. (Reprinted with permission from Yamashita et al. Int J Pharm 267 (2003) 79-91).

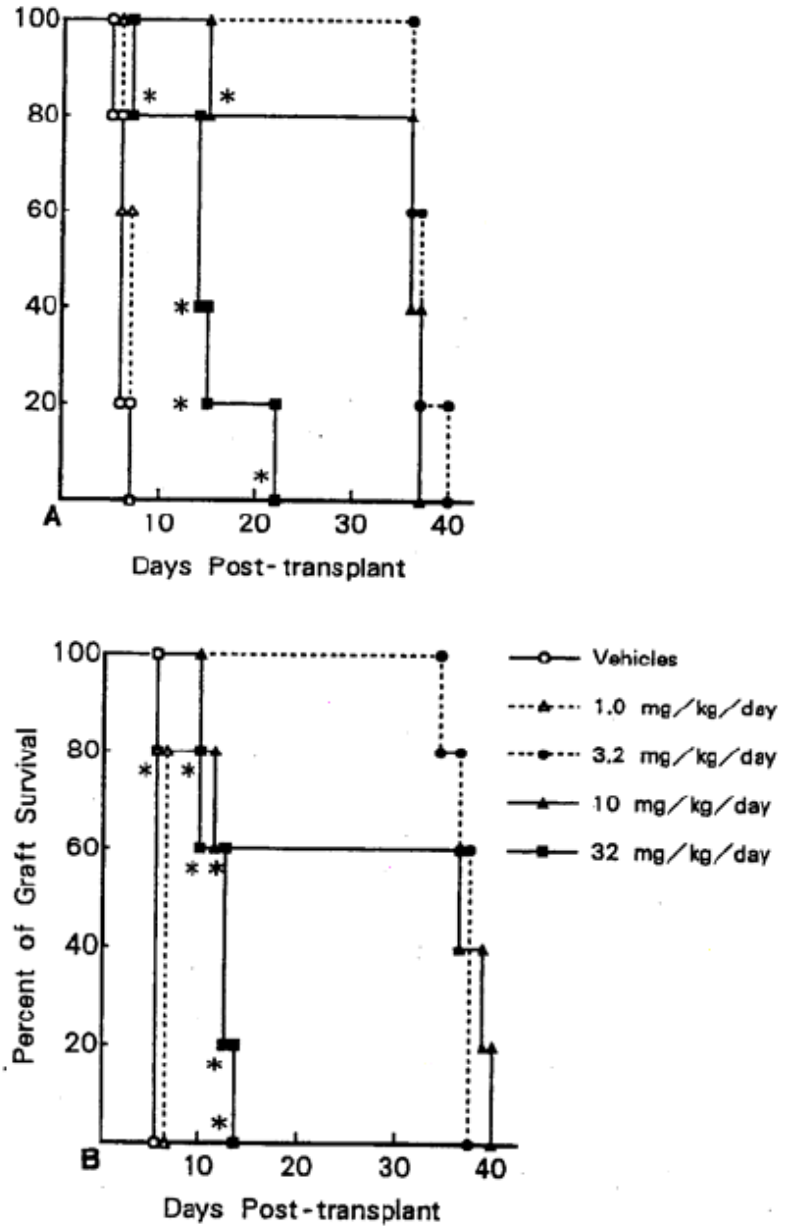

Figure 1.14 Results of (Top) SDF-tacrolimus and (Bottom) OEF-tacrolimus in the secondary rat skin allograph transplantation study. Dose 0, 1, 3.2, 10, and 32 mg/kg/day; dosage period, once daily for 30 days; number of animals: 5. * - died with living graft. (Reprinted with permission from Honbo et al. Trans Proc 19 (5, Supp 6) 1987, 17-22)

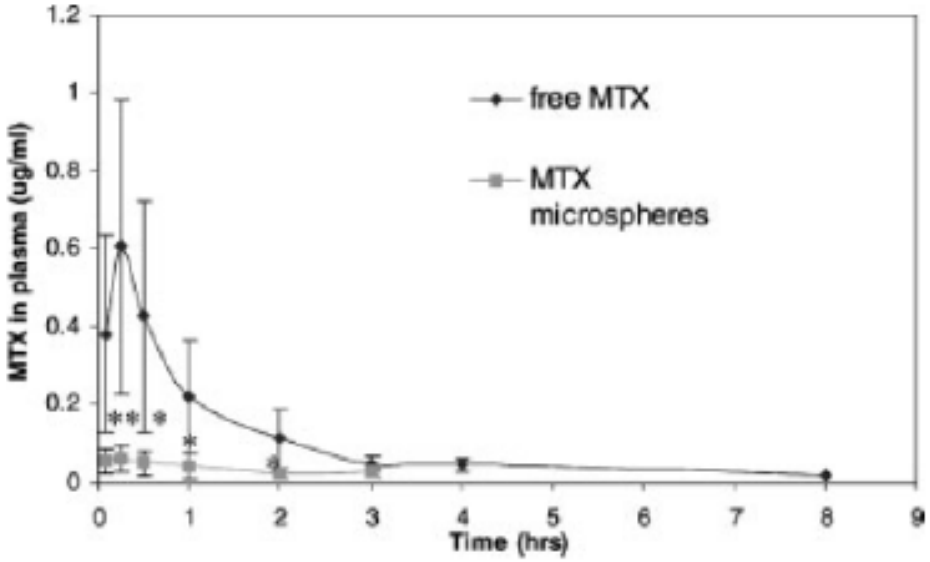

Figure 1.15 MTX concentrations in rabbit plasma after a single intra-articular injection of either free MTX or 25 mg of MTX loaded microspheres in 200 μL PBS. The dose of MTX injected was 1.5 mg. * Indicates statistical difference between MTX plasma concentrations of rabbits injected with free MTX and MTX loaded microspheres by paired t-test ($p<0.05$). (Reprinted with permission from Liang et al. J. Pharm. Sci. 93(4) 2004 943-955)

Repaglinide (REP)

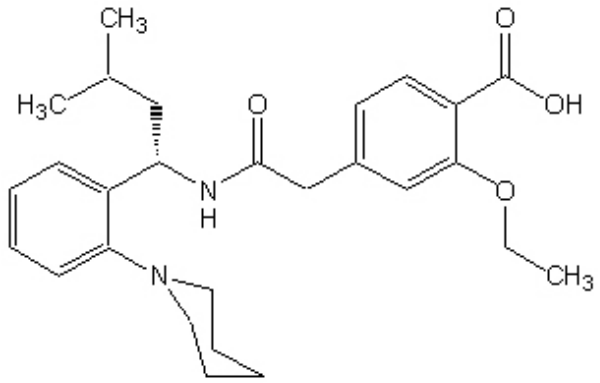

Repaglinide Related Compound B

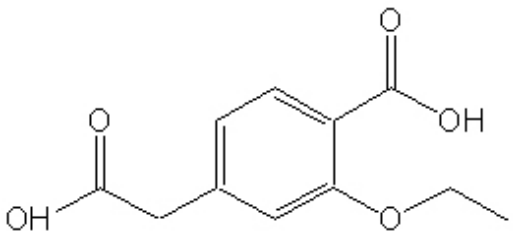

Repaglinide Related Compound A

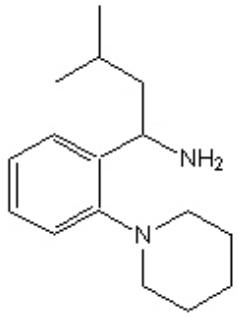

Figure 2.1: Structure of Repaglinide (REP), REP related compound B, and REP related compound A

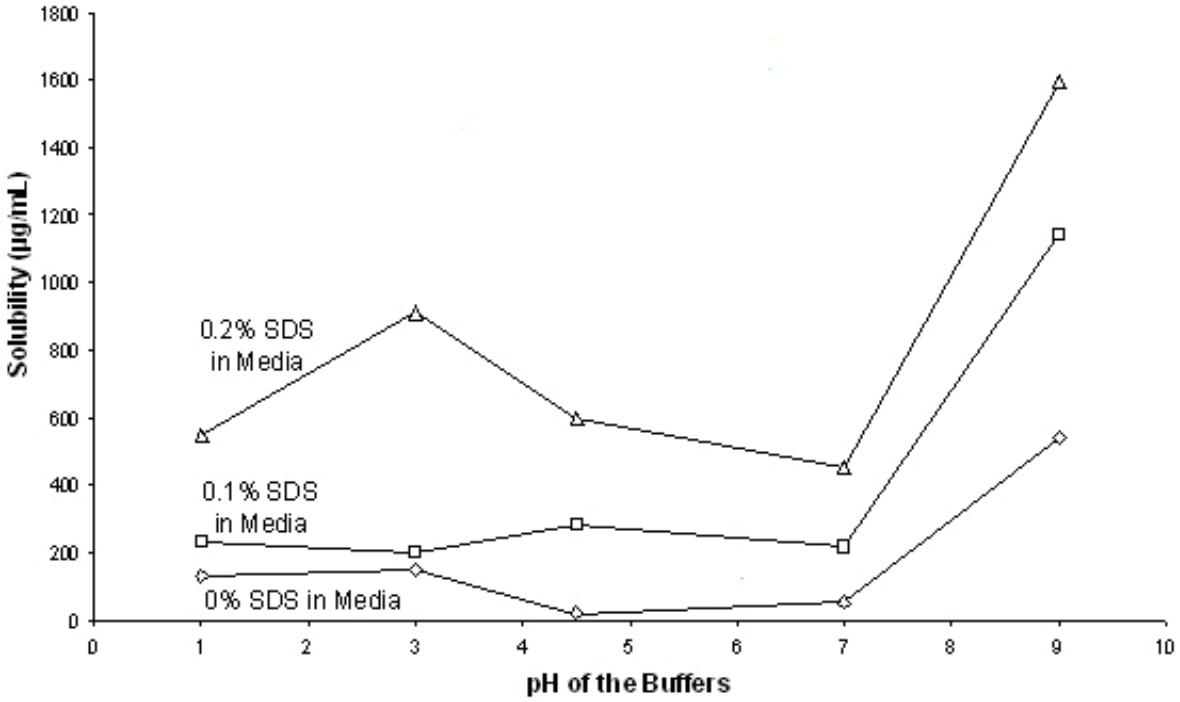

Figure 2.2: Solubility of repaglinide (µg/mL) in different pH buffers with differing %SDS added to the buffer

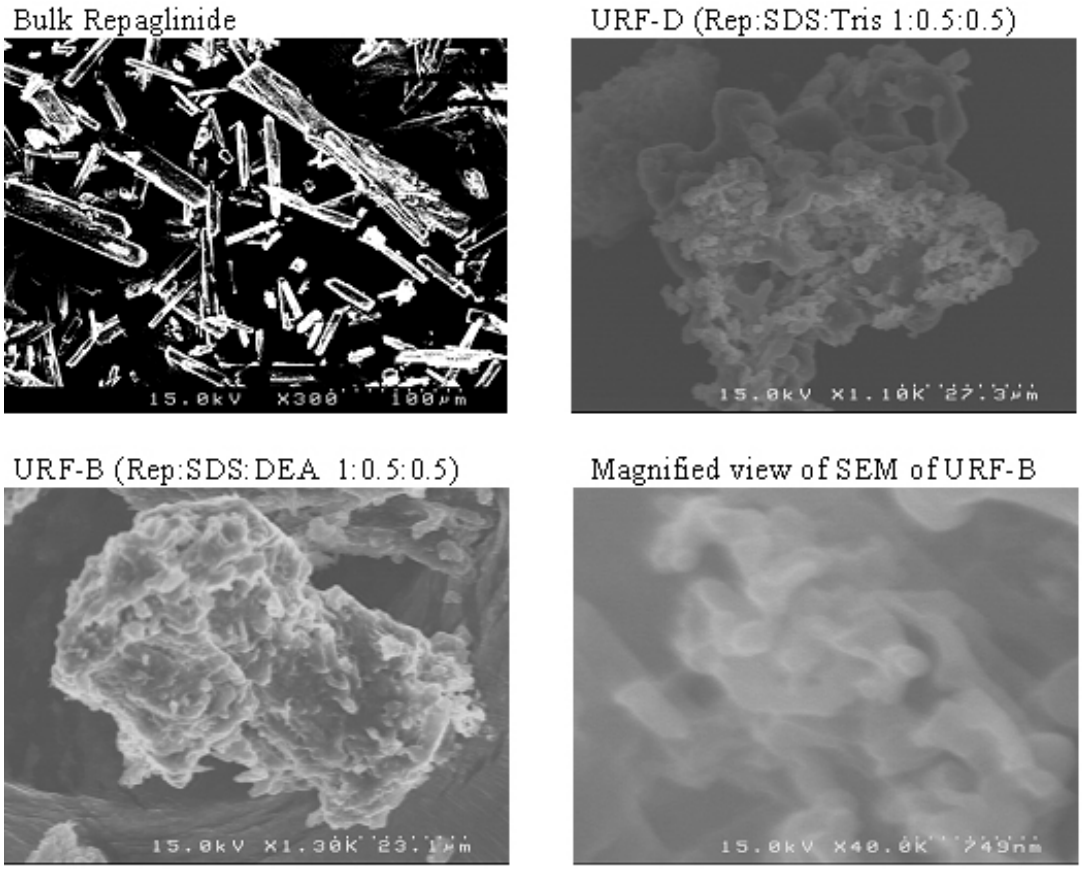

Figure 2.3: SEM micrographs of REP and REP-URF Formulations

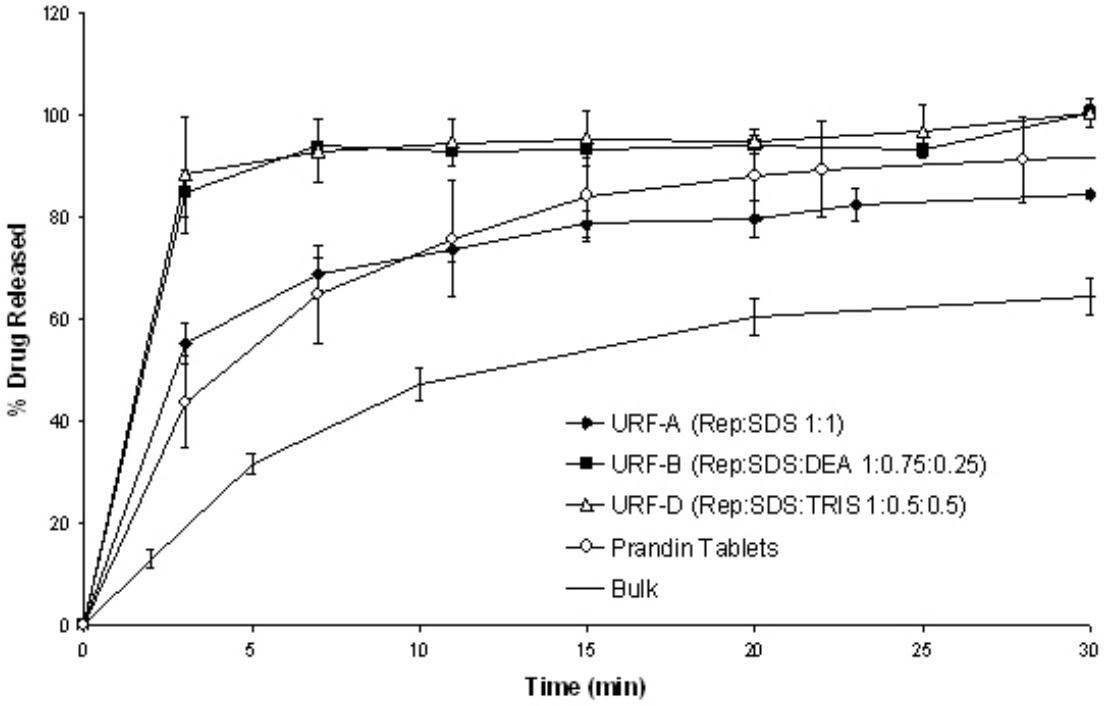

Figure 2.4: Dissolution performed under sink conditions: effect of adding an alkalizing agent to the URF formulation

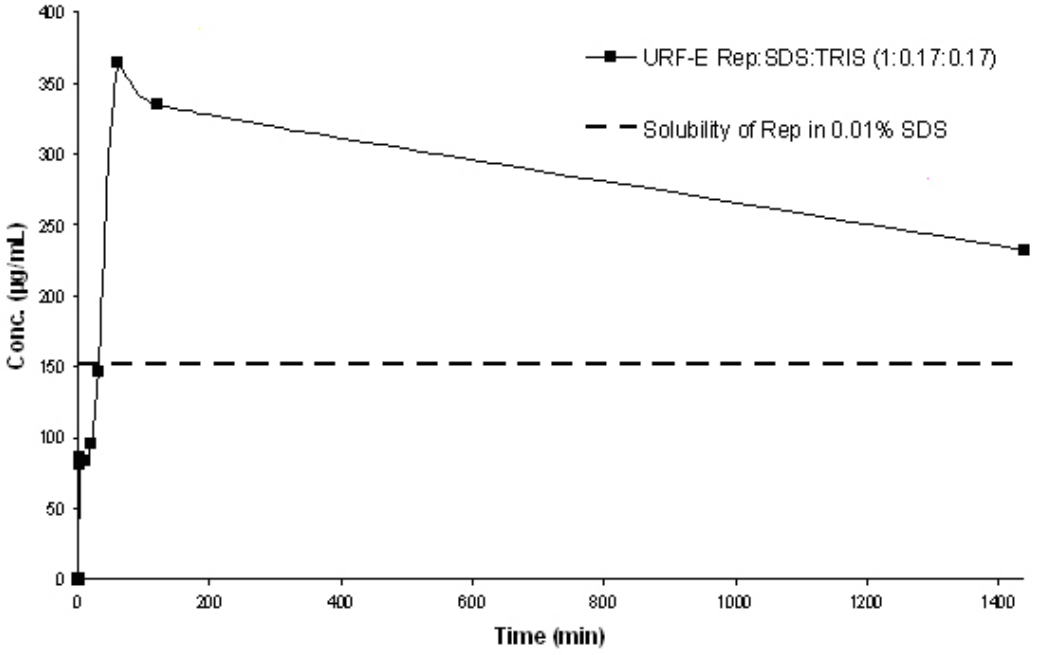

Figure 2.5: Dissolution of URF-E performed under supersaturated conditions, pH 4.5 citrate/sodium phosphate buffer, 50 RPM, 37^{o}C, 100 mL, paddle method

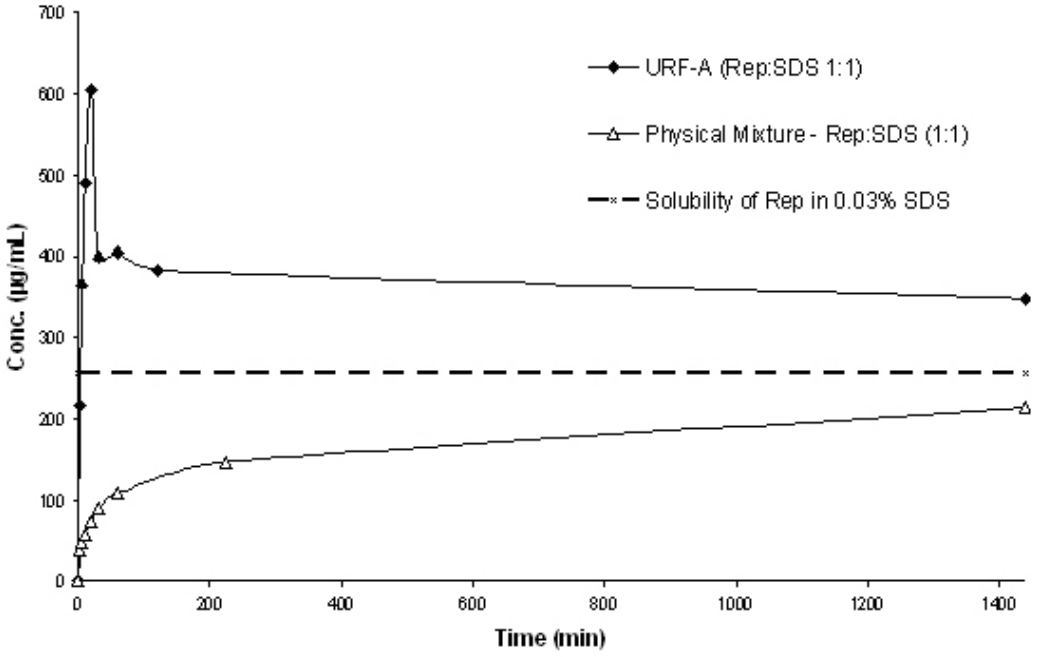

Figure 2.6: Dissolution of URF-A and REP/SDS Physical Mixture under supersaturated conditions - pH 4.5 citrate/sodium phosphate buffer, 50 RPM, 37^{o}C, 100 mL

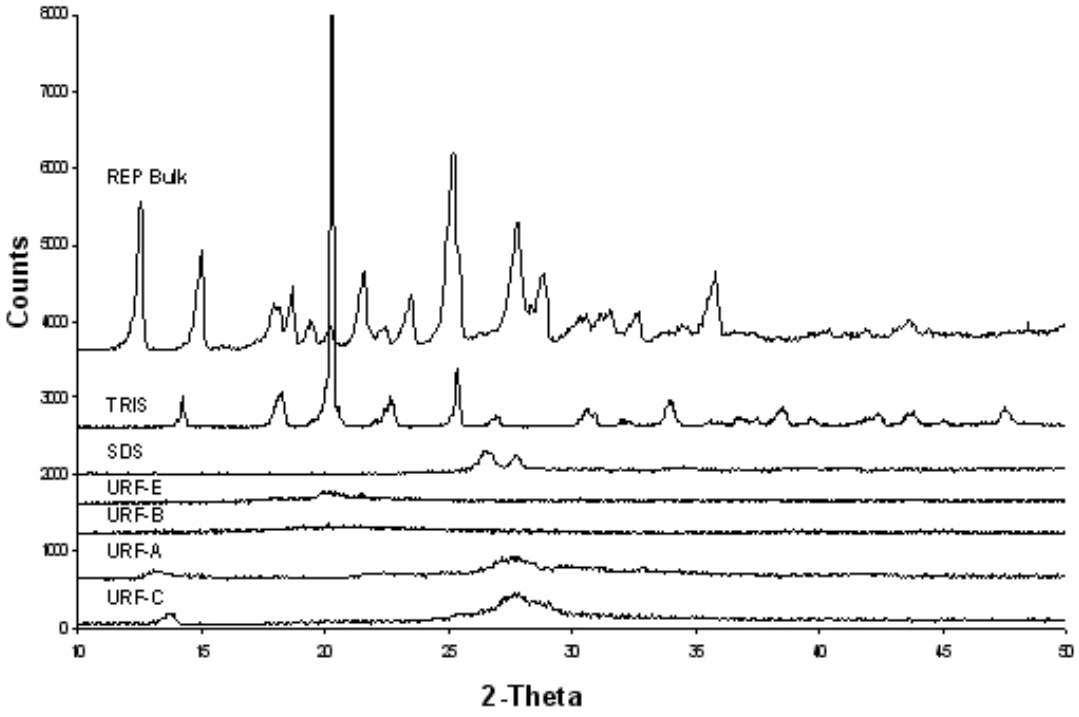

Figure 2.7: X-Ray Diffractograms of REP, excipients, and REP-URF Formulations

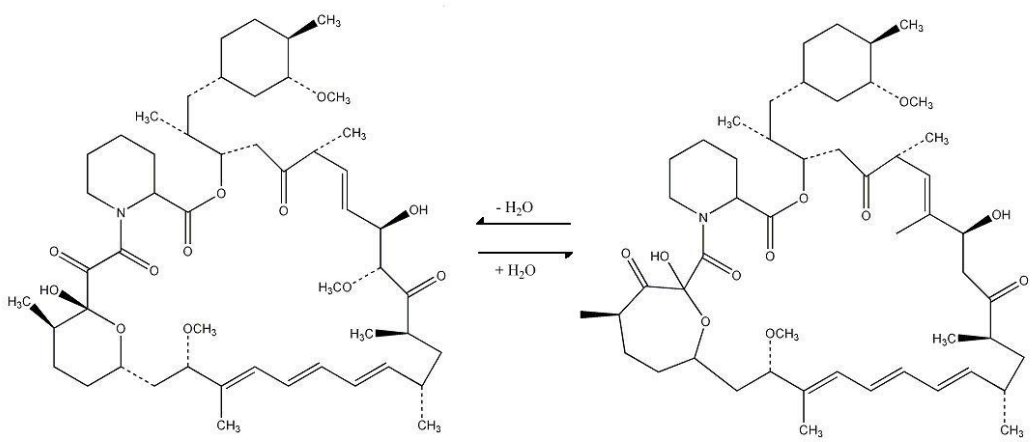

Figure 3.1: Isomerization of sirolimus in organic/aqueous solution

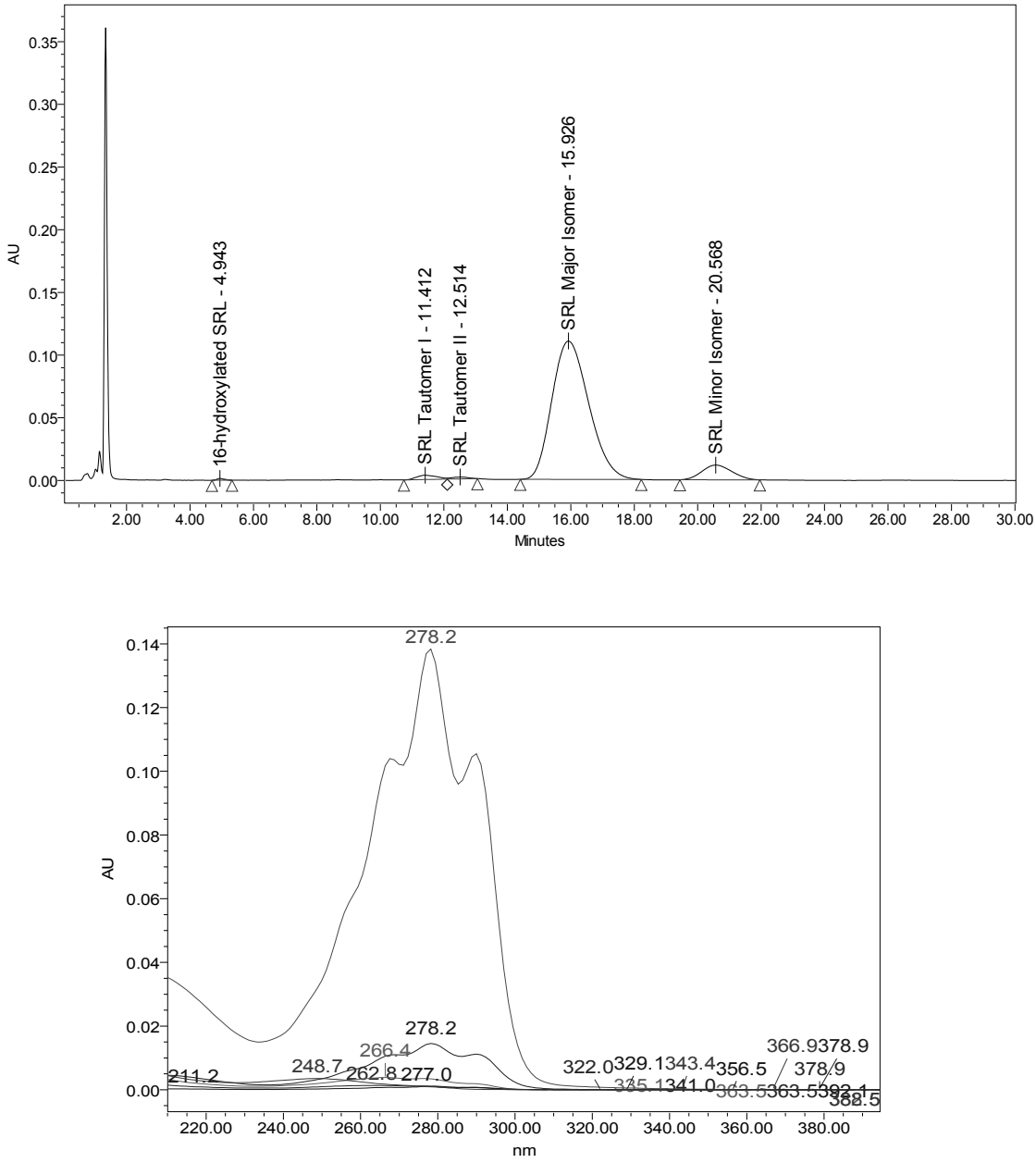

Figure 3.2: Working standard of SRL at 100µg/mL drug, along with the typical UV spectrum of a working standard, showing the characteristic SRL UV spectrum with a lambda max of 278.2 nm

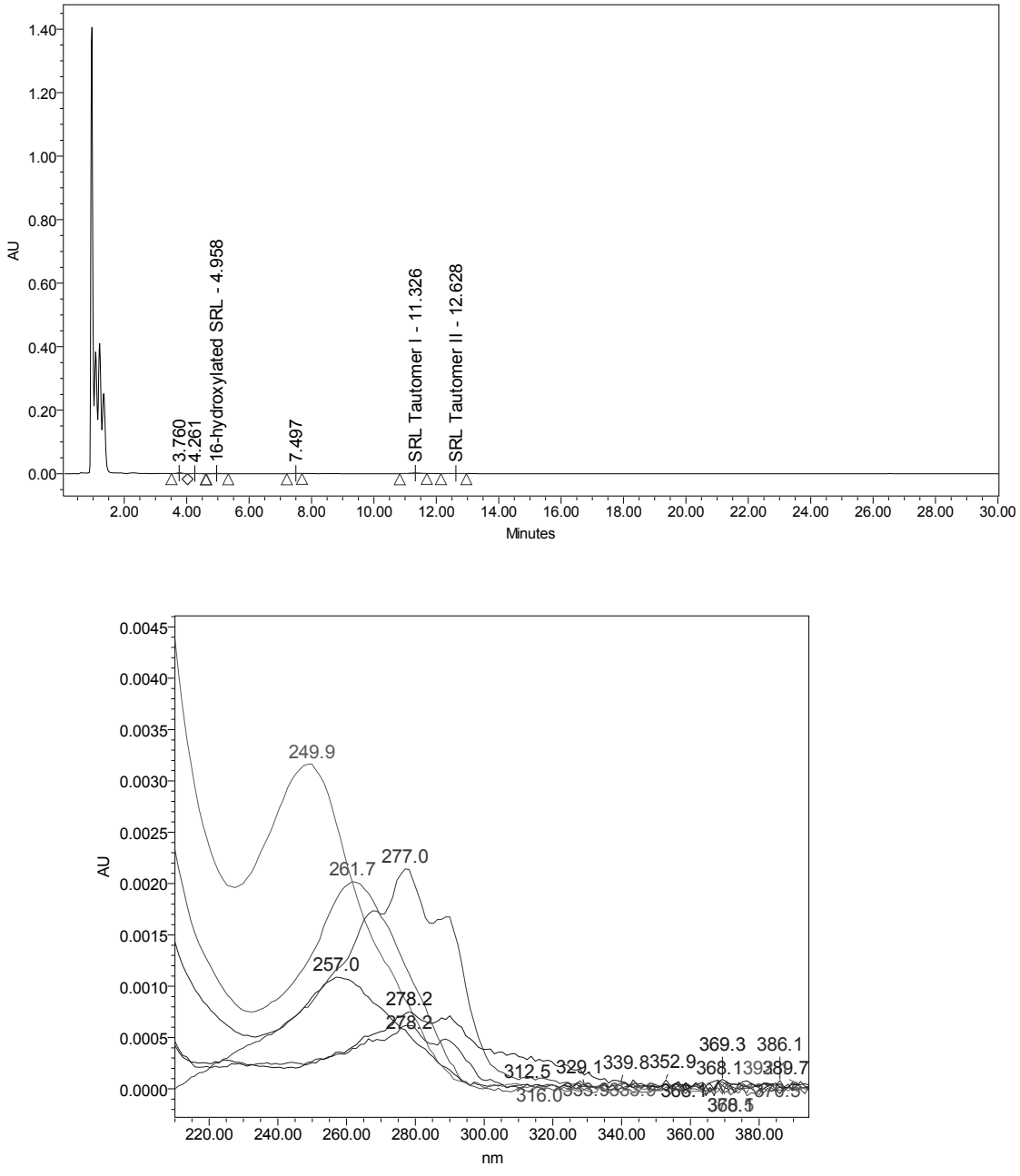

Figure 3.3: Base catalyzed degradation of SRL using 0.1N sodium hydroxide for 30 min at 25^{o}C (100µg/mL SRL added initially), and the UV spectrum of the resulting degradation confirming no SRL present in the solution.

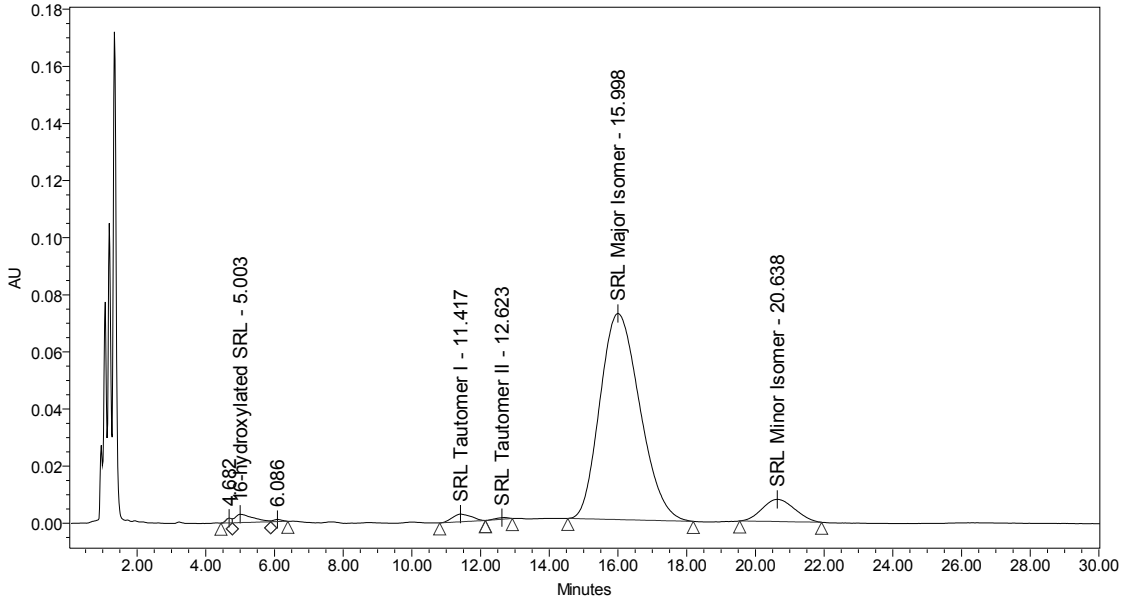

Figure 3.4: Acid catalyzed degradation of SRL using 0.1N hydrochloric acid for 1 hour at 25^{o}C (100µg/mL SRL added initially)

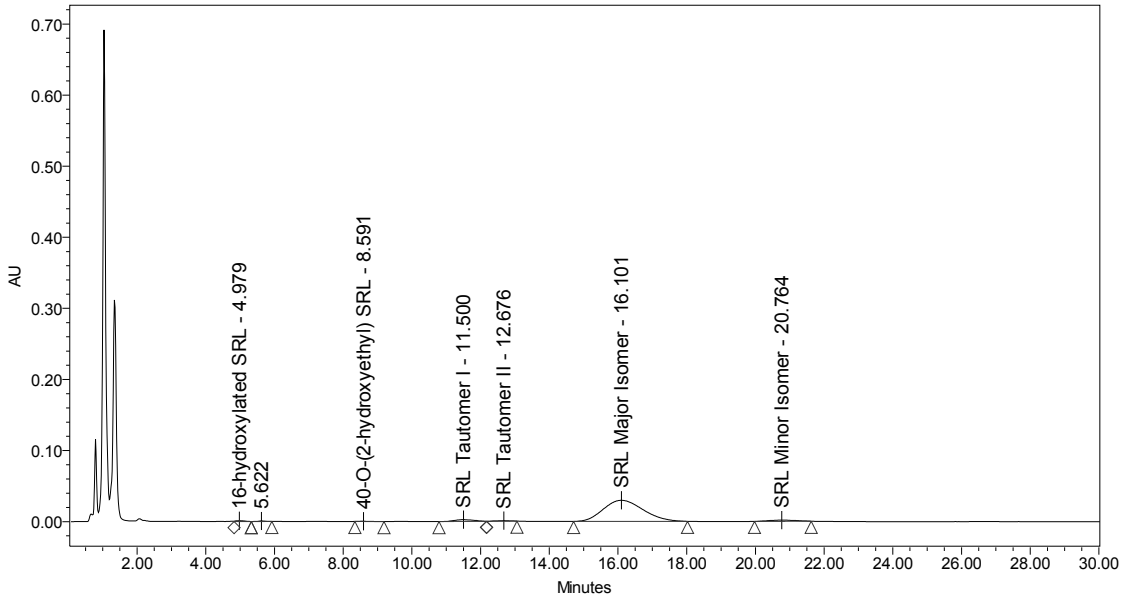

Figure 3.5: Oxidation catalyzed degradation of SRL using 3% hydrogen peroxide for 1 hour at 25^{o}C (100µg/mL SRL added initially)

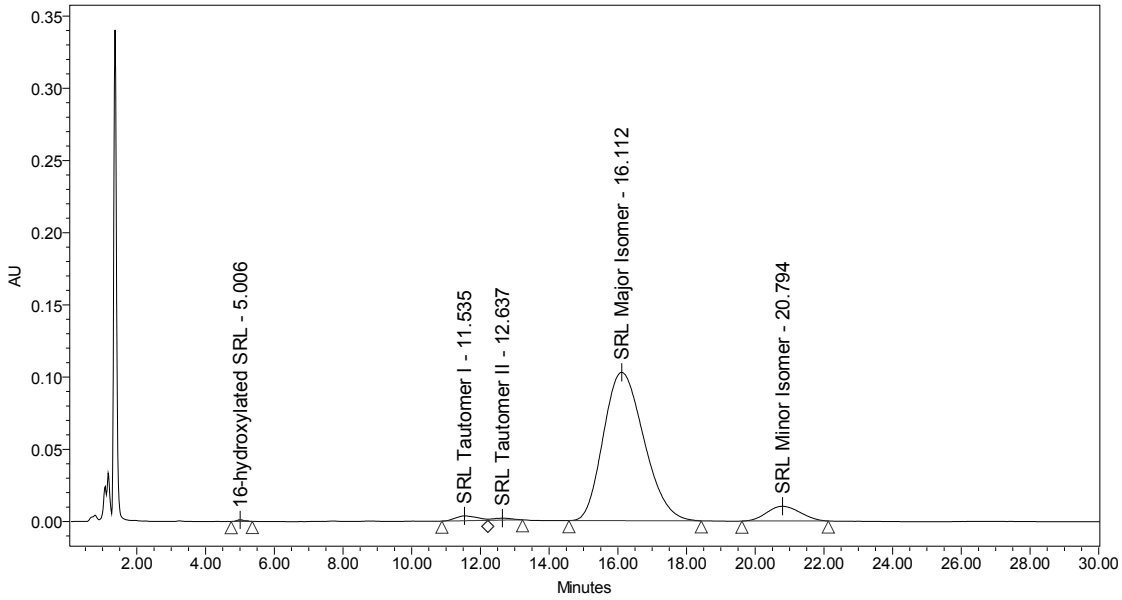

Figure 3.6: Thermal degradation of SRL using 100µg/mL SRL incubated at 40^{o}C for 6 hours

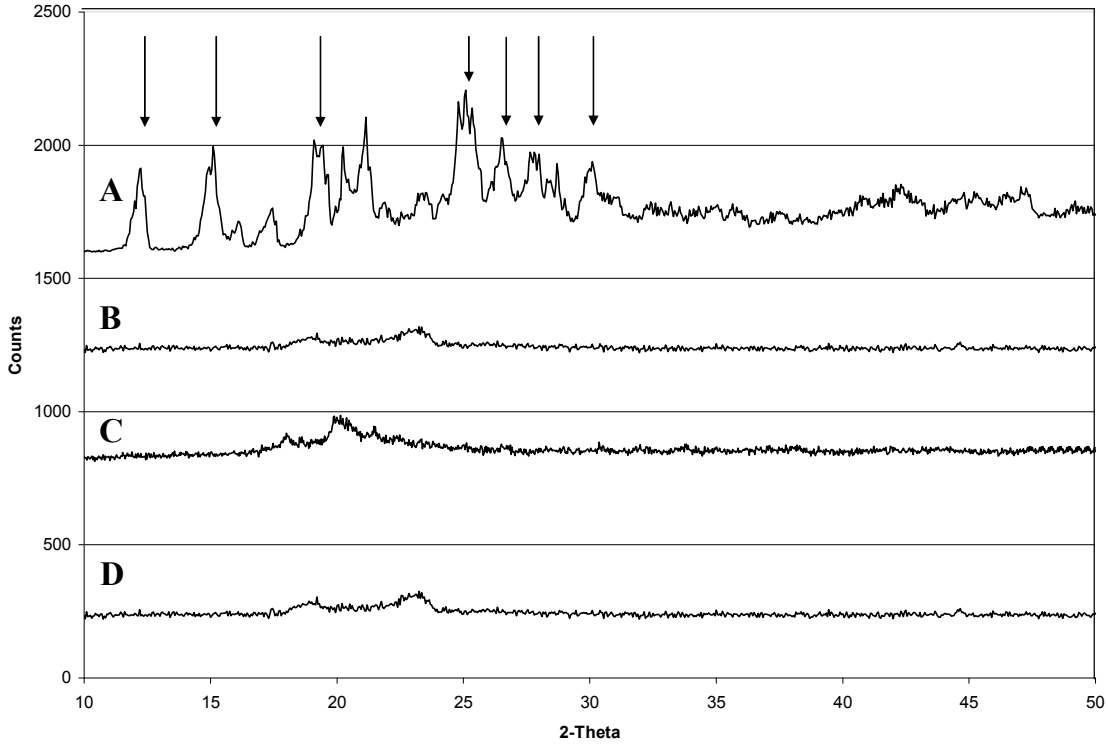

Figure 3.**7**: X-Ray diffraction pattern for A.) SRL bulk drug substance (crystalline); B.) URF-SRL Formulation 3 (SRL:SDS:P407 2:1:1), C.) URF-SRL Formulation 2 (SRL/HPMC E5, 1:1), and D.) URF-SRL Formulation 1 (SRL/P407, 1:1)

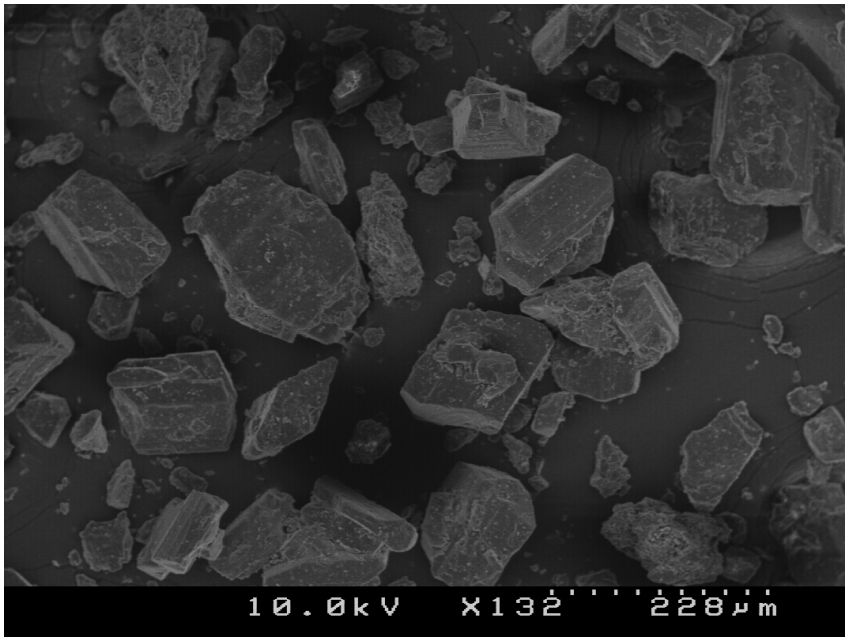

Figure 3.8: SEM's of SRL bulk material (crystalline)

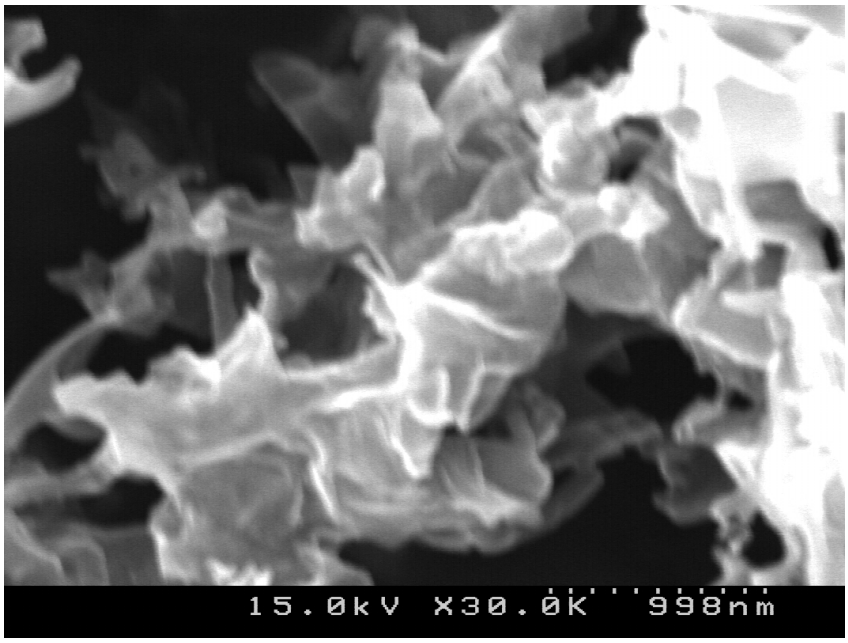

Figure 3.9: SEM of URF-SRL Formulation 1 (SRL:P407, 1:1)

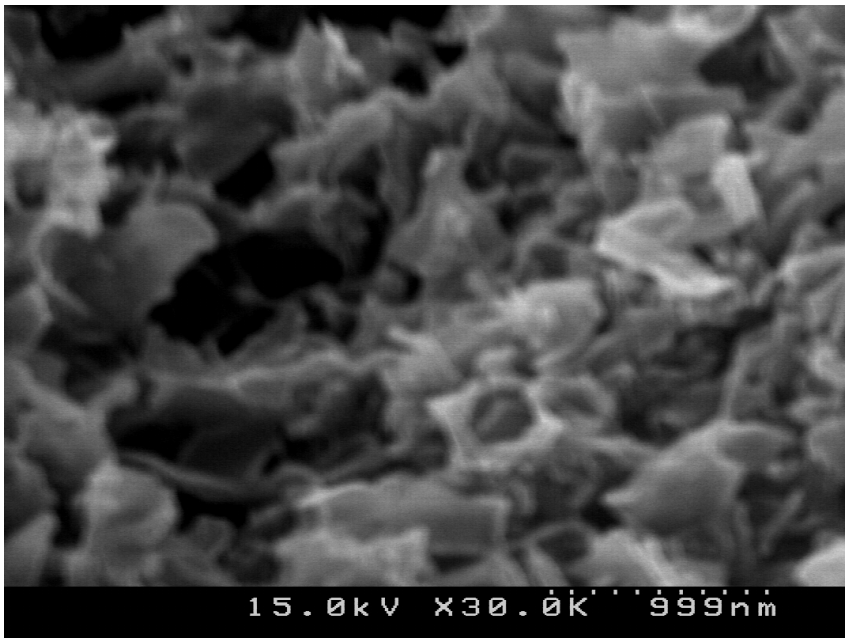

Figure 3.10: SEM of URF-SRL Formulation 2 (SRL:HPMC E5, 1:1)

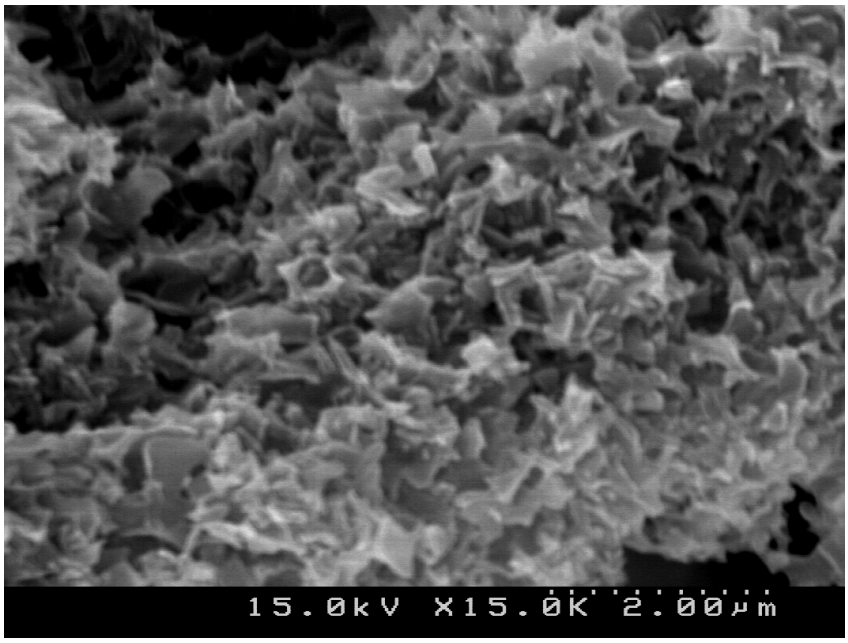

Figure 3.11: SEM of URF-SRL Formulation 2 (SRL:SDS:P407, 2:1:1)

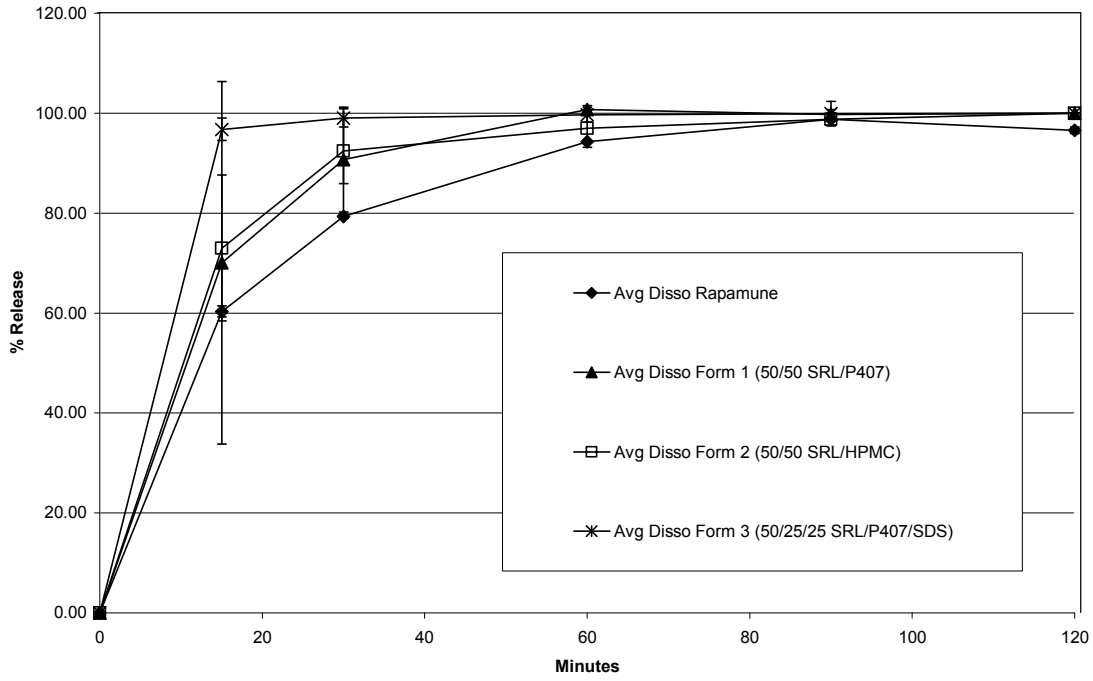

Figure 3.12: Sink dissolution of URF-SRL Formulations 1, 2, and 3 and Rapamune® Tablets. Dissolution conditions: 3-5mg SRL, 900 mL, 0.1% SDS media, 50 RPM, 37^{o}C, n=3.

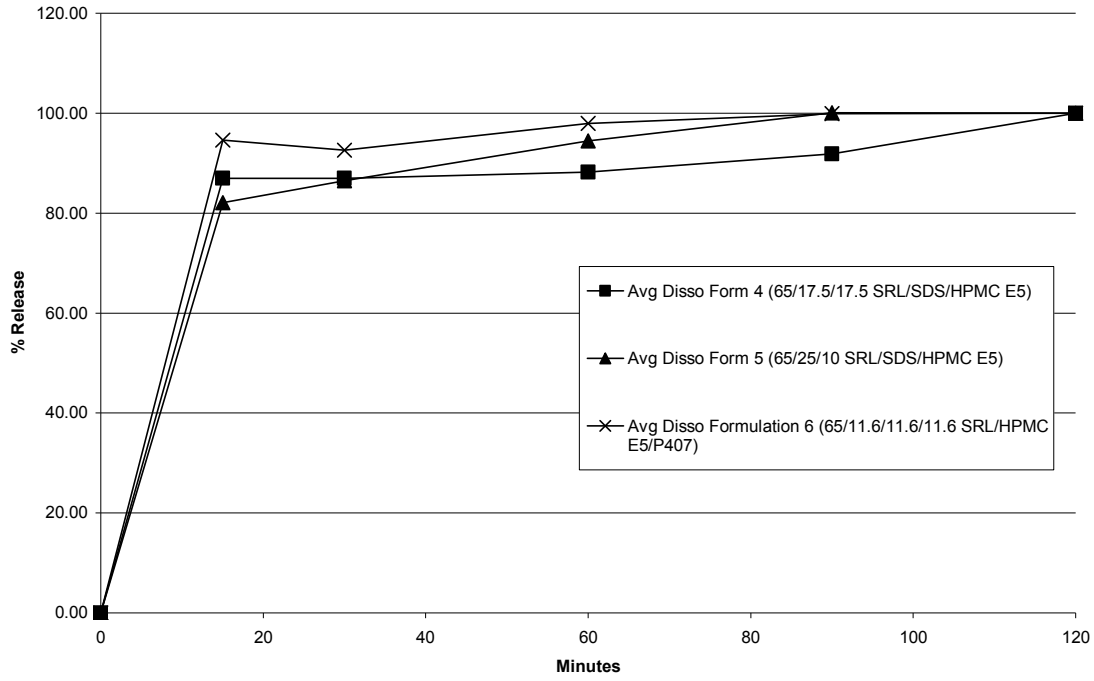

Figure 3.13: Sink dissolution of URF-SRL Formulations 4, 5, and 6 (high potency 65% SRL formulations). Dissolution conditions: 3-5mg SRL, 900 mL, 0.01% SDS media, 50 RPM, 37^{o}C, n=3.

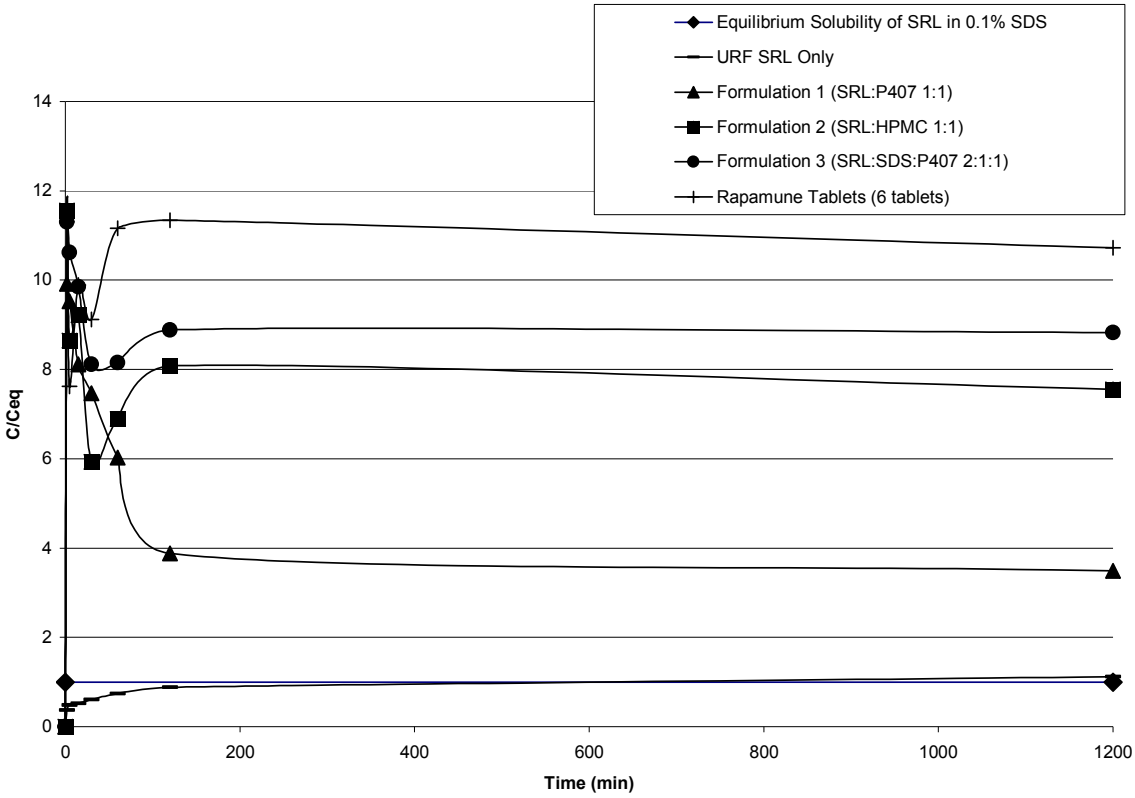

Figure 3.14: Supersaturated dissolution of URF-SRL Formulations 1, 2, and 3 and Rapamune® Tablets. Drug loading - 12.5X times aqueous equilibrium solubility - (6.5 mg SRL), 0.1% SDS in water,100 mL, small volume dissolution apparatus, 50 RPM, 37^{o}C, n=1

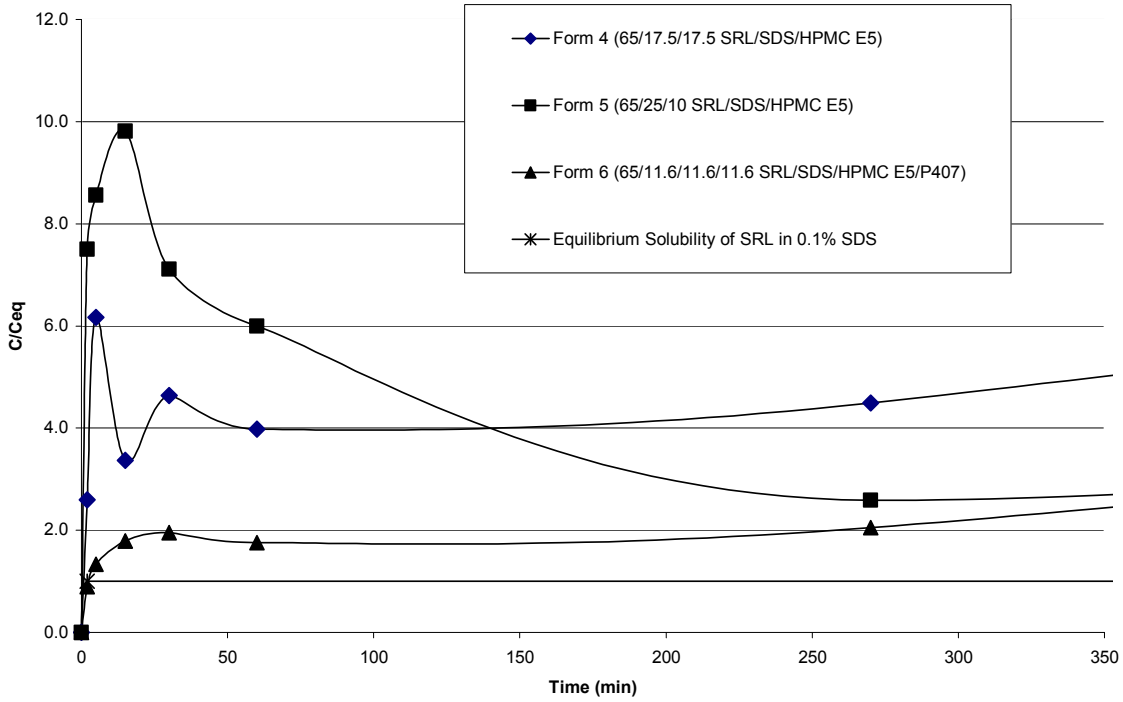

Figure 3.15: Supersaturated dissolution of URF-SRL Formulations 4, 5, and 6. Drug loading - 12.5 times equilibrium aqueous solubility (6.5 mg SRL), 100 mL, 0.1% SDS in water, small volume dissolution apparatus, 50 RPM, 37^{o}C, n=1.

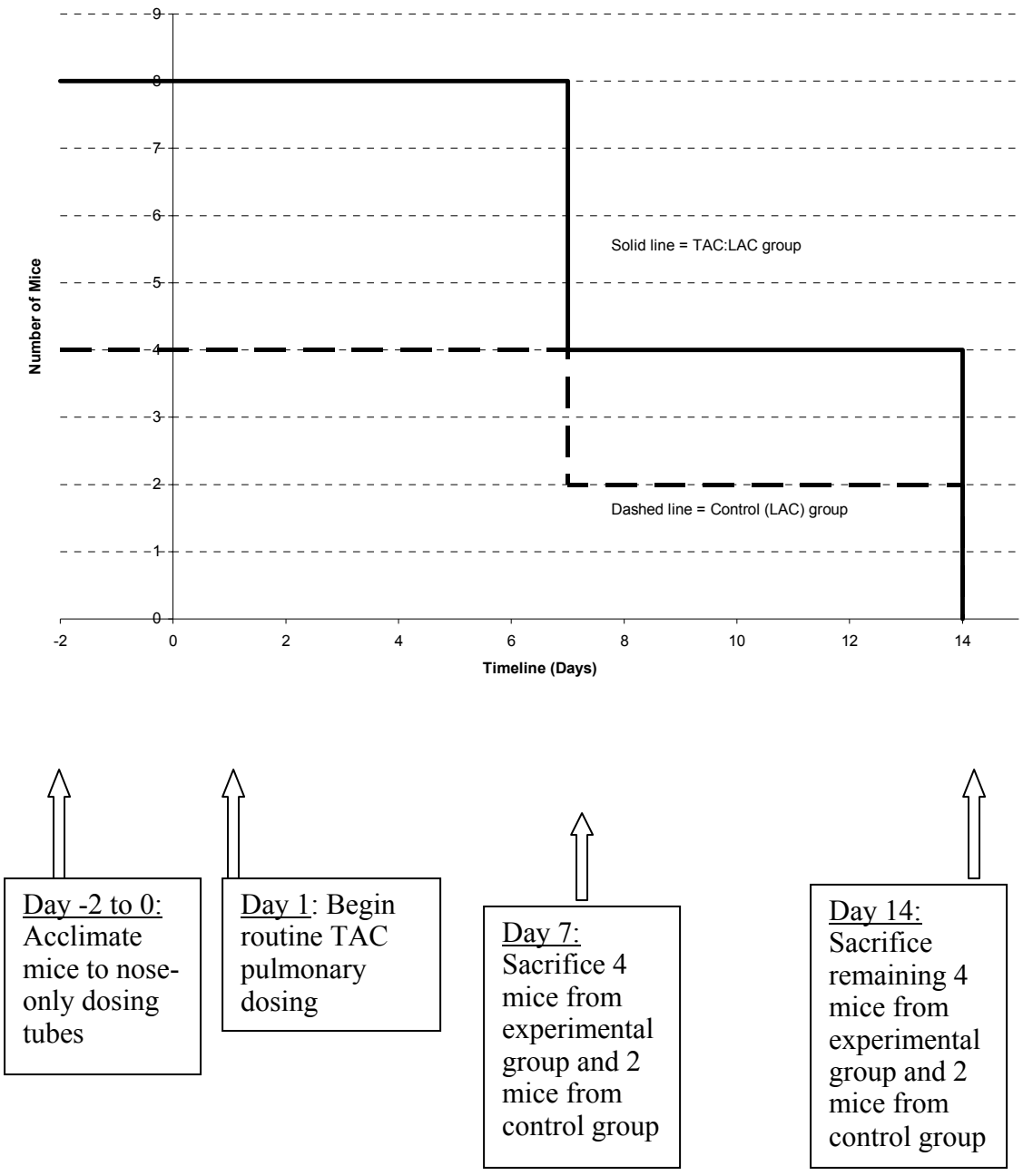

Figure 4.1: Timeline scheme of animal dosing for the TAC multi-dose study for 7 and 14 days.

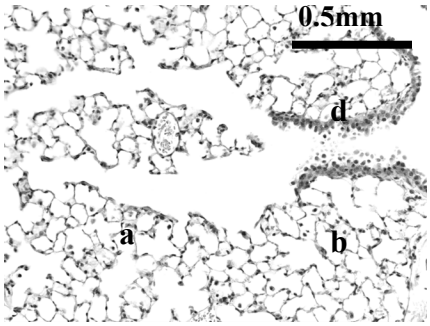

Figure 4.2: Lung tissue histology from TAC:LAC experimental group, day 7. a.) Alveolar Spaces; b.) Capillaries; c.) Lymph Tissue; d.) Arterioles with red blood cells present

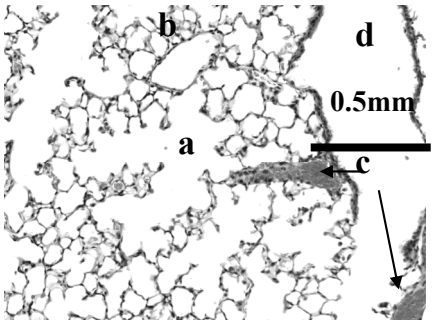

Figure 4.3: Lung tissue histology from TAC:LAC experimental group, day 14. a.) Alveolar Spaces; b.) Capillaries; c.) Lymph Tissue; d.) Arterioles with red blood cells present

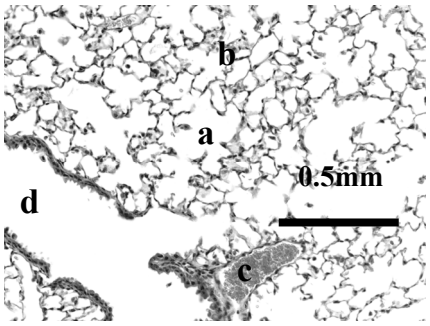

Figure 4.4: Lung tissue histology from LAC only control group, day 7. a.) Alveolar Spaces; b.) Capillaries; c.) Lymph Tissue; d.) Arterioles with red blood cells present

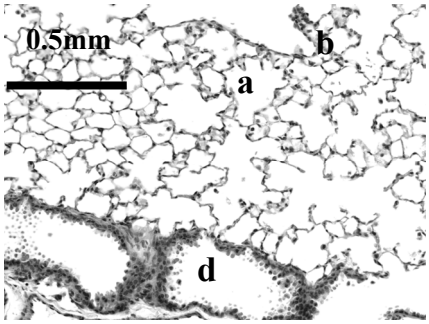

Figure 4.5: Lung tissue histology from LAC only control group, day 14. a.) Alveolar Spaces; b.) Capillaries; c.) Lymph Tissue; d.) Arterioles with red blood cells present

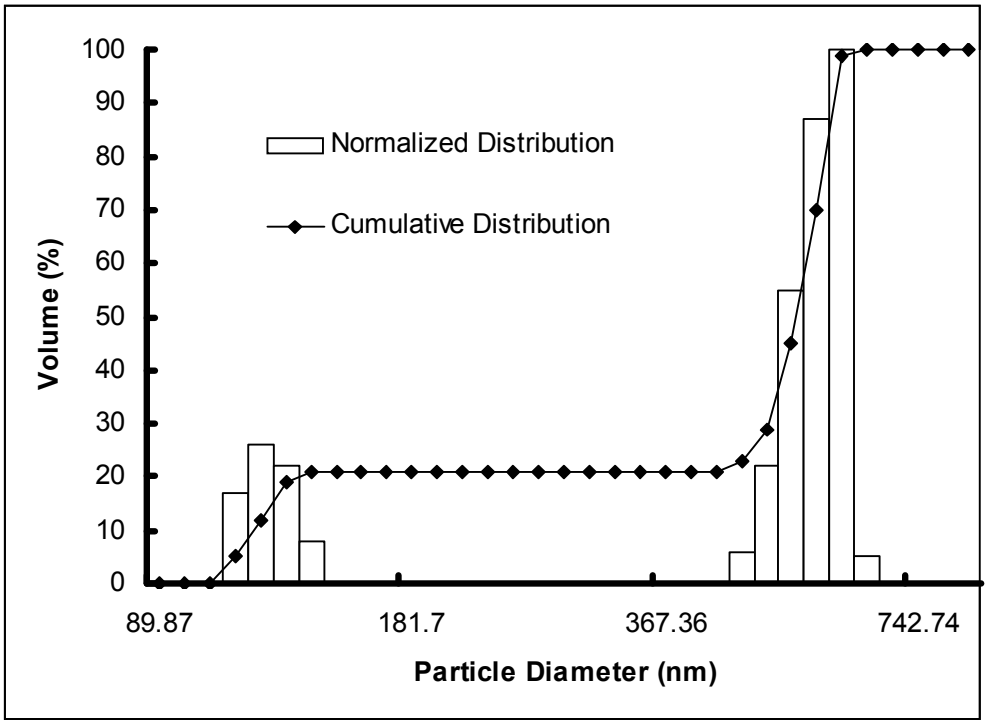

Figure 4.6: Particle sizing measurements by dynamic light scattering of the URF TAC:LAC (1:1) formulation when dispersed in DI water and sonicated for 15 minutes. The mean diameter was reported to be 468.3 nm, with almost 90% of particles, by volume, with diameters below 561 nm.

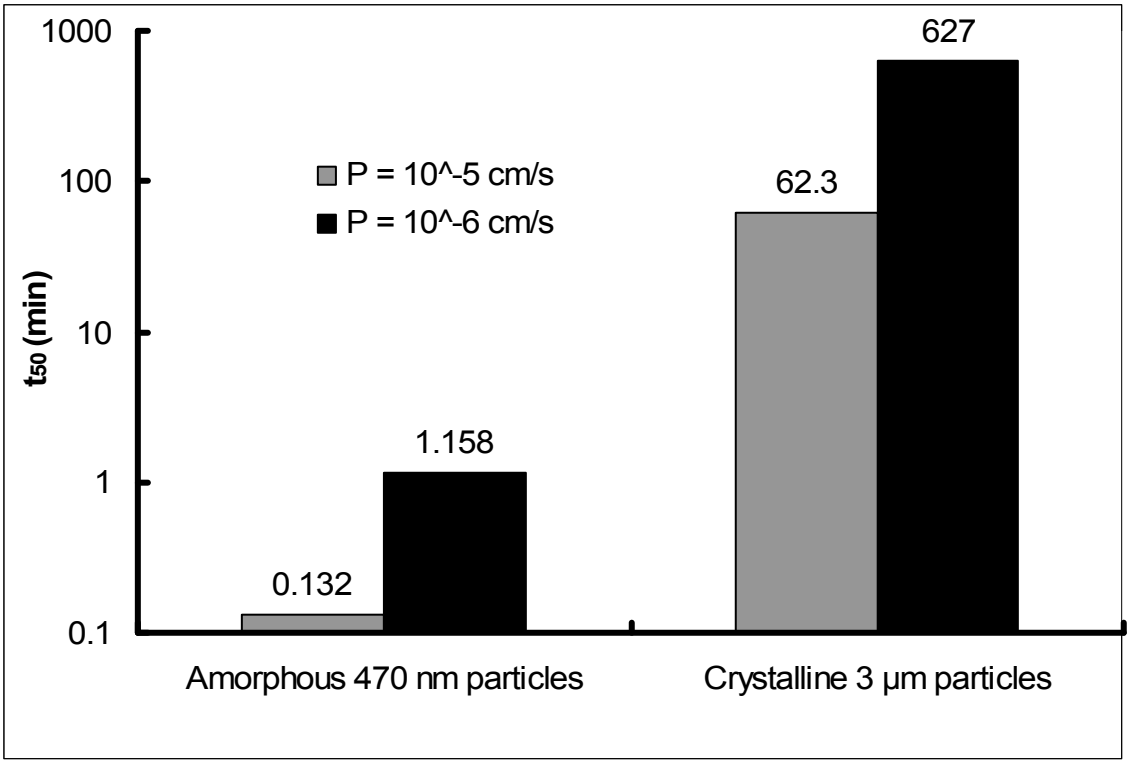

Figure 4.7: Predicted absorption half lives (time for 50% of drug to dissolve and permeate though lung epithelium) for amorphous and crystalline TAC drug particles at two different permeabilities for a deposited dose of 4.06 µg TAC/lung (~ 18.5 µg/g lung tissue), which was chosen based on results from a TAC:LAC single-dose pharmacokinetic study. The diffusion coefficient was estimated to be $4.02*10^{-6}$ cm^2/s.

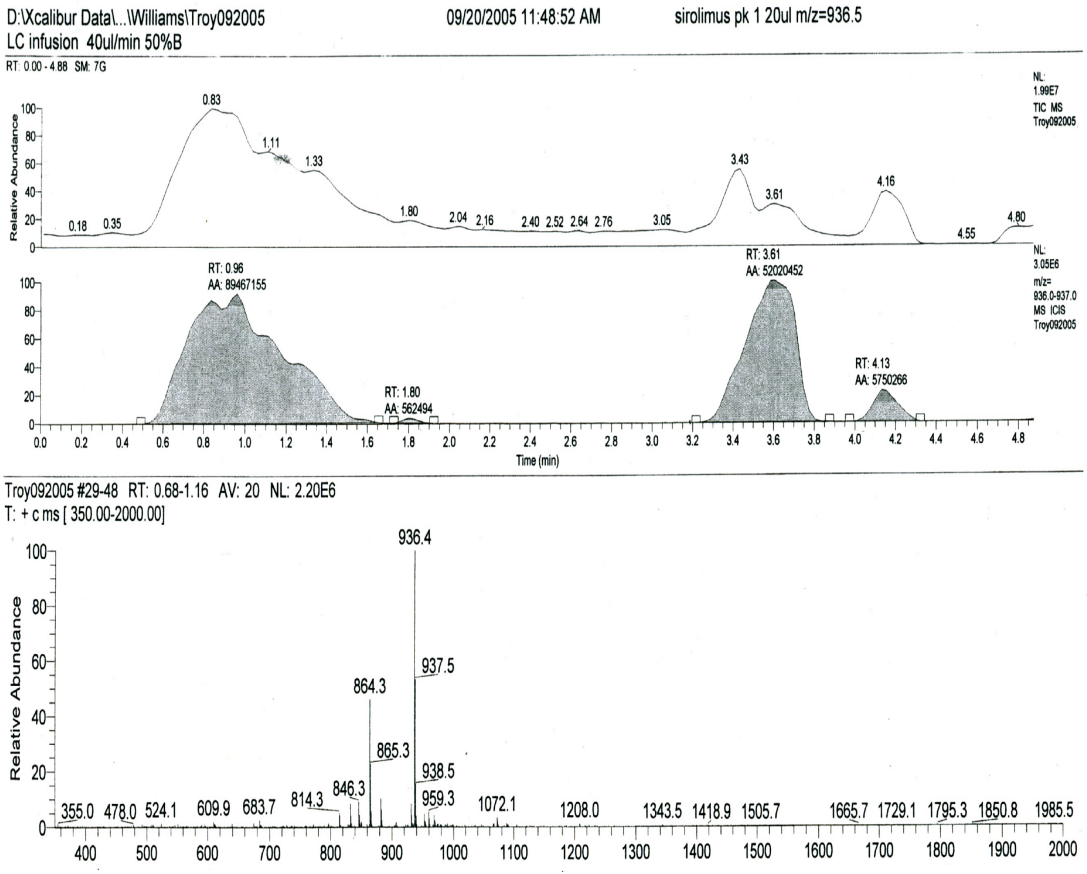

Figure A.1: Sirolimus fraction 1 (peak 1, major lactone isomer) analyzed by LC-MS, showing daughter ions and m/z values for the fractionated sample.

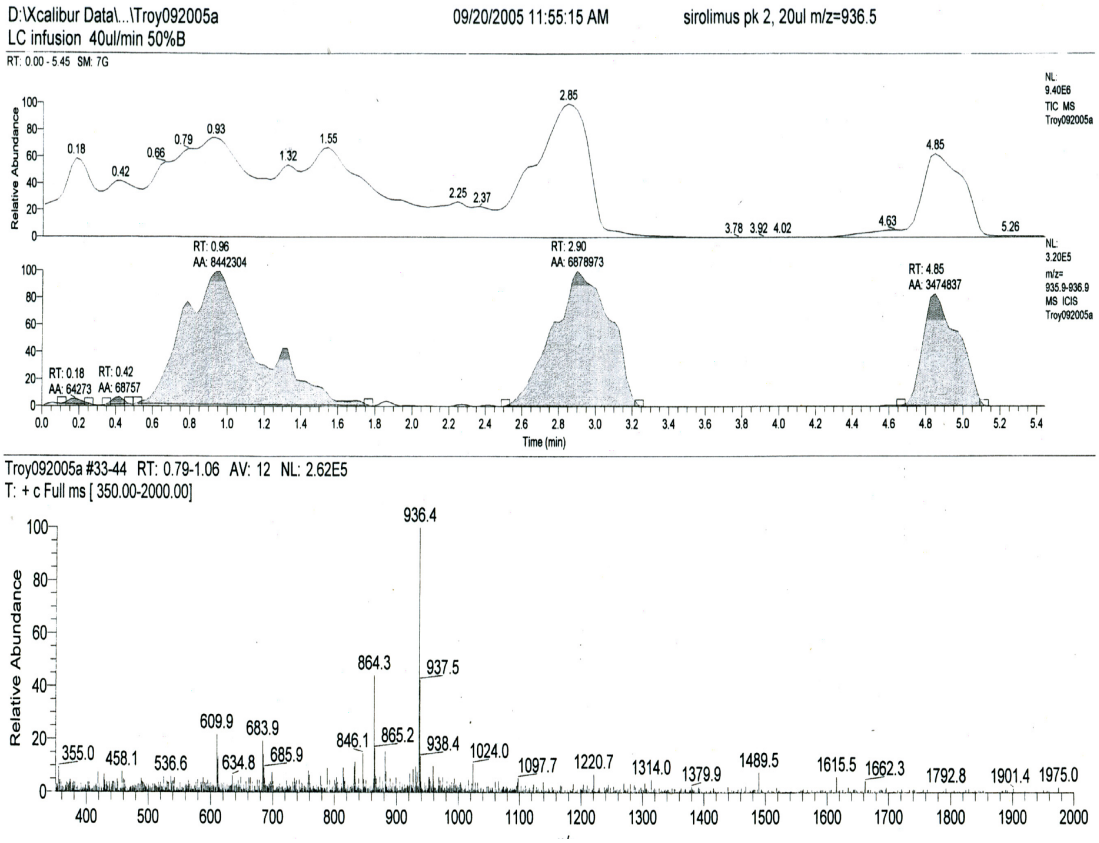

Figure A.2 Sirolimus fraction 2 (peak 2, minor lactam isomer) analyzed by LC-MS, showing daughter ions and m/z values for the fractionated sample

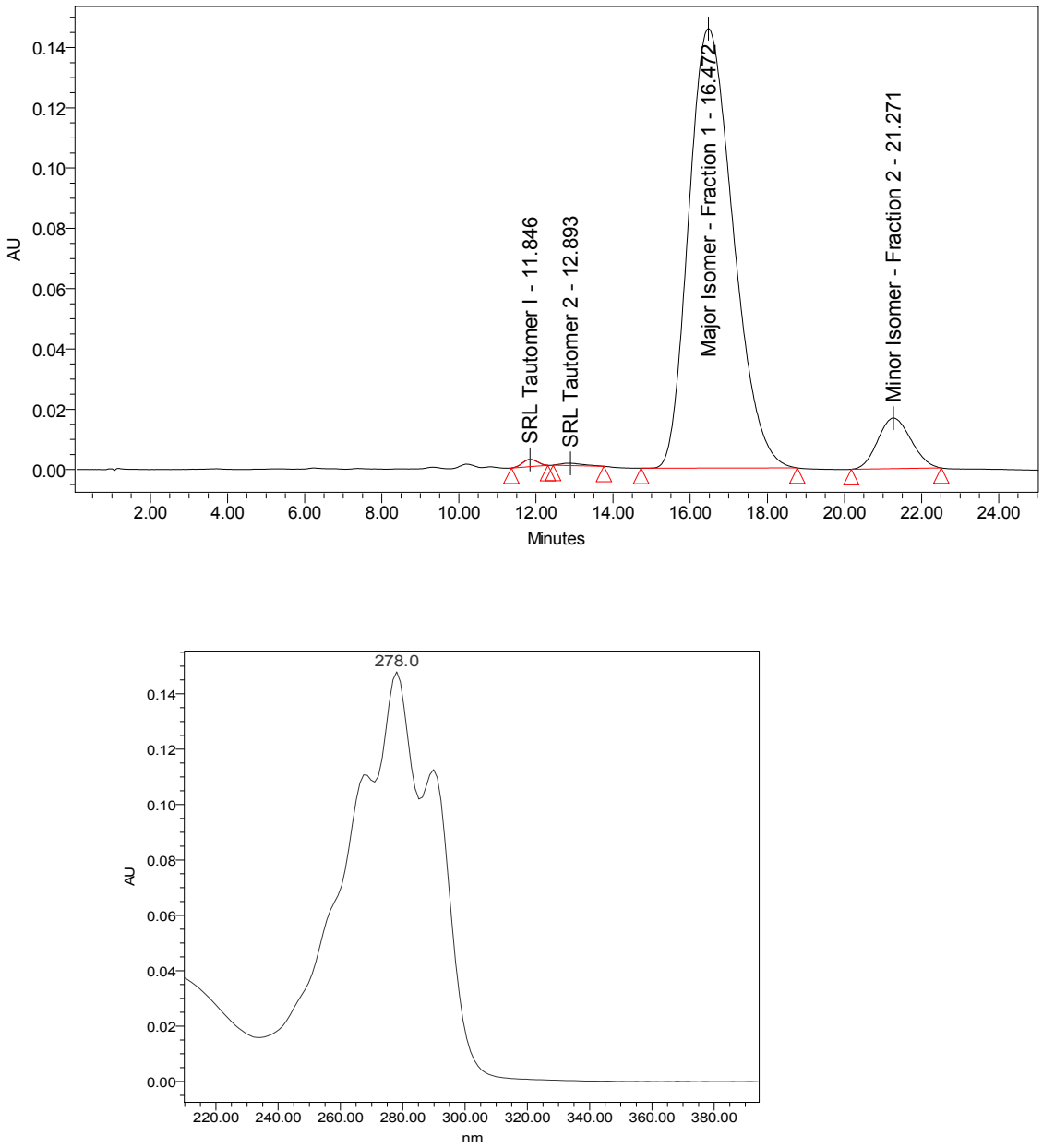

Figure A.3 Sample chromatogram and UV spectrum of a working standard SRL (50 µg/mL), showing both isomer peaks and identical UV spectra

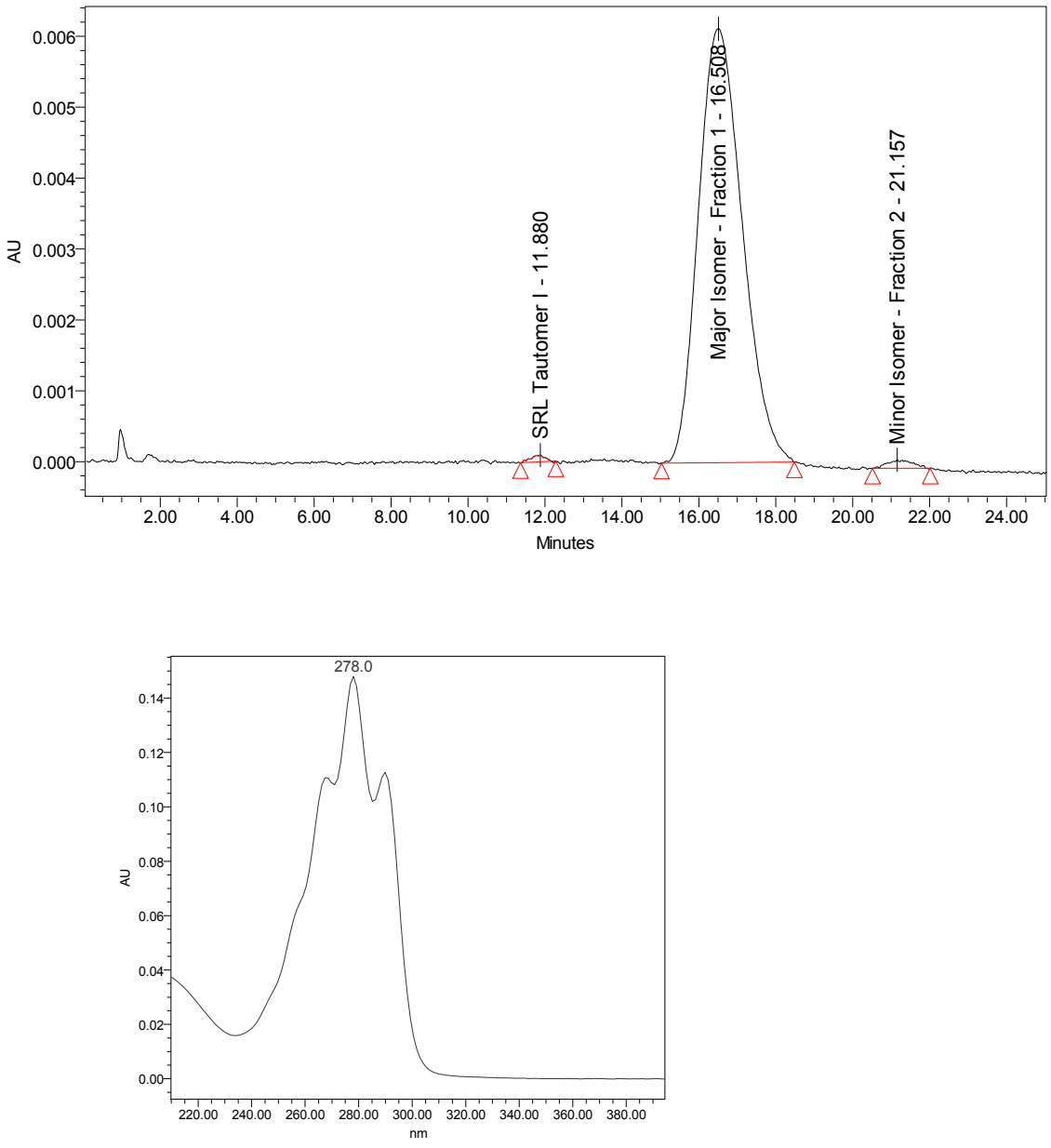

Figure A.4: Sample chromatogram and UV spectrum for fractionated sample 1 (peak 1, major lactone isomer) collected over 15-17 minutes

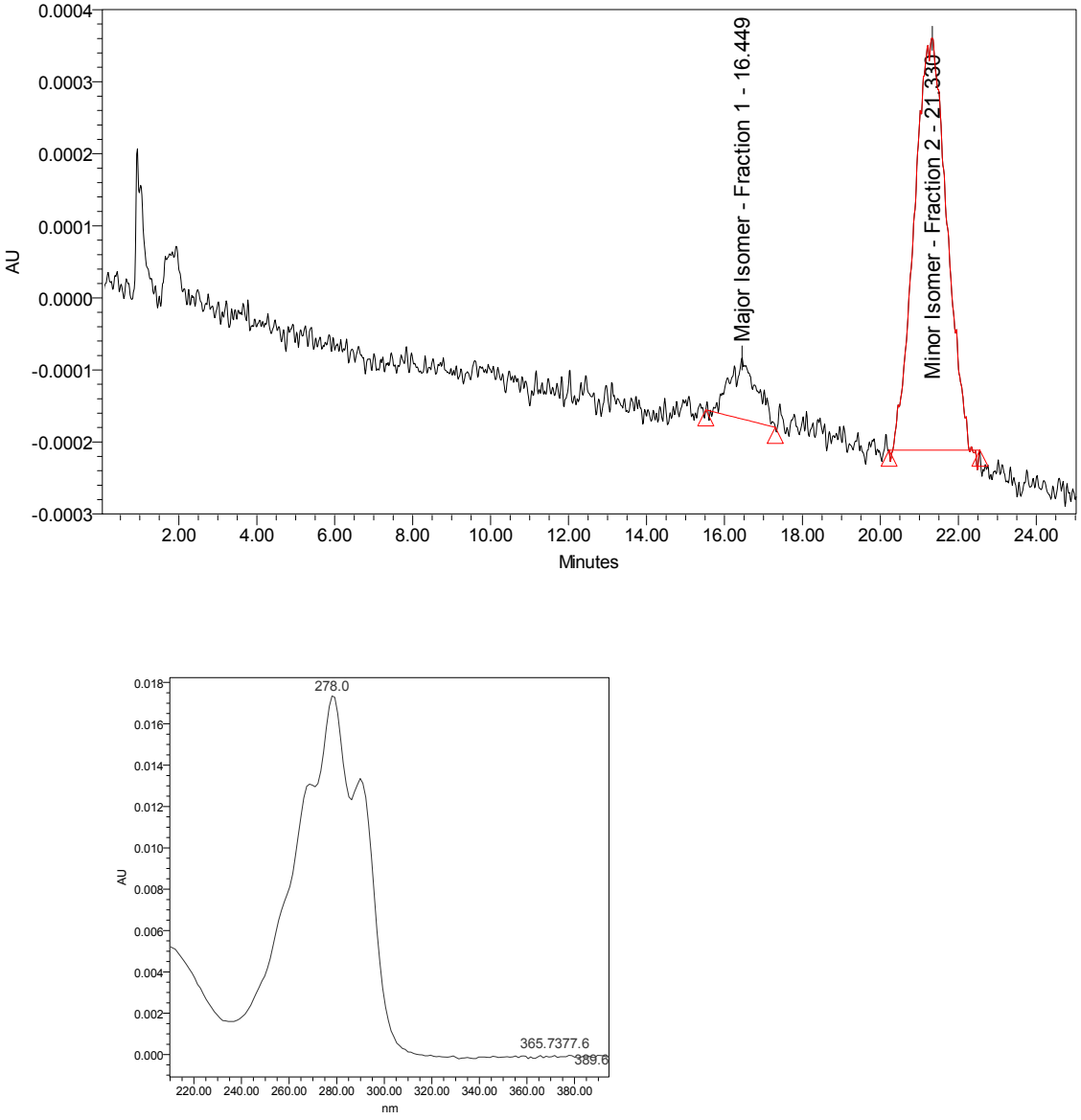

Figure A.5: Sample chromatogram and UV spectrum for fractionated sample 2 (peak 2, major lactam isomer) collected over 19-22 minutes

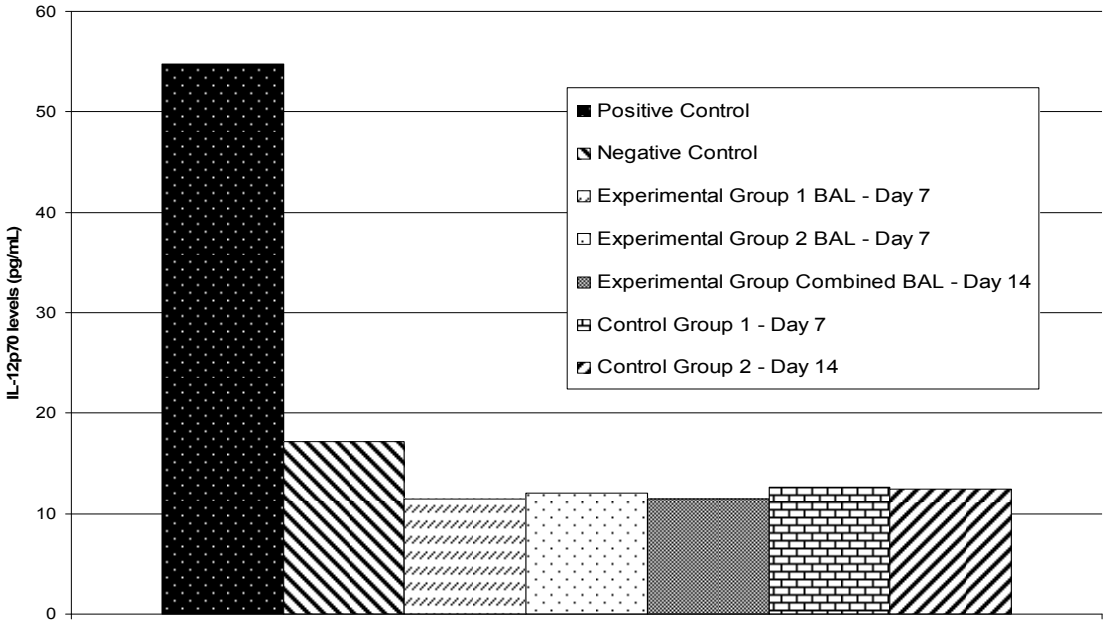

Figure E.1: IL-12p70 from Mouse ELISA kit showing no induction of the cytokine in BAL fluid.

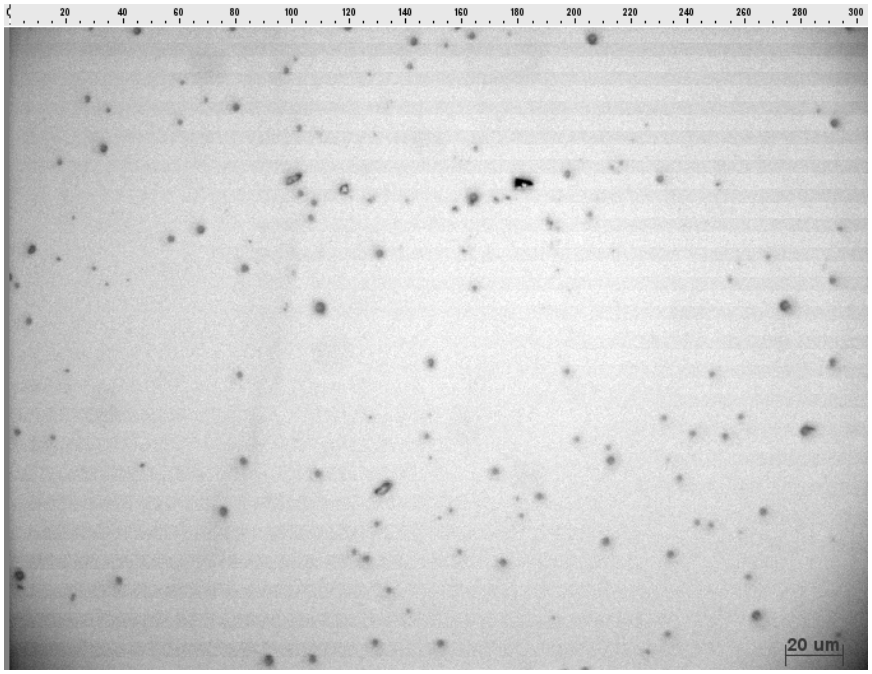

Figure F.1: Light microscope images of URF-TAC microparticles dispersed in RPMI 1640, 40X magnification; initial time point

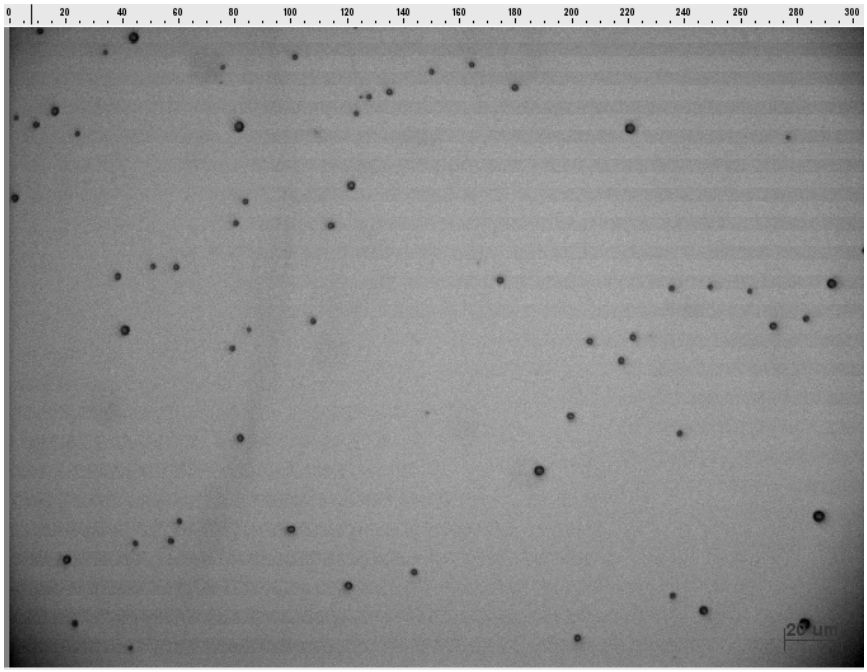

Figure F.2: Light microscope images of TAC:LAC microparticles dispersed in RPMI 1640, 40X magnification; initial time point.

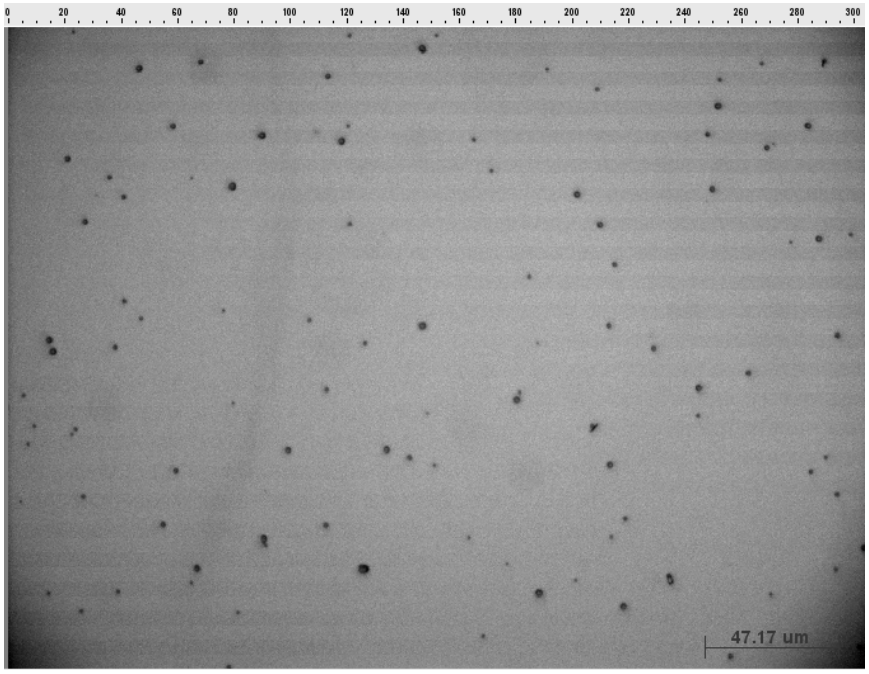

Figure F.3: Light microscope images of ITZ:mannitol:DPPC microparticles (control) dispersed in RPMI 1640, 40X magnification; initial time point

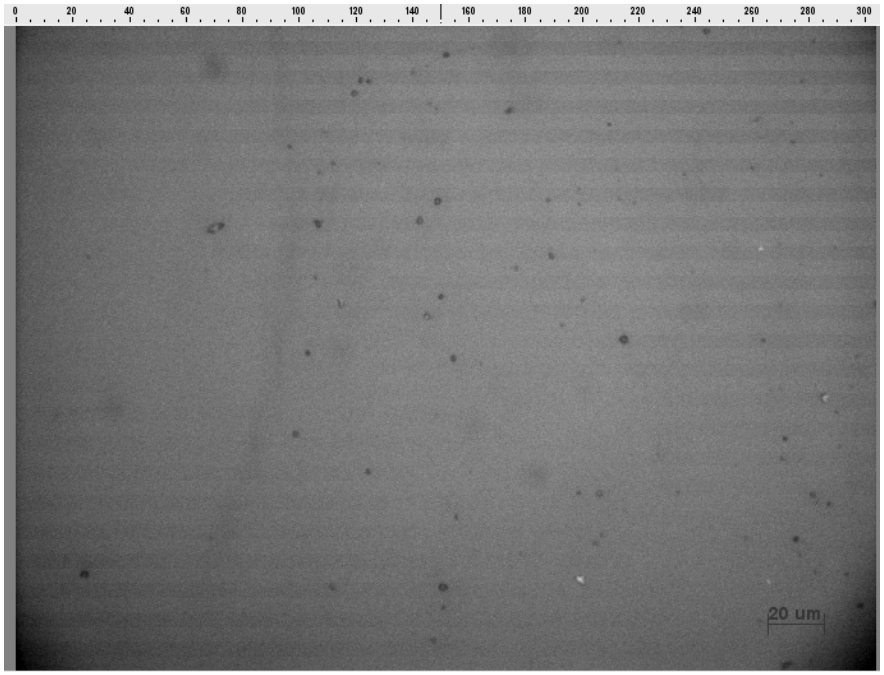

Figure F.4: Light microscope images of URF-TAC microparticles dispersed in RPMI 1640, 40X magnification; day 5 time point.

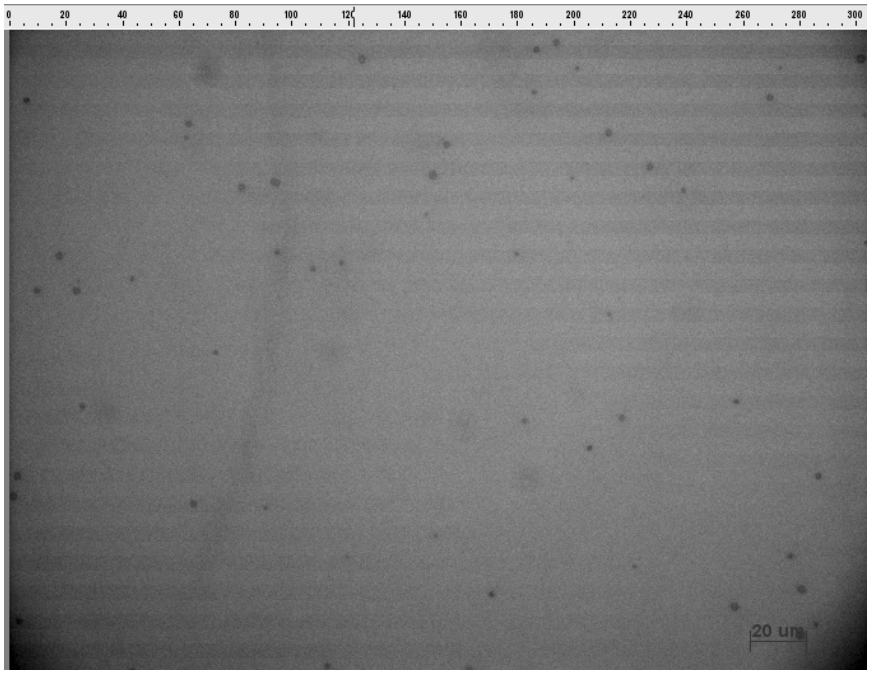

Figure F.5: Light microscope images of TAC:LAC microparticles dispersed in RPMI 1640, 40X magnification; day 5 time point.

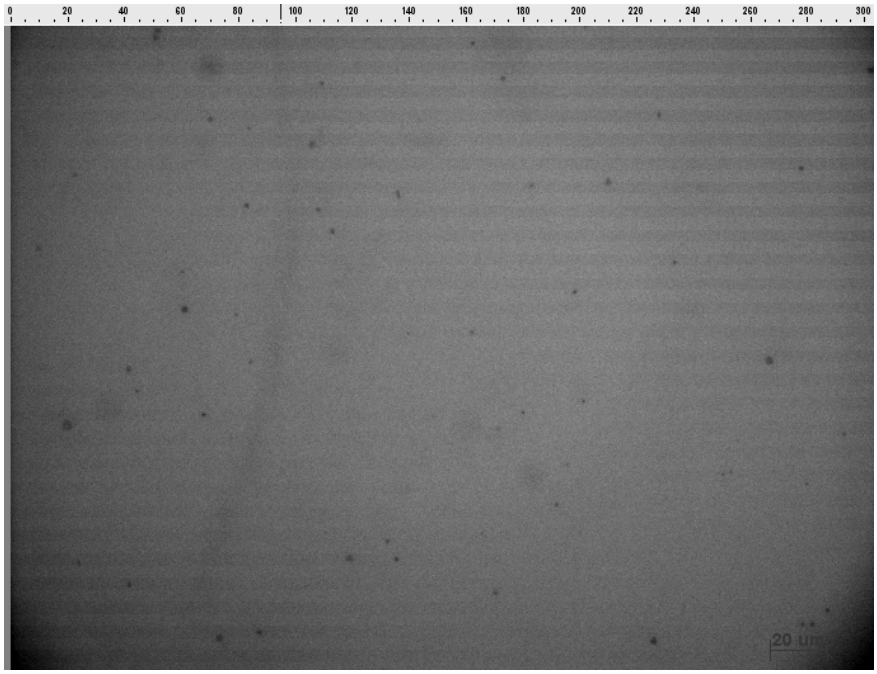

Figure F.6: Light microscope images of TAC:LAC microparticles dispersed in human serum, 40X magnification; day 5 time point

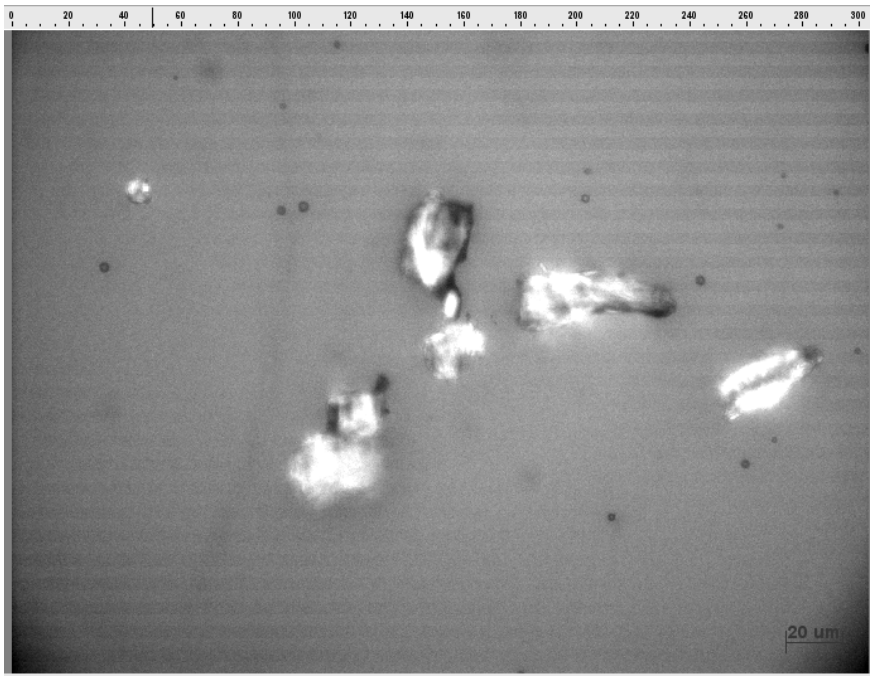

Figure F.7: Light microscope images of ITZ:mannitol:DPPC (control) microparticles dispersed in human serum, 40X magnification; day 5 time point.

Appendix A: Fractionation and Characterization of Sirolimus Isomers in Aqueous Solution

A.1 PURPOSE:

The purpose of this study was to determine the nature of the two sirolimus (SRL) isomers in aqueous solution and determine the ratio of the two isomers to each other under the specific high performance liquid chromatography (HPLC) method that was used to analyze SRL in the studies in Chapter 3. The literature (Sehgal, et al., 1994) reported an isomerization of SRL which occurs in the presence of water (shown in Figure 3.1), and they report a ratio of 4:1 major (lactone) to minor (lactam) isomers of SRL. The HPLC data that was generated showed a different ratio, using different HPLC conditions. Confirmation that the two peaks were, indeed, SRL isomers was established.

A.2 MATERIALS AND METHODS

A.2.1 Materials

The materials used in this study were described in Chapter 3.3.1.

A.2.2 Methods

The methods used in this study were described in Chapter 3.3.4 for the fractionation of the samples and separation of the isomers. The methods for analysis by LC-MS are described in Chapter 3.3.5. The LC-MS was validated by Dr. Herng-Hsiang Lo in the CRED Analytical Instrumentation Facility Core.

A.3 RESULTS

The results of this study show that the major isomer peak, eluting at about 16 minutes is the lactone form of the SRL molecule, while the minor isomer peak, eluting at about 21 minutes is the lactam form of the molecule. The peaks were fractionated, and both fractions were analyzed by LC-MS. The major isomer (Peak 1) and its mass spectrum are shown in Figure A.1. The minor isomer (Peak 2) and its mass spectrum are shown in Figure A.2. The daughter ions of each of the isomers are depicted in the mass spectra of each, showing that the m/z value for both peaks is 936 g/mole, which is the molecular weight of SRL. The chromatogram and UV spectra of the working standard solution at 50 μg/mL is shown in Figure A.3. After both fractions were separated, then immediately re-injected into the HPLC, the chromatograms show that traces of both isomers are present in both fractions (Figure A.4 and Figure A.5). Additionally, their UV spectra are identical (Figure A.4 and A.5). For comparison, the UV spectrum from the literature (Sehgal, et al., 1994) is shown in Figure A.6. Therefore, equilibrium is set up in the aqueous media of the mobile phase and diluent. As stated in Chapter 3.4, the ratio of major to minor isomer is about 85.7-87.5% major isomer and 12.5-14.3% minor isomer. This proves that the isomerization of SRL in the aqueous diluent and mobile phase separates the two isomers, and that in order to analyze for SRL, both isomers must be taken into account. In analyzing samples containing SRL, the peak areas for both the major and minor isomers were summed to determine the peak area of SRL in total. These values were then fit to the linear standard curve, and analysis was performed for the SRL.

A.4 ACKNOWLEDGEMENTS

The authors would also like to thank Dr. Herng-Hsiang Lo in the CRED Analytical Instrumentation Facility Core supported by NIEHS center grant ES07784 for his help with the mass spectrometry (LC-MS) analysis and interpretation.

Appendix B: Tabulation of Data from the Solubility Study of Repaglinide Under Different pH Conditions with Varying Levels of Surfactant

B.1 PURPOSE

The purpose of this study is to show the solubility of repaglinide, a poorly water soluble drug, using different pH buffers (to observe if there is an effect of pH), and different concentrations of surfactant (sodium lauryl sulfate): 0% SDS, 0.1% SDS, and 0.2% SDS to determine the optimum solubility of the drug under in vitro conditions. This method was modified from Higuchi and Connors et al, 1965.

B.2 MATERIALS AND METHODS

B.2.1 Materials

The materials used in this study were described in Chapter 2.3.1.

B.2.2 Methods

The methods used in this study were described in Chapter 2.3.1.1 for the determination of the solubility of repaglinide in each of the buffers described in Chapter 2.3.1.1, with sodium dodecyl sulfate (SDS) present at the three levels described in 2.3.1.1.

B.3 Results

Results show a pH-dependent dissolution of repaglinide. A wetting agent, such as SDS being present allows for increased solubility of the compound, but the solubility follows the same trend, with low solubility in acid conditions and higher solubility at basic conditions. The presence of SDS only slightly raises the solubility of the drug. The solubility vs. pH with varying amounts of SDS (all below the critical micelle concentration of SDS) is shown in Figure 2.2. The tabulation of the actual numbers (concentration of repaglinide vs. pH of the buffer) is shown in Table B.1.

Appendix C: Dissolution Under Sink Conditions - Tabulation of Repaglinide and Sirolimus Data

C.1 PURPOSE

The purpose of this study was to tabulate the data for the dissolutions performed under sink conditions (below 10% solubility of the drug in the media in which it is being tested). Two drugs, repaglinide and sirolimus had undergone processing using the Ultra Rapid Freezing Processing technique. Several different formulations were produced for each drug, with different excipients and different potency. This appendix serves as a tabulated summary of the % drug released over time, which in turn generated the dissolution curves in Figure 2.4 for repaglinide, and Figures 3.12 and 3.13 for sirolimus.

C.2 MATERIALS AND METHODS

C.2.1 Materials

The materials used in this study were the same ones used in Chapter 2.3.1 for the repaglinide formulations, and the materials used for sink dissolution measurements for the sirolimus formulations were the same ones used in Chapter 3.3.3. Although the drugs are different, and the media are different, as well as differences in other dissolution parameters, the appropriate chapters cover the experiments that were performed, and details their exact performance.

C.2.2 Methods

The USP methods that were used to generate the sink dissolution data for the repaglinide formulations are detailed in Chapter 2.3.7. Although the methods for generating the sink dissolution curves for sirolimus are much different than those or repaglinide, they were detailed in Chapter 3.3.3. The results were tabulated to generate the dissolution curves under sink conditions.

C.3 Results

The results show that there is rapid dissolution of repaglinide, containing surfactant and an alkalizing agent as excipients. Additionally, the amorphous nature of the nanoparticles allowed for reduced particle size, increasing the drugs dissolution rate. Figure 2.4 shows that the repaglinide formulations are performing better than the Prandin® commercial tablet. Results for sirolimus under sink dissolution conditions shows addition of wetting agents and surfactants, combined with processing using URF allow for faster dissolution than the commercial Rapamune® tablet. Figures 3.12 and 3.13 show that the dissolution formulations of the amorphous, high potency SRL formulations show better dissolution than the commercial product. Table C.1 show the time vs. % REP released, while Table C.2 shows the time vs. % SRL released for all formulations described in the text. These tables were used to generate the dissolution figures: Figure 2.4 for repaglinide, and Figures 3.12 and 3.13 for sirolimus.

Appendix D: Dissolution Under Supersaturated Conditions - Tabulated Data for Repaglinide and Sirolimus Supersaturated Dissolution

D.1 PURPOSE

The purpose of this study was to tabulate the data for the dissolutions performed under supersaturated conditions (12.5-times the equilibrium solubility of the drug in water). Two drugs, repaglinide and sirolimus had undergone processing using the Ultra Rapid Freezing Processing technique. Several different formulations were produced for each drug, with different excipients and different potency. This appendix serves as a tabulated summary of the % drug released over time, which in turn generated the dissolution curves in Figure 2.5 and 2.6 for repaglinide, and Figures 3.14 and 3.15 for sirolimus

D.2 MATERIALS AND METHODS

D.2.1 Materials

The materials used in these studies are the same as are used in Chapter 2.1 for repaglinide, and the materials used in the sirolimus dissolution under supersaturated conditions are the same as Chapter 3.1.

D.2.2 Methods

The methods used in these studies are the same as are used in Chapter 2.3.8 for repaglinide, and the methods used for the sirolimus dissolution under supersaturated conditions are the same as Chapter 3.3.4.

D.3 RESULTS

The results show that there is rapid supersaturated dissolution of repaglinide, containing surfactant and an alkalizing agent as excipients. Additionally, the amorphous nature of the nanoparticles allowed for higher apparent solubility, as compared to the equilibrium solubility in media. Figure 2.5 and 2.6 show that the repaglinide formulations are supersaturating the media, as well as prolonging the supersaturation of the drug in solution. Results for sirolimus under supersaturated dissolution conditions shows addition of wetting agents and surfactants, combined with processing using URF allow for increased supersaturation, even though the potencies of the formulations are extremely high (50-65% SRL). The commercial Rapamune® tablet, however, has high levels of surfactant and solubilizers (1:350 ratio of SRL to solubilizing excipients), allowing the drug to stay at an "apparent" supersaturation for long periods of time. Figures 3.14 and 3.15 show that the dissolution formulations of the amorphous, high potency SRL formulations show high initial supersaturation, and gradual recrystallization, but remaining high in supersaturation for long time periods. Table D.1 show the time vs. % REP released, while Table D.2 shows the time vs. % SRL released for all formulations described in the text. These tables were used to generate the dissolution figures: Figure 2.5 and 2.6 for repaglinide, and Figures 3.14 and 3.15 for sirolimus.

APPENDIX E: MOUSE IL-12 CYTOKINE ANALYSIS OF BAL LUNG FLUID FOLLOWING SEVEN AND FOURTEEN DAY CHRONIC EXPOSURE TO THE TAC:LAC FORMULATION

E.1 PURPOSE

The purpose of this study was to determine if TAC was effectively inhibiting cytokines (namely IL-12p70) during the multi-dose study. Cytokines like IL-12p70 are an indication of inflammation and irritation caused by a foreign substance (i.e. a drug administered by the pulmonary route). This study proves that TAC is functioning normally by inhibiting cytokine production and that no further inflammation or irritation is caused by the TAC:LAC formulation after the 7 and 14 day dosing period.

E.2 MATERIALS AND METHODS

E.2.1 Materials

ELISA was conducted to determine the induction of the interleukin IL-12p70 in BAL fluid collected from the mice using the Quantikine® mouse IL-12p70 ELISA test kit (R&D Systems, Minneapolis, MN). The kit contained all needed materials for analysis.

E.2.2 Methods

ELISA for analysis of Murine IL-12p70 in Bronchio-Alveolar Lavage (BAL) samples from the mice used in the TAC:LAC multi-dose study (Chapter 4) was conducted. The ELISA for analysis of murine IL-12p70 in BAL fluid was conducted as

per the manufacturer's instructions. Briefly, standards were diluted as per the instructions from the manufacturer, ranging in concentrations from 250 pg/mL to 7.8 pg/mL. All reagents were brought to room temperature, and prepared as instructed. A 50 µL aliquot of assay diluent was added to each well on the microtiter plate, then the standards, positive and negative controls, and samples were added to each well. Samples and standards were prepared in duplicate. The plate was covered with adhesive film and incubated at room temperature for 2 hours. Each well was washed 5 times with the diluted wash solution. A 100 µL aliquot of conjugate was added to each well, and the plate was covered and incubated another 2 hours. Each well was washed an additional 3 times with diluted wash solution. A 100 µL aliquot of substrate solution was added to each well, and the plate was covered and incubated at room temperature for another 30 min. A 100 µL aliquot of stop solution was added to each well, and the optical density was measured using the microtiter plate reader (µQuant Microtiter Plate Reader, Biotek Instruments, Inc., Winooski, VT) at 450 and 540 nm. Results were calculated using linear regression according to standard absorbances.

E.3 RESULTS

BAL fluid supernatant was analyzed for interleukin IL-12p70 induction by the lung tissue in the experimental and control group animals [68]. This cytokine interleukin is responsible for inflammation and irritation which might occur during the pulmonary dosing of drug/excipient to the lung tissue. The positive control used in the ELISA test, which was supplied with the kit, was tested at 54.8 pg/mL, within the specified range (32-56 pg/mL). The BAL fluid obtained from animals dosed with amorphous TAC:LAC composition produced by URF or the lactose control were similar to the negative control in IL-12p70 cytokine levels, showing a lack of interleukin induction by the lung tissue in any of the groups. Since the IL-12p70 was not detected above the negative control level in the mouse IL-12 ELISA test, it is observed that there is not induction or elicitation of the interleukin caused by the drug or the excipient. Given that the present study was a multiple dose, chronic exposure study, it can be concluded that the drug and excipient are safe and can be administered via the pulmonary route without fear of irritation or inflammation in the lung tissues. These results were expected since TAC inhibits cytokine production in cells, including IL-12p70. The table for the ELISA data is given in Table E.1, and the graph of the data in the table are given in Figure E.1.

APPENDIX F: STABILITY OF TAC NANOPARTICLES IN RMPI GROWTH MEDIUM, HUMAN SERUM, AND WHOLE BLOOD

F.1 PURPOSE

Before beginning the MLC and PHA studies, the TAC nanoparticle formulations (URF-TAC and TAC:LAC) were evaluated for stability in the RPMI growth medium, human serum, and whole blood. The objective of the study was to observe aggregation, dissolution, recrystallization, or other physical changes that might occur during the MLC or PHA studies.

F.2 MATERIALS AND METHODS

F.2.1 Materials

The materials used in this study are detailed in Chapter 5.3.1. A Zeiss Axioskop 2 with an Axiocam MRc5 light microscope (Carl Zeiss Vision GmbH; Aalen, Germany) was used to view the test samples for aggregation, recrystallization, dissolution, or other changes in physical state.

F.2.2 Methods

Dispersions of these formulations were compared to a formulation of an anti-fungal drug, itraconazole (ITZ), containing mannitol and dipalmitoylphosphatidylcholine under the same conditions as a control. Dispersions of the three formulations were made in normal saline at a concentration of 1 mg/mL. After 2 minutes of probe sonication in an

ice bath, followed by 5 minutes of standing, and another 1 minute of sonication at room temperature, a uniform dispersion of all three formulations was obtained. The dispersions were plated in a 96-well plate along with each of the three media which they were to be observed in (RPMI 1640, serum, and blood). A 50 μL sample of each dispersion was added to a 200 μL sample of each of the media. The plate was shaken on a plate shaker. The plate was incubated at 37^{o}C, and the samples were observed both visually and under a light microscope at 12 hours, 24 hours, 3 days, and 5 days. Samples were observed for aggregation, recrystallization, and other physical changes. Microscope photos were taken of each of the samples at each time point to compare to each other.

F.3 RESULTS

The stability studies of both URF-TAC and TAC:LAC nanoparticles in Roswell Park Memorial Institute (RPMI) growth medium shows that the drug is stable, releasing the contents and acting as a drug reservoir, perhaps slowly dissolving and extending release of the drug over the incubation time needed for the cell culture assays (3 and 5 days). Experiments performed in human serum showed similar results to the RPMI stability study, showing TAC nanoparticle aggregates with smaller apparent sizes at days 3 and 5. Unfortunately, due to the presence of red and white blood cells in the whole blood, it was difficult to distinguish a TAC nanoparticle from a cell or cell fragment. The whole blood data was not used in the stability study for this reason.

Light microscope photos were taken at specific time points (initially, one-half day, 1 day, 3 days, and 5 days). It was apparent that the TAC nanoparticles (both the URF-TAC and TAC:LAC did not dissolve in the RPMI growth medium, human serum, or whole blood (as far as could be observed). Particles of sizes 3-10 μm were observed

initially and at the end of the study, at day 5, the particle sizes were still visible, but slightly smaller in size than the initial particles (3-7 μm). Photos of the microscopic samples were taken and are shown in Figures F.1 through F.6. Figure F.1 shows the URF-TAC formulation dispersed in RPMI initially, while Figure F.2 shows the TAC:LAC formulation dispersed in RPMI initially, and Figure F.3 shows a control (Itraconazole formulation containing mannitol and DPPC). The control sample was added because it has been known to be dispersible in saline and stable for up to 5 days. Figure F.4 shows the same URF-TAC formulation at day 5, while Figure F.5 shows the same TAC:LAC formulation in RPMI at day 5. Figure F.6 shows the control in human serum at day 5, revealing crystals precipitating from the serum. Overall, the two URF formulations show small aggregates of the primary drug (3-7 μm) when stability of the nanoparticles is observed over the 5 day incubation period. TAC nanoparticles are compatible with the RPMI and human serum, showing no recrystallization or aggregation beyond about the 5-10 μm size range. Additionally, the TAC particles did not appear to dissolve completely at this concentration (1 mg/mL), instead remaining as discreet aggregates of the nanosized primary drug particles.

APPENDIX G: DYNAMIC LASER LIGHT SCATTERING OF TAC NANOPARTICLES AND DISSOLVED TAC IN ETHANOL IN RPMI GROWTH MEDIUM TO DETERMINE PARTICLE SIZES

G.1 PURPOSE

Dynamic light scattering was used to determine the nature of each dilution, to observe whether or not particles were present in each of the dilutions, and the size of the particles, if any were present. The dilution of Prograf® TAC in ethanol, further dilutions of the Prograf® in RPMI 1640, and dilutions of URF-TAC and TAC:LAC used in the MLC and PHA study were observed using DLS, placed in ampules, and read using the laser at wavelength 630 nm. Results are reported as the mean geometric diameter of the particles in the samples.

G.2 MATERIALS AND METHODS

G.2.1 Materials

Materials used in this study are described in Chapter 5.3.1. Additionally, a dynamic light scattering (DLS) instrument was used. In the DLS experiments, the dispersion was circulated through a custom-built cylindrical light-scattering cell. Threaded stainless steel caps secured two sapphire windows (Crystal Systems, 0001 orientation, 2.54-cm diameter, 0.70-cm thickness) in the scattering cell, with a 0.7-cm path length. Black oxide (Fe_3O_4) coating on the surfaces of the scattering cell reduced stray light. A custom-built goniometer held the coherent light source (a 17-mW He-Ne

laser, Melles Griot 05-LHP-925, λ) 632.8 nm), a plano-convex glass lens (Melles Griot 01 LPX 125, focal length 6.00 cm, diameter 3.00 cm), and the light-scattering cell. The scattered light was focused by a SELFOC microlens (0.25 pitch) and transmitted by an optical fiber (NSG America, single mode, specified wavelength of 630 nm) to an avalanche photodiode (Brookhaven Instruments BI-APD). The externally measured detection angle was corrected for refraction to obtain the actual scattering angle. Data analysis was by a digital autocorrelator (Brookhaven BI- 9000AT) and a non-negative least-squares (NNLS) routine (Brookhaven 9KDLSW32). The distribution was determined in terms of the scattering intensity. Each reported diameter corresponds to the maximum of the distribution and is the average of at least two runs

G.2.2 Methods

Samples of URF-TAC and TAC:LAC (at 1 mg/mL) were dispersed in saline using a probe sonicator, while Prograf® TAC was dissolved in absolute ethanol and filtered. These formulations, diluted with RPMI according to the scheme in Chapter 5.4.1 (0.4-0.5 ng/mL for MLC and 0.29 for PHA) along with absolute ethanol, RPMI, and distilled water were tested using the DLS apparatus. Samples were placed in ampules, laser light was passed through the samples, and the scattering of the laser light was used to generate particle sizes in the dispersions. The results were generated, giving a polydispersity curve and a mean geometric diameter of the particles in suspension.

G.3 RESULTS

In the dynamic light scattering experiment, it was shown that TAC dissolved in absolute ethanol had no particles, resulting in no scattering of the laser light. This was in comparison to distilled water which showed the same result. The RPMI 1640 solution, without any added drug, showed particle size diameters of 330 nm, due to the addition of human serum, L-glutamine, vitamins, antibiotics, and other agents. After the first dilution of the dissolved TAC in ethanol, however, there was a large particle distribution that seemed to show TAC crystals growing as a result of the lower solvent power of the RPMI 1640 solution when compared to ethanol itself. The mean particle size diameter increased to 582 nm, showing crystal growth of the TAC in the solution of RPMI 1640. The histogram of the particle size distribution showed a large polydispersity of particles in the solution. The second dilution of dissolved TAC in ethanol showed similar results with a mean particle size of 590 nm, and similar polydispersity of particle sizes. This recrystallization of TAC from solution in the RPMI 1640 could account for the lower values for inhibition obtained from the nanoparticulate TAC formulations.

The dynamic light scattering from the nanoparticulate formulations of TAC in saline showed aggregates of the primary drug particles of 100-200 nm in size. These aggregates were not as large as the particles seen in the recrystallized ethanol TAC. For the URF-TAC first dilution in RPMI, the mean particle size was shown to be 314 nm, while the second dilution in RPMI was shown to be 453 nm. The differences in particle sizes was probably due to the sonicated dispersion added directly to the RPMI in the first dilution, then aggregation of those particles after the second dilution. Similar results were observed with the TAC:LAC formulation, which showed 393 nm mean particle size in the first dilution, with the second dilution showing a mean particle size of 649 nm.

The growth of aggregates in the RPMI upon subsequent dilutions was not unexpected, since the TAC is a hydrophobic drug, and after sonication, the particles desire to reduce interfacial tension by aggregating to larger sizes. None the less, the crystalline URF-TAC showed smaller particles with less polydispersity than the Prograf® dissolved in ethanol, accounting for the apparent differences in proliferation of lymphocytes *in vitro*. The amorphous TAC:LAC formulation, however, could supersaturate the media *in vitro*, causing less proliferation of the lymphocytes that was observed.

Appendix H: Lowered TAC:LAC Pulmonary Dosing in Rats - Pharmacokinetic Study at One Hour

H.1 PURPOSE

The purpose of this experiment was to show that lower dosing of aqueous nebulized TAC:LAC nanoparticles in a healthy rat model could produce the same anti-rejection capability lung levels as has been reported in previous studies (Ide, et al, 2007). A rat model study was performed at a lower dosing level to compare results with Ide et al. [69]. This research confirmed dosing of TAC:LAC nanoparticles at a lower dose (3.2mg/mL TAC) yielded the similar lung levels reached by Ide et al., although Ide et al. dosed the animals at a higher tacrolimus level (0.1% TAC), using a pressurized metered dose inhaler (pMDI) formulation.

H.2 MATERIALS AND METHODS

H.2.1 Materials

H.2.2 Methods

The drug materials, ELISA assay, and formulation materials, as well as the rodent dosing apparatus are described in Chapter 4.3.1. The rat models used in the study were Harlan Sprague Dawley rats weighing 290-300 grams (Harlan Sprague Dawley, Indianapolis, IN), which were rested and acclimated to the restraint chambers for 3 days prior to dosing.

H.2.2.1 Andersen Cascade Impaction for the Lower Dose

The Andersen Cascade Impactor was used to determine if there was any difference in the dose emitted, MMAD, or respirable fraction in the lower dosing (3.2 mg/mL TAC) vs. the higher dosing (1 mg/mL TAC) used in the multi-dose study in Chapter 4.

H.2.2.2 ELISA Mouse Lung Level TAC Analysis

The mouse ELISA lung analysis was performed using the Pro-TRAC II FK 506 ELISA kit (Minneapolis, MN). The lungs were homogenized with the Polytron rotor/stator apparatus. The lung tissue was diluted by half with saline, and the homogenate was analyzed according to the instructions given in the kit.

H.3 RESULTS

Andersen Cascade impaction results with the lowered TAC:LAC dosing showed a respirable fraction of 79.4% and a mass median aerodynamic diameter (MMAD) of 2.33μm. Lowered dosing in a rat model was achieved by nebulizing 6.4 mg of URF processed TAC:LAC containing 3.2 mg tacrolimus. Tacrolimus deposition in rat lung and whole blood levels averaged 398.7 ng/g ± 34.4 and 3.91 ng/ml ± 2.5, respectively one hour after dosing in four rats. These levels would be effective in a lung transplanted rat model according to a therapeutic lung level of 270.4 ng/g reported by Ide et al. [69]. Blood levels obtained in this study and in data presented by Ide were both similar, and therapeutically relevant. Lowered tacrolimus lung levels obtained in a rat model after

dosing URF processed TAC:LAC would be effective in preventing rejection of transplanted lung tissue in rats.

BIBLIOGRAPHY

Akashi T., Nefuji M, Yoshida M, et al. Quantitative Determination of Tautomeric FK 506 by Reversed Phase Liquid Chromatography. *J Pharm Biomed Analy* 1996 14 339-346.

Amidon GL. A theoretical basis for a biopharmaceutic drug classification: the correlation of in vitro drug product dissolution and in vivo bioavailability. *Pharm Res* 1995;13:413-420.

Apanius V, Penn D, Slev PR, et al. The nature of selection on the major histocompatibility complex. *Critic Reviews Immunol* 1997; 17:179-224.

Balandrand-Pieri N, Queneau P, Caroli-Bosc F, et al. Effects of Tauroursodeoxycholate Solutions on Cyclosporin A Bioavailability in Rats. *Drug Metabol Distrib* 1997; 25:912-916.

Baldrick, P. Bamford, DG. A toxicological review of lactose to support clinical administration by inhalation. *Food Chem Toxicol* 1997 35 (7), 719-733.

Beclovent Aerosol for Inhalation: professional literature. Research Triangle Park, NC: Glaxo Smithkline Pharmaceuticals, 1998.

Benameur H, Latour N, Schandene L, Van Vooren JP, Flamion B, Legros F. Liposome-incorporated dexamethasone palmitate inhibits in-vitro lymphocyte response to a mitogen. *J Pharm Pharmacol* 1995; 47:812-817.

Cattaneo D, Perico N, Gaspari F. Assessment of Sirolimus Concentrations in Whole Blood by High-Performance Liquid Chromatography with UV Detection. *J Chromatogr B*, 2002 774 187-194.

Ceyhan BB, Sungur M, Celikel CA, Celikel T. Effect of Inhaled Cyclosporin on the Rat Airway: Histologic and Brochioalveolar Lavage Assessment. *Respiration*, 2001 65 71-78.

Chakinala MM, Kollef MH, Trulock EP. Critical Care Aspects in Lung Transplant Patients. *J Intens Care Med* 2002; 17:8-33.

Chorny M, Mishaly D, Leibowitz A, Domb A, Golomb G. Site-specific Delivery of Dexamethasone from Biodegradable Implants Reduces Formation of Pericardial Adhesions in Rabbits. *J Biomed Materials Res A* 2006; 78A:276-282.

Cimolai N, Taylor GP, Mah D, et al. Definition and Application of a Histopathological Scoring Scheme for an Animal Model of Acute Mycoplasma-Pneumoniae Pulmonary Infection. *Microb Immunol* 1992 36 (5), 465-478.

Costantino HR, Firouzabadian L, Hogeland K, et al. Protein spray freeze drying. Effect of atomization conditions on particle size and stability. *Pharm Res*. 2000; 17(11):1374-1383.

Courrier, HM, Butz, N, Vandamme,TF. Pulmonary Drug Delivery Systems: Recent Developments and Prospects. *Crit Rev Therap Drug Carrier Syst* 2002 19 (4,5): 425-498.

Davis DL, Murthy JN, Gallant-Haidner H, et al. Minor Immunophilin Binding of Tacrolimus and Sirolimus Metabolites. *Clin Biochem* 2000 33 (1), 1-6.

Deen, MVD, Vries, ED, Timens,W, Scheper, R et al. ATP binding cassette (ABC) transporters in normal and pathological lung. *Respir Res* 2001 2 (59), 1-16.

Dressman JB, Reppas, C. In vitro-in vivo correlations for lipophilic, poorly water soluble drugs. *Eur J Pharm Sci* 2000; 11:S73-S80.

Duax WL, Cody V, Strong PD. Structure of the asthma drug beclomethasone dipropionate. *Acta Crystallograph B: Struct Crystallog Cryst Chem* 1981; B37:383-387.

Dubey DP, Yunis I, Yunis EJ. Cellular Typing: Mixed Lymphocyte Response and Cell-Mediated Lympholysis. In: Rose NR, Friedman H, Fahey JL, eds. *Manual of Clinical Laboratory Immunology*. Washington, DC: American Society for Microbiology, 1986:847-858.

Edsbacker S, Wollmer P, Nilsson A, Nilsson M. Pharmacokinetics and gastrointestinal transit of budesonide controlled ileal release (CIR) capsules. *Gastroenter* 1993; 104:A695.

Edsbacker S, Andersson T. Pharmacokinetics of Budesonide (Entocort EC) Capsules for Crohn's Disease. *Clin Pharmaco* 2004; 43:803-821.

Edsbacker S, Larsson P, Wollmer P. Gut Delivery of Budesonide, a Locally Active Corticosteroid from Plain and Controlled-Release Capsules. *Eur J Gastroenterol Hepatol* 2002; 14:1357-1362.

Faassen F, Kelder J, Lenders J, Onderwater R, Vromans H. Physicochemical Properties and Transport of Steroids Across CACO-2 Cells. *Pharm Res* 2003; 20:177-186.

Forbes B, Ehrhardt C. Human respiratory epithelial cell culture for drug delivery applications. *Eur J Pharm Biopharm* 2006 60 (2), 193-205.

Forsgren P, Modig J, Gerdin et al. Intrapulmonary deposition of aerosolized Evans blue dye and liposomes in an experimental porcine model of early ARDS. *Upsala J Med Sci* 1990 95 (2), 117-36.

Fruman DA, Wood MA, Gjertson CK, Katz HR, Burakoff SJ, Bierer BE. FK506 binding protein 12 mediates sensitivity to both FK506 and rapamycin in murine mast cells. *Eur J Immunol* 2005; 25:563-571.

Gallant-Haidner HL, Trepanier DJ, Freitag DG, Yatscoff SW. Pharmacokinetics and Metabolism of Sirolimus. *Therap Drug Monitor* 2000 22 (1), 31-35.

Geiser M. Morphological aspects of particle uptake by lung phagocytes. *Micros Res Tech* 2002 57 (6), 512-522.

Gottfried BS, Lee CJ, Bell KJ. The Leidenfrost Phenomenon: Film Boiling of Liquid Droplets. *Int J Heat Mass Transfer* 1966 9 1167-1187.

Goulet MT, Boger J. Degradative Studies on the Tricarbonyl Containing Macrolide Rapamycin. *Tetra Let* 1990 31 (34), 4845-4848.

Groneberg DA, Fischer A, Chung K, Daniel H. Molecular Mechanisms of Pulmonary Peptidomimetic Drug and Peptide Transport. *Am J Resp Cell Mol Biol*, 2004 30 251-260.

Geelhaar A, Weibel ER. Morphometric estimation of pulmonary diffusion capacity. 3. The effect of increased oxygen consumption in Japanese Waltzing mice. *Respir Physiology* 1971 11 (3), 354-66.

Grube E, Buellesfeld L. Rapamycin Analogs for Stent Based Local Drug Delivery. *Herz* 2004; 29:162-166.

Guo Z, Gatterman MS, Hood L, Hansen JA, Petersdorf EW. Oligonucleotide Arrays for High-Throughput SNPs Detection in the MHC Class I Genes: HLA-B as a Model System. *Genome Res* 2002; 12:447-457.

Guzman M, Molpeceres J, Garcia F, Aberturas MR, Rodriguez M. Formation and Characterization of Cyclosporin Loaded Nanoparticles. *J Pharm Sci* 1993; 82:498-502.

Hamelryck T, Dao-Thi M, Poortmans F, Chrispeels M, Wyns L, Lorris R. The crystallographic structure of phytohemmaglutinin-L. *J Biolog Chem* 1996; 271:20479-85.

Hancock BC, Zograffi G. Characteristics and significance of the amorphous state in pharmaceutical systems. *J Pharm Sci* 1997; 86:1-12.

Hickey T, Kreutzer D, Burgess DJ, Moussy F. Dexamethasone/PLGA Microspheres for Continuous Delivery of an Anti-Inflammatory Drug for Implantable Medical Devices. *Biomat* 2002; 23:1649-1656.

Higaki M, Ishihara T, Izumo N, Takatsu M, Mizushima Y. Treatment of Experimental Arthritis with Poly (D,L Lactic/Glycolic) Acid Nanoparticles Encapsulating Betamethasone Sodium Phosphate. *Ann Rheum Dis* 2005; 64:1132-1136.

Ho S, Clipstone N, Timmerman L, et al. Mechanism of Action of Cyclosporin A and FK506. *Clin Immunol Immunop* 1996; 80:S40-S45.

Hoeben, BJ, Burgess, DS, McConville, JT, et al.. In vivo efficacy of aerosolized nanostructured itraconazole formulations for prevention of invasive pulmonary aspergillosis. *Antimicrob Agents Chemotherapy* 2006 50 (4), 1552-1554.

Honbo T, Kobayahi M, Hane K, Hata T, Ueda Y. The Oral Dosage form of FK-506. *Transplant Proc* 1987; 19:17-22.

Hooks MA. Tacrolimus - A New Immunosuppresant - Review of the Literature. *Ann Pharmacother* 1994; 28:501-511.

Humphreys WG. Presystemic and First-Pass Metabolism. In: Wang B, Siahaan T, Soltero R, eds. Drug Delivery Principles and Applications. Hoboken, NJ: Wiley and Sons, 2005.

Hu JH, Johnston KP, Williams III RO. Nanoparticle engineering processes for enhancing the dissolution rates of poorly water soluble drugs. *Drug Dev Ind Pharm.* 2004;30:233-245.

Hu JH, Johnston KP, Williams III RO. Spray-freezing into liquid (SFL) particle engineering technology to enhance dissolution of poorly water soluble drugs: organic solvent versus organic/aqueous co-solvent systems. *Eur J Pharm Sci*. 2003;20:295-303.

Hu JH, Johnston KP, Williams III RO. Rapid dissolving high potency danazol powders produced by spray freezing into liquid process. *Int J Pharm*. 2004;271: 145-154.

Hu JH, Johnston KP, Williams III RO. Spray-freezing into liquid (SFL) particle engineering technology to enhance dissolution of poorly water soluble drugs: organic solvent versus organic/aqueous co-solvent systems. *Eur J Pharm Sci*, 2003 20 295-303.

Hu JH, Johnston KP, Williams III RO. Stable amorphous danazol nanostructured powders with rapid dissolution rates produced by spray freezing into liquid. *Drug Dev Ind Pharm* 2004 30 695-704.

Hu JH, Johnston KP, Williams III RO. Nanoparticle Engineering Processes for Enhancing the Dissolution Rates of Poorly Water Soluble Drugs. *Drug Dev Ind Pharm* 2004 30 (3), 233-245.

Hu JH, Rogers TL, Brown J, Young T, Johnston KP, Williams III RO. Improvement of Dissolution Rates of Poorly Water Soluble APIs Using Novel Spray Freezing into Liquid Technology. *Pharm Res* 2002 19 (9), 1278-1284.

Hutchinson, IV, Bagnall, AW,. Bryce, AP,. Pufong, AB et al.. Differences in the Mode of Action of Cyclosporine and FK 506. *Transplant Proc* 1998 30 (4), 959-960.

Ide N, Nagayasu T, Matsumoto T, et al. Efficacy and Safety of Inhaled Tacrolimus in Rat Lung Transplantation. *J Thorac Cardiovasc Surg* 2007 133 (2), 548-553.

Imuran Tablets: professional literature. Mississagua, Ontario: Glaxo-Smithkline Pharmaceuticals, 2005.

Jain AB, Fung JJ. Cyclosporin and Tacrolimus in Clinical Transplantation - A Comparative Review. *Clin Immunotherapeutics* 1996; 5:351-373.

Jang, S,. Weintjes, M, Au, J. Kinetics of P-glycoprotein Mediated Efflux of Paclitaxel. *J Pharmacol Exp Therap* 2001 298 (3), 1236-1242.

Juniper E, Price DB, Stampone P, Creemers J, Mol S, Fireman P. Clinically Important Improvements in Asthma-Specific Quality of Life, but No Difference in Conventional Clinical Indexes in Patients Changed from Conventional Beclomethasone to Approximately Half the Dose of Extrafine Beclomethasone Dipropionate. *Chest* 2002; 121:1824-1832.

Kalariya M, Padhi B, Chougule M, Misra A. Methotrexate Loaded Solid Lipid Nanoparticles for Topical Treatment of Psoriasis: Formulation and Clinical Implications. *Drug Del Tech* 2004; 4:65-71.

Kruijtzer C, Beijnnen J, Schellens J. Improvement of Oral Drug Treatment by Temporary Inhibition of Drug Transporters or CYP 450 in the Gastrointestinal Tract and Liver: an Overview. *Oncologist* 2002; 7:516-530.

Lamprecht A, Yamamoto H, Takeuchi H, Kawashima Y. Design of pH-Sensitive Microspheres for the Colonic Delivery of Immunosuppressive Drug Tacrolimus. *Eur J Pharm Biopharm* 2004; 58:37-43.

Lamprecht A, Yamamoto H, Ubrich N, Takeuchi H, Maincent P, Kawashima Y. FK-506 Microparticles Mitigate Experimental Colitis with Minor Renal Calcineurin Suppression. *Pharm Res* 2005; 22:193-199.

Lang JM, Oberling F, Mendel C, Grenier JF, Mayer S, Waitz R. Hydrostatics and lymphocyte reactivity to phytohemagglutinin. *Report of the Society of the Science of Biology and Its Affiliates* 1974; 168:112-116.

Lauricella AM, Garbossa G, Nesse A. Dissimilar behavior of lymph cells in response to the action of aluminum. In vitro and in vivo studies. *Int Immunopharmacol* 2001; 1:1725-1732.

Leuenberger H. Spray Freeze Drying: The process of choice for low water soluble drugs? *J Nanoparticle Res* 2002;4:111-119.

Liang L, Jackson J, Min W, et al. Methotrexate Loaded Poly (L-Lactic) Acid Microspheres for Intra-Articular Delivery of Methotrexate to the Joint. *J Pharm Sci* 2004; 93:943-955.

Liversidge GG, Conzentino P. Drug Particle Size Reduction for Decreasing Gastric Irritancy and Enhancing Absorption of Naproxen in Rats. Int J Pharm 1995; 125:309-315.

Lobo JM, Schiavone H, Palakodaty S, York P, Clark A, Tzannis S. SCF-Engineered Powders for Delivery of Budesonide from Passive DPI Devices. J Pharm Sci 2005; 94:2276-2288.

Loser K, Balkow S, Higuchi T, et al. FK-506 Controls CD40L-Induced Systemic Autoimmunity in Mice. *J Invest Dermatol* 2006 126 1307-1315.

Lum H, MitznerW. A species comparison of alveolar size and surface forces. *J Applied Physiol* 1987 62 (5), 1865-71.

Ma A, Qi S, Xu D, Zhang X, Daloze P, Chen H. Baohuoside-1, a Novel Immunosuppressive Molecule, Inhibits Lymphocyte Activation In Vitro and In Vivo. Transplantation 2004; 78:831-838.

Maluish AE, Strong DM. Lymphocyte Proliferation. In: Rose NR, Friedman H, Fahey JL, eds. Manual of Clinical Laboratory Immunology. Washington, DC: American Society of Microbiology, 1986:274-281.

Makino K, Yamamoto N, Higuchi K, et al. Phagocytic Uptake of Polystyrene Microspheres by Alveolar Macrophages: Effects of the size and surface

properties of the microspheres. *Colloids and Surfaces B: Biointerfaces*, 2003 27 33-39.

Mahalati K, Kahan BD. Clinical Pharmacokinetics of Sirolimus. *Clin Pharmaco*, 2001 40 (8), 573-585.

Maia CS, Mehnert W, Schafer-Korting M. Solid Lipid Nanoparticles as Drug Carriers for Topical Glucocorticoids. Int J Pharm 2000; 196:165-167.

Maia CS, Gysler A, Mehnert W, Muller RH, Schafer-Korting M. Local Tolerability of Solid Lipid Nanoparticles for Dermal Use. Proceedings of the International Symposium of Controlled Release of Bioactive Materials 1999; 26:399-400.

Mancinelli LM, Frassetto L, Floren LC, et al. The pharmacokinetics and metabolic disposition of tacrolimus: A comparison across ethnic groups. Clin. Pharmacol. Therapeut. 2001; 69.

Matteucci ME, Brettmann BK, Rogers, TL, et al.Design of Potent Amorphous Drug Nanoparticles for Rapid Generation of Highly Supersaturated Media. *Molecular Pharmaceutics,* 2007 in press

Marsh SG, Albert ED, Bodmer WF, et al. Nomenclature for Factors of the HLA System. *Tissue Antigens* 2005; 65:301-369.

McConville, JT, Overhoff, KA, Sinswat, P, et al. Targeted High Lung Concentrations of Itraconazole Using Nebulized Dispersions in a Murine Model. *Pharm Res* 2006 23 (5), 901-911.

Merisko-Liversidge E, Liversidge GG, Cooper E. Nanosizing: A Formulation Approach for Poorly Water Soluble Compounds. *Eur J Pharm Sci* 2003; 18:113-120.

Meissner Y, Pellequer Y, Lamprecht A. Nanoparticles in Inflammatory Bowel Disease: Particle Targeting vs. pH Sensitive Delivery. *Int J Pharm* 2006; 316:138-143.

Mitruka SN, Pham SM, Zeevi A, et al. Aerosol Cyclosporin Prevents Acute Allograft Rejection in Experimental Lung Transplantation. *J Thoracic Cardiovasc Surg* 1997; 115:28-37.

Mitruka SN, Won A, McCurry KR, et al. In the Lung Aerosol Cyclosporine Provides a Regional Concentration Advantage over Intramuscular Cyclosporine. *Clin Lung Heart/Lung Transplant* 2000; 19:969-975.

Miyaji S, Nishiyama T, Takada O, Hayahshi et al. Comparative Study of Immunosuppressants Effects of Various Immunosuppressants on Response of Canine Mixed Lymphocyte Culture. *Iryo* 1993; 47:200-204.

Mollison KW, Fey T, Krause RA, et al. Nephrotoxicity studies of the immunosuppressants tacrolimus (FK506) and ascomycin in rat models. *Toxicology,* 1998 125 169-181.

Molnar-Kimber KL. Mechanism of action of rapamycin (Sirolimus, Rapamune). *Transplant Proc* 1996; 28:964-969.

Morand EF. Corticosteroids in the Treatment of Rheumatologic Diseases. *Current Opin Rheumatol* 2000; 12:171-177.

Morris RE. Prevention and Treatment of Allograft Rejection in vivo by Rapamycin: Molecular and Cellular Mechanisms of Action. *Ann New York Acad Sci* 1992; 1:68-72.

Neoral Soft Gelatin Capsules and Oral Liquid: professional literature. East Hanover, NJ: Novartis Pharmaceuticals, 1998.

Nickmilder, M, Latinne, D, De Houx, J et al. Isolation and identification of a C39 demethylated metabolite of rapamycin from pig liver microsomes and evaluation of its immunosuppressive activity. *Clin Chem* 1998 44 (3), 532-538.

Ostrander KD, Bosch HW, Bondanza DM. An In-Vitro Assessment of a Nanocrystal Beclomethasone Dipropionate Colloidal Dispersion via Ultrasonic Nebulization. *Eur J Pharm Biopharm* 1999; 48:207-215.

Oberdoerster, G.. Effects and fate of inhaled ultrafine particles. ACS Symposium Series, 890 (Nanotechnology and the Environment), 2005 37-59.

Overhoff KA, Engstrom JD, Chen B, et al. Novel Ultra-Rapid Freezing Particle Engineering Process for Enhancement of Dissolution Rates of Poorly Water Soluble Drugs. *Eur J Pharm Biopharm* 2007 65 57-67.

Patton JS, Fishburn, CS. Weers, JG .The Lungs as Portal Entry for Systemic Drug Delivery. *Proc Am Thorac Soc*, 2004 1 338-344.

Pang KS. Modeling of Intestinal Drug Absorption: Roles of Transporters and Metabolic Enzymes. *Drug Metabol Disposit* 2003 31 (12), 1507-1519.

Parham P, Ohta T. Population Biology of Antigen Presentation by MHC Class I Molecules. *Science* 1996; 272:67-74.

Prograf Capsules: professional literature. Osaka, Japan: Fujisawa Pharmaceuticals, 2004.

Protopic Ointment: professional literature. Osaka, Japan: Fujisawa Pharmaceuticals, 2002.

Raghavan SL. Effect of cellulose polymers on supersaturation and in vitro membrane transport of hydrocortisone acetate. *Int J Pharm* 2000; 193:231-237.

Ran Y, Zhao L, Xu Q, Yalkowsky S. Solubilization of Cyclosporin A. *AAPS Pharm Sci Tech* 2001; 2.

Rapamune Tablets and Oral Liquid: professional literature. Philadelphia, PA: Wyeth Pharmaceuticals, 2004.

Report on Carcinogens, 11th Edition. In: *United States Department of Health and Human Services,* ed. Vol. 11: Public Health Service, National Toxicology Program, 2004..

Ricciutelli M, Di Martino P, Barboni L, Martelli S. Evaluation of rapamycin chemical stability in volatile-organic solvents by HPLC. *J Pharm Biomed Anal*, 2006 41 (3), 1070-1074.

Rocca-Serra JP, Vicaut E, Lefrancois G, Umile A. Efficacy and Tolerability of a New Non-Extrafine Formulation of Beclomethasone HFA-134a in Patients with Asthma. *Clin Drug Invest* 2002; 22:653-665.

Rogers TL, Johnston KP, Williams III RO. Solution-based particle formation of pharmaceutical powders by supercritical or compressed fluid CO2 and cryogenic spray-freezing technologies. *Drug Dev Ind Pharm*, 2001 27 (10), 1003-1015.

Rogers TL, Nelsen AC, Sarkari M, et al. Enhanced Aqueous Dissolution of a Poorly Water Soluble Drug by Novel Particle Engineering Technology: Spray-Freezing into Liquid with Atmospheric Freeze-Drying. *Pharm Res* 2003 20 (3), 485-493.

Rodriguez M, Antunez J, Taboada C, Seijo B, Torres D. Colon specific delivery of budesonide from Microencapsulated cellulosic cores: Evaluation of the efficacy against colonic inflammation in rats. *J Pharm Pharmacol* 2001; 53:1207-1215.

Salm P, Tresillian MJ ,Taylor PJ et al., Stability of Sirolimus (Rapamycin) in Whole Blood. *Therap Drug Monitor* 2000 22 (4), 423-426.

Sakagami M, Kinoshita W, Makino Y, et al. Mucoadhesive BDP Microspheres for Powder Inhalation - Their Unique Pharmacokinetic/Pharmacodynamic Properties. *Respir Drug Del* 1998; 4:193-199.

Sandimmune Capsules and Oral Liquid: professional literature. East Hanover, NJ: Novartis Pharmaceuticals, 1999.

Sanchez A, Seoane R, Quireza O, et al. In Vivo Study of the Tissue Distribution and Immunosuppressive Response of Cyclosporin A-Loaded Polyester Micro and Nanospheres. *Drug Deliv* 1995; 2:21-28.

Scammell JG, Denny WB, Valentine DL, et al. Overexpression of the FK506-Binding Immunophilin FKBP51 Is the Common Cause of Glucocorticoid Resistance in Three New World Primates. *Gen Compar Endocrin* 2001; 124:152-165.

Sehgal SN, Camardo JS, Scarola JA, et al. Rapamycin (Sirolimus, Rapamune). *Dialys Transplant* 1995:482-487.

Sehgal SN, Molnar-Kimber K, Ocain TD, et al. Rapamycin: A Novel Immunosuppressive Macrolide. *Medicinal Res Review* 1994; 14:1-22.

Segall M, Bach F. Pooled Stimulating Cells as a "Standard Stimulator" in Mixed Lymphocyte Culture. *Transplantation* 1976; 22:79-85.

Simamora P, Alvarez JM, Yalkowsky SH. Solubilization of Rapamycin. *Int J Pharm* 2001; 213:25-29.

Sinswat P, Matteucci ME, Johnston KP, Williams III RO. Dissolution rates and supersaturation behavior of amorphous repaglinide particles produced by controlled precipitation. *J Biomed Nanotech*, 2007 3 (1), 18-27.

Sinswat P, Overhoff KA, McConville JT, et al. Nebulization of Nanoparticulate Amorphous or Crystalline Tacrolimus - Single Dose Pharmacokinetics Study in Mice. *Eur J Pharm Biopharm*, 2007 in press

Smith G, Ryoo W, Johnston KP. Electrostatically Stabilized Metal Oxide Particle Dispersions in Carbon Dioxide. *J Phys Chem B* 2005; 109:20155-20165.

Soeda S, Akashi T, Maeda K, Kawagita T. Studies on the Development of Tacrolimus Production. *Seibutsu Kogaku Kaishi* 1998; 76:389-397.

Sorbera LA, Leeson PA, Castaner J. SDZ-RAD. *Drugs Fut* 1999; 24:22.

Streit F, Christians U, Schiebel H, et al. Sensitive and specific quantification of sirolimus (rapamycin) and its metabolites in blood of kidney graft recipients by HPLC/electrospraymass spectrometry. *Clin. Chem*., 42 (9), 1996 1417-1425.

Steffan, RJ, Kearney, M, Hu, DC, et al. Base Catalyzed Degradation of Rapamycin. *Tetra Letters*, 1993 34 (23), 3699-3702.

Suntres Z, Shek P. Liposomes promote pulmonary glucocorticoid delivery. *J Drug Targ* 1998; 6:175-182.

Suntres Z, Shek P. Prophylaxis against lipopolysaccharide-induced lung injuries by liposome-entrapped dexamethasone in rats. *Biochem Pharmacol* 2000; 59:1155-1161.

Tacca MD. Prospects for Personalized Immunosuppression: Pharmacologic Tools - A Review. *Transplant Proc*., 2004 36 687-689.

Tamura S, Tokunaga Y, Ibuki R, Amidon GL et al. The Site-Specific Transport and Metabolism of Tacrolimus in Rat Small Intestine. *J. Pharmacol. Exp. Therap*., 2003 306 310-316.

Trepanier DT, Gallant H, Legatt DF, Yatscoff RW. Rapamycin: Distribution, Pharmacokinetics, and Therapeutic Range Investigations: An Update. *Clin Biochem*, 1998 31 (5), 345-351.

Trexall Tablets: professional literature. Pomona, NY: Duramed Pharmaceuticals, 2005.

Van Os EC, Zins BJ, Sandborn WJ, et al. Azathioprine Pharmacokinetics After Intravenous, Oral, Delayed Release Oral, and Rectal Foam Administration. *Gut* 1996; 39:63-68.

Zins BJ, Sandborn WJ, McKinney JA, et al. A Dose Ranging Study of Azathioprine Pharmacokinetics After Single-Dose Administration of a Delayed-Release Oral Formulation. *J Clin Pharmacol* 1997; 37:38-46.

Vita

Troy Powell Purvis was born October 3, 1975 in Fort Worth, TX to O.J. "Jack" and Anita Purvis. He graduated from the Mississippi School for Math and Science in 1994, after which he accepted a full scholarship to attend Louisiana State University. He transferred to Mississippi State University where he began his education in the College of Arts and Sciences in 1995, seeking a degree in Chemistry, under the direction of Dr. William Henry. His research interests began in Dr. Henry's lab, using specialized equipment to synthesize novel air and water sensitive organometallic compounds, specializing in selective synthesis of single isomer organometallics and their characterization. He maintained a close working relationship with both his professors and fellow students, while earning high grades in all of his class work. He graduated *magna cum laude* in 1998, with an American Chemical Society certified Bachelor's of Science degree in Chemistry. Upon graduation, he began work at a pharmaceutical company (DPT Laboratories, San Antonio, TX) which spurred his interest in the pharmaceutical and analytical sciences. Moving to Austin, TX in 2001, Troy was hired at another smaller pharmaceutical company, Pharmaform, LLC. While working at Pharmaform, he was introduced to Dr. Robert "Bill" O. Williams, III, and after realizing the benefits of graduate education, he applied to the Pharmaceutics Division of the College of Pharmacy at the University of Texas in 2003. With Dr. Williams as his advisor, he wrote review articles for the *International Journal of Pharmaceutics*, a book chapter for *Advanced Formulation Design to Optimize Therapeutic Outcomes* (Drs.

Williams, McConville, and Taft, editors), and an original research paper for *AAPS Pharm Sci Tech* online journal. While earning his Ph.D., Troy was assigned various teaching assistant positions, working with Drs. Pearlman, Croyle, and Kerwin. He was also a teaching assistant for the Pharmaceutical Calculations and Compounding Laboratory, where he taught undergraduate pharmacy students the basics of pharmaceutical formulation compounding and pharmaceutical calculations. He was the head teaching assistant for this lab for one semester in 2005, which taught him about working with students and assisting in their learning process. In 2005, he was awarded a Competitive Pharmaceutics scholarship. He has attended and presented original research findings at many conferences and meetings throughout the United States and Europe. In collaboration with the University of Texas Health Science Center in San Antonio, TX, he has learned clinical implications of drug delivery, resulting in manuscripts that are soon to be published. Parts of his dissertation will be submitted for publication in high impact pharmaceutical and medical journals.

Permanent address: 109 Heron Court, Brandon, MS 39047

This dissertation was typed by Troy Powell Purvis.